The development of bacterial toxin and plant sugar-binding proteins for neuronal tracing and delivery

Jessica Leanne Haigh

Submitted in accordance with the requirements for the degree of
Doctor of Philosophy

The University of Leeds
School of Biomedical Sciences

September 2016

The candidate confirms that the work submitted is her own and that appropriate credit has been given where reference has been made to the work of others.

Acknowledgements

Firstly I must thank my primary supervisor Jim Deuchars; you have provided me with amazing guidance throughout my project and supplied endless enthusiasm. I am of course eternally thankful for the countless times you've called me a donkey, possibly not always deservedly so. I must also thank my co-supervisor Bruce Turnbull, you have been a fountain of knowledge. Your input has given me a real passion for such a niche area and you have no doubt steered my future direction as a scientist. Sue Deuchars, you have been a fantastic support and picked me up the in the times I have felt I wasn't achieving enough with my PhD. You've kept my project on the straight and narrow by reining in Jim and his magnificent, sometimes wacky, ideas.

Additionally I would to thank all the members of my supervisors' labs, you have all aided me in completing this PhD. Dan Williamson, Darren Machin, Ian Edwards - without you guys I wouldn't even have a project. Thank you kindly for all the time you gave up to teach me. Also thanks to Katherine, counting all those cells can't have been fun. Claudia thank goodness we have had each other through this unrelenting process, there is no doubt in my mind that I would have lost the plot without you in the office. Thank you for all the times you lent an ear to soak up my whining. Aaron Murray, Calvin Smith, Jenny Clancy, Kaisan Mahadi, Lauryn New, Lucy Peers, Matt Balmforth, Pierce Mullen, Varinder Phull, Yazi Al'Joboori, and Yusoff Merican: chatting and joking in the lab with you lot undoubtedly kept me sane and cheered me up on the darkest of days. You all made doing a PhD tolerable and even fun at times.

Massive thanks to all my friends who have provided more support and love than I could ever have asked for. Especially Verity Hammond, Sam Fraser, Nicole Jackson, and Grace Hoysted, you guys have been there for me when I needed a hug, a coffee and most importantly a beer (or two). Arthur Mercer you have been the best distraction and have given me something to look forward to during the laborious months of writing. Thanks for pretending to care about my boring thesis updates, and most importantly for making me smile every day.

Final thanks go to my family. Mum and Dad and Grandad, I can't thank you enough for everything you have given up to put me through university. Even Frankie, annoying as you are, you've always been there to call when I needed a chat. I hope I can make you all proud.

Abstract

The blood-brain barrier, while protective, presents a major obstacle for drug delivery to the central nervous system, thus ways to circumvent it for the treatment of neurological disorders are highly desired. Many pathogens and their toxins have evolved to hijack cell entry systems, initiating endocytosis following the binding of sugars on the plasma membrane. This project aims to repurpose these mechanisms to facilitate the delivery of therapeutic proteins to neurones.

Viruses with the ability to express sugar-binding proteins were assessed for their ability to target neurones for transduction following retrograde transport. This would allow for the tracing of neuronal circuits as well as potential delivery of therapeutic molecules to higher order neurones after peripheral administration. Canine adenovirus 2 and adeno-associated virus serotypes 2, 5, and 8 did not successfully transduce neurones in rats or mice; future work may pseudotype the viruses for re-targeting.

The sub-populations of neurones labelled by B subunits of cholera toxin (CTB) and the related heat-labile enterotoxin (LTB) following various routes of injection in mice were studied. In general, motor neurones, autonomic preganglionic neurones and primary afferents could be targeted following peripheral administration. A fusion protein of CTB and the calcium buffering protein parvalbumin was designed, expressed and tested both *in vitro* and *in vivo*; CTB successfully delivered its cargo to neurones. CTB was also engineered for alternative detection and novel conjugation methods; following administration *in vivo* all engineered CTB proteins could be detected.

This study provides a basis for the development of further CTB fusion proteins; the toxin represents a versatile delivery vehicle, both as an experimental tool and as a potential therapeutic in the treatment of neurodegenerative diseases.

Table of Contents

List of Figures

List of Tables

Abbreviations

AAV	Adeno-associated virus
Aβ	Amyloid-beta
AD	Alzheimer’s disease
ALS	Amyotrophic lateral sclerosis
AMAN	Acute motor axonal neuropathy
APP	Amyloid precursor protein
BBB	Blood-brain barrier
BoNTs	Botulinum neurotoxins
CAR	Coxsackievirus and adenovirus receptor
CAV-2	Canine adenovirus 2
CST	Corticospinal tract
CTB	Cholera toxin B subunit
CNS	Central nervous system
Cre	Cre recombinase
CSF	Cerebrospinal fluid
CuAAC	Copper-catalysed azide-alkyne cycloaddition
DL-TBOA	DL-threo-beta-Benzyloxyaspartate
DP	Differential power
DRG	Dorsal root ganglion
DVN	Dorsal vagal nucleus
EDAC	1-Ethyl-3-(3-dimethylaminopropyl)carbodiimide
EDTA	Ethylenediaminetetraacetic acid

EM	Electron microscopy
ER	Endoplasmic reticulum
GDNF	Glial-derived neurotrophic factor
GFP	Green fluorescent protein
GLP-1	Glucagon-like peptide-1
GluR2	Glutamate receptor 2
HRP	Horseradish peroxidase
HSPG	Heparin sulphate proteoglycan
IGF-1	Insulin-like growth factor-1
IM	Intramuscular
IML	Intermedial lateral column
IP	Intraperitoneal
LacZ	β-galactosidase
LTB	Heat-labile enterotoxin B subunit
MBP	Myelin basic protein
MMN	Multifocal motor neuropathy
NCX	Sodium calcium exchanger
NE	Nuclear envelope
NGF	Nerve growth factor
NMJ	Neuromuscular junction
NTS	Nucleus tractus solitarius
PBS	Phosphate buffered saline
PD	Parkinson’s disease
PEG	Polyethylene glycol
PEI	Polyethylenimine

PFA	Paraformaldehyde
PNS	Peripheral nervous system
PT	Pertussis toxin
PVDF	Polyvinylidene fluoride
ROS	Reactive oxygen species
QD	Quantum dot
SCI	Spinal cord injury
SERCA	Sarco/endoplasmic reticulum Ca^{2+}-ATPase
siRNA	Small interfering RNA
SNARE	Soluble N-ethylmaleimidesensitive factor attachment protein receptor proteins
SPAAC	Strain-promoted alkyne-azide cycloaddition
SOD1	Superoxide dismutase 1
SPN	Sympathetic preganglionic neurone
ST	Shiga toxin
TeNT	Tetanus toxin
TfR	Transferrin receptor
TMB	Tetramethyl benzidine
TTC	Tetanus toxin C fragment
VSV-G	Vesicular stomatitis virus G protein
VG	Viral genome
WGA	Wheat germ agglutinin
XII	Hypoglossal nucleus

Chapter 1
General Introduction

The treatment of neurological diseases is hindered by the blood-brain barrier (BBB); while acting to protect the central nervous system (CNS) from the entrance of foreign particles by allowing only restricted access of molecules, it also prevents the delivery of therapeutic drugs. One way to circumvent the BBB is by targeting peripheral neurones whose cell bodies are contained within the CNS. Entrance to these neurones at the terminals or along the axons means a drug may be internalised and retrogradely transported to the cell body. A carrier molecule is required to target the drug to the correct cells and to deliver it to the cell body after peripheral administration. Nature has already designed these carriers; bacterial toxins and viruses that target peripheral neurones can be re-purposed to deliver therapeutic cargo rather than their usual damaging payload.

1.1 Targeting neurones with bacterial toxins

Intracellular protein delivery to cells is hindered because entry is restricted; proteins cannot diffuse across the plasma membrane and so must use specific machinery to enter. Endocytosis is a common route for trafficking of proteins into cells; this may be mediated by clathrin-coated pits or caveolae, and in either route the proteins are trafficked into endosomes. Bacterial toxins have evolved to hijack cell entry mechanisms for delivery of toxic payloads in sufficient quantities to effectively modulate target molecules. Toxins may bind gangliosides to initiate cell entry, many of which are ubiquitously expressed including at neuronal plasma membranes. These natural cell entry mechanisms may be adapted to facilitate the delivery of therapeutic proteins for intracellular targeting in neurones.

1.1.1 Botulinum toxins

Botulinum neurotoxins (BoNTs) are produced by *Clostridium* bacteria and are the most potent lethal toxins known, causing muscle paralysis which, if leading to respiratory failure, results in death (Cherington, 1998). Their primary site of action is the neuromuscular junction where their protease activity blocks the release of acetylcholine (Dolly, 2003). There are seven BoNTs, named A to G according to the order of their discovery (Johnson, 1999), each possesses similar tertiary structures due to significant sequence divergence. The A, B and E serotypes cause human botulism (Arnon et al., 2001), with A and B exhibiting the longest duration of activity *in vivo* lasting from several weeks to months (Meunier et al., 2003). Commercially available BoNT/A (Botox™) and BoNT/B (Myobloc™) are used for cholinergic nerve and muscle dysfunction, as well as cosmetic treatments to reduce the appearance of wrinkles (Glogau, 2002; Bhidayasiri and Truong, 2005; Foster, 2005).

All BoNTs are synthesised as single polypeptide chains of 150 kDa, formed of a heavy chain (100 kDa) and a light chain (50 kDa) that are linked via a disulphide bond. The heavy chain contains the translocation domain and receptor binding domain, while the light chain is catalytic. The binding domain permits receptor-mediated endocytosis of the toxins by binding gangliosides GD1a and GT1b, along with SV2 in the case of BoNT/A and synaptotagmins for BoNT/B and BoNT/G (Schengrund et al., 1991; Nishiki et al., 1996; Yowler et al., 2002; Rummel et al., 2004; Dong et al., 2006). The interaction of BoNT/A and BoNT/B with synaptotagmin-I depends on the presence of gangliosides, while BoNT/G can interact directly with synaptotagmin-I and synaptotagmin-II in a ganglioside-independent fashion (Yowler et al., 2002; Rummel et al., 2004). Once contained within endosomes the light chain and translocation domain undergo conformational changes such that a channel is formed enabling the light chain to translocate into the cytosol. The mechanism of channel formation is not fully understood, it may be due to the acidic endocytic environment (Montecucco et al., 1989), or the translocation domain may enhance light chain stability and moderate its membrane interaction (Araye et al., 2016). When the partially unfolded light chain slips into the cytosol the disulphide bond between the two chains is reduced, the light chain protease is then released to exert its toxic effect (Simpson, 2004).

The toxic effects of BoNTs are mediated through three main targets, each a component of the soluble N-ethylmaleimidesensitive factor attachment protein receptor (SNARE) proteins. B, D, F and G target synaptobrevin on synaptic vesicles (Schiavo et al., 1994b; Schiavo et al., 2000) while A and E target the plasma membrane protein synaptosome-associated protein of 25 kDa (SNAP-25) (Blasi et al., 1993b; Schiavo et al., 1993), and C cleaves both SNAP-25 and syntaxin (Blasi et al., 1993a) (Figure 1.1). Cleavage of synaptobrevin results in vesicles that cannot undergo the normal cycle of endocytosis and exocytosis (Schiavo et al., 2000). Cleavage of syntaxin-SNAP-25 means vesicles are no longer able to dock at the plasma membrane (Oyler et al., 1989; Bennett et al., 1992). Ultimately, whichever SNARE protein is cleaved, the release of acetylcholine is inhibited producing the characteristic flaccid paralysis.

There is some evidence to suggest that BoNTs may be capable of transcytosis. Following direct injection of BoNT/E to the hippocampus SNAP-25 cleavage was restricted to the injected hemisphere. Whereas in animals treated with BoNT/A, cleaved SNAP-25 was detected on the contralateral side from 3 days after injection (Antonucci et al., 2008). Injections of BoNT/A into the optic tectum led to truncation of SNAP-25 in synaptic terminals within the retina; the authors suggest that the toxin retrogradely transported in retinal ganglion cells and then entered starburst amacrine

cells via transcytosis (Antonucci et al., 2008). When BoNT/A was injected into the eye of rats the toxin underwent anterograde transport and transcytosis from retinal ganglion cells to the tectum (Restani et al., 2011). *In vitro* analysis of cultured hippocampal cells in microfluidic chambers further highlights the ability of BoNT/A and BoNT/D to enter upstream neurones via transcytosis (Bomba-Warczak et al., 2016). Cultured neurones were labelled with reporter dyes to distinguish between projecting and non-projecting cells in the chamber. When BoNTs were added to the axon side of the chamber substrate cleavage was measured in second-order neurones suggesting the active toxin has exited first-order neurones and entered upstream.

The action of BoNTs at the neuromuscular junction has made them effective therapeutic molecules for treatment of neuromuscular conditions and disorders of the autonomic nervous system (Oyler et al., 1989). BoNT/A and BoNT/B are licensed for the treatment of dystonia, a disorder of variable muscle tone resulting in muscular spasms (Tarsy and Simon, 2006). Intradermal injection of BoNT/A is a highly effective treatment of autonomically mediated focal hyperhidrosis, characteristic excessive sweating is significantly reduced with results from a single treatment lasting around 6 months (Heckmann et al., 2001; Weinberg et al., 2014). As well targeting motor neurone and autonomic terminals BoNTs can also bind to nociceptive primary afferents making them a valuable tool for treatment of pain (Sim, 2011). BoNT/A was combined with the binding domain of tetanus toxin to increase the range of targeted neuronal populations, the chimera was found to inhibit mechanical sensitivity in a rat model of inflammatory pain and did not cause either flaccid or spastic paralysis following intrathecal administration (Ferrari et al., 2013). Another BoNT/A chimera known as BiTox was created by ‘stapling’ together the recombinant light chain/translocation domain and receptor-binding domain of BoNT/A (Mangione et al., 2016). BiTox injections attenuated A-nociceptive-mediated secondary mechanical hyperalgesia as well as neuropathic pain states in rats without causing motor deficits or impairing acute thermal and mechanical nociceptive thresholds. For both BoNT conjugates it is thought that the elongation of the toxin prevents entrance to the neuromuscular junction, and hence no motor effects are seen.

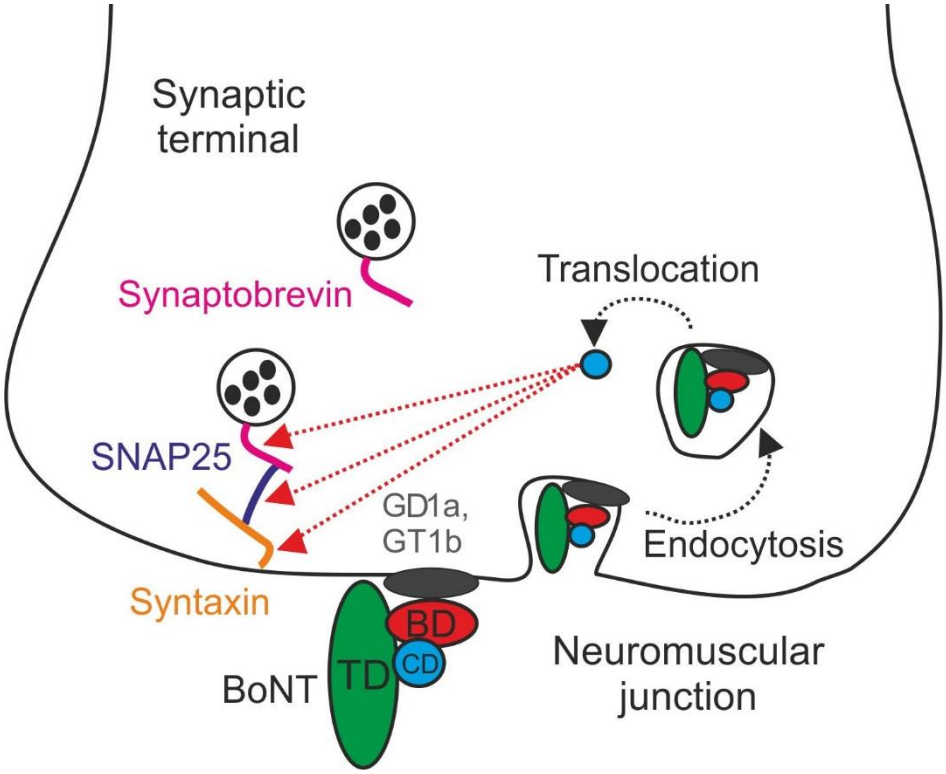

Figure 1.1 The mechanism of action of botulinum toxins

BoNTs are formed of the binding domain (BD, red), the catalytic domain (CD, blue) and the translocation domain (TD, green). After binding to GD1a and/or GT1b, BoNTs are endocytosed into the pre-synaptic terminal. The TD forms a channel in the endosome allowing the CD to escape into the cytosol. Depending on the serotype, CD protease activity occurs at synaptobrevin, syntaxin or SNAP25, leading to inhibition of neurotransmitter release as vesicles can no longer dock at the plasma membrane.

With BoNTs already licensed for medical use along with their strong neurotropism, the toxins are attractive candidates for delivery of cargo to neurones from the periphery. A 10 kDa aminodextran was coupled to the heavy chain of BoNT/A, the cargo was successfully delivered to cultured cortical cells and generally remained within endosomes (Goodnough et al., 2002). BoNT/D has been used to deliver enzymatically active cargo to the cytosol in neural cells (Bade et al., 2004). Bade et al. used a proteolytically inactive light chain to prevent endogenous BoNT activity, using the toxin instead as a transport system for delivery of cargo including luciferase, GFP and dihydrofolate reductase. There is further scope for all seven members of botulinum neurotoxin family to be manipulated as delivery vehicles or as neuronal silencers both as therapeutics and experimental tools (Davletov et al., 2005).

1.1.2 Tetanus toxin

Tetanus toxin (TeNT) produced by *Clostridium tetani* is the extremely potent neurotoxin that causes tetanus. Like BoNTs the target for cell entry is the neuromuscular junction, once internalised the toxin is transported retrogradely to the cell body in the spinal cord where it induces spastic paralysis by blockade of neurotransmitter release from spinal inhibitory neurones (Brooks et al., 1957).

The structure of TeNT is similar to that of BoNTs with a 100 kDa heavy chain and a 50 kDa light chain joined by a single disulphide bond. The light chain is the N terminal part of the toxin and folds around the active site zinc atom (Schiavo et al., 1994a) that has been suggested to participate in the hydrolysis of the peptide bond (Rossetto et al., 2001). The heavy chain is formed of the N-terminal translocation domain (HN), similar to that of BoNT. The C-terminal domain of the heavy chain is formed of the 25 kDa HC-N region whose function remains unknown, and the 25 kDa HC-C region that mediates the binding of the toxin to motor neurones at the neuromuscular junction via two polysialoganglioside binding sites (Fotinou et al., 2001; Rummel et al., 2003; Chen et al., 2009). Following retroaxonal transport TeNT does not accumulate within the soma, but rather continues to the dendrites (Schwab et al., 1979). The toxin is able then to cross the synapse, being discharged into the intersynaptic space to bind and enter the pre-synaptic membrane of synaptically connected cells. After endocytosis, conformational changes in HN and the light chain allow for translocation of the light chain into the cytosol where the disulphide bond is reduced (Pirazzini et al., 2011). The light chain then targets synaptobrevin for cleavage and so prevents fusion of synaptic vesicles with the plasma membrane (Schiavo et al., 1992) (Figure 1.2). Unlike most BoNTs, TeNT must enter two different populations of neurones: peripheral motor neurones and then synapsing spinal interneurones. The binding of TeNT at central and peripheral sites is different; L-HN injected intramuscularly in cats caused no motor deficit, but when injected directly into the spinal cord spastic paralysis was produced (Takano et al., 1989). It has been suggested that the protein receptor responsible for inclusion of the toxin in retrogradely transported endosomes in peripheral motor neurones is different to the protein receptor utilised at the interneurone synaptic membrane where TeNT then enters via synaptic vesicle endocytosis (Pellizzari et al., 1999). Nidogens act as the protein receptor on the motor neurone terminal causing TeNT to cluster and bind, initiating endocytosis (Bercsenyi et al., 2014); it is possible that the protein receptor at the interneurone surface is different.

The targeting of TeNT to peripheral motor neurones makes it a good candidate for protein delivery in diseases such as ALS, indeed a number of fusion proteins have

been made. TeNT fusion proteins utilise the binding domain, tetanus toxin fragment C (TTC), to gain entry to neurones and by replacing the toxic light chain therapeutic cargo may be delivered. Intramuscular injection of fusion proteins containing TTC and the enzyme superoxide dismutase (SOD1) highlighted the ability of TTC to transport another protein retrogradely, with both proteins detected within the CNS (Figueiredo et al., 1997). Glial-derived neurotrophic factor (GDNF) was introduced to an ALS mouse model as a TTC recombinant fusion protein (GDNF-TTC); mice survived on average 9 days longer and quality of life for symptomatic animals was improved (Ciriza et al., 2008). Insulin-like growth factor-I (IGF-I) has also been delivered with TTC in ALS mice via intramuscular and intrathecal injections (Chian et al., 2009). While the delivered protein was detected at high levels within the CNS, there was no significant effect on disease progression or survival of the mice. Functional effects of TTC fusion proteins have been measured *in vitro*, delivery of the anti-apoptotic protein Bcl-xL increased neurone survival following glutamate-induced apoptosis (Carlton et al., 2008). While the authors suggest that the protein remained biologically active, Bcl-xL functions in the mitochondria and there is no suggestion of how the complex was targeted to the functional cellular compartment. It is possible that TTC itself, rather than the delivered cargo, produced the anti-apoptotic effect, as TTC has been found to be neuroprotective. TTC rescued cultured cerebellar granule neurones from apoptosis, with both phosphatidylinositol 3-kinase (PI3K) and extracellular-signal-regulated kinase (ERK) dependent pathways implicated in neuroprotection (Chaib-Oukadour et al., 2004). It is therefore possible that TTC fusion proteins, if able to deliver a functional cargo, could also protect neurones through action of TTC alone.

Immunisation against tetanus toxoid does not block uptake of TTC (Fishman et al., 2006) and so TTC fusion proteins could be delivered by repeated administration. The authors suggest the uptake of the protein by nerve terminals following intramuscular injection is rapid enough to avoid clearance by the immune system. The neurotropism and ability to cross synapses make TTC a good protein for targeting and delivering therapeutic molecules in motor neurone diseases. The trans-synaptic property means that higher order neurones may too be targeted from the periphery. TTC may be used as a carrier of biological molecules to neuronal cytosol from peripheral sites of injection.

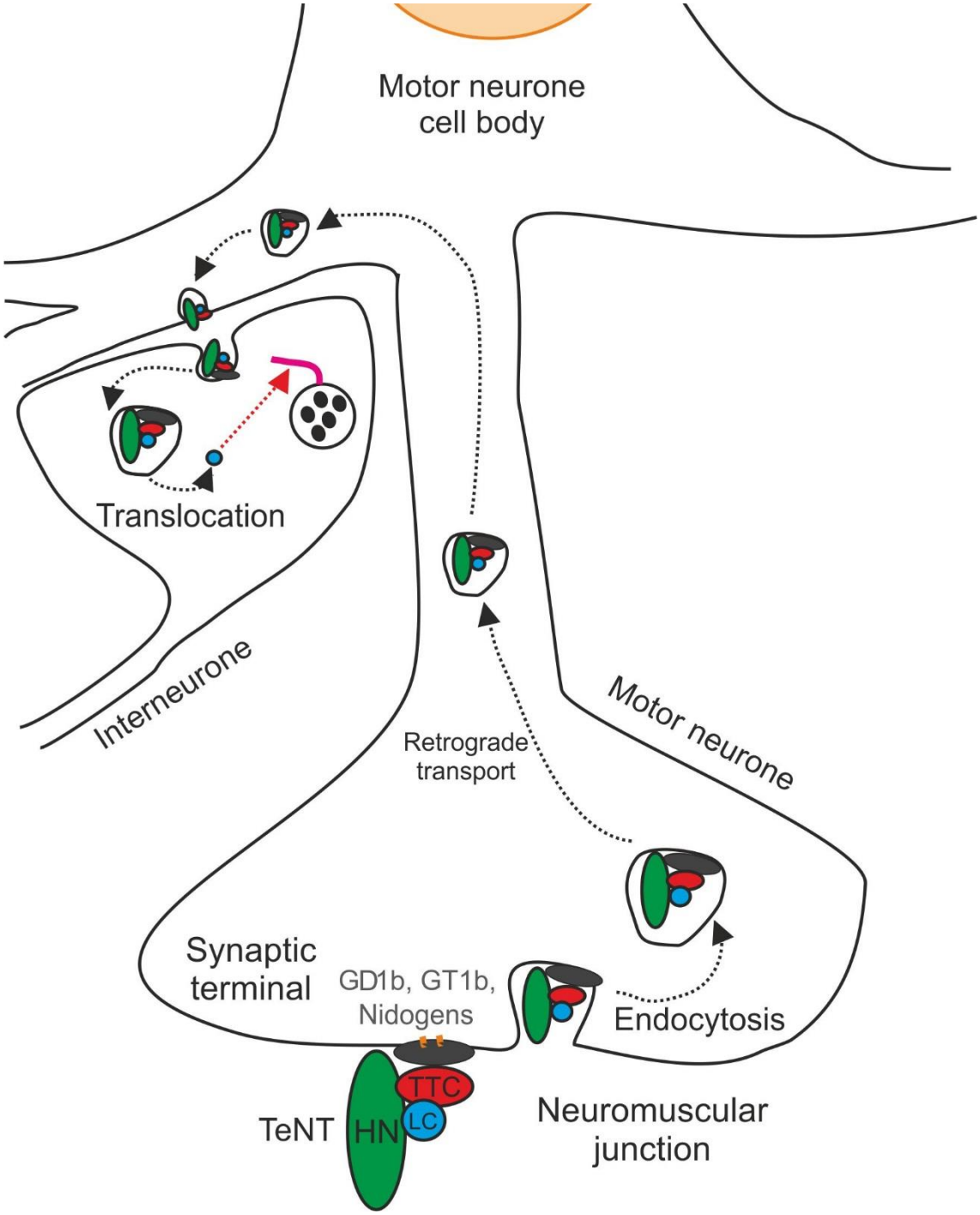

Figure 1.2 The mechanism of action of tetanus toxin

TeNT is formed of the catalytic light chain (LC, blue), the translocation domain (HN, green) and the binding domain (TTC). TTC binds to GD1b and GT1b along with nidogens on the motor neurone at the neuromuscular junction, allowing endocytosis of the toxin. It is then retrogradely transported to the cell body, where it exits at the dendrites to enter interneurones. The LC is then translocated out of the endosome into the cytosol where it targets synaptobrevin (pink) for cleavage; thus preventing neurotransmitter release as vesicles are unable to dock at the plasma membrane.

1.1.3 AB_5 toxins

AB_5 toxins are a group of virulence factors produced by several major bacterial pathogens; collectively they kill over a million people each year (Vanden Broeck et al., 2007). There are four families based on sequence homology and A-subunit catalytic activity. These comprise pertussis toxin (PT) produced by *Bordetella pertussis*, shiga toxin (ST) produced by *Shigella dysenteriae*, cholera toxin (CT) produced by *Vibrio cholerae* and the closely related heat-labile enterotoxins (LT) produced by enterotoxigenic *Escherichia coli*, finally subtilase cytotoxin (SubAB) produced by Shiga toxigenic *E. coli* (structures detailed in Figure 1.3). AB_5 toxins are named such due to their structure; the B-subunit forms a pentameric ring responsible for binding to the host cell surface, whereas the A subunit is comprised of an A2 linker peptide and the catalytically active A1-subunit that disrupts the host's cellular machinery. Despite similar structural architecture shared between AB_5 family members, they differ in their host cell surface receptor specificity (Table 1.1), intracellular trafficking and catalytic activity (Beddoe et al., 2010). While nervous tissue is not the primary target for any AB_5 toxins, the cell entry ligands for CT, LT-I and LT-IIs are expressed on neurones and so these toxins will be focused on.

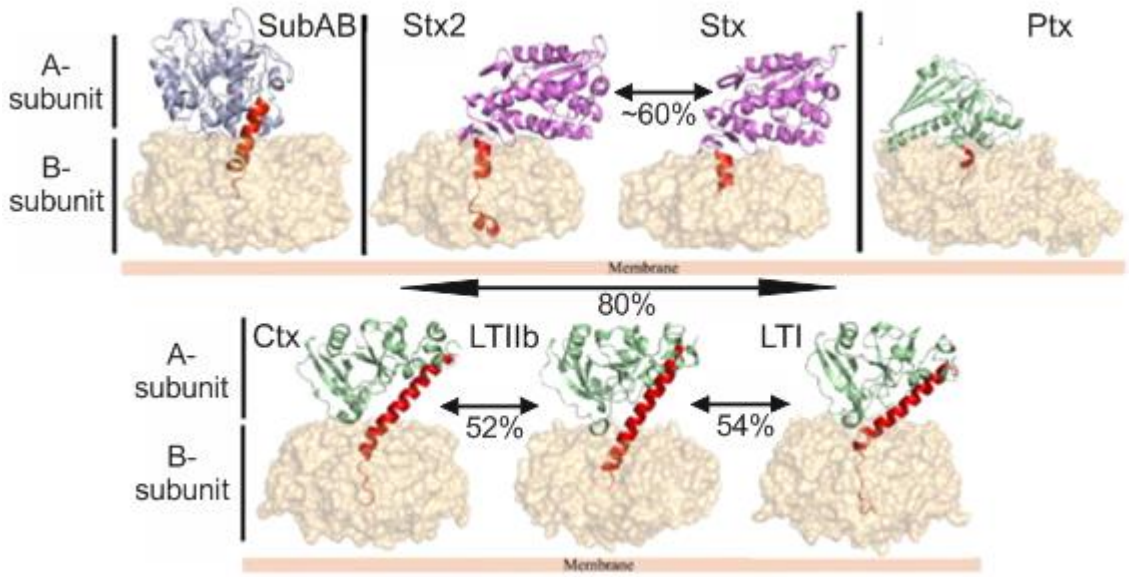

Figure 1.3 Crystal structures of AB_5 toxins

B-pentamers are shown at the membrane face, A2 linkers are red, and A1 catalytic subunits coloured according to respective catalytic activity (Light blue for subtilase activity, purple for RNA N-glycosidase activity and light green for ADP-ribosylase activity). Sequence homology between A subunits in families is indicated. Reprinted from Beddoe et al. (2010), with permission from Elsevier.

Toxin	Cell entry ligand	Reference
CT	GM1	(Merritt et al., 1994b)
LT	GM1	(Merritt et al., 1994b)
LT(IIa)	GD1b	(Fukuta et al., 1988)
LTB(IIb)	GD1a	(Fukuta et al., 1988)
PT	Unknown	(Wong and Rosoff, 1996)
ST	Gb3	(Waddell et al., 1988)
SubAB	Neu5Gc	(Byres et al., 2008)

Table 1.1 Cell entry ligands for AB_5 toxins

1.1.4 Heat-labile enterotoxins (LTs)

The gut is the primary target of LTs where infection with enterotoxigenic *Escherichia coli* and subsequent toxin release results in watery diarrhoea which, if untreated with rehydration therapy, can lead to death. LTs have been serologically separated into two groups, termed type I and type II, the latter being further divided into LT-IIa and LT-IIb (van den Akker et al., 1996). LT-IIa and LT-IIb share 68% sequence homology in the B pentamer (Fan et al., 2000), however LT-IIa binds GD1b, and LT-IIb shows affinity for GD1a (Fukuta et al., 1988). LT-I shares only 11% homology with the B pentamer of LT-IIb, and recognises the oligosaccharide moiety of GM1 (Merritt et al., 1994b). LT-I also binds with lower affinities to asialo-GM1 which lacks a sialic acid, GD1b, and gangliosides containing terminal N-acetyllactosamine disaccharide (Merritt et al., 1994a; MacKenzie et al., 1997). The homology between catalytic A subunits ranges from 56-71% but all function as ADP-ribosylating enzymes (Merritt and Hol, 1995).

After B-subunit binding of their cognate receptor, endocytosis is triggered, followed by retrograde transport via the Golgi to the ER. The A1-subunit is then unfolded via protein disulphide isomerase (Tsai et al., 2001) and retro-translocated into the cytosol via the Sec61 channel (Matlack et al., 1998) or the derlin-1-Hrd1 complex (Bernardi et al., 2008). It then undergoes refolding such that it gains catalytic activity, ADP-ribosylating an arginine residue in the α-subunit of the G_s protein (Moss and Richardson, 1978). This causes inhibition of GTPase activity of $G_{s\alpha}$ and renders adenylate cyclase constitutively active. This results in increased levels of cAMP in the host cell which opens several ion channels, including the cystic fibrosis transmembrane receptor; in the intestine this leads to the loss of fluid and electrolytes into the lumen (Sears and Kaper, 1996).

The gangliosides bound by LTs are expressed on neuronal membranes (Tettamanti et al., 1973). GM1 is enriched in the myelin of motor fibres, but reportedly in only trace amounts in sensory myelin as measured by thin layer chromatography of myelin fractions of ventral and dorsal roots, respectively (Ogawa-Goto et al., 1992). The ganglioside has also been reported to be enriched on the axolemmal surface of myelinated fibres and Schwann cells of the peripheral nervous system as measured by binding of CT-HRP (Sheikh et al., 1999). The B pentamer of LTs is non-toxic and is able to enter cells without the toxic portion, by replacing the toxic A subunit LTs could be repurposed as vehicles for delivering other proteins to neurones. The structurally similar CTB toxin subunit has been used widely as a neuronal tracer and delivery vehicle, but LTBs are widely ignored other than when used as adjuvants (Ma, 2016). There is one study utilising LT-IIa as a platform to deliver heterologous proteins into neurones (Chen et al., 2015). First the toxic A portion was replaced with β-lactamase, this was found to be catalytically active when delivered to Neuro-2a cells and cultured cortical neurones. The cargo was also found to be released from the B pentamer as the Pearson coefficient measurement of colocalisation of LTB and β-lactamase fell from 0.64 to 0.43. Next a single-chain, anti-BoNT/A camelid antibody was delivered with LT-IIa. The antibody inhibited SNAP25 cleavage when cultured neurones were exposed to BoNT/A. Chen et al. produced and purified both fusion proteins using *E.coli*, in theory any number of fusion proteins could be created to deliver any protein of interest to neurones.

Fusion proteins of LT-I and LT-II could be used to target motor neurones from the periphery to deliver therapeutic molecules in motor neurone diseases. They may also be tested centrally for the treatment of neurodegenerative disorders such as Alzheimer’s disease, Parkinson’s disease and Huntington’s disease where delivered proteins could reduce protein aggregation.

1.2 Cholera toxin (CT)

Cholera toxin is the causative agent of cholera, where-upon infection of the gut with *Vibrio cholerae* the virulence factor induces severe watery diarrhoea, leading to a loss of up to 30 litres of fluid a day (Sanchez and Holmgren, 2005). Cholera is rife within the developing world where sanitary provisions are poor and along with LT causes over a billion cases of diarrhoea annually. However, CT is not just a toxic agent - it also has a number of applications as an experimental tool and as a therapeutic.

1.2.1 Structure and ganglioside binding

CT is an AB_5 toxin of approximately 85 kDa, it shares 83% sequence homology with LT-I (Dallas and Falkow, 1980); it is formed of the catalytically active A subunit (28 kDa) and a homopentamer of B subunits (CTB, 58 kDa) which are non-covalently linked (Fan et al., 2000). The α-helical rod (A2) tethers the globular A1 to the pentamer with its C-terminal passing through the opening created by the doughnut arrangement of B subunits (Figure 1.4A). The B subunit monomers consist of a large α-helix that sits central within the pentameric structure, and two adjoining anti-parallel β-sheets (Figure 1.4B). The two β-sheets from each adjoining monomer form a virtually unbroken β-sheet core in a ring around the pentamer. Each B-subunit contributes residues to a carbohydrate binding site, located on the opposite face to the A subunit. Each monomer is able to interact with the terminal galactose of ganglioside GM1 through hydrogen bonding (Merritt et al., 1994b). The five binding sites have one of the highest known affinities for protein-carbohydrate interactions (K_d = 43 nM) (Turnbull et al., 2004).

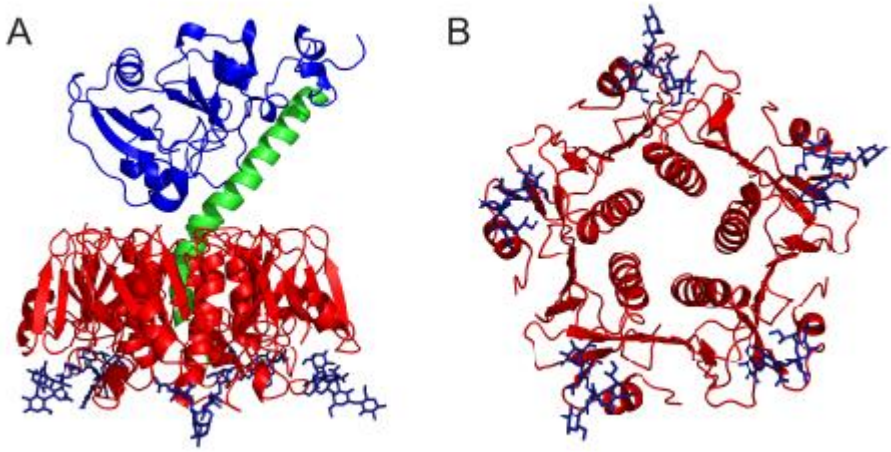

Figure 1.4 The structure of cholera toxin (composite of PDB 1S5E and 3CHB)

A) The AB_5 holotoxin structure with A-subunit formed of the catalytic A1 (blue) and linker A2 (green) and B-subunits in red bound to GM1 gangliosides in blue. B) A top down view of the B pentamer revealing its pentagonal shape.

1.2.2 Expression and secretion

The CT gene cassette, ctxAB, is responsible for horizontal gene transfer and is found on the virulence plasmid that is naturally occurring in *Vibrio cholerae* as well as its CTXϕ phage (De Haan and Hirst, 2004). The genes for the A-subunit and B-subunit

overlap in a polycistronic gene with the Shine Dalgarno sequence (a ribosomal binding site) for CTB located within the 3' region of the CTA gene (Pickett et al., 1989). The two toxin units are made separately and the holotoxin assembled in the periplasm. CTB monomers are targeted to the periplasm via a propeptide leader sequence; here this sequence is cleaved and a disulphide bond formed between cysteine's 9 and 86. CTB monomers then associate around the C-terminal of CTA2 to form the holotoxin (Tinker et al., 2005). Both the AB_5 toxin and the CTB pentamer can be secreted from the periplasm, but not the A subunit alone (Finkelstein and LoSpalluto, 1969; Hirst et al., 1984). Toxin secretion involves the type 2 secretion system (T2SS), a piston driven mechanism illustrated in Figure 1.5 (Reichow et al., 2010). The macromolecular complex spans the inner and outer membrane of the periplasm; a dodecameric hollow shaft loads the holotoxin and then a pseudopilus ejects it into the extracellular space.

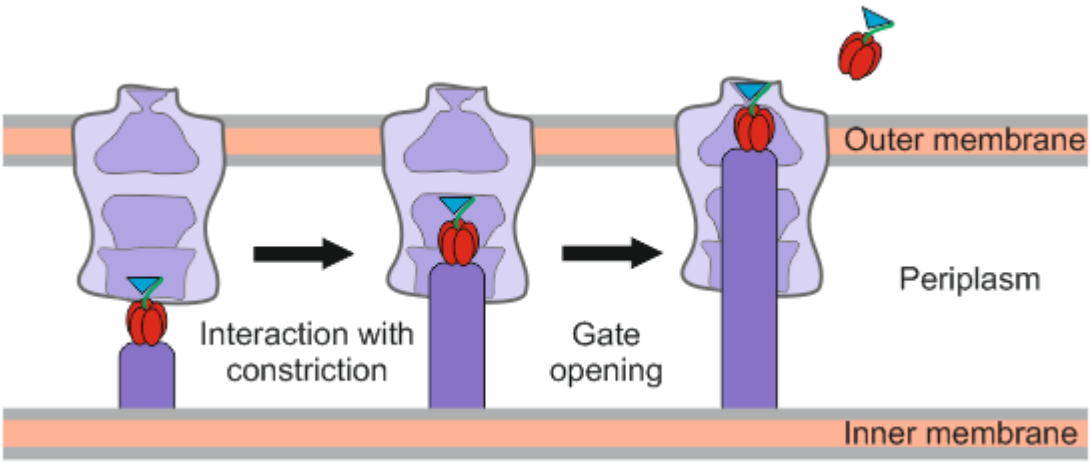

Figure 1.5 Schematic of the structure and proposed mechanism of the Type 2 secretion system (T2SS)

Cholera toxin either binds to the pseudopilus tip (dark purple) while the secretin (lilac) is closed, or binds directly to secretin. The pseudopilus tip extension pushes the cholera toxin free from the complex and the toxin then dissociates from the pseudopilus tip. Adapted from Reichow et al. (2010).

1.2.3 Mechanism of toxicity

Once secreted the CT binds GM1 (Holmgren et al., 1973), initiating receptor-mediated endocytosis and allowing the toxin entrance to host cells. Endocytosis may be caveolae-dependent (Orlandi and Fishman, 1998), clathrin-dependent (Torgersen et al., 2001), or noncaveolae/nonclathrin-mediated (Kirkham et al., 2005). Once internalised, endosomes are rapidly sorted to the trans-Golgi network where they then

enter the retrograde trafficking pathway to the ER (Figure 1.6). While it was initially thought that the Golgi apparatus was essential for this retrograde transportation (Majoul et al., 1996), later studies showed it was not mandatory. Treatment of BSC1 cells with Exo2, a chemical that rapidly blocks anterograde transport from the ER to the Golgi apparatus, did not affect the ability of CTB to reach the ER (Feng et al., 2004). The C-terminus of CTA2 contains the ER targeting motif KDEL (RDEL in LT-I) (Lencer et al., 1995); earlier studies indicated that this was vital for localisation of the toxins to the ER but toxins with mutations in the sequence are still able to enter (Fujinaga et al., 2003). Once in the ER the disulphide bond between the A1 and A2 subunits is cleaved by protein disulphide isomerase; A1 then unfolds and can be translocated through Sec61p into the cytosol (Schmitz et al., 2000). A1 catalyses ADP-ribosylation of $G_{s\alpha}$ leaving adenylate cyclase permanently activated in its GTP-bound state, thus enhancing its activity. This leads to elevated intracellular cAMP levels which cause protein kinase A to phosphorylate and open the chloride channel CFTR (Kunzelmann and Mall, 2002). The resulting chloride efflux produces the osmotic movement of water into the gut lumen and the characteristic watery diarrhoea seen in cholera patients.

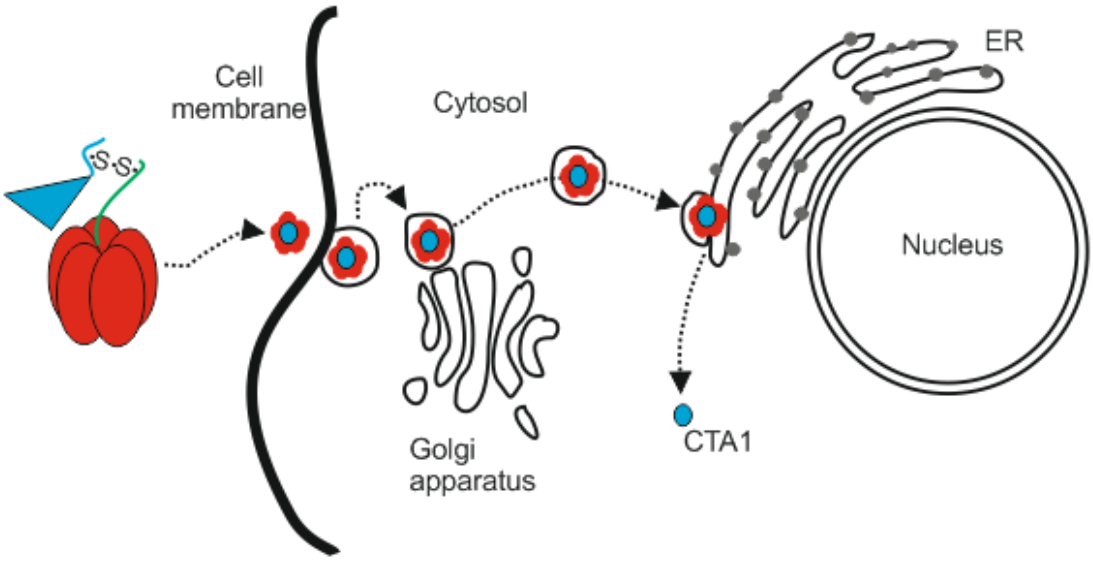

Figure 1.6 The retrograde trafficking of cholera toxin

The CTB subunit binds GM1 ganglioside on the plasma membrane, triggering endocytosis of the holotoxin. The toxin is then targeted via the Golgi apparatus to the ER; here the disulphide bond between CTA1 and CTA2 is cleaved, releasing CTA1 into the cytosol for it to have its catalytic effect.

The B-pentamer is not toxic in the absence of the A-subunit, and it continues to trigger endocytosis. CTB is a highly stable protein and has been produced on a large-scale previously (Lebens et al., 1993). For these reasons CTB is a good candidate for targeting therapeutic molecules to GM1-expressing cells.

1.2.4 CTB as an adjuvant

CT has adjuvant activity, that is, it enhances the immune response to an antigen when co-delivered (Northrup and Fauci, 1972). The strong mucosal responses are elicited through a combination of increasing the permeability of the mucosal epithelium, upregulating and enhancing co-stimulatory molecule presentation on antigen presenting cells, promoting isotype differentiation in B cells, and altering T cell proliferation along with cytokine production (Sanchez and Holmgren, 2008). Both the A and B subunits contribute to adjuvant activity but this may prove toxic. CTB alone when mixed with an antigen fails to induce adjuvant activity, but direct conjugates to an antigen have been successful and safer than AB_5-adjuvants.

CTB adjuvants are usually delivered intranasally or orally, and are now exploited to vaccinate against cholera due to the strong oral immunogenicity of CTB (Sinclair et al., 2011). CTB has been used in the promotion of mucosal tolerance to auto-antigens. CTB induces the formation of T regulatory cells and the production of IgA (Holmgren et al., 2005), and as such can reduce the priming of dendritic cells for Th2 response to inhaled antigens (Smits et al., 2009). Intranasal administration of CTB in allergic and naïve mice suppressed multiple features of asthma including allergen-triggered eosinophilia, Th2 cytokine synthesis and bronchial hyper-reactivity. In this study the adjuvant activity of CTB in auto-immune asthma was found to be both curative and preventative.

CTB has also been found to function as an immunomodulator capable of altering the properties of innate immune cells (Burkart et al., 2002). CTB induces MAPK phosphatase-1 expression and inhibits Janus kinase and p38 activation, this leads to a substantial attenuation of production of the common cytokines TNFα and IL-6 produced by lipopolysaccharide-stimulated macrophages (Chen et al., 2002). The reduction in cytokine production vastly reduces inflammation, and thus further immune responses are diminished.

Two subjects in clinical trials using intranasal LT-I adjuvants against human immunodeficiency virus and tuberculosis developed transient facial nerve paralysis (Bell ’s palsy) (Lewis et al., 2009) and this dampened enthusiasm for CT and LT-I based adjuvant therapies. It is thought that the ability of the toxin to bind and enter

neurones may have caused damage to the facial nerve, or an inflammatory response after intranasal administration could have affected the facial nerve. Investigations are continued in the toxin adjuvants as delivered via topical or mucosal routes (Bharati and Ganguly, 2011).

1.2.5 CTB as a neuronal tracer

GM1 is one of the four main brain gangliosides (GM1, GD1a, GD1b and GT1b) constituting 97% of all gangliosides in the normal human brain (Tettamanti et al., 1973), as such it was thought that CTB may be used to target neurones allowing for tracing (Stoeckel et al., 1977). CTB was found to trace neurones successfully in both retrograde (Luppi et al., 1987; Luppi et al., 1990) and anterograde (Lindh et al., 1989; Hirakawa et al., 1993) directions, with the toxin distributed throughout the cell body, neurites and terminals. When injected into a restricted site CTB enters any neurones that originate, terminate or pass through the injection site; the toxin is then transported along the length of the neurone. The neuronal populations labelled with CTB are varied, and the toxin may be administered peripherally or centrally. Spinal motor neurones can be labelled after intramuscular injection (Gramsbergen et al., 2000) and the distribution of corticospinal tract motor neurones has been monitored during development (Oudega et al., 1994). Injection of CTB into cervical region C1-3 allows for anterograde tracing of mossy fibre terminals in the cerebellum from their cell bodies in the spinocerebellar tract (Matsushita et al., 1991). Anterograde and retrograde transport of CTB was employed to assess somatosensory relay structures in the brain (Ericson and Blomqvist, 1988).

Distributions of CTB in the CNS following systemic administration have been studied, delivered either intraperitoneally or intravenously (Alisky et al., 2002; Havton and Broman, 2005). Motor neurones, preganglionic autonomic neurones and terminal projections of select primary afferents were labelled in the study by Havton and Broman. Alisky et al. describe labelling of many sensory afferents in the spinal cord in addition; the extra labelling is likely due to the 100-fold higher dose they used. Lower doses of CTB delivered systemically target myelinated neurones with axons in the periphery.

CTB can be used as a tracer for study at electron microscopy (EM) level. After systemic injection of CTB conjugated to horseradish peroxidase (HRP) rats were fixed with 1% paraformaldehyde with 2.5% glutaraldehyde, and CTB-HRP detected via tetramethyl benzidine (TMB) to be examined by both light and electron microscopy (Alisky et al., 2002). Motor neurones in the ventral horn contained scattered large crystalline reaction product granules in the cytoplasm, and no labelling of neuronal

terminals opposing the labelled neurones. Sympathetic preganglionic neurones (SPNs) in the intermediolateral nucleus (IML) contained reaction product in the cytoplasm, as well as in small clear vesicles and some dense core vesicles. CTB conjugated to colloidal gold particles (CTB-gold) is another tracer used for detection via EM (Llewellyn-Smith et al., 1990). CTB-gold was detected in neurones of the CNS after 12 hours and up to 42 days, following direct injection into brain and spinal cord parenchyma, and superior cervical ganglion. The tracer appeared as black punctate deposits in perikarya and proximal dendrites after silver intensification. Electron microscopy revealed CTB-gold deposits primarily associated with lysosomes.

CTB is a valuable tool for evaluating the connectivity and neurochemistry of pathways in the CNS, with uses as both a central and peripheral tracer, capable of travelling both retrograde and anterograde and persisting for weeks within neurones.

1.2.6 CTB fusion proteins

As a proven neuronal tracer capable of entering cells via endocytosis, it was logical to assess whether CTB could be used as a delivery agent of other proteins. Most CTB fusion proteins function as adjuvants, but other proteins have been delivered with the toxin (Table 1.2). One of the first fusion proteins made was with the plant toxin saporin, a ribosomal inactivating protein (Llewellyn-Smith et al., 1999). Disabling the cell's protein synthesis machinery initiates apoptosis, and by using CTB conjugates the toxin can be targeted to neuronal subsets. Saporin was chemically conjugated to CTB with N-succinimidyl 3-(2-pyridyldithio) propionate (SPDP) to form disulphide bridges between the two proteins (Picklo et al., 1994). Following injection of CTB-saporin into the superior cervical ganglion 84% of the SPNs supplying the ganglion had died after two weeks (Llewellyn-Smith et al., 1999). The toxin conjugate has also been used to measure physiological effects of targeted ablation of cardiac sympathetic neurones after injection to the stellate ganglion (Lujan et al., 2009). CTB-saporin has been used to develop a model of the impact of respiratory motor neurone death such as that seen in ALS, where the impact of compensatory responses may be measured without the complications attendant to ALS mouse models (Nichols et al., 2015). Intrapleural injection of the toxin conjugate was capable of killing motor neurones with access to the pleural space without damaging cells in other brainstem and spinal cord regions. The motor neurone survival was approximate to that in end-stage ALS rats allowing for assessment of mechanisms of preservation of breathing capacity despite the significant cell death. These studies provide evidence that CTB can deliver an active enzyme into specific subsets of neurones to alter their cellular activity.

CTB fusion proteins have been produced in various ways for delivery as adjuvants in a number of diseases, providing edible, safe and low-cost vaccines. Silkworm pupae were engineered to produce a fusion protein of CTB and amyloid-β peptide 42 (Aβ42), the toxic element of senile plaques formed in Alzheimer's disease (Li et al., 2014). The pupae were lyophilised and the powder administered orally to a mouse model of the neurodegenerative disease. This induced the production of anti-Aβ42 antibodies that reduced plaque formation, leading to improved memory and cognition as assessed by the water maze task. Oral vaccinations have also been produced in *E.coli* for the treatment of diabetes by delivering the epitope of the auto-antigen glutamic decarboxylase 65 (GAD65) (Gong et al., 2009). Non-obese diabetic mice showed prominent reduction in pancreatic islet inflammation, suggesting they had developed immunological tolerance against autoimmune diabetes. Another oral vaccination delivering proinsulin to protect against development of diabetes was expressed as a CTB fusion protein in lettuce and tobacco chloroplasts (Ruhlman et al., 2007). Delivery by gavage of the reconstituted lyophilised leaf material prevented pancreatic insulitis and protected insulin-producing β-cells from apoptosis in non-obese diabetic mice.

The ability of CTB to deliver a protein cargo to cells was tested with CTB-GFP, the fusion protein was expressed via the tobacco chloroplast genome and contained a furin cleavage site (Limaye et al., 2006). After oral administration of lyopholised leaf material in mice, GFP was detected in the intestinal mucosa, liver and spleen, whereas CTB remained in intestinal cells as detected by immunohistochemistry. Diabetic patients have to administer insulin injections daily and alternative methods are highly desired; CTB was tested as a delivery vehicle for glucagon-like peptide (GLP-1), a protein capable of increasing insulin secretion. CTB-GLP-1 was produced in tobacco chloroplasts, facilitating bioencapsulation of the fusion protein within plant cells for oral administration and transmucosal delivery in the gut (Kwon et al., 2013). The fusion protein reduced blood glucose levels to a similar level as intraperitoneal injection of GLP-1 without causing hypoglycaemia in mice. The study provides promising evidence for use of the bacterial toxin as a delivery vehicle in disease; CTB-GLP-1 could eliminate the need for injection in diabetic patients and increase patient compliance.

Conjugated to-	Function and outcome	Reference
Amyloid-β peptide (Aβ42)*	CTB-Aβ42 was produced in silkworm pupae that were then lyophilised, the powder was administered orally to mice to immunise them against the plaque protein. The Alzheimer's disease mice had reduced plaque deposition and improved memory and cognition.	(Li et al., 2014)
Exendin-4 (GLP-1 analogue)	EX4 was expressed as CTB-fusion protein in tobacco chloroplasts to facilitate bioencapsulation within plant cells and transmucosal delivery in the gut via GM1 receptors present in the intestinal epithelium. This stimulated insulin secretion similar to the IP injection of commercial EX4 but did not cause hypoglycaemia in mice.	(Kwon et al., 2013)
GAD65*	Oral administration of bacterial CTB-GAD((531-545)3) fusion protein showed the prominent reduction in pancreatic islet inflammation in non-obese diabetic mice.	(Gong et al., 2009)
GFP	Oral administration of CTB-GFP produced in leaf material resulted in GFP labelling of the intestinal mucosa, liver and spleen, while CTB remained in the intestinal cells	(Limaye et al., 2006)
ISS-ODNs (DNA immunostimulatory sequence oligdeoxynucleotides)*	In a mouse model of allergic rhinitis, a single intranasal delivery of low-dose ISS-ODN/CTB conjugate effectively protects previously sensitized mice from allergic hypersensitivity responses	(Won et al., 2009)
Myelin basic protein (MBP)	Oral administration of CTB-MBP lead to reduced B-amyloid plaques in the hippocampus of a mouse model of AD	(Kohli et al., 2014)
Proinsulin*	Expression of cholera toxin B-proinsulin fusion protein in lettuce and tobacco chloroplasts-oral administration protects against development of insulitis in non-obese diabetic mice.	(Ruhlman et al., 2007)
Saporin	Injection of CTB-saporin into specific ganglia ablates neuronal populations	(Llewellyn-Smith et al., 1999; Lujan et al., 2009; Lujan et al., 2010; Nichols et al., 2015)

Table 1.2 List of CTB fusion proteins made along with the proposed function and outcome

Fusions with * indicate an adjuvant

Oral administration of myelin basic protein (MBP) fused to CTB with a furin linker region was assessed for therapeutic effect in a mouse model of Alzheimer's disease (Kohli et al., 2014). MBP is a major structural protein of the CNS contributing to the stability and maintenance of the myelin sheath (Boggs, 2006). In the early stages of Alzheimer's disease demyelination is measured in association with Aβ plaques in white matter. During *in vitro* studies MBP was found to inhibit Aβ fibril formation and degrade Aβ plaques. Delivery of MBP to the CNS, past the BBB would therefore be potentially beneficial in reducing plaques. Treatment with CTB-MBP was successful in reducing amyloid load in the brain, with the number of plaques reduced by 70% in the hippocampus and cortex as detected by anti-Aβ antibody 2454 or thioflavin S. The ratio of insoluble amyloid (Aβ42) to soluble fraction was also reduced. Exactly how MBP crosses the BBB is unclear but MBP levels were increased in many brain regions and the reduction in Aβ plaque number and ThS intensity was uniform throughout. Possibly the leaky BBB in Alzheimer's disease patients allows entry of the protein once released into blood from the gut (van de Haar et al., 2016).

The production of CTB fusion proteins in chloroplasts or bacterial expression systems offers inexpensive production and facilitates storage of bioencapsulated proteins for several months without degradation. CTB has been used to successfully deliver proteins to neurones via direct injection as well as systemic routes. The toxin is a good candidate for a delivery vehicle of therapeutic molecules to neurones.

1.3 Gangliosides as cell entry ligands

A common element facilitating the uptake of toxins is their ability to bind gangliosides. The diverse coating of glycans on every cell surface provides a biochemical signature to be read by recognition molecules and forms each cell's distinctive face to its environment. In vertebrates this glycocalyx is composed of glycoproteins, glycolipids and proteoglycans. Within the nervous system the glycocalyx consists primarily of gangliosides, these are glycosphingolipids that are embedded in the outer leaflet of the plasma membrane, with one or more sialic acid residue in their glycan structure (Schnaar et al., 2014). While gangliosides are found in every vertebrate tissue they are markedly more abundant within the nervous system. Interestingly a number of viruses and bacterial toxins utilise gangliosides as cell entry ligands, initiating receptor-mediated endocytosis. Gangliosides represent important cell surface molecules for study to reveal mechanisms of cell entry by toxins, as well as elucidation of their role within the nervous system both physiologically and pathologically.

1.3.1 Synthesis and structure

Gangliosides consist of a glycan carried on a ceramide lipid to form a glycosphingolipid with one or more sialic acid residue linked via the sugar chain. Ceramides are composed of a sphingosine with a C2 primary amine that is N-acylated with a long chain fatty acid amide; ceramides of brain gangliosides typically have C1- and C3-hydroxyl groups and a C4-C5 double bond. The sphingosine chain of brain gangliosides is long at 18 to 20 carbons and the fatty acid amide is saturated, resulting in a rigid structure, enhanced lateral self-association and thus ganglioside-enriched domains.

A series of glycosyltransferases are employed to biosynthesise gangliosides in the Golgi apparatus (Prinetti et al., 2007), first the ceramide is glycosylated and then β4-galactose added, this terminal galactose is sialylated with a single Neu5Ac residue at its 3-hydroxyl to form GM3. The simple ganglioside GM3 acts as the main precursor for all other gangliosides (Figure 1.7). Gangliosides may be grouped into 0-, a- and b-series. 0-series gangliosides have no sialic acid on the first galactose residue and are rare in the adult mammalian brain. One sialic acid residue indicates a-series and two sialic acids denote b-series, these make up the majority of brain gangliosides.

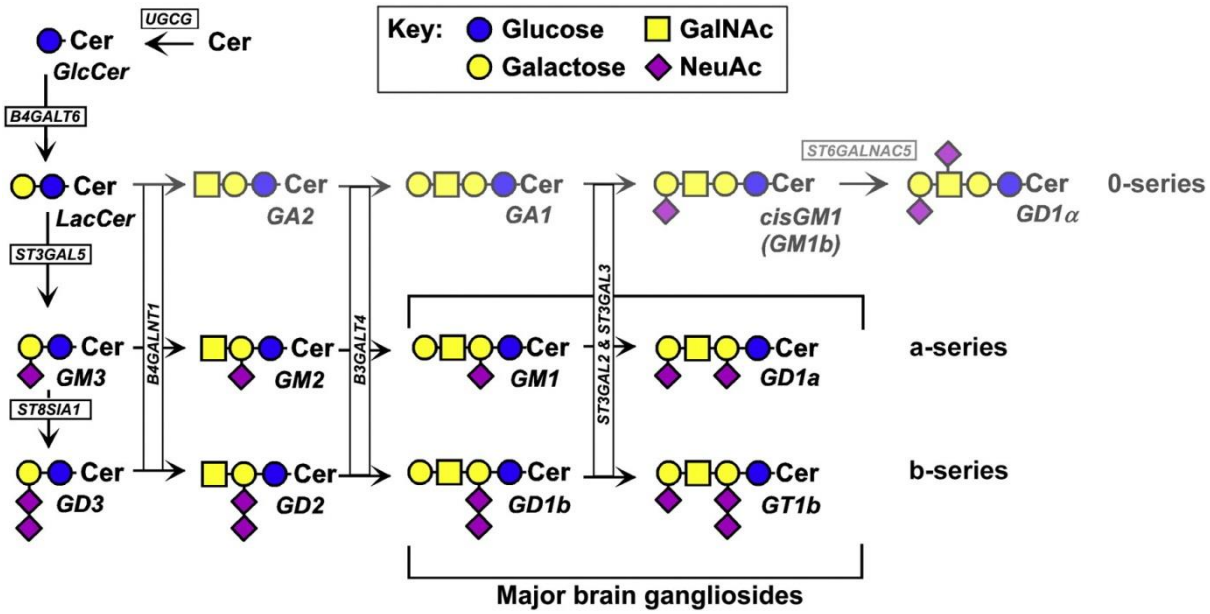

Figure 1.7 Ganglioside synthesis pathways of mammalian brain gangliosides

GM3 serves as the precursor for all brain gangliosides. The genes responsible for the expression of each glycosyltransferase are named in boxes. Reprinted from Schnaar (2016), with persmission from Elsevier.

1.3.2 GM1 expression

The a- (GM1 and GD1a) and b-series (GD1b and GT1b) gangliosides constitute 97% of brain gangliosides in mammals (Tettamanti et al., 1973). GM1 is the primary receptor for both CT and LT-I and so this ganglioside will be focused on. GM1 is a monosialoganglioside, with just one sialic acid residue (Figure 1.8).

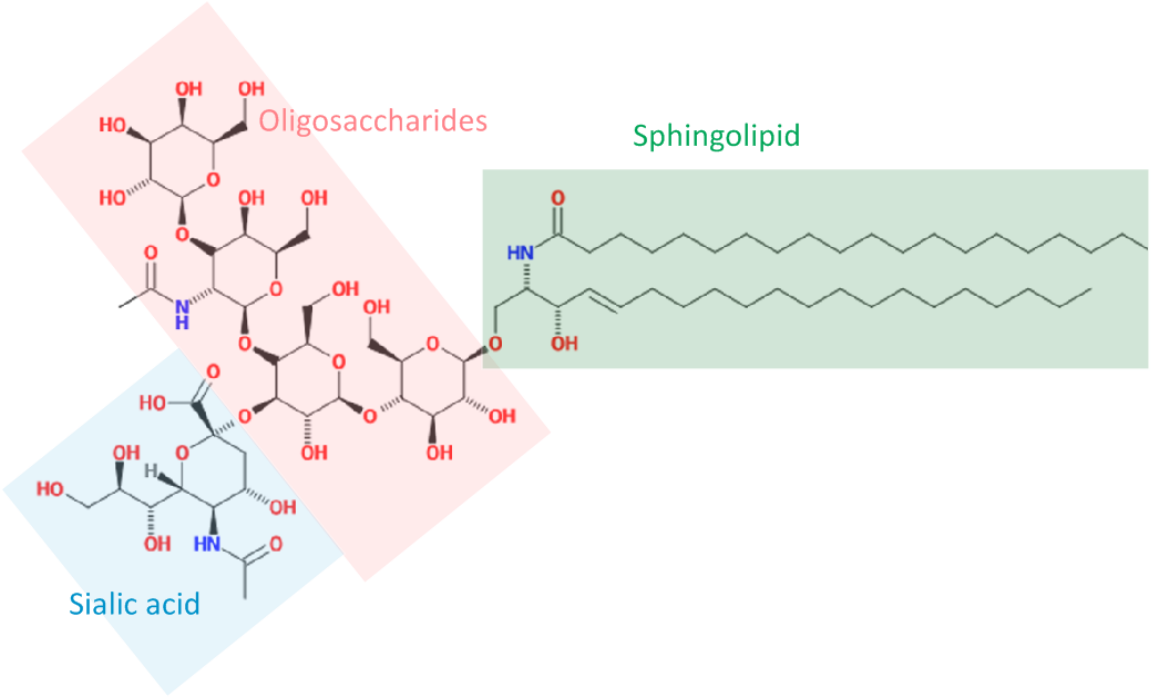

Figure 1.8 Structure of GM1 ganglioside

GM1 consists of a sphingolipid (green) embedded in the membrane and the oligosaccharides (pink) and sialic acid residue (blue) that extend beyond the cell. Adapted from Cavallo et al. (1993).

The ganglioside is expressed by mucosal cells in the small intestine, acting as the site for cholera and enterogenic *E.coli* toxin virulence (Holmgren et al., 1975). As detected by monoclonal antibody, GM1 was found to be widely expressed throughout brain regions in mice but predominantly in the white matter, and within the spinal cord the corticospinal tract was densely labelled (Vajn et al., 2013). Cultured neurones incubated with CT-HRP however suggest GM1 is present on the axolemmal surface of myelinated neurones, Schwann cells, oligodendrocytes (Kim et al., 1986; Sheikh et al., 1999). These differences could be attributed to potential alteration in ganglioside localisation in cultured cells, or difference in detection method. A more recent study by

Marconi et al. (2005) using monoclonal antibodies against the ganglioside showed discrepancy with previous results; GM1 was not shown to be expressed on oligodendrocyte precursors, though the results agreed with neurone expression. GD1a was expressed on nearly all oligodendrocytes, this ganglioside can be converted to GM1 by neuraminidase and so could serve as a pool *in vivo*. Marconi et al. tested post-mortem brain samples, while Kim et al. used cultured cells which may not be representative of in situ human tissue and may account for the differing results.

There are pools of gangliosides within intracellular loci as well as at the plasma membrane. GM1 is associated with the internal membranes of late endosomes and lysosomes due to retrograde transport within cells (Chinnapen et al., 2012). Upon ligand binding to GM1 a portion of plasma membrane is internalised to recycling endosomes and is eventually recycled back (Iglesias-Bartolome et al., 2009); it is thought this process may contribute to the uneven distribution of GM1 in various domains of neuronal plasma membrane. Transport of GM1 from the plasma membrane to sites of intracellular degradation have made it a useful tool in assessing the endocytic pathway (Mobius et al., 1999). GM1 is found at notable levels in the nuclear membrane of neurones where it is involved in calcium regulation (Wu et al., 1995).

1.3.3 GM1 function

Gangliosides reside in the extracellular portion of the plasma membrane; the ceramide and much of the glucose portion are engaged with the lipid leaflet with the glycan residues extending into the surrounding milieu (DeMarco and Woods, 2009). This glycan extension allows GM1 to act as a cell surface recognition site. Due to enhanced self-association GM1 tends to be found concentrated in lipid rafts (Sonnino et al., 2007) and this owes its function as a cell signalling and adhesion molecule. Lipid rafts are defined as detergent-resistant groups that are isolated as low-density fractions by density-gradient ultracentrifugation. Often additional lipids like cholesterol, phosphatidylinositols and sphingomyelin are concentrated within these microdomains (Simons and Sampaio, 2011). The clusters also contain lipid-modified proteins and may be viewed as ‘glycosignaling domains’ with roles in cell adhesion and cell-cell interactions (Hakomori et al., 1998). A number of functions have been proposed for GM1 in the nervous system, with the most well elucidated roles being differentiation through promotion of neurite outgrowth, and regulation of calcium homeostasis between nuclear and cellular cytoplasm.

The concentration of gangliosides increases during human development, with GM1 increasing 12-15-fold from the 10^{th} gestational week to age 5 years; this was assessed with post-mortem tissue of varying ages (Svennerholm et al., 1989). The most rapid

increase was seen during the period for dendrite arborisation and synaptogenesis, suggesting GM1 may be important to these events. In neurones cultured from the central and peripheral nervous system, as well as a neuroblastoma cell line, GM1 expression in the nuclear envelope (NE) was upregulated as the cells differentiated as detected by CTB-HRP and DAB cytochemistry (Kozireski-Chuback et al., 1999). The increased expression lagged behind neurite outgrowth but eventually reached plateau, suggesting a functional role for the ganglioside following the onset of morphological differentiation. GM1 facilitates the efflux of nuclear calcium ions, Neuro2a cells treated with a neuramidase purified from *Clostridium perfringens* have an increased concentration of GM1 in the NE and an enhanced calcium efflux was measured; when GM1 was reduced, the calcium efflux was also (Ledeen et al., 1998). It is thought that GM1 contributes to the reduced nuclear calcium concentration that characterises differentiated neurones.

GM1 promotes differentiation in a number of cell lines *in vitro*. The ganglioside interacts with TrkA, a receptor for nerve growth factor (NGF), to potentiate the effect of NGF (Rabin and Mocchetti, 1995). A cell line transfected with TrkA had increased TrkA phosphorylation and increased tyrosine phosphorylation of known TrkA targets after incubation with NGF or GM1. Mock transfected cells did not show this effect, suggesting GM1 interacts with TrkA to mimic some effects of NGF as well as to potentiate it. Using rat PC12 cells where NGF can be used to induce neuronal differentiation Mutoh et al. (1995) found that GM1 could enhance neurite outgrowth when applied with a dose of NGF usually insufficient to induce differentiation. There was more than 3-fold increase in autophosphorylation of TrkA when GM1 was added to the culture medium in comparison to NGF alone. Nishio et al. (2004) established that overexpression of GM1 in PC12 cells suppresses neurite formation normally induced by NGF. They suggest it modifies the intracellular location of TrkA and alters membrane fluidity, thereby preventing normal signal transduction of NGF. This would suggest an optimal concentration of the ganglioside is required for normal signal transduction.

Interactions of the ganglioside with other proteins that also facilitate differentiation have been studied. The binding of laminin-1 to GM1 in lipid rafts is crucial for neurite outgrowth. Ichikawa et al. (2009) suggest this binding enables a focal microdomain to form and enhance signal transduction by linking NGF-TrkA with laminin-integrin signalling, thereby promoting neurite outgrowth. Laminin-GM1 interactions have also been studied in cortical astrocyte culture, where addition of laminin causes re-organisation of GM1 into macrodomains that co-localise with dystrophin-associated

protein complex (Noel et al., 2009). This would suggest a role for GM1 in maintaining scaffolding of the cell by keeping the relevant proteins in rafts together.

Another important and well recognised role of GM1 in the nervous system is calcium homeostasis. GM1 tightly associates with a sodium calcium exchanger (NCX) on the inner membrane of the nuclear envelope, and this potentiates NCX activity (reviewed by Ledeen and Wu, 2007). The interaction was demonstrated by Xie et al. (2002), who noted that the plasma membrane of NG108-15 neuroblastoma cells had no association of NCX and GM1. This is due to splice variants of NCX that exist in different membrane compartments within a cell, and the nuclear envelope specific variant is able to interact with GM1. The negatively charged sialic acid group of the oligosaccharide chain of GM1 is thought to interact with the positively charged amino acid residues in the loop between transmembrane segments 5 and 6 of NCX (Xie et al., 2004).

The NCX/GM1 complex modulates transfer of calcium between the nucleoplasm and nuclear envelope and therefore the ER, which is continuous with the nuclear envelope. Initial experiments used isolated nuclei (Xie et al., 2004), but more recent proof comes from whole cell experiments where calcium sensors were transfected into various cell lines (with and without GM1) to monitor calcium dynamics in the nucleoplasm and nuclear envelope (Wu et al., 2009). Thapsigargin, a sarco/endoplasmic reticulum Ca^{2+}-ATPase (SERCA) inhibitor, caused a decrease in nuclear envelope/ER calcium and this could be rectified when calcium was added to cells with functional NCX/GM1. The alteration in calcium concentration was not seen when an NCX inhibitor was added to solution, nor did it occur in cells without working NCX/GM1. The NCX/GM1 complex therefore serves as an alternate route to SERCA for calcium transfer between cytosol and the ER.

Mice have been genetically engineered to lack GM1 by knocking out GM2/GD2 synthase, the enzyme required for its production. These mice are highly susceptible to kainate induced seizures which can be attenuated with intraperitoneal injection of LIGA20, a derivative of GM1 that can cross the blood-brain barrier and insert into the nuclear envelope, where it can potentiate NCX activity (Wu et al., 2005). Neurones cultured from these mice are highly vulnerable to calcium-induced apoptosis, and this could be rescued by GM1 and LIGA20. These results suggest a role of the NCX/GM1 complex in neuronal viability through prevention of excitotoxicity by calcium regulation.

Bringing together the two key roles of GM1 is the suggestion that GM1 ganglioside expression in the nuclear envelope alters calcium homeostasis following initiation of neurite outgrowth (Wu et al., 1995), to facilitate downstream calcium signalling in

differentiation (reviewed by Ledeen et al., 1998). During axonogenesis GM1 is upregulated and calcium concentration is altered, suggesting the ganglioside is crucial in the mechanism for signalling axon outgrowth.

GM1 selectively binds the GluR2 subunit of the α-amino-3-hydroxy-5-methyl-4-isoxazolepropionic acid (AMPA)-type glutamate receptor (Prendergast et al., 2014) and it is thought that the ganglioside may alter the receptor trafficking. Ganglioside-binding proteins from rat cerebellar granule neurones were identified using affinity capture followed by quantitative proteomic mass spectrometry. The potential for GM1 to regulate excitatory neurotransmitter receptor presentation at synapses may explain why congenital deficits in ganglioside biosynthesis result in intellectual deficits and seizure susceptibility.

GM1 has proven roles in calcium homeostasis, neuronal differentiation, axon outgrowth, receptor-mediated endocytosis and protein subunit trafficking.

1.3.4 Involvement of gangliosides in motor neuropathies

Auto-antibodies toward GM1 have been implicated in a number of motor neuropathies, including multifocal motor neuropathy (MMN) and an axonal subtype of Guillain-Barré syndrome known as acute motor axonal neuropathy (AMAN). While GM1 is ubiquitously expressed, the motor targeting of antibodies may be due to motor neurones having an increased density of GM1 in comparison to sensory neurones (Ogawa-Goto et al., 1992). Whether these antibodies directly induce the disease state is yet to be elucidated, but there is a growing body of evidence suggesting their involvement.

The pathogenic effect of anti-ganglioside antibodies likely depends on the local glycolipid environment of the plasma membrane as this can alter accessibility and avidity of the antibodies to their targets. *In vitro*, anti-ganglioside antibodies bind at the nodes of Ranvier and activate the complement cascade (Paparounas et al., 1999). Anti-GM1 antibodies alter distribution of TrkA in lipid rafts, thus affecting NGF induced autophosphorylation (Ueda et al., 2010). NGF activity is required for neuronal survival, and so diminishing this results in neurone death.

MMN is an inflammatory neuropathy characterised by progressive and asymmetric distal limb weakness, a hallmark of MMN being conduction block without abnormalities in sensory transmission. IgM auto-antibodies against GM1 have been found in about 50% of patients; however this number varies between 20-85% in the literature. One study found that increased titres of anti-GM1 are associated with more severe muscle weakness (Cats et al., 2010).

In peripheral nerves of mice lacking gangliosides including GM1, K^+ channels were mislocalised from juxtaparanodes and nodal Na^+ channel clusters were broadened (Susuki et al., 2007). Electrophysiological recordings showed slowed nerve conduction and a decrease in nodal sodium current in peripheral nerves. Binding of anti-GM1 antibodies at paranodal junctions may therefore disrupt sodium and potassium channel clusters, preventing the rapid propagation of action potentials, thus reflecting the conduction block seen in MMN. With roles for GM1 in maintenance and repair via NGF, anti-GM1 antibodies may prevent these functions. This would lead to axonal damage seen in motor neurones of MMN patients, and contribute to muscle weakness.

AMAN is a paralytic disorder characterised by motor axonal degeneration with little demyelination or lymphocytic inflammation seen, and importantly sensory neurones are spared. The syndrome was first described as a subtype of Guillain-Barré syndrome by Feasby et al. (1986). The subtype is particularly common in Northern China (Ho et al., 1995). Most patients have suffered an antecedent infection with *Campylobacter jejuni* and this is thought to trigger anti-GM1 IgG antibody production. The axolemma is the site of attack by the auto-antibodies (Hafer-Macko et al., 1996); since this is crucial for maintenance of membrane potential, damage will lead to disruptions in electrochemical gradients and therefore cell death.

There is molecular mimicry between a lipo-oligosaccharide on the surface of *C. jejuni* and GM1 ganglioside (Yuki et al., 1993). Therefore one suggested mechanism of disease progression is that anti-GM1 antibodies are made to clear the bacteria; however these then go on to attack GM1 expressed on motor neurones, preventing the ganglioside function and leading to axonal damage. The antibodies produced may lack specificity with some able to recognise a moiety shared by GM1 and GD1b (O'Hanlon et al., 1996). This may be why a very small subset of patients suffer sensory symptoms, as anti-GD1b antibodies are associated with acute sensory ataxic neuropathy.

Further evidence for the role of anti-GM1 in AMAN comes from reports of patients developing the disorder following injection of a ganglioside preparation to treat non-specific pain syndrome. The injection of exogenous gangliosides was immunogenic for all patients in one particular study, triggering high anti-GM1 IgG antibodies targeted to the nodes of Ranvier of motor neurones and causing axonal degeneration (Illa et al., 1995). Yuki et al. (2001) used this idea to create an animal model of AMAN where GM1 caused sensitisation. Rabbits had flaccid limb weakness with anti-GM1 deposited on peripheral motor fibres with no demyelination or lymphocytic infiltration, as characterised in human AMAN.

It is interesting to note the differing symptoms of the two disorders where anti-GM1 antibodies are usually measured. MMN sees demyelination and slowed nerve conduction with IgM antibodies, while AMAN has no demyelination or inflammation, instead there is axonal damage leading to paralysis with IgG antibodies measured. While there are likely a number of factors contributing to both diseases, it is possible the differing types of antibodies produced play a role. The specific function of the classes of immunoglobulins for the distinctive processes per disease is unknown, but it is possible to hypothesise. IgM macromolecules may interfere with remyelination of the motor fibres they bind to in MMN and this could cause the characteristic conduction block (Kaji and Kimura, 1999). IgG antibodies undergo retrograde transport to the soma following absorption from the nerve terminal (Engelhardt and Appel, 1990a); this internalisation may cause the damage and dysfunction of axons seen in AMAN.

Intravenous immunoglobulin (IVIg) infusion is an effective treatment for both disorders but the mechanism of action is unknown. The progression of MMN is halted, but the effect declines over time allowing the disease to advance again. Using the rabbit model of AMAN, IVIg treatment was confirmed effective at improving recovery rate of motor function (Nishimoto et al., 2004). One suggestion is that the treatment may accelerate the catabolism of the endogenous pathogenic auto-antibodies via interactions with Fc receptors (Reilly and McKenzie, 2002). The complement system may be activated due to the large quantity of antibody infused; this would enhance clearance of all antibodies. Interestingly neither of these appears to be the mode of action in MMN or AMAN as titres of auto-antibodies were not reduced (Van den Berg et al., 1998). It may be that IVIg is able to neutralise the antibodies or their downstream effects in some way to reduce damage, or prevent binding of the auto-antibody to its target. The fact that the treatment is effective suggests immune system involvement, and this is likely the auto-antibodies.

1.3.5 Involvement of gangliosides in neurodegeneration

Alterations in the ganglioside content in the brains of Alzheimer's disease (AD) patients suggest a role for GM1 in neurodegenerative disease. As further evidence, the depletion of gangliosides in knockout rodent models leads to neurodegeneration with symptoms similar to those in Parkinson's disease (PD), discussed below.

A fundamental process in AD pathogenesis is the deposition of amyloid-beta (Aβ), a derivative of amyloid precursor protein (APP). GM1 appears to have a role in AD pathology via altering Aβ production and seeding plaque formation. The processing of APP is dependent on lipid rafts, GM1 increases Aβ secretion and it has been suggested this may be by increasing gamma-secretase activity (Zha et al., 2004). GM1

clusters in detergent-resistant membrane microdomains where it promotes the interaction of secretases such as BACE1 with APP (Ehehalt et al., 2003), thereby having a direct role in the amount of amyloidogenic protein produced. GM1 expression was found to be increased in the brains of AD patients, even though total ganglioside expression was reduced (Yanagisawa, 2005). Alteration in ganglioside composition of the cell membrane alters lipid raft integrity affecting cell signalling, as well as altering production of amyloidogenic protein it could also lead to cell death seen in AD via activation of apoptotic pathways.

The ganglioside has also been implicated in fibril formation, where it acts as a seed to initiate the formation of plaques. Aβ has a high affinity for GM1 gangliosides, it has been suggested the N-terminal interacts both electrostatically and via hydrogen bonds with GM1 clusters (Yanagisawa and Ihara, 1998). The Aβ oligomers are recruited to ganglioside rich domains where they undergo conformational change from random coils to alpha helices, and as the protein density increases the structure becomes rich in beta sheets necessary for the formation of insoluble amyloid fibrils (Ikeda et al., 2011). Aβ-GM1 complexes have been measured in brains with early pathological signs of AD, further implicating its role as a seed. This membrane bound structure may be thought of as a seed, acting as a binding site for polymerisation of Aβ. The recruitment of oligomers also causes lipid peroxidation of the membrane and calcium dyshomeostasis when studied in primary fibroblasts from familial AD patients (Evangelisti et al., 2012), these would likely cause damage and cell death. As well as extracellular effects, recent studies suggest intracellular clusters of GM1 may contribute to amyloid fibril formation. GM1-bound Aβ accumulated preferentially in endosomes in aged monkeys (Kimura and Yanagisawa, 2007); and in PC12 cells blocking of the endocytic pathway induced Aβ aggregation by accelerating the release of exosome-associated GM1 (Yuyama et al., 2008). These findings indicate a role for abnormal endocytic trafficking in Aβ-based pathology in AD.

GM1 can also serve as a neuroprotective agent, intracerebroventricular administration of the ganglioside halts cognitive decline and improves motor function of AD patients (Svennerholm et al., 2002). Exactly how exogenous GM1 proves to be therapeutic while endogenous GM1 is implicated in disease progression is unknown. Exogenous GM1 prevented neurotoxicity caused by Aβ in hippocampal slice culture when incubated for 24 hours (Kreutz et al., 2011). Pre-treatment with the ganglioside prevented activation of GSK3β, a signalling molecule involved in the initiation of apoptosis in AD models. While GM1 is able to prevent neuronal death *in vitro* and slow symptom progression in patients, the danger of causing autoimmune neuropathies

must be noted. A safer alternative may be to use LIGA20, a derivative of GM1 that can cross the blood-brain barrier.

Deficiency of GM1 has been shown in the brain of patients with Parkinson's disease and GM2 synthase knockout mice that are deficient in GM1 develop PD-like symptoms (Wu et al., 2012). The symptoms were alleviated following administration of LIGA20, with the loss of tyrosine hydroxylase expressing neurones reduced. A five year study of subcutaneous GM1 injections in PD patients saw either reduction or stabilisation of motor symptoms and was indicated as safe over the period (Schneider et al., 2010). A further study by Schneider et al. (2013) validated these results in a randomised, controlled, delayed start trial. The motor symptoms of early-start patients were significantly improved 6 months into the trial, whereas the delayed group, who had at this point no GM1 treatment, had a worsening of theirs. The study provides evidence that GM1 ganglioside injections slow the rate of progression of PD.

The multifaceted roles of GM1 in neuronal physiology and pathology are revealed by the gangliosides enrichment in specialised subdomains of the neuronal plasma membrane. GM1 exerts neurotrophic and neuroprotective effects, including promotion of neuronal differentiation, neurite outgrowth and neuronal survival, both *in vitro* and *in vivo*. While the ganglioside is involved in neurodegenerative processes, exogenous application has proven to be therapeutic against several types of neuronal damage.

1.4 Amyotrophic lateral sclerosis

Amyotrophic lateral sclerosis (ALS) is a progressive disease causing muscle weakness due to deterioration of motor neurones. As of yet there are no successful treatment strategies, with patients usually dying 2-5 years after onset of symptoms (Turner et al., 2013). This presents a major unmet clinical need in the development of therapeutics targeted to motor neurones for treatment of the disease. CTB and LTB are capable of targeting motor neurones and thus may be useful in directing therapeutics for the treatment of ALS.

1.4.1 ALS overview

ALS is a rare disease, affecting about 2.2 people per 100,000 per year in Europe (Kiernan et al., 2011), but the economic, societal and personal burden is substantial (Schepelmann et al., 2010). The disease is categorised into two forms: the sporadic form (SALS) constituting 90-95% of cases has no obvious genetic component, while the remaining 5-10% of cases are familial (FALS) due to their associated genetic inheritance factor (Kiernan et al., 2011). The age of clinical onset of ALS is highly variable, but usually occurs between the ages of 50 and 65 (Logroscino et al., 2008; Logroscino et al., 2010). In rodent models of FALS neuronal abnormalities are detected as early as embryonic development (Williamson and Cleveland, 1999; Bories et al., 2007; van Zundert et al., 2008). These are usually overexpression models so care must be taken when extrapolating to humans, but the animals do not develop clinical abnormalities until late into adulthood, just as in the human disease course. Aberrant activity within the cells of ALS patients may start early in life and become clinically apparent much later, meaning there is scope to detect these early changes and target treatment before irreparable damage occurs.

The most common symptoms seen in both sporadic and familial ALS are muscle weakness, twitching and atrophy; these result in difficulty speaking, swallowing and eventually breathing, with pneumonia a common cause of death among patients (Zarei et al., 2015). Symptoms emerge due to failing axonal connections that lead to lower motor neurone and muscle denervation (Saxena and Caroni, 2011). As the axons retract they are initially compensated for by sprouting and collateral re-innervation from more resistant neurones, but eventually these neurones are damaged as well. Animal models highlight that only following this initial axonal dysfunction and retraction does the cell body become visibly abnormal and die, and this is confirmed by a rare post-mortem report from a patient who died early in the disease (Fischer et al., 2004). Autopsy revealed denervation and re-innervation changes in the muscle but motor neurones were normal, this has led to the suggestion that ALS pathology begins at the distal axon and proceeds in a ‘dying back’ pattern. As well as motor neurones, neurones in the prefrontal and temporal cortex are affected in ALS, but to varying degrees (Ringholz et al., 2005). Around 15% of ALS patients suffer concomitant frontotemporal lobe degeneration (FTLD) resulting in frontal executive dysfunction (Lillo and Hodges, 2009).

There is no cure for ALS, and only one licensed drug serving to lengthen survival time by 2-3 months; riluzole is often used to extend the time before ventilation support is required (Carlesi et al., 2011). The mechanism of action remains unknown but riluzole

may reduce the excitotoxic effects of glutamate. The drug has been shown to trigger pre-synaptic inhibition possibly through a reduction in calcium influx mediated by P/Q-type calcium channels, and this in turn inhibits the subsequent glutamate release from nerve terminals (Wang et al., 2004). Riluzole also inactivates voltage-gated sodium channels and is a non-competitive NMDA receptor antagonist as measured electrophysiologically in Xenopus oocytes (Debono et al., 1993). There are no treatments to halt or reverse the progressive motor neurone loss seen in ALS, and the only other therapies are palliative to aid management of symptoms and improve quality of life.

1.4.2 Familial ALS

Mutations in several genes have been found to cause FALS and contribute to the development of SALS; these include SOD1, C9ORF72, TARDBP, FUS and most recently NEK1. Each gene contributes to normal functioning of neurones along with other cells, and exactly why motor neurones are more susceptible to the pathogenic effects is unknown.

There are over 150 known mutations in the cytosolic copper/zinc superoxide dismutase 1 (SOD1), and they account for around 20% of FALS cases (Rosen et al., 1993; Robberecht and Philips, 2013). SOD1 is a cytosolic enzyme involved in free radical scavenging, mutants of which are misfolded and targeted for degradation through ubiquitylation yet somehow the mutant protein escapes (Basso et al., 2006). Once free within the cytoplasm the misfolded protein impairs the cell's degradation machinery by altering the proteasomal pathway and autophagy (Bendotti et al., 2012; Chen et al., 2012). Increased numbers of autophagosomes have been detected in spinal motor neurones of ALS patients as measured by electron microscopy; interestingly both degenerated and normal-appearing motor neurones showed features of autophagy (Sasaki, 2011). Accumulation of mutant SOD1 leads to initiation of a stress response, following on from this an unfolded protein response mounts either due to further accumulation of protein or an external stressor such as ageing (Saxena and Caroni, 2011). This leads to microglial activation, aberrant axonal transport and irregular mitochondrial function, ultimately resulting in axonal retraction and denervation followed by cell death.

Identification of a hexanucleotide repeat in chromosome 9 open reading frame 72 (C9ORF72) was the most recent major discovery in FALS (DeJesus-Hernandez et al., 2011; Renton et al., 2011). The mutation accounts for 40% of FALS cases and established a molecular link between ALS and FTLD (Majounie et al., 2012). The usual function of C9ORF72 is unknown but it is a homologue of the DENN proteins, which

are highly conserved GDP-GTP exchange factors for Rab GTPases (Levine et al., 2013). C9ORF72 was found to regulate endosomal trafficking and autophagy in primary cultured neurones, with strong colocalisation found between the protein and Rab7 and Rab11 in ALS patient motor neurones (Farg et al., 2014). How repeat expansions in C9ORF72 cause the motor neurone disease remains to be elucidated. Levels of C9ORF72 mRNA in the frontal cortex were reduced by 38% as measured by RT-PCR in samples from ALS patients (DeJesus-Hernandez et al., 2011). This suggests the expanded allele does not generate mature mRNA, however confirmation at the protein level has proven difficult as current available antibodies are not reliable. Probing via fluorescence in situ hybridisation reveals nuclear foci of the expanded hexanucleotide repeat in neurones of the frontal cortex and spinal cord (DeJesus-Hernandez et al., 2011). Such repeats can form a sink for nuclear RNA-binding proteins where they are unable to carry out their usual post-transcriptional functions, resulting in expression of erroneous proteins. The hexanucleotide repeat is capable of forming G-quadruplexes and this can facilitate the binding of other proteins (Fratta et al., 2012). Possibly G-quadruplexes formed of C9ORF72 pre-mRNA containing the expansion cause a toxic gain-of-function.

Transactive response DNA-binding protein 43 (TDP43) is a transcriptional repressor encoded for by the TARDBP gene (Ou et al., 1995). Motor neurones of the majority of ALS patients contain inclusion bodies of ubiquitylated and phosphorylated TDP43, and have abnormal nuclear TDP43 staining (Neumann et al., 2006). Mutations in TARDBP account for around 5% of FALS cases even though TDP43 aggregates are found in most ALS patients, both familial and sporadic (Neumann et al., 2006). Whether these aggregates are involved in causing ALS or are a by-product is not yet known. TDP43 protein binds DNA and RNA, and is involved in transcription, splicing and transport (Lee et al., 2012), and thus mutations may cause a loss of these essential functions. Mutant TDP43 forms aggregates in cell culture, and recent studies have shown that cytoplasmic TDP-43 aggregates colocalise with stress granule markers where translation is repressed (Dewey et al., 2012). With the protein sequestered to the cytoplasm the nuclear levels are reduced, however it is uncertain whether these changes are sufficient to cause the disease *in vivo*. Indeed, a mouse model expressing mutant TDP43 was found to induce an ALS phenotype without aggregate formation and without abnormal processing of TDP43 in spinal motor neurones (Arnold et al., 2013). Both overexpression and knockout of TDP43 is harmful to cells, suggesting a need for tight regulation of TDP43 (Lee et al., 2012).

Fused in sarcoma (FUS) is an RNA-binding protein encoded by the FUS gene, mutations in which cause around 5% of FALS cases (Kwiatkowski et al., 2009; Vance et al., 2009). FUS is normally a nuclear protein that like TDP43 binds both DNA and RNA, with roles in regulating transcription, alternative splicing and DNA repair (Sama et al., 2014). In contrast, mutant FUS accumulates in cytoplasmic inclusions within neurones and post-mortem analysis revealed lower motor neurone degeneration in patients with FUS mutations (Vance et al., 2009). FUS uses transportin to shuttle between the cytoplasm and the nucleus (Zinszner et al., 1997); mutant FUS disrupts this nuclear import causing the mislocalisation to the cytoplasm where it is recruited into stress granules, much like TDP43 (Dormann et al., 2010). The true mechanism of FUS toxicity is yet to be elucidated, and while it appears similar to TDP43 the two mutant proteins do not colocalise in inclusions, nor do they share binding partners (Lagier-Tourenne et al., 2012). Further exploration of the functionally related proteins may provide new insights into mechanisms underlying ALS pathogenesis.

The most recent genetic factor for ALS to be elucidated was mutant NEK1, responsible for around 3% of FALS cases (Kenna et al., 2016). NEK1 is a member of the highly conserved NIMA kinase family and among other functions, regulates the formation of primary cilia (Shalom et al., 2008), disruption of which has been linked to brain dysgenesis, hydrocephalus and intellectual disability (Lee and Gleeson, 2010). Disruption of other neuronally expressed NEK proteins has been shown to disrupt neuronal morphology, neurite outgrowth, as well as microtubule stability and dynamics when measured *in vitro* (Chang et al., 2009; Cohen et al., 2013). With suggested roles for NEK1 in cilia formation, DNA-damage response, microtubule stability, neuronal morphology and axonal polarity (Kenna et al., 2016) it is clear that disruption of these mechanisms could lead to motor neurone cell death. More research into the mechanisms of mutant NEK1 is required, but findings could help direct new treatments.

1.4.3 Causes of cell death in ALS

The pathogenic events in ALS are varied with a host of genetic and environmental factors leading to motor neurone cell death. Dysfunction in axonal transport, cytoskeletal disarrangement, mitochondrial dysfunction, aberrant RNA metabolism, protein aggregates and glutamate/calcium excitotoxicity are just some mechanisms. Glial cells are also involved in pathogenesis, with activated astrocytes and microglia increasing neuroinflammation.

ALS-causing mutations in TDP43 and FUS highlight the role of aberrant RNA metabolism and production of toxic RNA species in disease progression, and many more proteins linked to the disease are involved in RNA processing, reviewed by

Lemmens et al. (2010). As well as alterations in mRNA splicing and sequestering of proteins to the cytoplasm as seen with TDP43 and FUS, many other steps of RNA synthesis and processing are affected in ALS. The stability of mRNA through binding partners if affected can lead to cell damage. Aggregates of neurofilament are found in motor neurones of SALS and FALS patients (Troost et al., 1992), and also in SOD1 mouse models (Lin et al., 2005). The RNA-binding protein p190RhoGEF usually acts to stabilise neurofilament mRNA, but it also binds unassembled neurofilament protein; the dynamic competition between the two binding sites results in a homeostatic mechanism where the mRNA degrades when unassembled protein accumulates. As p190RhoGEF forms aggregates with unassembled neurofilament light protein it is unavailable to stabilise mRNA; such aggregates have been detected in presymptomatic SOD1 transgenic mice, suggesting a role as an early pathological change (Lin et al., 2005).

While it is the motor neurones that die in ALS, other cell types contributing to pathogenesis include microglia, astrocytes and T cells, reviewed by Philips and Robberecht (2011). Neuroinflammatory responses are usually transient, acting to clear a specific factor, but persistence of damaging factors in ALS causes a sustained response which becomes detrimental rather than curative. Activated microglia and astrocytes have been detected with immunohistochemistry in port-mortem tissue of ALS patients and transgenic mice (Engelhardt and Appel, 1990b; Nagy et al., 1994; Hall et al., 1998). Rodent models of ALS have provided evidence for the role of non-neuronal cells in ALS disease progression. Selective deletion of mutant SOD1 from motor neurones delayed disease onset, while diminishing levels in microglia had little effect on the early disease phase but later disease progression was slowed (Boillee et al., 2006). Further to this, delivery of small interfering RNA (siRNA) to motor neurones to knockdown mutant SOD1 in transgenic mice delayed disease onset, but did not modify the disease cause once started (Ralph et al., 2005). Astrocytes derived from ALS patients when co-cultured with motor neurones were found to be toxic, with the number of motor neurones reduced by 50% when compared to non-ALS astrocyte control cultures. When mutant SOD1 astrocytes were transplanted into the cervical region of the spinal cord of wild-type rats, a focal toxicity of motor neurones was induced, and forelimb function declined (Papadeas et al., 2011). These data suggest a role for different cell types in the onset and progression of ALS.

Motor neurones are highly susceptible to glutamate-induced excitotoxicity; this is partly determined by the permeability of AMPA-type glutamate receptors. Calcium permeability of AMPA receptors is mediated by the presence of the glutamate

receptor 2 (GluR2) subunit (Mishina et al., 1991), with those lacking the subunit being more permeable to calcium ions. Motor neurones have relatively low levels of GluR2 and are thus more prone to calcium overload (Van Damme et al., 2002). Post-transcriptional RNA editing of GluR2 where glutamine (Q) is substituted by arginine (R) in the putative second membrane domain (M2) reduces the calcium permeability (Mishina et al., 1991). AMPA receptors containing unedited GluR2 have high calcium conductance, in contrast to the edited GluR2 which has a low calcium conductance. GluR2-editing defects have been detected in the motor neurones of ALS patients as measured by RT-PCR from laser microdissected autopsy samples; in addition, cerebellar Purkinje cells from ALS patients had over 99% GluR2 editing efficiency and non-disease control samples had no deficiencies in editing (Kwak and Kawahara, 2005). This suggests failed GluR2 editing occurs in a disease specific and region selective manner. Modification of GluR2 by RNA editing is a biologically crucial event, and the reduction in editing in ALS motor neurones likely contributes to selective motor neurone cell death via glutamate/calcium excitotoxicity. Expression of the excitatory amino acid transporter (EAAT2) by astrocytes is decreased in ALS patients (Rothstein et al., 1992) and rodent models (Bruijn et al., 1997) meaning glutamate clearance is reduced. This may result in increased glutamate levels in the synapse and prolong glutamate stimulation of motor neurones. During progression of ALS, motor neurones in the oculomotor nucleus and Onuf's nucleus tend to be spared while most others are destroyed (Kanning et al., 2010). The calcium-buffering capacity, of spinal motor neurones is limited in comparison to the spared motor neurones, further increasing their susceptibility to excitotoxicity (Vanselow and Keller, 2000).

1.4.4 Calcium binding proteins and ALS

The expression profile of calcium binding proteins across subpopulations of motor neurones may contribute to their selective vulnerability in ALS. Particularly vulnerable populations of neurones within the brainstem and spinal cord are those with low levels of calcium buffer proteins such as calbindin-D28k and parvalbumin. Immunohistochemistry of human autopsy specimens for calbindin-D28k and parvalbumin revealed that populations lost early in ALS such as cortical, spinal and cranial nerve motor neurones were absent of immunoreactivity. Motor neurones damaged late or infrequently in ALS such as those in Onuf's nucleus and oculomotor, trochlear, and abducens nerve neurones expressed markedly higher levels (Alexianu et al., 1994). Additionally, expression of calretinin and parvalbumin in spinal motor neurone axons, but not cell bodies, was further decreased in ALS patients when compared to healthy controls (Hayashi et al., 2013).

Oculomotor neurones may be resistant to cell death in ALS due to an increased calcium buffering capacity. Using patch-clamp recordings in sliced tissue and microfluorometric-calcium measurements quantitative analysis of calcium homeostasis was measured (Vanselow and Keller, 2000). Endogenous calcium binding ratios were around 6-fold larger in oculomotor neurones when compared with vulnerable hypoglossal nucleus and spinal cord neurones. Local calcium elevations around open calcium channels were reduced and peak amplitudes of global calcium transients for a given influx were lower.

Overexpression of parvalbumin in a mSOD1 mouse model was used to assess whether increasing calcium binding protein expression could rescue motor neurones in ALS (Beers et al., 2001). The transgenic mice expressed rat parvalbumin under control of the rat calmodulin promoter; transcripts were detected in hypoglossal and spinal motor neurones, but not within glial cells. Administration of sera from ALS patients increases calcium within axon terminals of control mice (Engelhardt et al., 1995), but this was attenuated in parvalbumin overexpressing mice. Clinical progression of ALS was altered in the parvalbumin expressing transgenic mice when compared to mSOD1 mice. Motor neurone cell death was significantly reduced, disease onset was delayed by 17% and survival prolonged by 11%. ALS immunoglobulins increase intracellular calcium currents in a differentiated motor neurone cell line (VSC4.1) as assayed by whole-cell patch-clamp recording (Mosier et al., 1995). When VSC4.1 cells were transfected with calbindin-D28k cDNA under control of a phosphoglycerate kinase promoter they became resistant to ALS sera-mediated cytotoxicity (Ho et al., 1996).

Calcium dysregulation is clearly involved in ALS pathogenesis, with calcium binding proteins offering some protection against this. Efforts to upregulate calcium binding proteins or deliver them to motor neurones should be further studied as a potential therapeutic in ALS.

1.5 Calcium binding proteins

Calcium is a widely used regulator and initiator of physiological functions within biological systems. Calcium binding proteins act to modulate intracellular calcium signals, affecting both the temporal and spatial aspects of transient calcium rises. Under basal conditions intracellular calcium concentration ranges from 20-100 nM, yet the dissociation constant for most calcium buffers ranges from 200 nM to 1.5 μM (Schwaller, 2010). Therefore in a resting cell, calcium buffers remain in their calcium-free state, binding calcium ions only when intracellular levels increase. The intracellular

calcium concentration, calcium binding affinity, binding and release kinetics and intracellular mobility all affect the way a calcium buffer can alter calcium signalling.

Calcium buffers do not show any significant conformational change upon calcium binding and function purely to shape the amplitude and duration of calcium signals, as well as to limit the spatial spreading of local signals. Calcium sensors on the other hand do undergo a conformational change after binding calcium and subsequently interact with various target molecules with the ability to affect downstream regulatory processes within the cell.

1.5.1 Parvalbumin

Parvalbumin is a calcium binding protein of the EF-hand type encoded by the PVALB gene, at 110 amino acids in length and 12 kDa in weight it is a small and relatively stable protein and it does not undergo any post-translational modifications (Fohr et al., 1993). The EF-hand motif consists of two alpha helixes linked by a short approximately 12 amino acid loop (Kretsinger and Nockolds, 1973); in parvalbumin these can bind both calcium and magnesium ions. The calcium ion is bound by both the protein backbone and the side chains of the negative amino acids, glutamate and aspartate, which form a charge-interaction with the positively charged ion. Parvalbumin is commonly divided into three domains: AB, CD, and EF, each containing a helix-loop-helix motif. The AB domain contains a two amino acid deletion within the loop region such that it does not bind metal ions, domain CD contains the N-terminal binding site, and domain EF contains the C-terminal binding site (Kretsinger and Nockolds, 1973). The two calcium binding sites in parvalbumin do not exhibit co-operative binding (Cates et al., 2002) nor do they change conformation upon metal ion binding (Henzl and Tanner, 2008). Both sites are high-affinity binding sites, and as measured by fluorescence calcium imaging are nearly indistinguishable (Eberhard and Erne, 1994). Parvalbumin has a high affinity for calcium ions (dissociation constant $K_d > 10^8\ M^{-1}$) and an intermediate affinity for magnesium ions ($K_d > 10^4\ M^{-1}$) (Eberhard and Erne, 1994; Henzl et al., 2003). These properties along with the fact that the cytoplasmic magnesium concentration (0.1-1 mM) exceeds that of calcium (50-100 nM) in basal conditions explains why parvalbumin binding sites are over 80% occupied by magnesium ions in a resting cell. Remaining sites are either calcium-bound or metal-free. Parvalbumin is often described as a slow-onset calcium buffer (Schwaller, 2010). This is because when a stimulus induces a rise in cytosolic calcium levels, magnesium ions must first dissociate from the binding sites before being replaced by calcium ions. Due to the slow binding kinetics the rate in intracellular calcium rise is not affected by parvalbumin, but the initial rate of calcium decay is increased. The hallmark of

parvalbumin is its ability to convert monoexponential calcium decay into biexponential decay, where the unbinding of calcium ions in the later phase of decay prolongs it (Lee et al., 2000a; Collin et al., 2005).

High levels of parvalbumin are measured in a subset of fast-spiking GABAergic interneurones throughout the hippocampus, cerebellum and neocortex (Schwaller et al., 2002). It is also expressed in fast-twitch muscle fibres (Celio and Heizmann, 1982), and epithelial cells in the early distal convoluted tubule in the nephrons of the kidney (Olinger et al., 2012). Within the CNS, the parvalbumin induced biexponential calcium decay is observed in hippocampal neurones (Lee et al., 2000b), molecular layer interneurons in the cerebellum (Collin et al., 2005), presynaptic terminals of the calyx of Held (Muller et al., 2007) and Purkinje cell dendrites (Schmidt et al., 2007). At cerebellar interneurone synapses this parvalbumin slow decay component leads to a robust, delayed transmitter release subsequent to presynaptic bursts of action potentials (Collin et al., 2005).

The differential expression of parvalbumin between motor neurone subpopulations is hypothesised to contribute to their selective vulnerability to calcium-induced excitotoxicity. In situ hybridisation of rat CNS tissue demonstrated that ALS-resistant motor neurones robustly expressed parvalbumin mRNA, while no measurable expression was measured in ALS-sensitive populations (Elliott and Snider, 1995). Immunohistochemistry for parvalbumin protein expression further evidenced the hypothesis (Alexianu et al., 1994). A transgenic mouse line was created that overexpressed parvalbumin throughout the CNS; the mice had no apparent phenotype (Van Den Bosch et al., 2002). Calcium imaging of cultured spinal motor neurones from these animals revealed neuroprotective effects of parvalbumin against kainate-induced cell death as compared to non-transgenic controls. The authors suggest parvalbumin may reduce the calcium load on mitochondria, which in motor neurones in the absence of a diffusible buffer function as the main buffering organelle.

1.5.2 Calmodulin

Calmodulin is a 16.7 kDa protein encoded by CALM1 in humans, it is the prototypical calcium sensor (Chin and Means, 2000). Calmodulin comprises four EF-hand domains, the first pair combine to form a globular N-terminal domain and the second pair forming a globular domain at the C-terminus; the two domains are separated by a short flexible linker (Chattopadhyaya et al., 1992). The affinity of calmodulin for calcium ranges (K_d = 5×10^{-7} M to 5×10^{-6} M) with the affinity of the C-terminal pair of EF-hands up to 5-fold higher than the N-terminal pair (Klevit, 1983; Beccia et al., 2015). In the absence of calcium the two globular domains adopt different conformations. The N-terminal

domain is ‘closed’ with the helices of both EF hands packed together, while the C-terminal domain is ‘semi-open’ where a hydrophobic patch is partially exposed and accessible. The C-terminal domain can interact with target proteins at resting intracellular calcium levels (Swindells and Ikura, 1996). As intracellular calcium rises, each EF-hand binds a calcium ion and this leads to substantial alterations in the interhelical angles such that hydrophobic groups are exposed in a methionine-rich crevice of each domain that is separate from the calcium-binding loops (Yuan et al., 1999).

Calmodulin binding proteins can be categorised into six groups based on their modes of regulation in the presence or absence of calcium, reviewed by Chin and Means (2000). Briefly, group A irreversibly bind calmodulin irrespective of calcium concentration; group B bind in the absence of calcium but dissociate reversibly in the presence of calcium; group C effectors form low-affinity, inactive complexes with calmodulin at low concentrations of calcium. Group D effectors are inhibited by calcium-bound calmodulin; group E effectors are regulated by calcium-bound calmodulin; and group F effectors are phosphorylated by calmodulin-regulated kinases. The targets of calmodulin are diverse with functions including muscle contraction, metabolism, memory, apoptosis, inflammation and the immune response (Tidow and Nissen, 2013).

Calmodulin is ubiquitously expressed and is involved in the regulation of many essential physiological processes. In hippocampal neurones calmodulin translocates from the cytoplasm to the nucleus to activate a calmodulin-dependent kinase (CaMK IV) allowing for the rapid phosphorylation of CREB (Deisseroth et al., 1998). Calmodulin therefore affects transcription, alteration of which could have severe consequences for cells. Calmodulin may have a role in cell death seen in motor neurone diseases. Isoforms of CaMKs were elevated in both cytosolic and particulate fractions of spinal cords from ALS patients as measured by immunoblotting of post-mortem tissue (Hu et al., 2003). CaMK can accelerate the formation of mitochondrial reactive oxygen species (ROS) (Odagiri et al., 2009); due to low levels of antioxidants and the high flux of ROS generated during energy metabolism, motor neurones are particularly vulnerable to oxidative stress. In terms of treating a disease, altering calmodulin levels would have various downstream effects some of which could negatively affect the cell. Delivering calmodulin as a therapeutic would require close monitoring and is potentially not viable.

1.5.3 Calbindin-D28k

Calbindin-D28k is a 28 kDa calcium binding protein encoded for by the CALB1 gene; it contains 6 EF-hand domains organised in a globular domain, four of which bind calcium with medium-to-high affinity (Cheung et al., 1993). EF-hands 2 and 6 have lost their calcium binding capacity, while the other 4 sites bind calcium with high/medium affinity and magnesium with low affinity ($K_d \approx 700$ µM) (Kojetin et al., 2006). The binding of magnesium ions increases the cooperativity of calcium binding (Berggard et al., 2002b). Calbindin-D28k undergoes calcium-induced structural changes upon binding of calcium as measured by circular dichroism and NMR (Venters et al., 2003; Kordys et al., 2007). The on-rates of calbindin-D28k fast binding sites ($k_{on} \approx 8. \times 10^7$ $M^{-1}s^{-1}$) are fast enough to affect the early rising phase of calcium transients. Peak amplitude is significantly increased in Purkinje cells of calbindin null mutant mice when compared to controls (Airaksinen et al., 1997). The time to peak is not altered however, suggesting that the initial rise in calcium is governed by density and kinetics of the calcium channels rather than calcium binding proteins.

Calcium-loaded calbindin-D28k directly interacts with a number of intracellular target proteins, suggesting a role as a calcium sensor as well as a calcium buffer. NMR revealed interaction of calbindin-D28k with Ran-binding protein M (RanBPM), a protein required for microtubule assembly and regulation of GTP-bound Ran activity (Lutz et al., 2003). Myo-inositol monophosphatase (IMPase) was found to bind both apo- and calcium-bound calbindin-D28k as measured by bacteriophage display and fluorescence spectroscopy, activating IMPase up to 250-fold (Berggard et al., 2002a). IMPase is a key enzyme in the regulation of the activity of the phosphatidylinositol-signalling pathway, and therefore important in second messenger signalling. Another crucial binding partner is caspase-3, an initiator of apoptosis. Calbindin-D28k modulates apoptosis in osteoblasts that mineralise bone (Bellido et al., 2000).

Calbindin-D28k is expressed in high levels in the brain; it is also expressed in the kidney, bone and pancreas (Christakos et al., 1989). In the kidney calbindin-D28k is involved in the transcellular movement of calcium in the distal tubules (Borke et al., 1989). In the pancreas the calcium binding protein controls insulin release in the islet cells (Sooy et al., 1999). In the mature CNS calbindin-D28k is predominantly expressed in neurones as detected by immunohistochemistry (Celio, 1990). Specifically, calbindin-D28k was primarily detected in long-axon neurones including thalamic projection neurones, striatonigral neurones, nucleus basalis Meynert neurones, cerebellar Purkinje cells, large spinal-, retinal-, cochlear- and vestibular ganglion cells. It was also detected in some short-axon cells represented by spinal cord interneurones in layer II

and interneurones of the cerebral cortex. Cultured hippocampal neurones evidence a role for calbindin-D28k in neuroprotection against excitotoxicity. The cultured cells were relatively resistant to both glutamate and calcium induced neurotoxicity and were better able to reduce free intracellular calcium levels when compared to calbindin-D28k-negative neurones (Mattson et al., 1991). Calbindin-D28k null mice develop normally, with no structural deficits detected in the CNS by light microscopy; however mice are severely impaired in motor coordination tests suggesting a functional deficit in the cerebellar pathway (Airaksinen et al., 1997).

Like parvalbumin, calbindin-D28k is implicated in motor neurone vulnerability in ALS due to low expression levels in neurones lost early in the disease and markedly higher levels in resilient motor neurones (Alexianu et al., 1994). Organotypic slice culture of rat spinal cord slices was used to examine whether potent neuroprotective factors can increase the expression of calbindin-D28k in the postnatal spinal cord. Glial-derived neurotrophic factor, neurturin and insulin-like growth factor all increased calbindin-D28k immunoreactivity in motor neurones after 4 weeks (Spruill and Kuncl, 2015). Upregulation of the calcium binding protein may represent a mechanism by which motor neurones can be protected from glutamate and calcium-induced excitotoxicity. However delivery would need to be targeted and downstream effects of the protein must be taken into account.

1.5.4 Calretinin

Calretinin is a 31 kDa protein encoded for in humans by the CALB2 gene; it shares 58% homology with calbindin-D28k (Rogers, 1987). The protein contains 6 EF-hand domains, four of which are capable of binding calcium with high affinity, and one with low affinity (Schwaller et al., 1997). Calcium binding is high affinity and cooperative with a change of confirmation occurring as measured via the intrinsic tryptophan fluorescence intensity (Kuznicki et al., 1995). Calretinin also shows affinity for copper (Cu^{2+}) ions, upon binding it antagonises calcium binding to calretinin (Groves and Palczewska, 2001). Calretinin shares some kinetics of both slow (parvalbumin) and fast (calbindin-D28k) calcium buffers in modifying dendritic calcium transients (Faas et al., 2007), this is predominantly due to cooperative calcium binding.

Calretinin is generally expressed in neurones of the CNS and in the retina (Rogers, 1987). The subcellular localisation of calretinin is altered during development as measured by confocal microscopy in brainstem auditory neurones of chicks (Hack et al., 2000). Calretinin changes from being diffusely expressed throughout the cytoplasm to being highly concentrated beneath the plasma membrane. The authors suggest this may be an adaptation to spatially restrict calcium influxes. Calretinin is expressed in

high levels in cortical interneurons predominantly in cortical layers II and III, acting to inhibit projection neurones within the cortical minicolumn and synchronise their activity (Barinka and Druga, 2010).

Calretinin-deficient granule cells exhibit faster action potentials and generate repetitive spike discharge showing an enhanced frequency increase with injected currents. These alterations disappear when 0.15 mm of the exogenous fast-calcium buffer BAPTA is infused in the cytosol to restore the calcium-buffering capacity. Calretinin null mice are impaired in motor coordination tests, this is because calretinin is normally enriched in cerebellar granule neurones (Schiffmann et al., 1999). The calretinin-deficient granule cells display faster action potentials with injected currents as measured by patch-clamp recording (Gall et al., 2003). These alterations can be attenuated with addition of BAPTA, a fast-calcium buffer, suggesting calcium binding proteins are essential to modulate intrinsic neuronal excitability. Calretinin is expressed in 53% of ventral horn motor neurones in primates as measured by immunohistochemistry (Fahandejsaadi et al., 2004). In an SOD1 transgenic mouse model, calretinin immunoreactivity was decreased in the cerebral cortex and hippocampus when compared to wild-type controls (Chung et al., 2005). Furthermore, a reduction in calretinin-positive axons was measured in the anterolateral column of the spinal cord of post-mortem ALS CNS tissue (Hayashi et al., 2013). These data suggest a loss of the calcium binding protein may be associated with motor neurone cell death in ALS.

1.6 Viruses for gene delivery in the CNS

Viruses represent another approach for targeting neurones for delivery of exogenous material. Neurotropic viruses can be used for viral vector-mediated gene delivery, either as experimental tools in neuroscience or as therapeutics in the treatment of neurodegenerative diseases. Using a viral strategy allows for targeted correction of the underlying cellular and molecular abnormalities of a disease. Factors to take into account for a viral vector for neural delivery include transgene capacity, transduction efficiency, kinetics (onset, duration of expression, and elimination), biodistribution profile and immunogenicity. In order to treat motor neurone diseases a peripheral or systemic site of injection would be preferred, and so a virus must be able to enter neurones at the axon or terminals and retrogradely transport to the cell body for transduction.

1.6.1 Canine adenovirus type 2 (CAV-2)

Human adenoviruses (hAd) have demonstrated robust expression and have the potential for both long- and short-term gene transfer, making them attractive candidates for gene delivery. However clinical use of hAd vectors has been limited by pre-existing vector immunity, with efficacy and duration of transduction negatively affected (Wold and Toth, 2013). To circumvent this, vectors derived from non-human adenoviruses were generated and tested with the hypothesis that they would be more clinically useful due to the potential lack of immunological memory (Paillard, 1997). CAV-2 vectors were tested in a variety of mammalian cell lines; they successfully transduced the cells and the humoral response directed against human adenovirus 5 does not inhibit CAV-2 plaque formation (Klonjkowski et al., 1997). Despite humans and dogs cohabitating for over 30,000 years (Thalmann et al., 2013) CAV-2 has not been known to cross the species barrier and is unable to replicate in humans; it was therefore hoped to be used as a successful gene delivery vector without some of the clinical disadvantages of hAd vectors.

Adenoviruses are 150-mDa non-enveloped pathogens, with a linear double-stranded DNA genome of 28-48 kb packaged into a 90 nm icosahedral shell. Initial CAV-2 vector genomes were created by *in vivo* homologous recombination in *E.coli* to form an E1-deleted CAV-2 genome, E1 is essential for replication and amplification of the virus (Bergvall et al., 2013). Plasmids containing recombinant CAV vectors from which the E1 region had been deleted were generated and transfected into a CAV E1-transcomplementing cell line (Kremer et al., 2000). More recently CAV-2 vectors have been produced in a helper-dependent system where all viral coding regions are deleted. This resulted in vectors with a high cloning capacity of around 30 kb and allowed for transgene expression of over a year in the immunocompetent rat brain without immunosuppression (Soudais et al., 2004).

During the development of CAV-2 vectors it was found that they preferentially transduce neurones following intranasal, intramuscular and intracerebral administration (Soudais et al., 2001). In the rat olfactory cavity, CAV-2 transduced sensory olfactory neurones after 15 days while columnar epithelial cells remained unlabelled. Direct injections to the striatum in rats preferentially transduced dopaminergic neurons of the substantia nigra pars compacta, neurones in layer IV of the neocortex and thalamus. Therefore as well as neurones at the injection site, those projecting to it were also transduced. Injection of the vector into the gastrocnemius of neonatal mice (P4) successfully transduced innervating motor neurones with GFP detected in the lumbar region while myofibres were poorly transduced. This provides evidence that CAV-2 can

be administered to the peripheral nervous system, taken up by terminals and retrogradely transported to the CNS for transduction.

CAV-2 like other adenoviruses uses Coxsackievirus and adenovirus receptor (CAR) to enter cells and access the endocytic trafficking pathway (Soudais et al., 2000). CAR is highly expressed in the developing nervous system as measured by in situ hybridisation and Western blot in mice (Honda et al., 2000), and remains detectable within the adult nervous system (Salinas et al., 2009). Incubation of CAV-2 vectors with cultured motor neurones revealed CAV-2 entering the cells and trafficking in a bi-directional manner, though a preference was found for retrograde transport (Salinas et al., 2009). Genetic inhibition of dynein (retrograde transport) and kinesin (anterograde transport) impaired CAV-2 axonal transport suggesting a role for these molecular motors. Endocytosis and transport of CAV-2 occurs within pH-neutral/Rab7^{+} endocytic vesicles and is mediated by clathrin (Salinas et al., 2009). These vesicles likely provide a protective environment were the virus is not subject to degradation or pH-induced conformational changes. Interestingly this pathway is also used by neurotrophins, as well as tetanus toxin suggesting that the endogenous pathway is hijacked by virulence factors (Deinhardt et al., 2006).

CAV-2 vectors have been utilised to characterise neural circuits. CAV-2 expressing Cre recombinase (Cre) was co-injected with an AAV that contains the floxed inverted sequence of the designer receptor exclusively activated by designer drugs (DREADD). This allowed for activation of the gene in specific populations of neurones where both viruses infected. IP injection of clozapine-N-oxide activated the DREADD in the mesolimbic dopamine system; by activating specific neural pathways the consequent changes in behaviourally relevant paradigms can be probed (Boender et al., 2014). The same vector was injected into the central nucleus of the amygdala to identify a subpopulation of neurones from the parabrachial nucleus that project to the amygdala with a role in appetite suppression (Carter et al., 2013). The retrograde transport of CAV-2 has also been used to determine the molecular profiling of neurones based on their connectivity. Mice were genetically engineered to express ribosomes tagged with anti-GFP camelid nanobodies, which could then be tagged by GFP delivered via CAV2-GFP. Immunoprecipitation for GFP allowed identification of marker genes for neurones on the basis of their projections. The system can be engineered to selectively capture translating mRNAs from neurones retrogradely labelled with GFP, and has been used to profile neurones projecting to the nucleus accumbens (Ekstrand et al., 2014).

CAV-2 vectors are ideal tools for the study of the pathophysiology of neurodegenerative diseases due to their neurotropism and ability to retrogradely transport. CAV-2 has been used to examine dopamine signalling in discrete dopaminergic circuits (Hnasko et al., 2006). A transgenic line of mice with a floxed non-functional tyrosine hydroxylase gene are dopamine-deficient. Injection of CAV2-Cre into the central caudate putamen restores enzyme expression to the midbrain neurones that project there as CAV-2 transduces the neurones and retrogradely transports to the cell bodies. The behaviour of virally rescued mice was then assessed; studies such as this highlight the role of CAV-2 in dissecting neural circuits in health and disease.

CAV-2 vectors have been tested as a gene therapy vehicle in mice to deliver DNA for a deficient enzyme. Mucopolysaccharidoses (MPS) are a group of metabolic diseases caused by a deficiency in lysosomal enzymes in the brain. MPS VII is caused by deficiency in the enzymatic activity of β-glucuronidase, this leads to accumulation of glycosaminoglycans within lysosomes and causes progressive CNS lesions (Vogler et al., 1994). Intracranial administration of CAV-2 expressing β-glucuronidase in a mouse model of MPS VII restores the global enzyme activity, reduces glycosaminoglycan accumulation and corrects the histological hallmarks (Ariza et al., 2014). Mice also showed significant improvement in cognitive function as measured by various behavioural tests. CAV-2 represents a good candidate delivery vector in the treatment of lysosomal storage diseases due to its global and sustained expression.

With proven ability to deliver transgenes to correct protein deficiencies and ability to enter motor neurones and transport retrogradely (Salinas et al., 2009), CAV-2 is a candidate vector for viral-mediated gene delivery in motor neurone diseases.

1.6.2 Adeno-associated virus (AAV)

AAVs are ideal vectors for gene delivery in neural tissue as they can infect both dividing and non-dividing cells, they are neurotropic, support long-lasting expression and do not exhibit pathogenicity. They can also be produced and purified easily, and in large amounts such as those required for clinical trials. There are 11 human serotypes (AAV1-AAV11) and over 100 from non-human primates (Choi et al., 2005); the many available serotypes have increased the vector's potential as a delivery vehicle due to increased scope of tropism (Daya and Berns, 2008). All the serotypes are non-enveloped, single-stranded DNA parvoviruses, with a diameter of 25 nm and a genome of 4.7 kb (Srivastava et al., 1983). Productive infection by AAV only occurs in the presence of a helper virus, either adenovirus or herpes virus. In the absence of a helper virus AAV2 integrates into a 4 kb region on chromosome 19 (q13.4),

establishing latency (Linden et al., 1996). This locus is near to several muscle-specific genes; whether integration into this site is suitable for human gene therapy was unknown but tissue culture experiments suggest that it is safe (Dutheil et al., 2000). Further studies revealed that AAVs integrate poorly into the host genome and so should be safe (Daya and Berns, 2008).

The first recombinant AAV (rAAV) was generated with serotype 2 where 95% of the viral genome was removed, however wild-type virus was required for production (Samulski et al., 1982). The next generation of rAAVs were created with all the necessary genes for production contained within plasmids such that wild type viruses are not required and thus increasing the safety of the vector (Ferrari et al., 1997). With AAV2 generated first, a lot of the initial viral therapy studies utilised this serotype; however later studies revealed other serotypes had increased transduction efficiency within the CNS with more cells transduced and increased levels of gene expression. In general serotypes 1, 2, 5, 8 and 9 are deemed neurotropic and are the most studied in the brain and spinal cord (Weinberg et al., 2013).

In CNS tissue, AAV8 is deemed to be most efficacious in transducing CNS tissue when compared to AAV5; and AAV5 more efficacious than AAV2 (Harding et al., 2006; Weinberg et al., 2011). AAV8 also has greater efficacy than AAV1; however AAV8 has proven to be neurotoxic where GFP expression caused death of dopaminergic neurones, therefore caution is warranted when attempting to increase transgene expression (Klein et al., 2006). The patterns of AAV transgene expression can vary considerably after direct infusion into the CNS; factors affecting this include viral structure, vector purity, promoter used and CNS milieu. Dependent on the application different serotypes may prove more effective and so the properties of each must be considered. For example in the substantia nigra (SN), injection of AAV2 leads to transduction of SN pars compacta (SNc) neurones with little expression in SN reticularis (SNr) (Klein et al., 1998). The same injection with AAV1 and AAV5 transduces both SNc and SNr (Burger et al., 2004). Each serotype can enter different subpopulations of neurones with differing efficacies, and so this must be taken into account when deciding which one to use.

Most studies with AAVs in the CNS have focused on central administration direct into parenchyma where they can travel in both retrograde and anterograde directions (Castle et al., 2014). However this raises the question whether AAVs might be delivered in the peripheral nervous system for transduction of neurones within the CNS (Table 1.3). AAV9 can cross the BBB in both neonatal and adult mice when administered intravenously (Foust et al., 2009). There was extensive transduction of

dorsal root ganglia (DRGs), motor neurones in the spinal cord and widespread transduction of neurones and astrocytes in the brain of neonates. In adult mice there was robust transduction of astrocytes throughout the CNS but neuronal transduction was limited. AAV2 was used to deliver small interfering RNA (siRNA) to spinal motor neurones via injections into the lower hind limb (Miller et al., 2005). The siRNA down-regulated mutant SOD1 in an ALS mouse model and produced a functional effect by delaying loss of grip strength. Intramuscular injection of the quadriceps in an SOD1 ALS mouse model with AAV2-GFP successfully labelled spinal cord motor neurones with no evidence of glial transduction (Kaspar et al., 2003). Two neurotrophic factors were then delivered, GDNF and IGF-1, before disease onset. At the usual age of symptom onset (90 days) GFP-treated mice had a decline in hindlimb function as assessed by the rotarod test. IGF-1 treatment delayed onset by 31 days, and GDNF by 16 days. Survival was also increased by delivery of neurotrophic factors; IGF-1 treated mice survived on average 37 days longer than control mice, and GDNF improved life span by 11 days. The beneficial effects of IGF-1 delivery were not solely restricted to neurones, astrogliosis was reduced as assessed by glial fibrillary acidic protein (GFAP) staining suggesting IGF-1 delayed activation of astrocytes. Kaspar et al. (2003) prove that AAV2 can be used to deliver proteins via retrograde transport in motor neurones after peripheral delivery to muscles. Furthermore, the delivered neurotrophic factors are functional in the ALS mouse model, prolonging motor neurone survival, decreasing parenchymal gliosis, delaying motor function decline and prolonging survival. These effects were evident even when AAV2 was administered at the time of symptom onset; as such effects are comparable to when treatment would be given in human disease. AAV8-GFP can transduce neuronal tissue after intraperitoneal injection in neonates, with GFP immunoreactivity detected in the white matter of the spinal cord, DRGs and peripheral nerve fibres (Zheng et al., 2010). Adult mice injected with AAV8-LacZ into the gastrocnemius had transduced cells in the white matter of the spinal cord, the ipsilateral sciatic nerve and in the muscle. When AAV9-GFP was injected into the gastrocnemius of adult mice it transduced motor neurones along the whole spinal cord along with spinal astrocytes and peripheral organs (Benkhelifa-Ziyyat et al., 2013). Delivery of AAV9 vectors expressing survival of motor neuron (Smn) protein in spinal muscular atrophy mice increased lifespan by increasing Smn levels. While this is promising, the biodistribution should be taken into account in terms of off-target effects of transgene expression.

A recombinant AAV2/6 formed of a serotype 2 genome packaged in the serotype 6 capsid has been observed to retrogradely transport in both mice and primates (Towne et al., 2008; Towne et al., 2010). Intramuscular injection of AAV2/6-GFP to the

gastrocnemius in primates resulted in transduction of muscle fibres at the site of injection and motor neurones in the lumbar spinal cord; GFP signal was not detected in glial cells or interneurones, nor in upper motor neurones of the motor cortex, suggesting that the vector could not cross synapses (Towne et al., 2010). There was also no detectable immune response. AAV2/6 is able to target motor neurones from the periphery with little off-target transduction, giving the serotype potential as a therapeutic vehicle in spinal cord injury and motor neurone diseases.

AAVs can be used to target cells of the CNS after peripheral administration and different serotypes may be tested depending on the type of cell to be targeted. Their low immunogenicity, lack of toxicity and ability to provide long-lasting gene expression make them ideal for viral-mediated gene delivery of the CNS.

Serotype	Delivered	Route	Transduced cells and outcome	Reference
AAV2	siRNA	IM	Delivery of siRNA to downregulate mutant SOD1 in ALS mice resulted in delayed loss of grip strength.	(Miller et al., 2005)
AAV2	GFP	IM	GFP expressed in spinal motor neurones with no evidence of glial transduction in mice.	(Kaspar et al., 2003)
AAV2	IGF-1, GDNF	IM	Delivery of the neurotrophic factors delayed symptom onset and improved survival in ALS mice.	(Kaspar et al., 2003)
AAV2/6	GFP	IM	GFP was detected in muscle fibres at the site of injection as well as in the supplying motor neurones in primates, there was no GFP detected in glial cells or interneurones.	(Towne et al., 2010)
AAV8	GFP	IP	In neonatal mice GFP was detected in the white matter of the spinal cord, DRGs and in peripheral nerve fibres.	(Zheng et al., 2010)
AAV8	LacZ	IM	In adult mice LacZ was detected in the white matter of the spinal cord, the sciatic nerve and in the muscle.	(Zheng et al., 2010)
AAV9	GFP	IM	Motor neurones were transduced along the length of the spinal cord, as well as astrocytes and peripheral organs in mice.	(Benkhelifa-Ziyyat et al., 2013)
AAV9	Smn	IM	Smn expression levels were increased in spinal muscular atrophy mice and lifespan was increased.	(Benkhelifa-Ziyyat et al., 2013)
AA9	GFP	IV	Expression of GFP in DRGs, motor neurones and astrocytes of neonates; astrocytes were transduced in adult mice but neuronal transduction was limited.	(Foust et al., 2009)

Table 1.3 List of AAV serotypes used to transduce cells of the CNS after peripheral administration, along with route and outcome

Abbreviations: DRG – dorsal root ganglion, GDNF – glial-derived growth factor, GFP – green fluorescent protein, IGF-1 – insulin-like growth factor 1, IM – intramuscular, IP – intraperitoneal, IV – intravenous, Smn – survival of motor neuron protein, SOD1 – superoxide dismutase, siRNA – small interfering RNA

1.7 Hypotheses and Aims

Techniques to circumvent the BBB are highly desired, both as experimental tools in neuroscience and as therapeutics for neurodegenerative diseases; bacterial toxins and viruses have shown promising results as vehicles capable of this task. There are two main aims of this study. The first is to assess the ability of bacterial toxins and virally delivered sugar-binding proteins to enter neurones. The second is to develop these vehicles for neuronal tracing and the delivery of other molecules. Hypotheses have been developed relating to either the first aim, second aim or both. It is hypothesised that:

1. LTB will have a similar pattern of labelling in the CNS as CTB after systemic administration in mice.
2. Bacterial toxins may be utilised to deliver a functional protein to neurones either by direct or systemic administration of engineered fusion proteins.
3. CTB may be engineered for methods of detection other than immunohistochemistry.
4. AAV and CAV-2 vectors may be used to transduce neurones via peripheral delivery.

Chapter 2
General Methods

2.1 Common buffers, solutions and media

Analytical grade reagents were obtained from Sigma Aldrich, Thermo Scientific, Alfa Aesar, VWR International and BDH Chemicals.

2.1.1 General buffers

HEPES buffer – 50 mM HEPES, 200 mM NaCl, 5 mM $CaCl_2$ (pH 7.5)

HEPES buffer ITC – 25 mM HEPES, 150 mM NaCl (pH 7.4)

Phosphate-buffered saline (PBS) – 10 mM Na_2HPO_4, 1.8 mM KH_2PO_4, 137 mM NaCl, 4 mM KCl (pH 7.4)

PBST (0.1%)- 10 mM Na_2HPO_4, 1.8 mM KH_2PO_4, 137 mM NaCl, 4 mM KCl, 0.1% (v/v) Triton X-100

Ligase buffer – 50 mM Tris-HCl, 10 mM $MgCl_2$, 10 mM dithiothreitol (DTT), 1 mM ATP (pH 7.5)

Tris buffered saline (TBS) – 50 mM Tris, 150 mM NaCl, pH 7.6

2.1.2 Bacterial growth media

LB growth medium – 1% (*w/v*) tryptone, 1% (*w/v*) NaCl, 0.5% (*w/v*) yeast extract

High salt LB growth medium – 1% (*w/v*) tryptone, 2% (*w/v*) NaCl, 0.5% (*w/v*) yeast extract

2xYT growth medium – 1.6% (*w/v*) tryptone, 0.5% (*w/v*) NaCl, 1% (*w/v*) yeast extract

Agar gels – 1.5% (*w/v*) agar, 1% (*w/v*) tryptone, 1% (*w/v*) NaCl, 0.5% (*w/v*) yeast extract

Pfu buffer – 20 mM Tris HCl, 10 mM KCl, 10 mM $(NH_4)_2SO_4$, 2 mM $MgSO_4$, 1% (*v/v*) Triton X-100, 1 mg mL^{-1} BSA (pH 8.8)

Restriction buffer – 50 mM CH_3CO_2K, 20 mM Tris-acetate, 10 mM $Mg(CH_3COO)_2$, 1 mM DTT (pH 7.9)

2.1.3 Mini-prep buffers

Buffer N3 – 4.2 M GuHCl, 0.9 M KAc

Buffer QG – 20 mM Tris-HCl (pH 6.6), 5.5 M GuSCN

Buffer P1 – 50 mM Tris-HCl (pH 8.0), 10 mM EDTA, 100 µg mL^{-1} RNase A

Buffer P2 – 200 mM NaOH, 1% (*w/v*) SDS

Buffer PB – 5.0 M GuHCl, 30% (*v/v*) isopropanol

Buffer PE – 10 mM Tris (pH 7.5), 80% (*v/v*) ethanol

2.1.4 Electrophoresis

Agarose gel electrophoresis loading buffer – 2.5% (*w/v*) Ficoll 400, 11 mM ethylenediaminetetraacetic acid (EDTA), 3.3 mM Tris-HCl, 0.017% (*w/v*) SDS, 0.15% (*w/v*) Orange G

SDS-PAGE loading buffer – 50 mM Tris-HCl (pH 6.8), 2% (*w/v*) SDS, 10% (*v/v*) glycerol, 1% (*v/v*) β-mercaptoethanol, 12.5 mM EDTA, 0.02% (*w/v*) bromophenol blue

SDS-PAGE running buffer – 25 mM Tris, 192 mM glycine, 0.1% (*w/v*) SDS

SDS-PAGE separating gel (12%) – 380 mM Tris (pH 8.8), 12% (*w/v*) acrylamide, 0.32% (*w/v*) bis-acrylamide, 0.1% (*w/v*) SDS, 0.1% (*w/v*) ammonium persulfate, 0.01% (*v/v*) tetramethylethylenediamine (TEMED)

SDS-PAGE stacking gel (5%) – 95 mM Tris (pH 6.8), 5% (*w/v*) acrylamide, 0.13% (*w/v*) bis-acrylamide, 0.1% (*w/v*) SDS, 0.1% (*w/v*) ammonium persulfate, 0.02% (*v/v*) TEMED

Sodium bicarbonate buffer – 10 mM Na_2CO_3, 90 mM $NaHCO_3$ (pH 9.0)

TAE buffer – 40 mM Tris-acetate, 1 mM EDTA

2.1.5 Western blot

PBS-Tween – PBS with 0.1% (v/v) Tween

Transfer buffer – 39 mM glycine, 78 mM Tris Base, 20% (v/v) methanol

Blocking buffer - 5% (w/v) skimmed milk powder in PBS-Tween (0.1%)

2.1.6 Cell culture media

HEK293 cell media – DMEM/F-12, GlutaMAX™, 10% FBS (*v/v*), 5% penicillin/streptomycin (Sigma)

Acetic acid buffer – 0.2 M acetic acid, 0.5 M NaCl, pH 2.8

2.2 Design, expression and purification of a CTB-parvalbumin fusion protein

2.2.1 Media, reagents and equipment

Oligonucleotide sequences (Integrated DNA Technologies), dNTPs, Pwo polymerase, DNA standard ladders (Bioline), Protein molecular weight markers (Fermentas), agarose (Fisher Scientific), ethidium bromide (Alfa Aesar), QIAquick PCR purification (Qiagen), QIAquick gel extraction kit (Qiagen), restriction enzymes (NEB), T4 DNA ligase (NEB), calcium chloride (Sigma), β-mercaptoethanol (Sigma), ampicillin (Sigma), pSAB2.2 (Ross, 2013), QIAprep spin Miniprep kit (Qiagen), Lysogeny broth (LB) mixture (Fisher Scientific), agar (Acros Organics), IPTG (Generon), ammonium sulphate, imidazole (Acros Organics), HEPES (Fisher Scientific), Ni-NTA agarose resin (Qiagen).

Thermocycler, Nanodrop 2000 (Thermo Scientific), Universal Hood II gel documentation system (BioRad), Avanti J30-I centrifuge (Beckman Coulter), Pico 17 and Fresco 21 centrifuges (Thermo Scientific), 0.22 µm and 0.8 µm filter (Satorius Minisart), Sanger sequencing (GATC Biotech), E. coli XL10-Gold ultracompetent cells (Agilent Technologies), E. coli C41(DE3) cells (Agilent), ISF1-X shaker incubator (Kuhner).

2.2.2 Assembly PCR overview

The DNA sequence for a C-terminal fusion protein of CTB (11.6 kDa) and human parvalbumin (12 kDa) was designed with a glycine-asparagine linker region and constructed using assembly PCR (also known as polymerase cycling assembly) (Xiong et al., 2008). The technique employs a similar principle to standard PCR however the provision of the template strand differs (Figure 2.1). While usually a single whole template strand is required, in assembly PCR the template is made up of several short oligonucleotide sequences (approximately 70 bp) that alternate between sense and anti-sense and overlap by about 20 bp at either end. The oligonucleotides act as primers due to the overlap of complementary sequences, and are extended to the end of the adjacent oligonucleotide. Over subsequent PCR cycles the extended parts continue to assemble and eventually provide a full template (Smith et al., 2003). An excess of shorter ‘terminal’ forward and reverse primers complementary to the 5’ ends of the sense and antisense strands ensures the whole gene can be exponentially amplified, much like standard PCR.

Assembly PCR takes advantage of the relative ease of chemically synthesising short oligonucleotide sequences. It is possible to create other fusion proteins with the same

oligonucleotides along with new ones ordered for another gene, and also mutants can be easily generated.

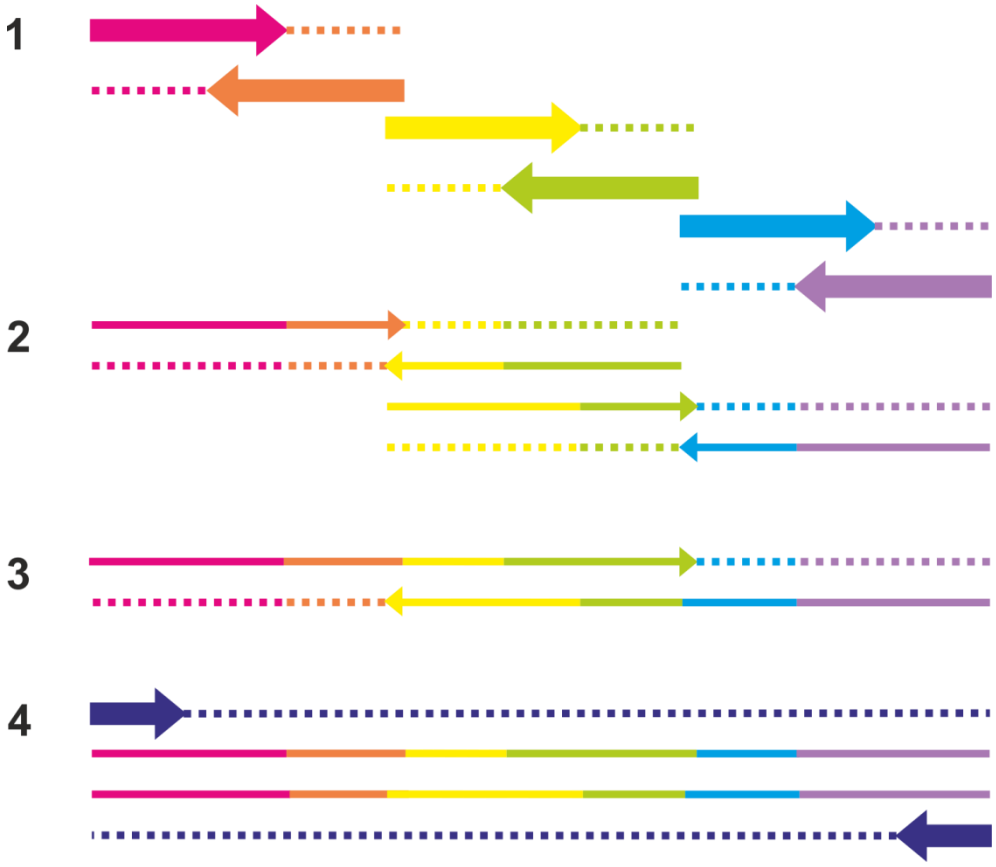

Figure 2.1 Overview of assembly PCR

1) Each coloured arrow represents an oligonucleotide sequence. The short region of complementary overlap between neighbouring sequences means they can assemble, and are extended (dotted lines) via DNA polymerase during PCR. 2 and 3) These newly extended sequences (multi-coloured arrows) assemble due to their overlapping lengths of complimentary DNA, and are extended (dotted lines). 4) Eventually the full gene sequence is produced. The shorter terminal primers (dark purple arrows) anneal to the 5’ ends of both the sense and antisense strands. This allows for extension of the whole sequence (dotted dark purple lines), resulting in exponential amplification.

2.2.3 Oligonucleotide design

Oligonucleotide sequences (Table 2.1) for assembly PCR were designed using the Assembly PCR Oligo Maker programme (Rydzanicz et al., 2005), and their properties confirmed with the OligoCalc programme (Kibbe, 2007). Primer sequences used for amplification were designed to insert the coding sequences for PstI and SphI restriction enzymes to facilitate cloning. Primer sequences were also designed for the linker region such that CTB and parvalbumin sequences could be made separately.

2.2.4 Assembly PCR

Using assembly PCR the gene for CTB was produced, as was that for the linker with parvalbumin. Then using a forward primer for CTB (5' CTGTTCAGGCGCATG 3') and reverse primer for parvalbumin (5' CTAAGTTTTCCCTGCAGG 3') the whole CTBparv gene (715 bp) was encoded.

The PCR reaction mix (50 µL total) consisted of the relevant oligonucleotides (10 nM each), terminal forward and reverse primers (2 µM each), dNTPs (200 µM each) and Pwo polymerase (0.01 U μL^{-1}) in Pfu buffer (20 mM Mg). See table 2.1 for list of oligonucleotides. The program ran for 30 cycles of melting at 95 °C for 30 seconds, annealing at 50 °C for 30 seconds, and extending at 72 °C for 120 seconds.

Nomenclature	**Sequence (5' – 3')**
CTB FT	CATGCGCCTGAACAG
Linker FT	GCAATTAGTATGGCAAAC
CTB A (with SphI)	CTGTTCAGGCGCATGCAGGAGGTGGCACTCCTCAAAATA TTACTGATTTGTGCGCAGAATACCACAACAC
CTB B	CTCTTTTTCCCGCTAGCGATTCTGTATACGAAAAGATCTT ATCATTTAGCGTATATATTTGTGTGTTGTGGTATTCTGCG
CTB C	GCTAGCGGGAAAAAGAGAGATGGCTATCATTACTTTTAA GAATGGTGCAATTTTTCAAGTAGAGGTACCAGGTAGTC
CTB D	GCAATCCTCAGGGTATCCTTCATACGTTCGATTGCCTTTT TTTGTGAATCTATATGTTGACTACCTGGTACCTCTACTTG
CTB E	GATACCCTGAGGATTGCATATCTTACTGAAGCTAAAGTC GAAAAGTTATGTGTATGGAATAATAAA

CTB F (no stop codon)	GTTTGCCATACTAATTGCGGCGATCGCATGAGGCGTTTT ATTATTCCATACACATAA
Parv A	GCAATTAGTATGGCAAACGGCGGTAATAACAATAACAAT AACAATAACAATAACGGCG
Parv B	CGCCTTCTTGATGTCCTCAGCGTTCAGCAAGTCTGTCAT CGACATACCGCCGTTATTGTTATTGTT
Parv C	AGGACATCAAGAAGGCGGTGGGAGCCTTTAGCGCTACC GACTCCTTCGACCACAAAAAGTTCTTC
Parv D	CACCTTCTTCACATCATCCGCACTCTTTTTCTTCAGGCCG ACCATTTGGAA GAACTTTTTGTGGTC
Parv E	GATGATGTGAAGAAGGTGTTTCACATGCTGGACAAGGAC AAAAGTGGCTTCATCGAGGAGGATGAG
Parv F	GACAGGTCTCTGGCATCTGGGGAGAAGCCTTTTAGGAT GAATCCCAGCTCATCCTCCTCGATGA
Parv G	ATGCCAGAGACCTGTCTGCTAAAGAAACCAAGATGCTGA TGGCTGCTGGAGACAAAGATGGGGAC
Parv H	GCTTTCAGCCACCAGAGTGGAGAATTCGTCAACCCCAAT TTTGCCGTCCCCATCTTTGTCTC
CTB RT	GTTTGCCATACTAATTGC
Parv RT (with PstI)	CTAAGTTTTCCCTGCAGG

Table 2.1 C-terminal CTB-parvalbumin fusion protein oligonucleotide sequences and primers, restriction enzyme sites highlighted

2.2.5 Determination of DNA concentration

All DNA concentrations (ng μL^{-1}) were determined by spectrophotometry at 260 nm and calculated using the equation; [DNA] = 50 × A_{260}

2.2.6 Agarose gel electrophoresis

Assembly PCR products were run on an agarose gel to visualise. Gels of 1.5% (w/v) agarose in TAE buffer with 3% (v/v) ethidium bromide were prepared. DNA samples were mixed with loading buffer, and once loaded were run at 100V for 25 minutes at constant voltage. Gels were visualised by trans-UV illumination using a Universal Hood II gel documentation system.

2.2.7 Purification of PCR product from reaction mixture (PCR clean up)

Once DNA fragments were confirmed a PCR clean up protocol was followed (QIAquick PCR purification) to remove unincorporated primers, left over dNTPs, salts and Pwo polymerase. Manufacturer recommended protocol was followed, with all centrifugation steps taking place at 17 900 x g at room temperature (21 °C). After addition of buffer PB (5 volumes) to the PCR reaction mix, the solution was passed through a silica membrane (to which DNA is adsorbed) by centrifugation for one minute. The membrane was washed twice by centrifugation for one minute with 750 µL buffer PE to remove salts, and finally DNA was eluted in 30 µL water by centrifugation for one minute.

2.2.8 Standard PCR

To amplify the gene, standard PCR was used with the assembly PCR product as the template and CTB FT and Parv RT as the forward and reverse primers (Table 2.1). The reaction mix is the same as in 2.2.4 but with 10 nM gene to be amplified in place of the parts, and the cycles are also identical.

2.2.9 Restriction digest

The insert and vector pSAB2.2 (see appendix 8.2.2 for plasmid sequence) were digested for 1 hour at 37 °C with the restriction enzymes PstI (20 U μL^{-1}) and SphI (4 U μL^{-1}), where 1 U is the amount required to digest 1 µg of λ DNA in a 50 µL reaction in one hour. Calf intestinal alkaline phosphatase (CIP) was added to the vector reaction mixture to prevent re-annealing. After digestion the insert underwent PCR clean up, while the linearised vector was gel extracted. This was accomplished using a QIAquick gel extraction kit and following the manufacturer-recommended protocol with all centrifugation steps taking place at 17 900 x g at room temperature. The vector underwent agarose gel electrophoresis, and using UV light to illuminate the gel the target band was excised using a scalpel. This was then dissolved in 3 gel volumes of buffer QG at 50 °C. After addition of 1 gel volume of isopropanol to increase the DNA yield, the solution was passed through a silica membrane by centrifugation for one minute. DNA is adsorbed to the membrane, but RNA, protein and metabolites pass through. The membrane was then washed with 750 µL PE buffer by centrifugation for one minute to remove salts, before a further minute of centrifugation to remove residual ethanol. The linearised vector was then eluted in 30 µL water by centrifugation for one minute.

2.2.10 Ligation

Digested insert and digested vector at a molar ratio of 5:1 were ligated for 30 minutes at room temperature (21 °C) in the presence of T4 DNA ligase (40 U μL^{-1}) where U is the amount required to give 50% ligation of HindIII fragments of λ DNA (5' DNA termini concentration 0.12 μM) in a total reaction volume of 20 μL in 30 minutes at 16 °C. The reaction took place in 10 μL ligase buffer with 50 ng of digested vector.

2.2.11 Production of chemically competent cells

A starter culture was prepared in 5 mL LB growth media with appropriate antibiotic and incubated overnight at 37 °C and 200 rpm. All centrifuge steps were completed at 3 000 x g and 4 °C. The overnight culture was centrifuged for 10 minutes and the supernatant discarded, while the pelleted cells were resuspended in 2 mL LB growth medium and used to inoculate 100 mL LB growth media. This was incubated at 37 °C and 200 rpm until the OD_{600} reached approximately 0.5, at this point the flask was placed on ice for 15 minutes. Sterile 0.1 M calcium chloride (50 mL) was syringe filtered through a 0.22 μm filter and placed on ice. The cooled LB growth media was then centrifuged for 10 minutes, the supernatant discarded, and cells resuspended in 10 mL $CaCl_2$ and incubated on ice for 20 minutes. This was then centrifuged for 10 minutes, resuspended in 4 mL of $CaCl_2$ and again incubated for 20 minutes on ice. After a final centrifugation step for 10 minutes, the cells were resuspended in 0.5 mL $CaCl_2$, and aliquoted competent cells stored at -80 °C for future use.

2.2.12 Transformation

Ligation reaction product (2 μL) was used to transform 10 μL E. coli XL10-Gold ultracompetent cells by heat shock. After addition of 0.4 μL β-mercaptoethanol to increase transformation efficiency cells were incubated at 4 °C for 15 minutes, 42 °C for 45 seconds, and 4 °C for 5 minutes. Transformation products were added to 1 mL of pre-warmed LB and incubated for one hour at 37 °C. Then 150 μL of LB was plated onto LB agar (1.5% (w/v), 100 μg mL^{-1} ampicillin) and incubated overnight at 37 °C. Both positive and negative controls were transformed alongside the experimental condition. Whether transformed uncut vector yielded colonies proved if the transformation was successful. With transformed cut vector it was possible to decipher whether the vector sample was completely cut. Transforming cells with just water checked for plasmid contamination of the cells.

Single colonies were picked and used to inoculate 5 mL of LB growth media with ampicillin (100 μg mL^{-1}). After incubation overnight at 37 °C and 200 rpm, a mini-prep protocol was followed to extract plasmid DNA. The DNA sequence was confirmed to be

as desired by Sanger sequencing (Sanger and Coulson, 1975; Sanger et al., 1977) via GATC Biotech. The plasmid was then transformed into the overexpression strain E. coli C41(DE3) cells as before.

2.2.13 Mini-prep – small scale plasmid DNA extraction

This was conducted using a QIAprep spin Miniprep kit and the manufacturer-recommended protocol was followed. Bacterial cells were pelleted from cultures by centrifugation at 4 500 x g for 10 minutes, and then resuspended in buffer P1 (250 µL). All further centrifugation steps took place at 17 900 x g at room temperature (21 °C). Buffer P2 (250 µL) was added to lyse the cells by alkaline lysis. After 5 minutes buffer N3 (350 µL) was added to neutralise the suspension and adjust to high salt binding conditions whilst precipitating SDS. The precipitate of SDS, genomic DNA, and cell debris was pelleted by centrifugation for 10 minutes. The supernatant was then passed through a silica membrane by centrifugation for 1 minute, where the plasmid DNA was adsorbed. The membrane was washed by centrifugation for 1 minute with buffer PB (500 µL) to remove endonucleases, and then with buffer PE (750 µL) to remove salts. The DNA could then be eluted in 50 µL of water by centrifugation for 1 minute, and concentration of plasmid measured using the Nanodrop.

2.2.14 CTBparv protein overexpression

Single colonies were taken from the plate to inoculate 5 mL of LB growth media with ampicillin (100 µg mL^{-1}). The starter cultures were incubated at 37 °C and 200 rpm overnight. Starter culture (3 mL) was added to LB growth media (2 x 1 L) which was then incubated at 37 °C and 200 rpm until the OD_{600} had reached between 0.6 and 0.8. At this point protein overexpression was induced with 0.5 mM IPTG and incubation continued for 24 hours at 30 °C and 150 rpm.

2.2.15 CTBparv protein purification

The induced cultures were centrifuged at 10 000 x g for 10 minutes at 4 °C to pellet the cells. The bacterial pellets were discarded, and the supernatant retained. To the supernatant, 570 g ammonium sulphate L^{-1} was added, and the mixture incubated at room temperature (21 °C) on a stirrer for 2 hours to precipitate the protein, or overnight at 4 °C. The solution was then centrifuged at 17 696 x g for 30 minutes at 4 °C in order to pellet the protein. The supernatant was discarded and each protein pellet resuspended by agitation for 10 minutes in 10 mL HEPES buffer with 10 mM imidazole (lysis buffer). These solutions were then pooled and centrifuged for 10 minutes at 4 000 x g, after which the resuspended protein was vacuum-filtered through a 0.8 µm filter.

2.2.16 Ni-NTA affinity chromatography overview

Nickel-nitrilotriacetic acid (Ni-NTA) affinity chromatography was used to purify the protein. Each CTB monomer has three histidine residues, two of which (His13 and His94) are known to contribute to Ni^{2+} co-ordination (Dertzbaugh and Cox, 1998). Pentamer formation results in these His residues acting similarly to a His-tag, thus enhancing co-ordination and allowing the pentameric protein to bind the Ni-NTA resin.

Histidine contains an imidazole ring that allows the binding to Ni^{2+} on the column. Flushing the column with buffer containing a high concentration of free imidazole means the bound protein will be washed off the column to be collected (Porath, 1992).

2.2.17 Ni-NTA column purification

The protein sample was passed down a Ni-NTA column that had been pre-equilibrated with lysis buffer containing 10 mM imidazole. The column was washed with 25 mL HEPES with 25 mM imidazole so that any non-specifically bound proteins are removed. The protein is eluted with 25 mL HEPES buffer with 250 mM imidazole and collected in 5 mL fractions.

2.2.18 Determination of protein concentration

Using the equation $[\text{Protein}] = \frac{A_{280}}{\varepsilon}$ the concentration (M) of CTBparv was calculated. Spectrophotometric analysis at 280 nm of the protein was used to give A_{280}, and the molar extinction coefficient (ε) of 11,585 M^{-1} cm^{-1} was provided by the ProtParam tool (ExPASy).

2.2.19 CTB protein expression

A stab from a stock of *Vibrio sp.60* containing the pATA13 plasmid (Aman et al., 2001) encoding CTB was used to inoculate 5 mL of high salt LB growth media with ampicillin (100 µg mL^{-1}). This starter culture was incubated at 37 °C and 200 rpm for 20 hours, and then 3 mL added to high salt growth media (1 L). When the OD_{600} had reached approximately 0.5, IPTG (0.5 mM) was added to induce protein overexpression and the incubation continued for 24 hours. The cells were isolated by centrifugation at 17 000 x g for 30 minutes, after which the cell pellet was discarded and the supernatant retained. Procedure was then followed as in 2.2.15 to purify the protein followed by Ni-NTA column purification.

2.3 Protein characterisation

2.3.1 Media, reagents and equipment

Acrylamide (Fisher Scientific), instant blue (Generon), EDTA (Fisher Scientific), calcium chloride (Sigma), 1,4-butanedioldiglycidyl (Sigma), Sepharose 4B (Sigma), 1,6-diaminohexane (Sigma), EDAC (Sigma), ethanol (Sigma). GM1 oligosaccharide was prepared by Darren Machin from GM1 (Carbosynth) using recombinant Leech endoglycosylceramidase, amplex red assay kit (Fisher Scientific).

X-cell blot II module (Invitrogen), C-DiGit blot scanner (LI-COR), ÄKTA FPLC system (GE Healthcare) with S200 26/60 column (GE Healthcare), MicroCal iTC200 System (GE Healthcare), SnakeSkin® pleated dialysis tubing (Thermo Scientific).

2.3.2 SDS-PAGE

Running gels of 12% (w/v) acrylamide (37.5:1 acrylamide:bis-acrylamide) with a 5% (w/v) acrylamide stacking gel were prepared (see section 2.4.1). Prior to loading, protein samples were mixed with loading buffer, and the gels run at 180 V in running buffer. Gels were stained with Instant Blue for half an hour, washed in water on a rocker overnight, and then visualised by trans-illumination using the gel documentation system.

2.3.3 ÄKTA protein purification

Proteins were separated for analysis using the ÄKTA fast protein liquid chromatography (FPLC) system. Protein was loaded (1.5 mL) and run on the S200 26/60 column at 4°C into 0.22 µm filtered HEPES buffer. Fractions of 5 mL were collected and analysed by SDS-PAGE (2.3.2).

2.3.4 Mass spectrometry

To assess the mass of protein, liquid chromatography mass spectrometry (LC-MS) was employed. Protein samples were prepared by diluting in water to 10 µM, and 10 µL injected directly via the autosampling system. The HPLC utilised a Dionex Ultimate 3000 UPLC system using a gradient of acetonitrile and water both with 0.1% formic acid as the eluent system. This was linked to a Bruker MaXis Impact mass spectrometer equipped with electrospray ionisation (ESI). Data processing was performed with ESI Compass 1.3 DataAnalysis V4.0 software (Bruker Daltonik).

2.3.5 Western blot

Western blot was used to assess whether each part of the fusion protein was present when detected with antibodies. Gels of 12% (w/v) acrylamide (37.5:1 acrylamide:bis-

acrylamide) were prepared. Protein samples were made up in loading buffer with 30 µg, 3 µg and 0.3 µg CTBparv. Once loaded, the gels were run at 30 mA for 30 minutes in running buffer.

Sponges and filter paper were soaked in transfer buffer. Polyvinylidene fluoride (PVDF) membrane was activated in methanol for 1 minute, washed in distilled water and then soaked in transfer buffer for 10 minutes. Proteins were transferred from the SDS gel onto a PVDF membrane for 30 minutes at 30 V in the transfer cell. The membrane was rinsed in PBS-Tween, and then blocked for 2 hours at room temperature (21 °C) in 5% blocking buffer to reduce non-specific binding. The membrane was incubated with primary antibody (Table 2.2) diluted in blocking buffer overnight at 4 °C with agitation. After washing in PBS-Tween for 15 minutes, three times, the membrane was incubated with appropriate secondary antibodies diluted (1:20 000) in blocking buffer for 1 hour at room temperature (Anti-mouse-HRP, 7076; anti-rabbit-HRP 7074, Cell signalling). The membrane was washed again as previous, and protein bands detected using chemiluminescent substrate from Amersham (RPN 2232) following manufacturer guidelines. Blots were visualised with a C-DiGit blot scanner.

2.3.6 Isothermal titration calorimetry

2.3.6.1 Isothermal titration calorimetry overview

Isothermal titration calorimetry (ITC) allows for the sensitive measurement of the thermodynamic parameters of reactions in solution. The enthalpy change (ΔH), association constant (K_a) and stoichiometry of a reaction (N) can be directly measured. The dissociation constant (K_d) can be derived from K_a ($1/K_a$). The technique will allow measurement of whether CTB fusion proteins retain ability to bind the ligand GM1, and may also be used to assess calcium binding properties of proteins

2.3.6.2 Isothermal titration calorimetry method

ITC was carried out using a MicroCal iTC200 System with cell temperature at 25 °C, reference power set to 5, and a stirring speed of 750 rpm. A total of 202.8 µL (sample cell volume) CTBparv protein at 11 µM was loaded into the sample cell, and 38.5 µL of the ligand GM1-oligosaccharide at 88 µM was added to the sample cell over 20 injections; 1 x 0.5 µL over the duration of 1 second, 19 x 2 µL over the duration of 4 seconds, with 120 seconds recovery between injections. Buffers were matched by dialysis to HEPES buffer prior to ITC using SnakeSkin® pleated dialysis tubing with 7000 MWCO. Titrations of buffer into buffer, and ligand into buffer were carried out as controls to measure heat of dilution. Data was fitted using NITPIC (Keller et al., 2012),

thermodynamic parameters calculated using SEDPHAT, and presented using GUSSI (NIH).

To assess the calcium binding properties of CTBparv ITC was utilised. CTBparv was incubated at room temperature (21 °C) with 10 mM ethylenediaminetetraacetic acid (EDTA) to remove calcium ions. The protein (1 mL) was then dialysed four times, using SnakeSkin® pleated dialysis tubing with 7000 MWCO into buffer (1 L) with 0.025 M HEPES, 0.15 M NaCl, pH 7.4 (Henzl et al., 2003), to remove EDTA. Following dialysis CTBparv concentration was measured as 8.9 μM (section 2.2.18). Ligand should be titrated at 7-10 times the concentration of protein, however since parvalbumin has two calcium binding sites, 16 times as much calcium chloride was titrated. A total of 202.8 μL CTBparv protein at 8.9 μM was loaded into the sample cell, and 38.5 μL of the ligand $CaCl_2$ at 142.2 μM was added to the sample cell over 20 injections; 1 x 0.5 μL over the duration of 1 second, 19 x 2 μL over the duration of 4 seconds, with 120 seconds recovery between injections.

CTBparv was incubated with EDTA-agarose (see 2.3.7) to remove calcium ions. First CTBparv was dialysed into ITC buffer using SnakeSkin® pleated dialysis tubing with 7000 MWCO. 400 μL CTBparv at 21.4 μM was added to EDTA-agarose in a mini-spin column and mixed, this was left incubating at room temperature for 1 hour. It was then spun at 2.6 rpm for one minute to rescue the protein. Following a final round of dialysis, CTBparv was diluted to 10 μM, and calcium chloride was made up at 160 μM with dialysed ITC buffer. The same protocol was followed as previous.

2.3.7 Preparation of EDTA-agarose

Calcium ions were sequestered from CTBparv by passage over EDTA-agarose. The chelating matrix was prepared using carbodiimide-mediated coupling of EDTA to aminohexyl agarose (Haner et al., 1984; Pepper, 1994).

In a 50 mL falcon tube, 10 mL of 0.6 N NaOH and 10 mL of 1,4-butanedioldiglycidyl were added to 10 mL Sepharose 4B; this was incubated overnight with constant agitation at 25 °C. The suspension was filtered through a sintered-glass funnel and washed extensively with hot water. 1 g of 1,6-diaminohexane was dissolved in 10 mL of 1 M sodium carbonate and the pH adjusted to 13 with NaOH. This solution was added to the epoxy-activated agarose, and pH readjusted to 13 if required. The suspension was then incubated for 24 hours with vigorous agitation at 25 °C. Following incubation the excess reagents were removed by filtration and the gel washed with water. The aminohexyl agarose is resuspended in 25 mL of 0.5 M EDTA, pH 6, and then 0.5 g of 1-Ethyl-3-(3-dimethylaminopropyl)carbodiimide (EDAC) added. The gel

suspension was incubated at room temperature (21 °C) with constant agitation for 4 hours. The pH was measured and readjusted to pH 6 if necessary, and then another 0.5 g of EDAC added. The incubation was continued for another 4 hours, and then the gel washed extensively with water, followed by 10 mM Ca^{2+} to remove excess EDTA. The agarose was then put into a column and stored in 20% ethanol at 4 °C.

Prior to protein loading, the gel was acidified dilute HCl (pH 2) to remove bound divalent ions, and then neutralised with ITC buffer.

2.3.8 Enzyme-linked immunosorbent assay (ELISA)

An ELISA was used to test whether anti-CTB antibody (Sigma, C3062) could detect both CTB and LTB. A black flat-bottomed high-binding Greiner plate (655077) was coated with GM1 by adding 100 µL of 20 µg/mL in ethanol and left to evaporate overnight. The plate was then washed three times by adding 200 µL of PBS. The wells were blocked with 1% bovine serum albumin (BSA) in PBS for 30 minutes at 37 °C and then washed three times with PBS with 0.1% BSA and 0.05% Tween (assay buffer). CTB and LTB were added to the wells at 1 µM in 0.1% BSA and 0.05% Tween, each in triplicate and left for 30 minutes at room temperature (21 °C). Following another round of assay buffer washes the primary antibody was added at 1:5 000 in assay buffer, rabbit anti-CTB (Sigma, C3062), and left to incubate for 30 minutes at room temperature. The antibody was removed and the wells washed three times with assay buffer. A secondary HRP-linked antibody, anti-rabbit HRP (Cell Signalling, 7074), was then added at a dilution of 1:10 000 in assay buffer and left at room temperature for one hour. The antibody was removed and the plate washed three times with assay buffer. The detection solution containing 5 µM amplex red with 5 µM hydrogen peroxide in PBS was added at 200 µL per well. The change in fluorescence (excitation 531 nm, emission 595 nm) was then measured on the EnVision plate reader (Perkin Elmer) over 5 minutes. The end-point fluorescence units were noted and compared to those of wells where only the secondary antibody was added.

2.4 Cell culture

2.4.1 Media, reagents and equipment

DMEM/F-12, GlutaMAX™ (Life Technologies), Foetal bovine serum (Sigma), penicillin/streptomycin (Sigma), TrypLE™ Select (Life Technologies), poly-D-lysine (Sigma), HBSS, collagenase type 1A (Sigma), dispase (Sigma), laminin (Generon).

Centrifuge (Denley BS-400), T75 flasks (CellStar), 13 mm glass coverslips (12392128, Fisher Scientific), 24 well plates (662160, CellStar).

2.4.2 HEK293 cell culture

HEK 293 cells were used to assess cell entry of CTBparv as they express the ganglioside GM1 and thus it was expected CTBparv could be endocytosed.

Human embryonic kidney (HEK293) cells were grown in Dulbecco's modified Eagle's medium (DMEM) with 10% foetal bovine serum (FBS) and 5% penicillin/streptomycin. When cells reached around 90% confluency they were split into new flasks. After two washes with sterile PBS, cells were incubated at 37 °C for 5 minutes with TrypLE™ Select to detach them from the flask. They were then resuspended in 4 mL DMEM and centrifuged for 5 minutes at 1000 x g. The supernatant was discarded, and the pelleted cells resuspended in 1 mL DMEM. For general passage, 150 µL of the cell suspension was added to 20 mL DMEM in a T75 flask.

2.4.3 Poly-D-lysine coating

Glass coverslips were coated with 0.01% poly-D-lysine to improve adherence of cells. The solution was left for 1 hour, removed, and then washed with PBS before adding cells.

2.4.4 Incubation of HEK 293 cells with CTB and CTBparv

HEK 293 cells were incubated with CTB and CTBparv to assess whether the proteins could be endocytosed. Approximately 100 000 cells were seeded onto 13 mm sterile glass coverslips coated with poly-D-lysine in 24 well plates and maintained in DMEM. They were left for 48 hours to attach to the coverslip and reach at least 80% confluency. Media was then removed and replaced with DMEM containing 1 µg of CTB or CTBparv. Cells were incubated for 1, 2, 4, 8 and 24 hours, washed in PBS for 5 minutes, washed in acetic acid buffer for 6 minutes followed by a final PBS wash for 5 minutes, and fixed with 4% PFA for 30 minutes. HEK 293 cells were also incubated for 4 hours with decreasing amounts (1 µg, 500 ng, 100 ng) of CTBparv to assess the minimal dose that could be detected. Following fixation cells underwent immunohistochemistry as described in section 2.6.3.

2.4.5 Dorsal root ganglia (DRG) culture

Dorsal root ganglia from all spinal cord levels were extracted from 7 – 10 day old rats. They were dissociated in HBSS with collagenase type 1A (1 mg/mL) and dispase (1 mg/mL) at 37 °C for 13 minutes. Cells were then mechanically triturated and returned to be incubated a further 2-3 minutes. The solution was gently triturated again,

with care taken not to introduce bubbles and the cells were washed twice by centrifugation for 5 minutes at 800 rpm and 4 °C. The pellet was resuspended in 600 µL of pre-warmed DMEM, and 85 µL plated onto poly-D-lysine and laminin coated glass coverslips. After 4 hours the wells were flooded with 1 mL of pre-warmed DMEM and incubated for 24 hours. Medium was removed and replaced with 500 µL DMEM containing 2 µg/ml of CTBparv. After 24 hours DRGs were fixed with 4% PFA for 30 minutes at room temperature (21 °C). They then underwent immunohistochemistry protocol (2.6.3), and were imaged on the LSM880 with Airyscan.

2.5 *In vivo* experimentation

2.5.1 Media, reagents and equipment

HEPES (Thermo Scientific), isoflurane (IsoFlo, Abbott), sodium pentobarbitone (Animalcare), veterinary wound powder (Battles), buprenorphine (Vetergesic, Animal Health), paraformaldehyde (Sigma), 25% glutaraldehyde (Merck), sucrose (Thermo Scientific), gelatine (Sigma), FSC 22 Clear (Leica).

Vicryl absorbable sutures (W9105, Ethicon), black braided silk with 16mm curved needle (W2502, Ethicon), glass micropipettes (1B150-4, WPI Inc), micropipette puller (P-97, Sutter Instrument Company), Hamilton syringe (701N), stereotaxic frame (Stoelting), cryostat (CM1850, Leica), vibrating microtome (VT1000S, Leica).

2.5.2 Animals

All experiments were performed under Home Office Licence, in accordance with the regulations of the UK Animals (Scientific Procedures) Act, 1986. Experiments were carried out on young C75Bl/6 adult mice (20–25 g) or young Wistar rats (65-85 g) of both genders, bred in house. For surgical procedures, muscle was sutured with coated vicryl absorbable sutures and the skin with black braided silk with 16mm curved needle; sutures were dusted with veterinary wound powder to prevent infection. All animals were administered 0.05 mg/kg buprenorphine intramuscularly after any surgery deemed ‘moderate’ by the Home Office.

2.5.3 Heat-labile enterotoxin B (LTB) injections in mice

LTB was produced by the Turnbull lab. Unanaesthetised mice (n=4, each) were injected intraperitoneally (IP) with 2000, 1000 or 500 µg LTB dissolved in 100 µL of 0.1 M phosphate buffered saline (PBS) using a sterile 0.5 cc syringe; mice were perfused after 3 days. For intravenous (IV) injections mice (n=3, each) were deeply anaesthetised with isoflurane and 500, 250 or 125 µg of LTB dissolved in 50 µL of 0.1

M PBS was administered to the right jugular vein. Mice undergoing IV injections were perfused after 5 days.

2.5.4 Cholera toxin B (CTB) injections in mice

Unanaesthetised mice were injected intraperitoneally with 2000, or 500 µg CTB (n=3, each) dissolved in either HEPES buffer or PBS. They were perfused after 3 days. For intramuscular (IM) injections of the tongue, mice (n=3) were deeply anaesthetised with isoflurane. The tongues were stretched out of their mouths using forceps, and 2 µL HEPES buffer with 80 µg CTB injected with a glass micropipette attached to a 10 µL Hamilton syringe. Mice were perfused after 3 days. For IM injections to the gastrocnemius mice (n=2) were anaesthetised with isoflurane and the left leg taped down, the area over the gastrocnemius was shaved. An incision was made to expose the muscle and a series of four 1 µL injections were made along the entire motor end plate (Mohan et al, 2014). A total of 80 µg was injected manually via graded glass micropipettes attached to a 10 µL Hamilton syringe. Care was taken not to damage the fasciae or the blood vessels. Mice were perfused after 4 days.

2.5.5 CTBparv injections in mice

Unanaesthetised mice (n=3, each) were injected intraperitoneally with 2000, 1000 or 500 µg CTBparv dissolved in 100 µL of HEPES buffer using a sterile 0.5 cc syringe and perfused after 3 days. Young (P14) mice (n=2) were injected IP with 500 µg of CTBparv and perfused after two days. For IM injections of the tongue, mice were deeply anaesthetised with isoflurane and 2 µL HEPES buffer with 50 µg CTBparv injected with a glass micropipette attached to a 10 µL Hamilton syringe. Mice were perfused after 1, 4, 7 and 13 days (n=3, each day). IM injections to the gastrocnemius (n=2) were performed as in 2.5.4.

2.5.6 Transcardial perfusion for fixation of tissue

Animals were deeply anaesthetised with sodium pentobarbitone (60 mg/kg, IP) and pedal reflexes tested to verify that the animals were fully sedated. First the abdomen was dissected transversely and then a thoracotomy performed to access the heart. The left ventricle was pierced, a blunt needle inserted and clipped into place. After the right atrium had been cut, the animals were flushed with 0.1 M phosphate buffer, followed by perfusion with approximately 150 mL of 4% PFA.

2.5.7 Tissue preparation

For IP injected animals, organs (brain, spinal cord, heart, liver, kidney and small intestine) and dorsal root ganglia (DRGs) were removed and post-fixed in 4% PFA for 24 hours at 4 °C. For all other injection routes the relevant portion of spinal cord or

brainstem was removed and post-fixed. The kidney, liver, small intestine and DRG samples were then set in gelatine and fixed in 4% PFA with 0.25% glutaraldehyde in 0.1 M phosphate buffer. Hearts were cryoprotected with 20% sucrose, embedded in FSC 22 Clear and kept at -80 °C. They were sectioned on a cryostat at 50 µm thickness and mounted immediately onto gelatinised slides. All other organs were sectioned at 50 µm thickness on a vibrating microtome and free floating sections collected in PBS. All brainstem and spinal cord sections were sectioned transversely. For cell counting, sections were cut serially and each third section taken for immunohistochemistry.

2.6 Immunohistochemical techniques

2.6.1 Media, reagents and equipment

PBS tablets (Oxoid), Triton X-100 (BDH Chemicals), Alexa Flour ®488 and ®555 (Invitrogen), biotinylated secondary antibodies (Vector Labs), Streptavidin Pacific blue (Invitrogen), Vectashield mounting medium (Vector Labs), sodium citrate (BDH Chemicals), 30% v/v hydrogen peroxide (Sigma), ExtrAvidin®-Peroxidase (Sigma), DAB kit (Vector Labs), xylene (Sigma), DPX (BDH Lab Supplies).

2.6.2 Immunohistochemistry overview

Immunohistochemistry utilises the binding of antibodies to antigens as a way to visualise the presence of proteins in a tissue. Primary antibodies are raised against the protein of interest; these may be polyclonal – binding to multiple different epitopes within the protein, or monoclonal – binding to one epitope. Then a secondary antibody with a visualisation tag is used, this is raised against the animal that the primary antibody came from.

2.6.3 Fluorescent immunohistochemistry

Sections of brainstem and spinal cord, as well as other organs, underwent immunohistochemical analysis to visualise proteins (see Table 2.2 for details of primary antibodies). Brainstem, spinal cord and other organs from animals that received no injections were processed alongside experimental tissues as controls.

Sections underwent three 10 minute washes in PBS and were then pre-incubated with 10% donkey serum diluted in PBS for 30 minutes. Next they were incubated in the appropriate primary antibodies diluted in PBST (PBS with 0.1% Triton X-100) for 12-24 hours at 4 °C. Following three 10 minute washes in PBS, the sections were incubated in species-specific secondary antibodies conjugated to Alexa Flour ®488 or ®555 at

1:1000, or a biotinylated secondary antibody at 1:250 followed by Streptavidin Pacific blue; all for approximately two to three hours. Sections were then washed in PBS, air-dried onto glass microscope slides and mounted under a coverslip with Vectashield mounting medium.

Immunohistochemistry for CD24 antibody required antigen retrieval techniques, before being incubated in donkey serum, slices were heated at 70 °C in 10 mM sodium citrate for 30 minutes. The ChAT antibody was incubated with PBS with 0.2% Triton, and left for 48 hours.

2.6.4 Diaminobenzidine (DAB) immunohistochemistry

Immunohistochemistry with DAB was used to label LTB or CTB positive cells and produce a permanent reaction product. Tissue sections were washed three times for 10 minutes with PBS before being incubated with 1% hydrogen peroxide in PBS for 30 minutes to quench endogenous peroxidase. After another three washes in PBS the sections were incubated with a primary antibody raised against CTB (Table 2.2) for 12-24 hours at 4 °C. The sections were washed in PBS and then incubated in biotinylated donkey anti-chicken for 4 hours. Following another set of PBS washes the sections were incubated in ExtrAvidin®-Peroxidase at 1:1500 overnight at 4 °C. This was then visualised with a DAB kit, with slices immersed in the solution for 2 minutes and washed in distilled water. Sections were then mounted onto gelatinised slides and air dried overnight. After dehydration in graded alcohols (50%, 70%, 95%, 100% and 100%) and clearing in xylene, the sections were mounted under coverslips with DPX.

2.6.5 Microscopy and Image Capture

For both fluorescent and DAB immunohistochemistry, the slides were examined using a Nikon Eclipse E600 microscope equipped with epifluoresence and Q-Imaging Micropublishing 5.0 camera. Images were obtained using AcQuis image capture software and adjusted for brightness and contrast using CorelDraw x6 software.

In addition, some tissue sections were selected to be visualised and captured using a confocal microscope (Zeiss LSM 510 Meta Confocal Microscope) and Zeiss LSM Image browser software. High resolution images were captured with the Zeiss LSM 880 Confocal Microscope with Airyscan.

Primary antibody to	Abbreviation	Raised in	Dilution	Source	Catalogue #	Reference
Cholera toxin B subunit	CTB	Chicken Rabbit	1:10000 1:10000	Abcam Sigma	AB19106 C3062	(Jalabert et al., 2011)
Choline acetyltransferase	ChAT	Goat	1:500	Chemicon	AB144	(Xu et al., 2009)
c-kit		Rabbit	1:500	Agilent	A4502	(Garrity et al., 2009)
Isolectin B4	IB4	Biotinylated	1:1000	Vector Labs	B-1205	
Lysosomal-associated membrane protein 1	LAMP-1	Rat	1:100	DSHB	1D4B	
mCherry		Rabbit	1:5000	Badrilla	A010-mCherry-50	
NeuN		Mouse	1:1000	Millipore	MAB377	(Mullen et al., 1992)
Parvalbumin	Parv	Mouse	1:2500	Swant	PV235	(Celio, 1990)
Tetanus toxin C	TTC	Rabbit	1:500	Rockland	100-401-894	(Chian et al., 2009)
Vesicular glutamate transporter 1	vGLUT1	Guinea pig	1:20000	Millipore	AB5905	(Oliveira et al., 2003)
Wheat germ agglutinin	WGA	Rabbit	1:20000	Sigma	T4144	(Dobi et al., 2010)

Table 2.2 List of all antibodies used

2.8 CTB-azide

2.8.1 Media, reagents and equipment

CTB-azide (produced by Daniel Williamson, Turnbull lab), biotinylated alkyne (EVU103, Kerafast).

2.8.2 *In vivo* testing of CTB-azide in mice

CTB-azide was tested for retrograde transport and detection with click chemistry *in vivo* via tongue injections. Mice (n=4) were administered 50 µg of CTB-azide into the tongue (as described in section 2.5.4) and perfused after two days. The brainstem was removed and re-sectioned as described in section 2.5.7.

2.8.3 Copper-Catalysed Azide-Alkyne Cycloaddition (CuAAC)

Copper-catalysed azide-alkyne cycloaddition (CuAAC) (Rostovtsev et al., 2002) allows for the bioconjugation of two molecules in a 'one-pot' reaction. The azide group within CTB can be reacted with a biotinylated alkyne. The subsequent biotinylated CTB could then be detected without an antibody, using avidin tagged with a fluorophore or peroxidase instead.

For the click reaction, the conditions from a 5-ethynyl-2′-deoxyuridine (EdU) and biotinylated azide reaction in animal tissue were used (Salic and Mitchison, 2008). Fixed slices were incubated in 0.2% PBST for 30 minutes and then washed twice for 10 minutes in Tris buffered saline (TBS). A solution containing 100 mM Tris (from 2 M Tris, pH 8.5), 1 mM Cu(II)SO_4, 10 µM biotinylated alkyne and 100 mM ascorbic acid was added to the wells, and left to incubate for 30 minutes at room temperature (21 °C) hidden from light. Following two 10 minute washes in TBS, the slices were incubated with Streptavidin Alexa Fluor® 555 at 1:1000 in PBS for two hours. To assess whether CTB was labelled by the click reaction, immunohistochemistry (section 2.6.3) for CTB was also used to check for double labelling. Controls of brainstem slices without CTB-azide underwent the click reaction to check for non-specific labelling.

2.9 AB_5-streptavidin-Alexafluor 555

2.9.1 *In vivo* testing of AB_5-streptavidin-Alexafluor 555 in mice

AB_5-streptavidin-555 (produced by Daniel Williamson, Turnbull lab) was tested for retrograde transport *in vivo* via tongue injections. Mice (n=2) were administered 30 µg of AB_5-streptavidin-555 into the tongue (as described in section 2.5.4) and perfused after 3 days. The brainstem was removed and re-sectioned as described in section

2.5.7. Slices underwent immunohistochemistry as described in section 2.6.3 with antibodies for either CTB or LAMP1 (Table 2.2).

2.10 CTB-quantum dot

2.10.1 Media, reagents and equipment

Silver enhancement kit (Nanoprobes), gold chloride (Sigma), osmium tetroxide (Taab Laboratory Equipment Ltd), durcupan resin (Sigma), uranyl acetate (Taab Laboratory Equipment Ltd), lead citrate (Taab Laboratory Equipment Ltd), Leica Ultracut.

2.10.2 *In vivo* testing of a CTB-quantum dot in mice

CTB conjugated to quantum dots (CTB-QD, produced by Emma Poole, Zhou lab, and Daniel Williamson, Turnbull lab) was tested for retrograde transport *in vivo* via tongue injections. Mice (n=2) were administered 2 µL of CTB-QD (2.78 µM) into the tongue (as described in section 2.5.4) and perfused after 3 days. The brainstem was removed and re-sectioned as described in section 2.5.7. Slices underwent immunohistochemistry as described in section 2.6.3 with antibodies for CTB. Mice were injected with just QD as a control.

2.10.3 Silver enhancement

Brainstem slices underwent silver enhancement to visualise QDs using HQ Silver (Nanoprobes). Manufacturer's guidelines were followed and slices imaged using Nikon Eclipse E600 microscope.

2.10.4 Processing for electron microscopy

Animals for EM were fixed with 4% PFA with 1% glutaraldehyde via transcardial perfusion (described in section 2.5.6). Slices (50 µm) then underwent silver enhancement and were incubated in gold chloride to fix the silver. Following three 10 minutes washes in PB, slices were incubated in 0.5% osmium in 0.1 M PB for 30 minutes to fix membrane lipids; osmium also acts as a stain for EM as it is electron dense. Following another round of washes in PB and then in distilled water the slices were dehydrated in increasing concentrations of acetone for 7 minutes each (50%, 70%, 90%, 100%, 100%). Resin is then added in increasing ratios mixed with acetone (25%, 50%, and 80%) for 30 minutes each and then the slices placed in resin in a small metal planchette and left overnight for acetone to evaporate.

A clean glass slide and the planchette are placed on a hotplate. Each section is removed from the planchette, placed onto the slide and mounted with a plastic

coverslip. The slides are then incubated at 60 °C for 48 hours for the resin to polymerise. After removing the plastic coverslip the slide is heated and using a scalpel the resin around the slice scored until the slice is freed. The resin embedded slice can then be glued on top of a resin block and the excess surrounding resin trimmed away with a razor blade. Resin is then trimmed from the top of the block with a glass knife using the ultracutter. A diamond knife is used for cutting 70 nm sections of resin embedded tissue; the sections are collected copper slot grids coated with formvar. After drying the grids are incubated in uranyl acetate for 3 minutes; this enhances contrast via interaction with lipids and proteins. Ultra-thin sections are washed in distilled water and left to dry. The grids are then incubated in 1% lead citrate for 3 minutes to enhance contrast through interaction with proteins and glycogens; sections undergo a final wash in distilled water.

Finally, ultra-thin slices can be imaged using an FEI G2 Spirit with LaB6 gun equipped with Gatan 2k CCD camera, operating on 120kV. Images were put together using CorelDraw x6 software.

2.11 Viral tracing studies

2.11.1 Media, reagents and equipment

Isoflurane (IsoFlo, Abbott), sodium pentobarbitone (Animalcare), veterinary wound powder (Battles), buprenorphine (Vetergesic, Animal Health), paraformaldehyde (Sigma).

Vicryl absorbable sutures (W9105, Ethicon), black braided silk with 16mm curved needle (W2502, Ethicon), glass micropipettes (1B150-4, WPI Inc), micropipette puller (P-97, Sutter Instrument Company), Hamilton syringe (701N), stereotaxic frame (Stoelting).

2.11.2 Adeno-associated virus (AAV)

AAV2 containing pAAV-EF1a-mCherry-IRES-WGA-Cre (UNC Gene Therapy Vector Core) was tested for its' ability to transfect neurons from the periphery via a number of different routes in both rats and mice (Table 2.3). AAV2 (2.7×10^{12} virus molecules/mL) was injected into the tongues of mice (n=3 per serotype) in 2 µL with a glass micropipette attached to a 10 µL Hamilton syringe. Mice were perfused after 4 or 6 weeks. For nodose ganglion injections rats were deeply anaesthetised with isoflurane. An incision was made lateral to the midline and using blunt dissection the vagus nerve exposed, 1 µL of AAV2 was injected and rats perfused after 4 weeks (n=1 per route).

AAV2 was delivered intranasally in a rat with 1 µL applied into the left nostril; the rat was perfused after 4 weeks. For fourth ventricle (4V) injections, mice (n=2) were anaesthetised with isoflurane and a craniotomy and durotomy performed over the area of interest, then 1 µL of AAV2 injected with a glass micropipette beneath the cerebellum; mice were perfused after 6 weeks.

Route	Species
Tongue	mouse
Nodose ganglion	rat
4V	mouse
Intranasal	rat

Table 2.3 Injection routes for AAVs, tested serotypes listed with species

2.11.3 Canine adenovirus 2 (CAV-2)

CAV-2 (Montpellier Vectorology (PVM)) expressing GFP-TTC (3.7×10^{16} viral genomes (VG)/mL) was injected peripherally to transduce neurones, with the GFP-TTC able to retrogradely transport and cross synapses, allowing for elucidation of networks. A reporter virus expressing DsRed (5.7×10^{12} VG/mL) was used to transduce and select first order neurones. The routes tested are listed in table 2.4. Gastrocnemius injections were completed as described in section 2.5.4, with 1 µL of each virus injected. Rats were culled after 4 weeks (n=2) or 5 weeks (n=2). Tongue injections were completed as described in section 2.5.4, with 1 µL of each virus injected; mice were culled after 3 weeks (n=1) or 4 weeks (n=3). Nodose ganglion injections were completed as in section 2.11.2, 1 µL of CAV-2-GFP-TTC was injected and the rat (n=1) was culled after 4 weeks. SCG injections were carried out as described in section 2.11.2, 1 µL of CAV-2-GFP-TTC was injected and the rats (n=3) were culled after 4 weeks. For sciatic nerve injections rats were anaesthetised with isoflurane. A midline incision was made along the posterior aspect of the right hindlimb and connective tissue eased away to expose the muscles. The biceps femoris was cut across, and via blunt dissection the sciatic nerve was exposed. With a glass micropipette inserted parallel to the nerve, 1 µL of each virus was slowly injected. The area was rinsed with saline to wash away virus that may have spilled. Rats were culled after 4 weeks (n=1), or 5 weeks (n=1). Injections to the peroneal nerve were made in a similar manner to sciatic nerve injection. 1 µL of each virus was slowly injected, and the mouse was culled after 4 weeks. For injections to the adrenal gland (n=1), the left side of the lower back was shaved and a longitudinal incision of about 1 cm made from the last rib. Using blunt dissection the muscle was parted to expose the kidney and 1 µL of each virus injected into the adrenal gland with a glass micropipette attached to a 10 µL Hamilton syringe. The

mouse was perfused after 4 weeks. CAV-2 was delivered intranasally in a rat with 1 µL applied into the right nostril; the rat (n=1) was culled after 4 weeks.

Route	Species
Gastrocnemius	rat
Tongue	mouse
Nodose	rat
SCG	rat
Sciatic nerve	rat
Peroneal nerve	mouse
Adrenal gland	mouse
Intranasal	rat

Table 2.4 Injection routes for CAV-2 listed with species tested

2.11.4 Testing virus expression with cell culture

An adenovirus producer cell line (911 cells) created from human retinoblast cells were used to assess infection efficiency (Fallaux et al., 1996). The 911 cells were cultured as in 2.4.2. Cells were seeded at 100,000 per well on poly-D-lysine coated glass coverslips in a 24 well plate in DMEM and left to settle overnight. Then CAV2-GFP-TTC was added at 3.7×10^{11} VG and CAV2-DsRed at 5.7×10^{7} VG to the cells. After 24 hours cells were washed with PBS and fixed with 4% PFA for 30 minutes. The cells then underwent immunohistochemistry for TTC as in 2.6.3. AAV was added to cells at 2.7×10^{10} virus molecules/mL. After 24 hours cells were washed with PBS and fixed with 4% PFA for 30 minutes. Coverslips were mounted with Vectashield onto glass slides and viewed with a Nikon Eclipse E600 microscope as in 2.6.5.

Chapter 3

The distribution of CTB and LTB within the brain and spinal cord following systemic and central administration

3.1 Introduction

The toxins produced by *Vibrio chlorerae* and *Escherichia coli*, cholera toxin (CT) and heat-labile enterotoxin (LT-I) respectively, are structurally similar (83% homology at amino acid level (Dallas and Falkow, 1980)). The non-toxic pentameric B subunits (CTB and LTB) are responsible for binding to the cell membrane and allowing endocytosis of these AB_5 toxins. The ganglioside GM1 acts as the main receptor for the toxins, and while ubiquitously expressed in vertebrates it is found in high relative abundance in the nervous system (Ogawa-Goto et al., 1992; Sheikh et al., 1999). For this reason CTB has been widely used as a neuronal tracer, both retrograde (Luppi et al., 1987; Luppi et al., 1990) and anterograde (Angelucci et al., 1996). It is a useful tracer due to its effective uptake and transport by neurones in the central and peripheral nervous system, as well as its ease of detectability.

Due to the non-toxic nature of CTB it was considered it may be used systemically. Distributions of CTB in the central nervous system (CNS) following systemic administration have been studied with immunohistochemistry in mice (Alisky et al., 2002) and with a CTB-HRP conjugate in rats (Havton and Broman, 2005). In general it was concluded that motor neurones, autonomic preganglionic fibres and primary afferents were labelled with CTB in the brainstem and spinal cord. This means that CTB was able to reach the CNS after peripheral administration, essentially crossing the blood-brain barrier (BBB) once inside the peripheral neurones.

While the predominant ganglioside both LTB and CTB bind to is GM1 (Merritt et al., 1994b), they do both also bind GD1b with lower affinity (Fukuta et al., 1988). LTB is more promiscuous than CTB, also interacting with asialo-GM1, lactosylceramide, as well as some galactoproteins (Fukuta et al., 1988). The expression profiles of the other receptors have not been fully characterised so it is not known whether LTB may enter some other neuronal populations when compared to CTB.

Therapeutic targeting of the CNS is made challenging by the BBB which acts to prevent the entry of bacteria and large molecules such as drugs or proteins from the bloodstream meaning that treatment of neurological disease proves difficult. CTB and LTB could provide a means to deliver therapeutic molecules to the CNS following systemic administration by entering neurones with axons in the periphery, circumventing the BBB.

3.1.1 Summary and objectives

CTB and LTB represent potential therapeutic tools to target foreign proteins to peripheral neurones. The labelling patterns of LTB in mice have never been studied following either central or peripheral injection. It is hypothesised that they would be similar to those seen after CTB administration since both toxins bind to GM1; however the additional receptor interactions of LTB may allow for more widespread cell targeting. This could be advantageous if wanting to target many cells types, but if neurones are the predominant target it may prove to be a disadvantage with too many off-target effects. While the systemic administration of CTB has been studied in mice, the administration of LTB has not, nor has the comparison of injected doses.

Research questions:

1. What are the labelling patterns of LTB within the brainstem and spinal cord following systemic (IP and IV) injection?
2. What are the labelling patterns of CTB within the brainstem and spinal cord following systemic (IP and IM) injection?
3. Do LTB and CTB enter the same subsets of neurones following IP injection?

The labelling patterns in the CNS will be assessed using immunohistochemistry, the epitope recognised by anti-CTB is also present on LTB and so the same antibody can be used to detect both toxins. By injecting a range of doses the neuronal subsets labelled at high and low doses can be compared. Also, following systemic administration of the toxins other organs will be assessed for off-target labelling.

The results from this study will identify and compare the labelling patterns of CTB and LTB within the CNS following various routes of central and peripheral administration in mice. This will provide rationale for using CTB/LTB conjugates as therapeutic tools to target specific subsets of neurones within the CNS.

3.2 Materials and methods

CTB was produced as described in section 2.2.19 and LTB was produced by the Turnbull lab and gifted for *in vivo* testing. An antibody raised against CTB was tested via an ELISA to confirm it detected both CTB and LTB, see section 2che.3.8. All tracing studies were carried out in C75Bl/6 mice, see table 3.1 for routes of injection, doses and n numbers for each protein tested. For detailed methods of LTB injections see General Methods section 2.5.3. For detailed CTB injections see General Methods

section 2.5.4. All tissue was prepared as described in General Methods section 2.5.6 and 2.5.7 and all antibodies used are listed in table 2.2. Fluorescent images were acquired as described in section 2.6.3, and diaminobenzidine (DAB) images as described in section 2.6.4.

To calculate any change in the number of CTB-positive cells labelled for a high versus low dose of CTB, first the number of ChAT cells were counted in each CTB labelled region, then the number of CTB-positive cells counted. This allowed the calculation of the proportion of CTB labelled cells to be counted in each section. For each condition 3 sections were counted from each animal (n=3 per dose), sections were collected serially and each third section counted to prevent cells being counted twice. All counts stated represent the average proportion of CTB labelled ChAT-positive cells ± standard error of the mean (SEM). Statistical analysis was carried out using a Student's t-test, two sample with unequal variance.

Route	Dose (µg)	Protein	n
IP	2000, 1000, 500	LTB	4 per dose
IV (jugular)	500, 250, 125	LTB	3 per dose
IP	2000, 500	CTB	3 per dose
IM (tongue)	80	CTB	3
IM (gastrocnemius)	80	CTB	2

Table 3.1 Route, dose and n number for each protein tested

3.3 Results

3.3.1 CTB was successfully produced

CTB was successfully overexpressed in *Vibrio sp.60* and purified on a nickel column, elutions contain the pentameric toxoid and the boiled sample contains the monomer (Figure 3.1A).

Comparison of labelling with CTB and LTB *in vivo* was to be assessed using immunohistochemistry, given the similarity between the two toxoids (Dallas and Falkow, 1980) it was hypothesised that a polyclonal antibody directed against CTB would also recognise LTB. Anti-CTB (Sigma, C3062) has been used previously to detect LTB in Western blot (Turner et al., 2011). An ELISA indicated that the antibody recognised both CTB and LTB when 1 µM of each toxoid was incubated on GM1 coated plates, as compared to a control with no toxoid applied (Figure 3.1B).

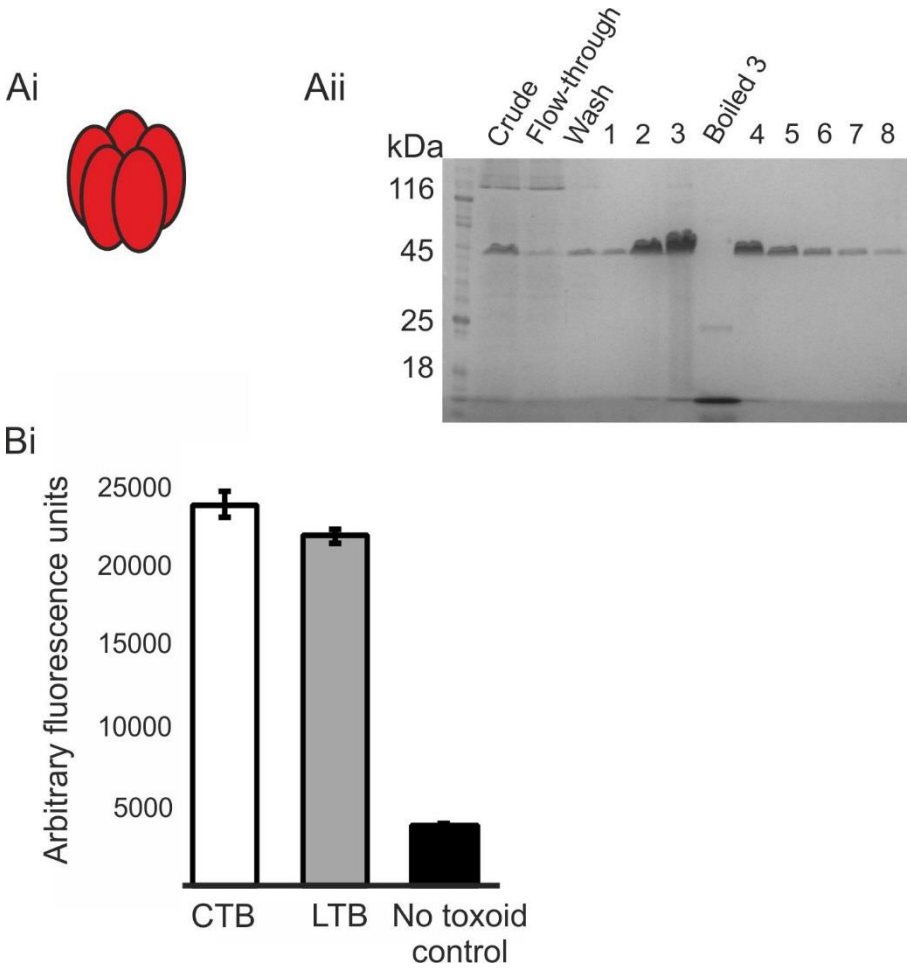

Figure 3.1 Expression and purification of CTB

A) Schematic of CTB, each red oval represents a monomer unit (Ai). SDS-PAGE analysis of nickel-column purified protein with boiled sample to visualise monomer units (Aii). B) ELISA analysis of 1 µM LTB and CTB binding GM1 as detected by anti-CTB, results are average of triplicate ±SEM.

3.3.2 Systemic administration of LTB – intraperitoneal

LTB was administered IP to assess the central labelling patterns following systemic administration. The areas that were labelled within the CNS were identical for each injected dose (2000, 1000 and 500 µg) after IP injection. In the brainstem there was labelling of the nucleus solitarius (NTS), the dorsal vagal nucleus (DVN), the hypoglossal nucleus, area postrema, nucleus ambiguus (Figure 3.2), and in more rostral sections the facial motor nucleus. Double labelling with ChAT confirmed the LTB-positive cells in each region were motor neurones. LTB labelled cells in the DVN and hypoglossal colocalise with ChAT-positive cells (Figure 3.2B). Again, in the nucleus ambiguus LTB-positive cells were always also labelled with ChAT (Figure 3.2C). There was no noticeable difference in labelling along the rostro-caudal axis of the nucleus ambiguus at any dose, there were LTB-positive cells throughout.

In the spinal cord there was LTB labelling of ChAT-positive cells in the ventral horn at all levels (Figure 3.3), indicating that motor neurones were labelled. In the cervical region the dorsal horn was not labelled at 500 or 1000 µg (Figure 3.3A). In the thoracic region, primary afferents were labelled in the dorsal horn, along with sympathetic preganglionic neurones (SPNs) in the intermediolateral column (IML) and cells in the central autonomic area (Figure 3.2B); this pattern was seen for all doses. The lumbar region contained LTB-positive primary afferents at every dose, along with the majority of motor neurones labelled in the ventral horn. There was no colocalisation between LTB and IB4, a marker of non-myelinated nociceptive fibres, suggesting that the terminals labelled in the dorsal horn were those of myelinated neurones (Figure 3.4).

3.3.3 Systemic administration of LTB – intravenous

To compare labelling following systemic routes of delivery, LTB was also delivered intravenously. For IV injections of LTB to the jugular vein, each dose (500, 250 and 125 µg) labelled similar regions within the CNS, and labelling was almost always unilateral. Within the brainstem there was labelling of the DVN, the hypoglossal nucleus, area postrema, nucleus ambiguus (Figure 3.5A), and in more rostral sections the facial motor nucleus (Figure 3.5B). Notably, the NTS was not labelled as it was following IP injections. In the spinal cord LTB-positive cells were found at all levels (Figure 3.6). Motor neurones were labelled unilaterally in the ventral horn for all doses along the entire length of the cord. In the cervical region the primary afferents of the dorsal horn were labelled for all doses. However the thoracic and lumbar region only had LTB-positive afferents at the highest dose of 500 µg.

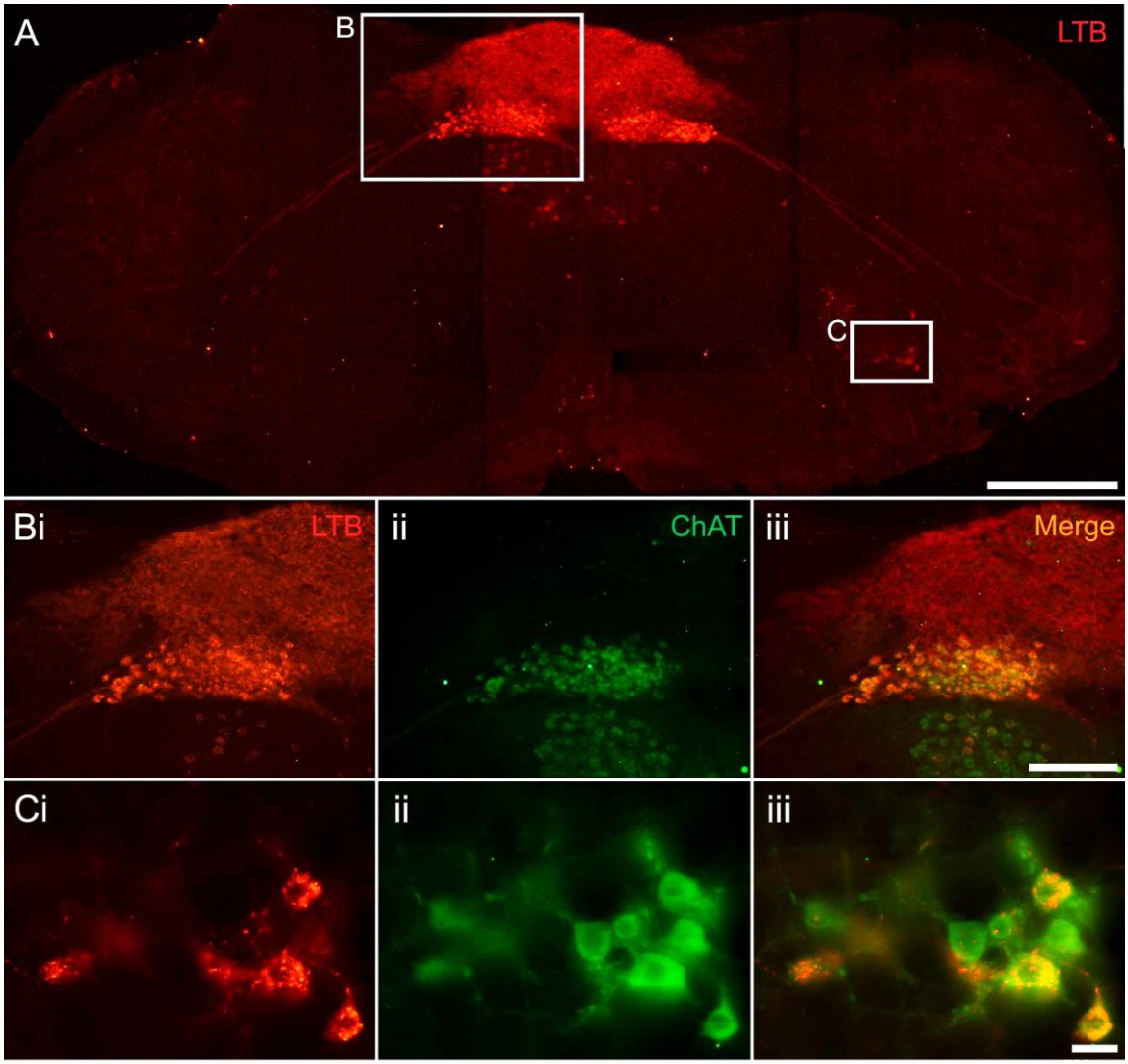

Figure 3.2 LTB labels neurones of the area postrema, DVN, NTS, hypoglossal nucleus and nucleus ambiguus following IP injection

Mice were injected IP with 1000 µg of LTB and were fixed after three days. Brainstem slices were obtained from removed brains and were then subjected to immunohistochemistry. A) Whole brainstem slice stained with anti-CTB (red). B) The DVN and hypoglossal nucleus stained with anti-CTB (red, Bi), anti-ChAT (green, Bii) and merged (Biii). C) The nucleus ambiguus stained with anti-CTB (red, Ci), anti-CHAT (green, Cii) and merged (Ciii). Scale bars: A = 500 µm; B = 200 µm; C = 25 µm.

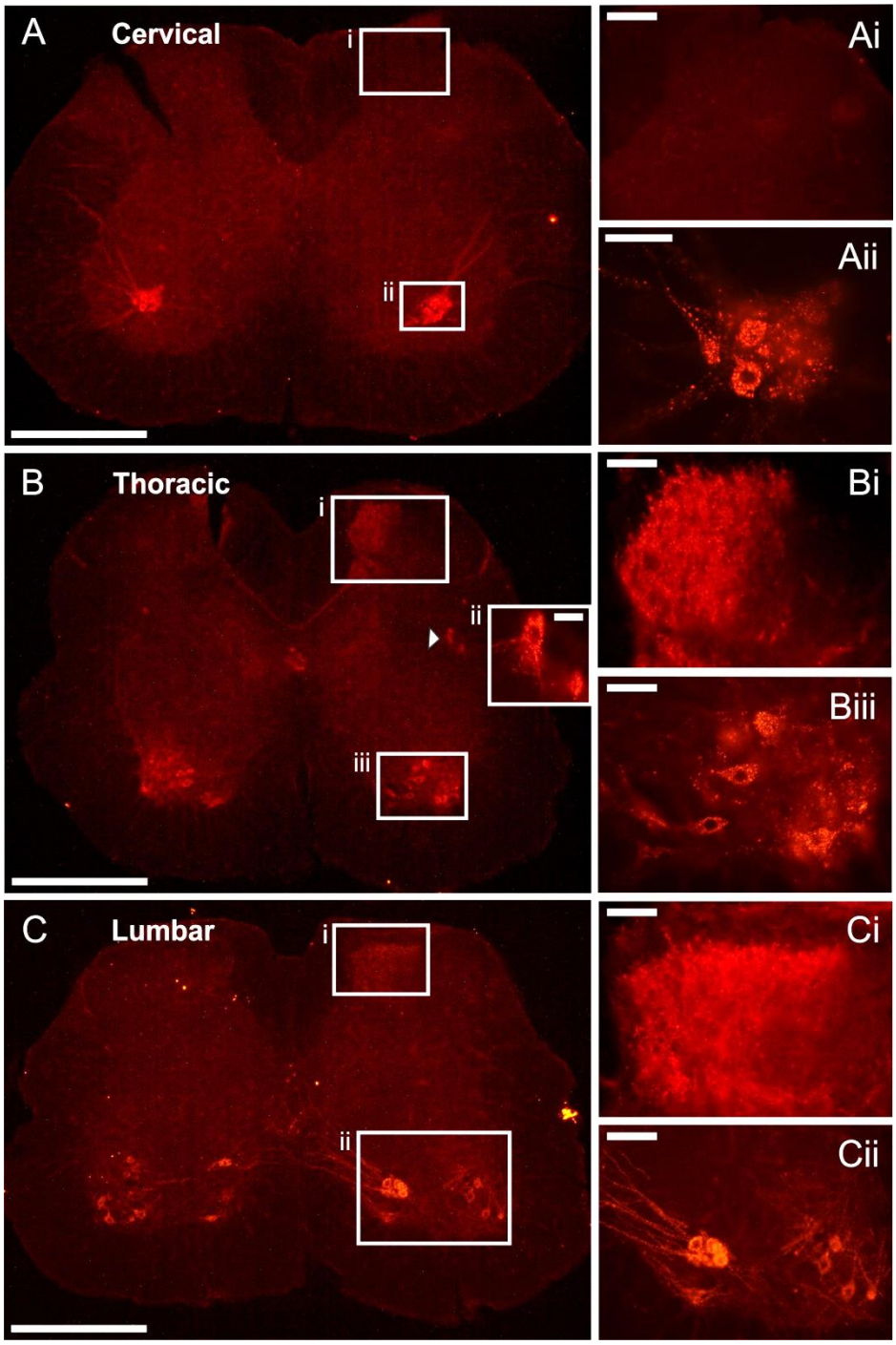

Figure 3.3 LTB labels neurones in the dorsal horn and ventral horn of the spinal cord following IP injection

Mice were injected IP with 1000 µg of LTB and were fixed after three days. Slices were obtained from removed spinal cords and were then subjected to immunohistochemistry. A) Cervical spinal cord slice stained with anti-CTB in the dorsal horn (Ai) and ventral horn (Aii). B) Thoracic spinal cord slice stained with anti-CTB in the dorsal horn (Bi), IML (Bii) and ventral horn (Biii). C) Lumbar spinal cord slice stained with anti-CTB in the dorsal horn (Ci) and ventral horn (Cii). Scale bars: A, B, C = 500 µm; Ai, Bi, Biii, Ci, Cii = 100 µm; Aii = 50 µm; Bii = 25 µm.

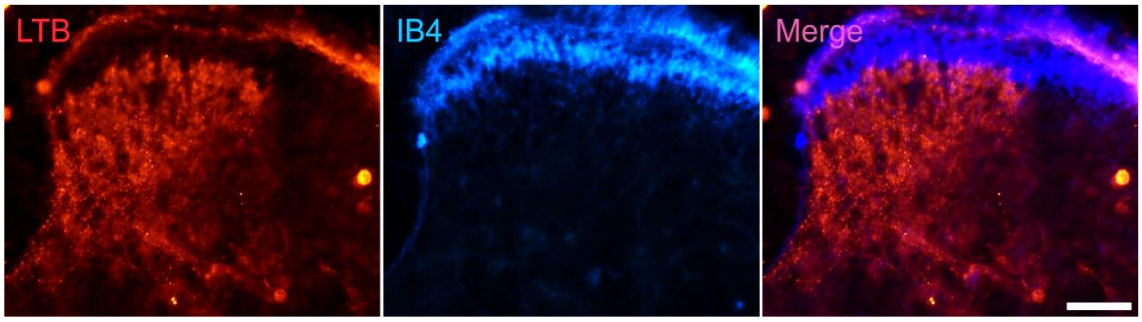

Figure 3.4 LTB does not label IB4-positive non-myelinated fibres in the dorsal horn following IP injection

Mice were injected IP with 1000 µg of LTB and were fixed after three days. Slices were obtained from removed spinal cords and were then subjected to immunohistochemistry. Dorsal horn section of spinal cord stained with anti-CTB (red, Ai), isolectin B4 (blue, Aii) and merged (Aiii). Apparent co-labelling in the top right is an artefact of secondary antibodies binding to remaining meninges. Scale bar = 50 µm.

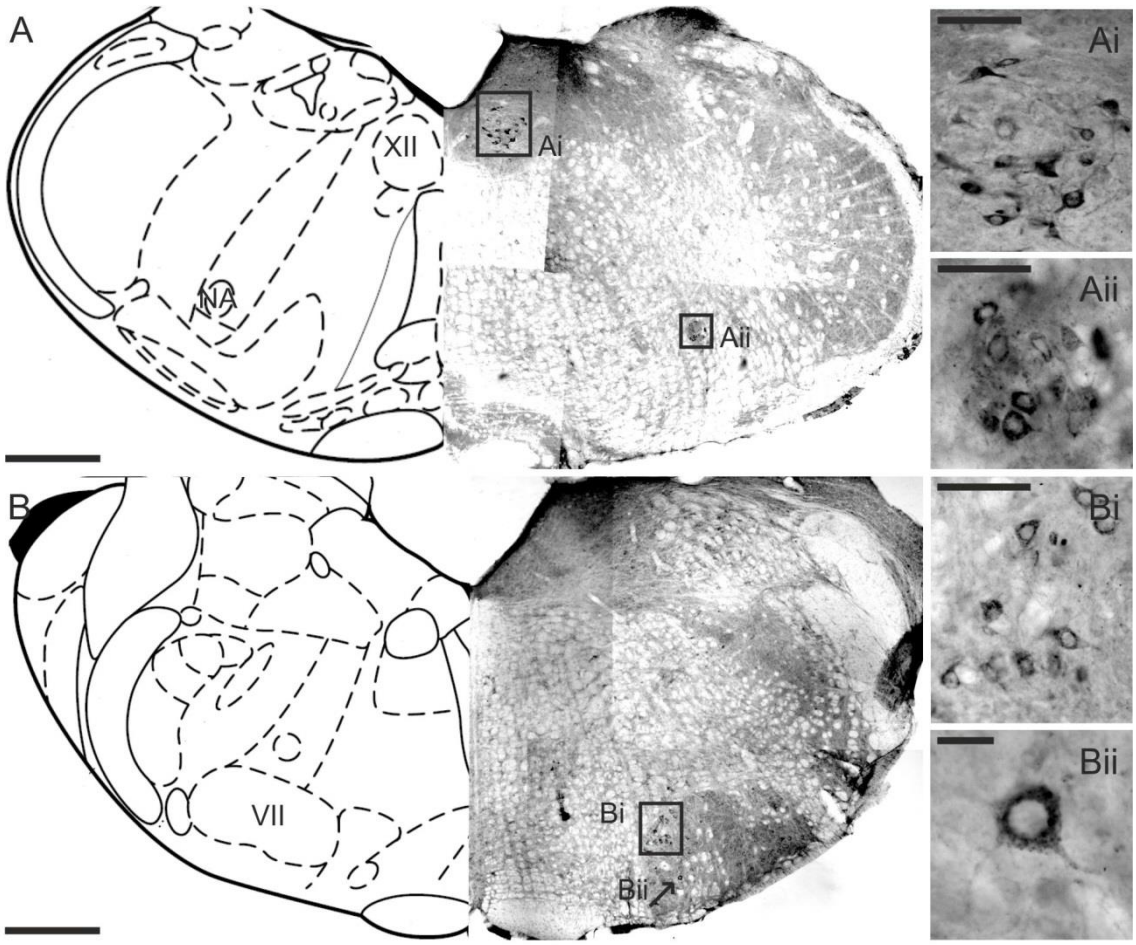

Figure 3.5 LTB labels neurones in the hypoglossal nucleus, facial motor nucleus and nucleus ambiguus following IV injection to the jugular vein

Mice were injected IV with 500 µg of LTB to the jugular vein and were fixed after five days. Brainstem slices were obtained from removed brains and were then subjected to immunohistochemistry with DAB. A) Whole brainstem slice (-13.24 mm from Bregma) stained with anti-CTB in the hypoglossal nucleus (XII, Ai) and nucleus ambiguus (NA, Aii). B) Whole brainstem slice (-11.00 mm from Bregma) stained with anti-CTB in the facial motor nucleus (VII, Bi) with clear punctate labelling (Bii). Scale bars: A, B = 500 µm; Ai, Aii, Bi = 100 µm; Bii = 20 µm.

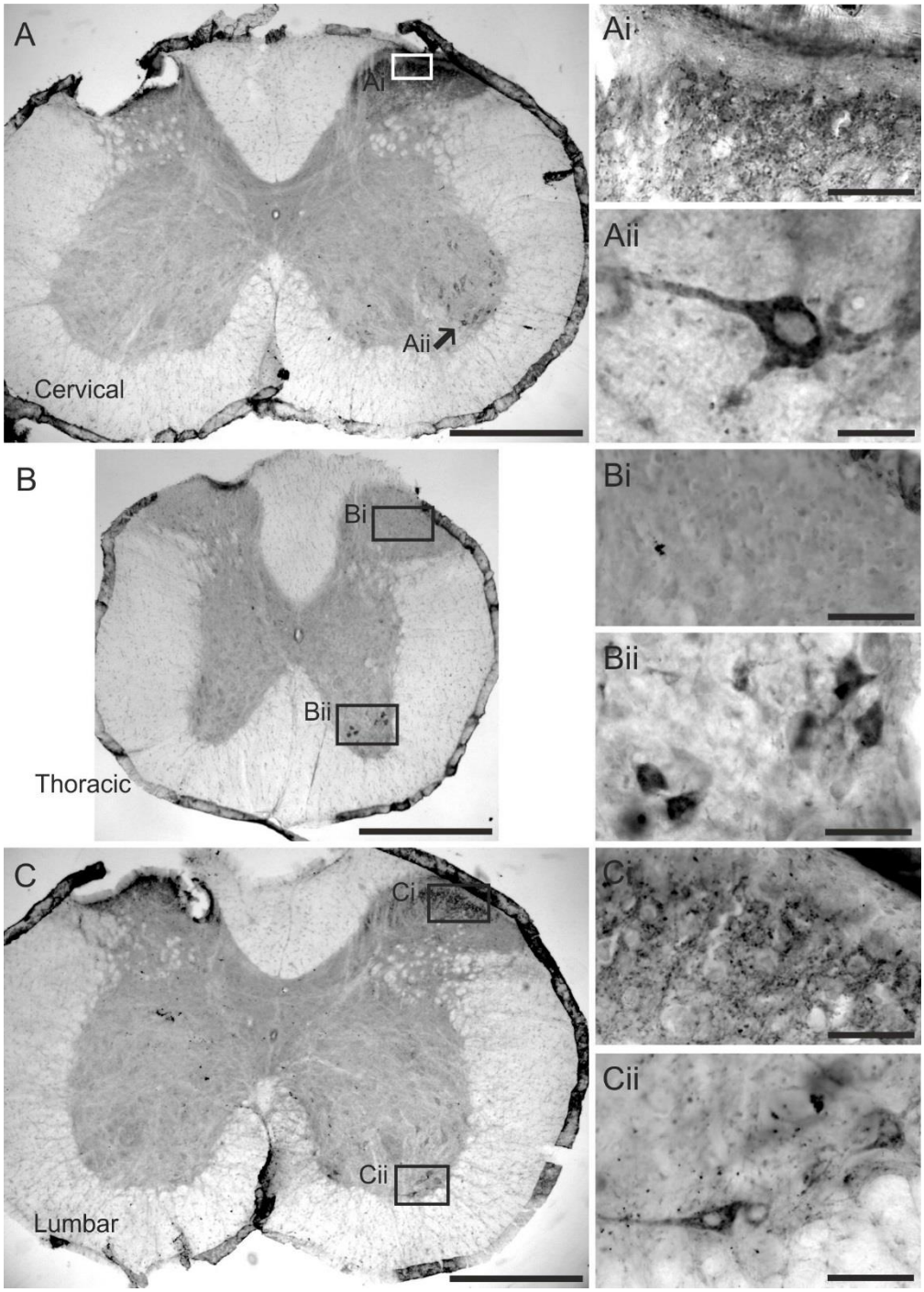

Figure 3.6 LTB labels neurones in the dorsal horn and ventral horn of the spinal cord following IV injection to the jugular vein

Mice were injected IV with 500 µg of LTB to the jugular vein and were fixed after five days. Slices were obtained from removed spinal cords and were then subjected to immunohistochemistry with DAB. A) Cervical spinal cord slice stained with anti-CTB in the dorsal horn (Ai) and ventral horn (Aii). B) Thoracic spinal cord slice stained with anti-CTB in the dorsal horn (Bi, this animal is not representative of other mice at this dose where the dorsal horn contained staining) and ventral horn (Bii). C) Lumbar spinal cord slice stained with anti-CTB in the dorsal horn (Ci) and ventral horn (Cii). Scale bars: A, B, C = 500 µm; Ai, Bi, Bii, Ci, Cii = 50 µm; Aii = 20 µm.

3.3.4 Systemic administration of CTB – intraperitoneal

CTB was injected intraperitoneally at a high dose (2000 µg) and a low dose (500 µg) to assess if this caused any difference in labelling of neuronal subsets in the brainstem and spinal cord. While many of the same areas were labelled with each dose, in general fewer cells were labelled with the low dose. All CTB labelling was bilateral.

After administration of 2000 µg of CTB, the area postrema, NTS, DVN, hypoglossal nucleus, nucleus ambiguus, and facial motor nucleus were labelled (Figure 3.7A). CTB-positive afferents can be seen in the NTS (Figure 3.7B), and the CTB-positive cells bodies in the DVN can be seen to colocalise with ChAT (Figure 3.7Biii). Motor neurones of the hypoglossal nucleus were labelled for CTB reactivity (Figure 3.7C); although not all ChAT-positive cells were CTB-positive. Most cells of the nucleus ambiguus were labelled for CTB (Figure 3.7D). In the cervical region of the spinal cord primary afferents in the dorsal horn were labelled (Figure 3.8Ai). There was no labelling around the central canal (Figure 3.8Aii). Most motor neurones were labelled in the ventral horn (Figure 3.8Aiii-iv) when compared to ChAT-positive cells (Figure 3.8B). In the thoracic region the dorsal horn was strongly labelled (Figure 3.9Ai). Sympathetic preganglionic neurones (SPNs) were CTB-positive in the intermediolateral column (IML) (Figure 3.9Aiii). CTB-positive fibres can be seen around the central canal (Figure 3.9Aii) and in some slices cell bodies were labelled in the central autonomic area. The motor neurones of the ventral horn were well labelled (Figure 3.9iv). There were CTB-positive primary afferents in the dorsal horn of the lumbar region of the cord (Figure 3.10Ai). Autonomic preganglionic neurones are labelled in the lumbar dorsal commissural nucleus (Figure 3.10Aii) along with those in the IML (Figure 3.10Aiii). Motor neurones of the ventral horn were CTB-positive (Figure 3.10Aiv). There were CTB-positive cells in the dorsal root ganglia (Figure 3.11A) and these did not colocalise with IB4-positive cell bodies (Figure 3.11B). This suggests that the cell bodies labelled were those of myelinated neurones since IB4 is a marker of non-myelinated neurones.

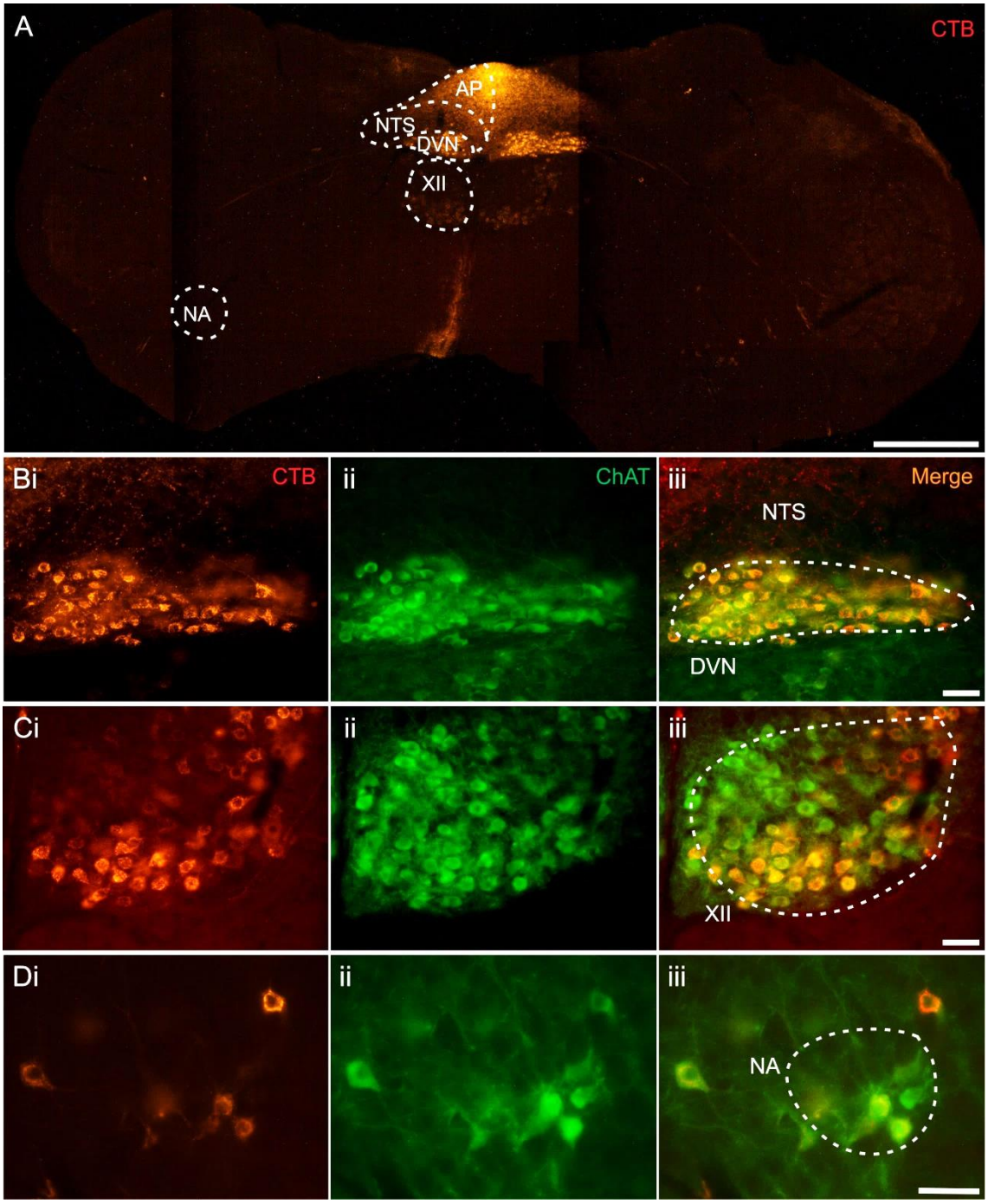

Figure 3.7 CTB labels neurones in the area postrema, nucleus tractus solitarius, dorsal vagal nucleus, hypoglossal nucleus and nucleus ambiguus following high dose IP injection

Mice were injected IP with 2000 µg of CTB and were fixed after three days. Brainstem slices were obtained from removed brains and were then subjected to immunohistochemistry. A) Whole brainstem slice stained with anti-CTB (red). B) The DVN and NTS stained with anti-CTB (red, Bi), anti-ChAT (green, Bii) and merged. C) The hypoglossal nucleus stained with anti-CTB (red, CI), anti-ChAT (green, Cii) and merged (Ciii). D) The nucleus ambiguus stained with anti-CTB (red, Di), anti-ChAT (green, Dii) and merged (Diii). Scale bars: A = 500 µm; B, C, D = 50 µm.

Figure 3.8 CTB labels neurones in the dorsal horn and ventral horn of the cervical spinal cord following high dose IP injection

Mice were injected IP with 2000 µg of CTB and were fixed after three days. Slices were obtained from removed spinal cords and were then subjected to immunohistochemistry. A) Cervical spinal cord slice stained with anti-CTB (red) in the dorsal horn (Ai), central canal (Aii) and ventral horn (Aii-iv). B) Ventral horn neurones stained with anti-CTB (red, Bi), anti-ChAT (green, Bii), DAPI (blue, Biii) and merged (Biv). Scale bars: A = 250 µm; Ai-iv = 25 µm; Bi-iv = 20 µm.

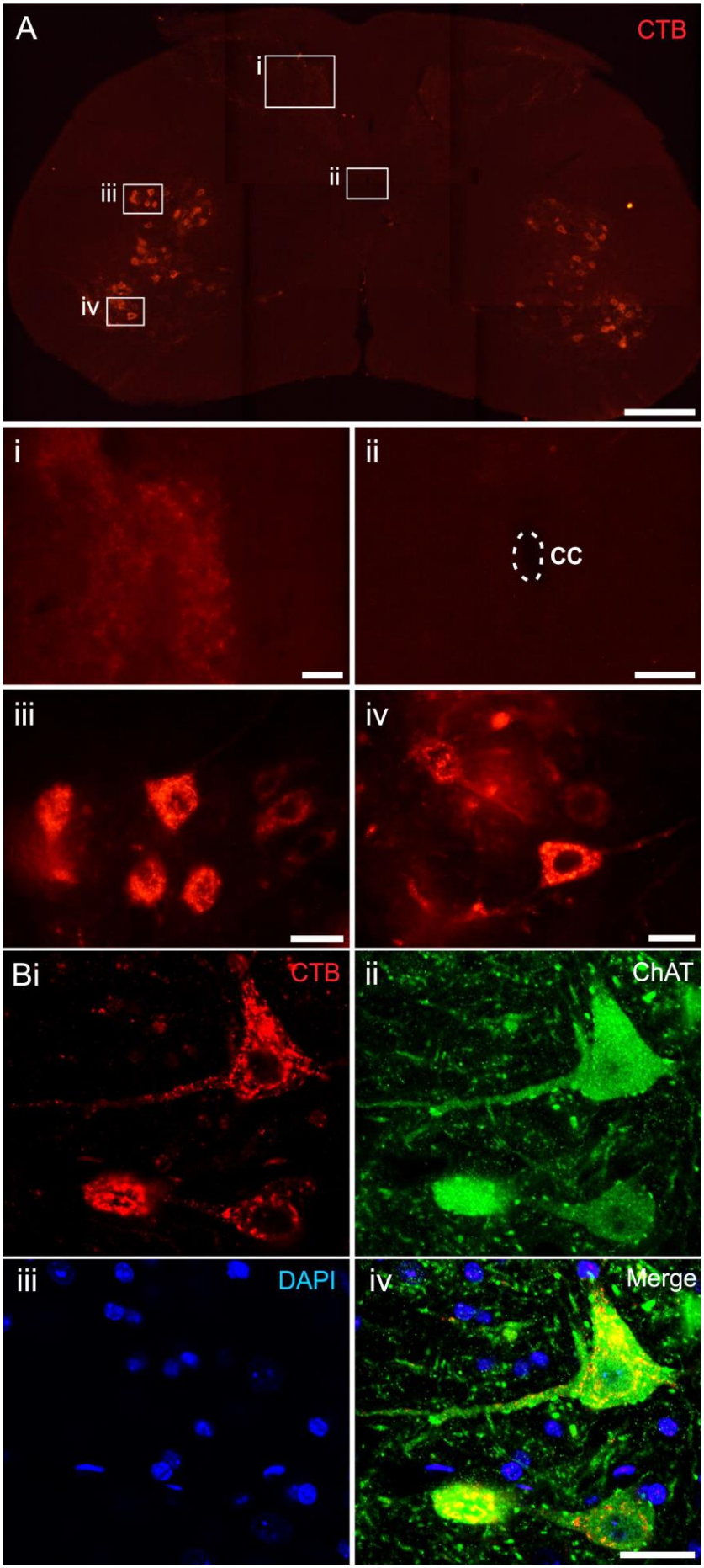
A
CTB
i
ii
iii
iv
i
ii
cc
iii
iv
Bi
CTB
ii
ChAT
iii
DAPI
iv
Merge

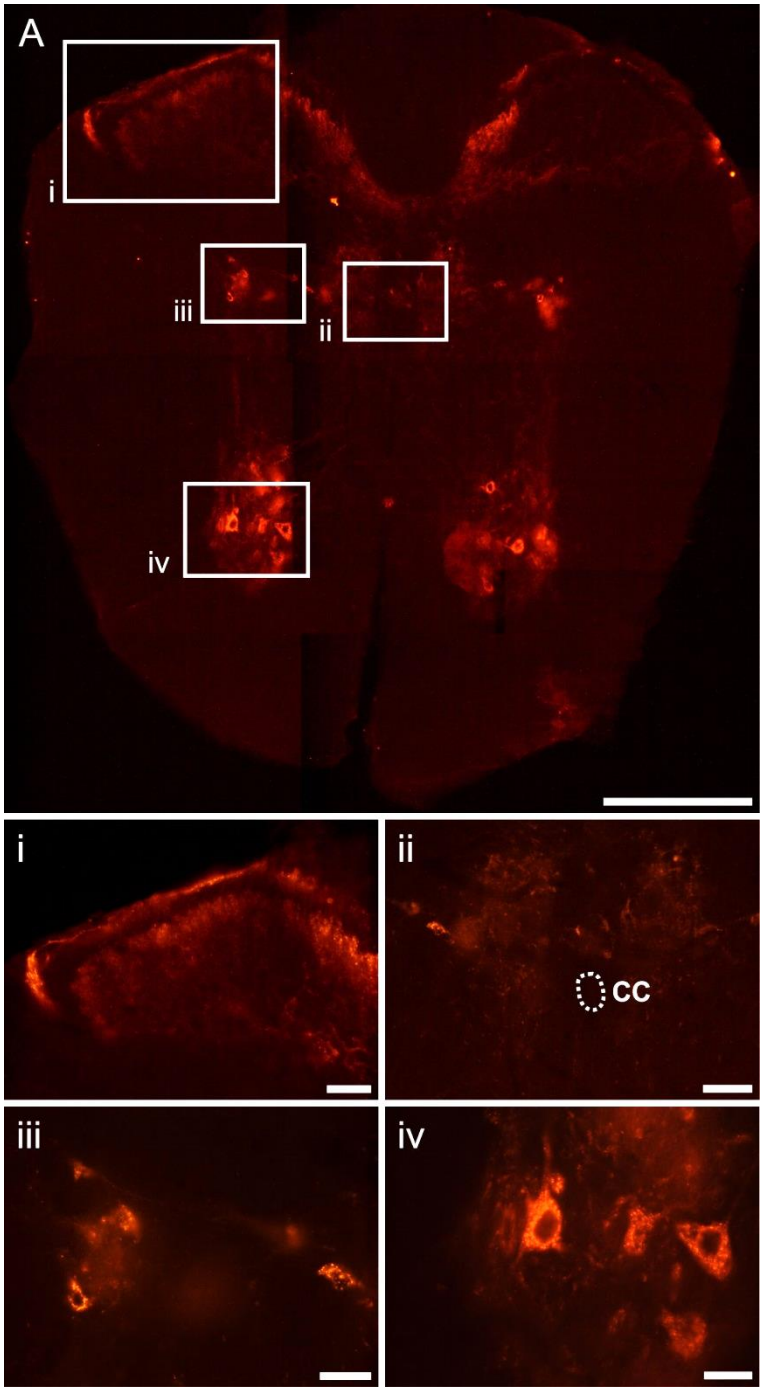

Figure 3.9 CTB labels neurones in the dorsal horn and ventral horn of the thoracic spinal cord following high dose IP injection

Mice were injected IP with 2000 µg of CTB and were fixed after three days. Slices were obtained from removed spinal cords and were then subjected to immunohistochemistry. A) Thoracic spinal cord slice stained with anti-CTB (red) in the dorsal horn (Ai), central canal (Aii), IML (Aiii) and ventral horn (Aiv). Scale bars: A = 250 µm; Ai-ii = 50 µm, Aiii-iv = 25 µm.

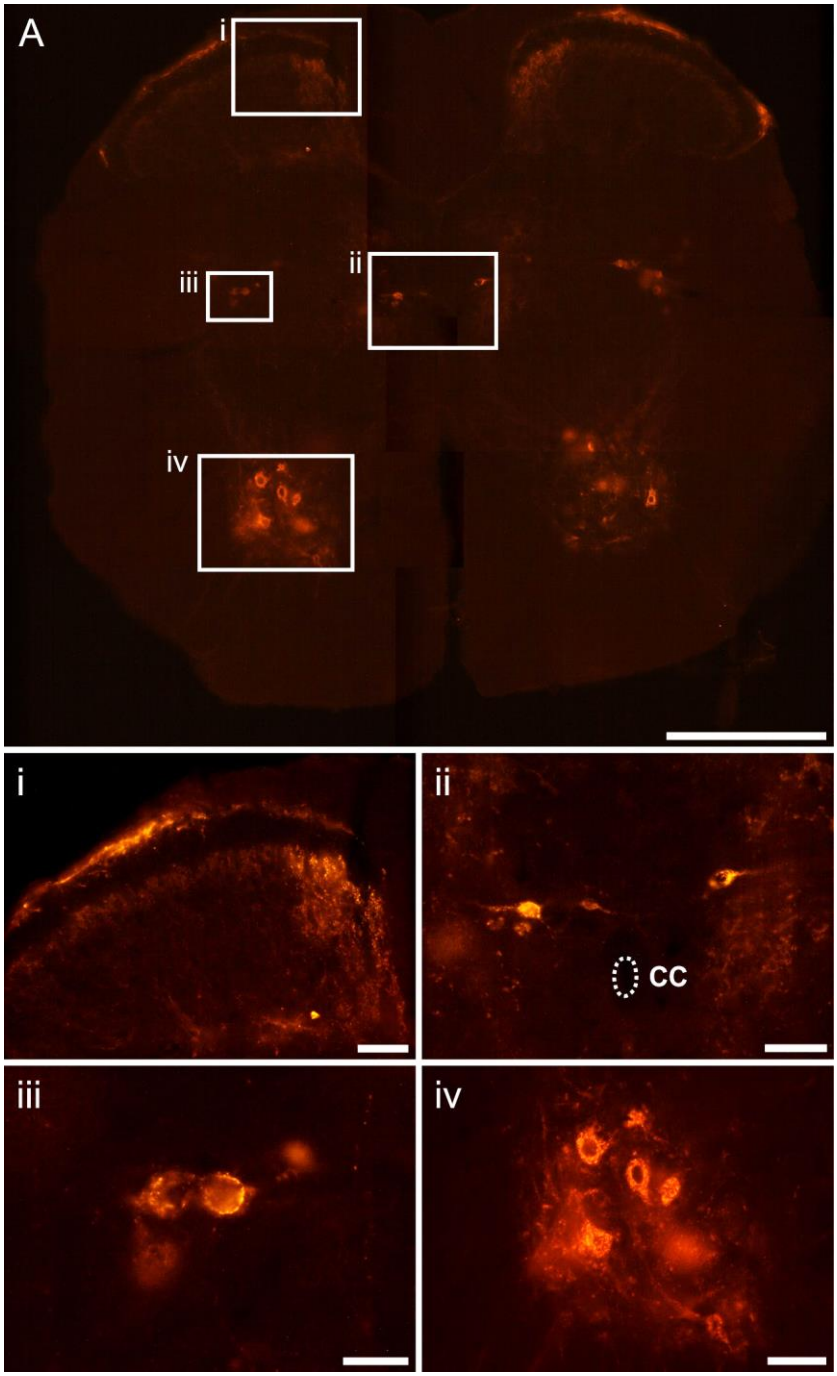

Figure 3.10 CTB labels neurones in the dorsal horn and ventral horn of the lumbar spinal cord following high dose IP injection

Mice were injected IP with 2000 µg of CTB and were fixed after three days. Slices were obtained from removed spinal cords and were then subjected to immunohistochemistry. A) Lumbar spinal cord slice stained with anti-CTB (red) in the dorsal horn (Ai), central canal (Aii), IML (Aiii) and ventral horn (Aiv). Scale bars: A = 250 µm; Ai-ii, iv = 50 µm, Aiii = 25 µm.

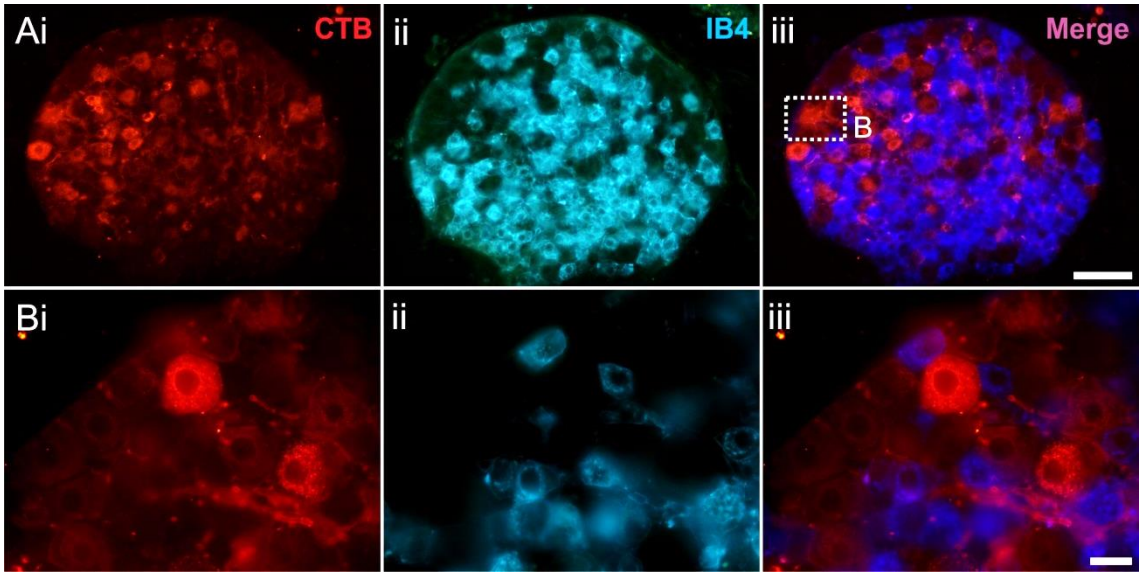

Figure 3.11 CTB does not label IB4-positive cell bodies in the dorsal root ganglia following high dose IP injection

Mice were injected IP with 2000 µg of CTB and were fixed after three days. Slices were obtained from removed DRGs and were then subjected to immunohistochemistry. A) Whole DRG slice stained with anti-CTB (red, Ai), isolectin B4 (blue, Aii) and merged (Aiii). B) DRG section stained with anti-CTB (red, Bi), isolectin B4 (blue, Bii) and merged (Biii). Scale bars: A = 100 µm; B = 25 µm.

After administration of 500 µg of CTB, the area postrema, NTS, DVN, nucleus ambiguus, and facial motor nucleus were labelled (Figure 3.12A). The DVN was well labelled with the majority of ChAT-positive cells also positive for CTB (Figure 3.12B). The hypoglossal nucleus was not labelled with CTB at this low dose (Figure 3.12C). The nucleus ambiguus and facial motor nucleus were partially labelled, but only in two mice of the three (Figure 3.11D, an example where the nucleus ambiguus was not labelled). In the spinal cord, primary afferents were CTB-positive in the thoracic (Figure 3.14Ai) and lumbar (Figure 3.13Ai) regions, but not in the cervical (Figure 3.11Ai). Around the central canal, there were no labelled fibres or cells in the cervical region (Figure 3.11Aii), but there were some positive cells in the thoracic (Figure 3.12Aii) and lumbar (Figure 3.13Aii) regions. In the IML, there were no labelled fibres or cells in the cervical region (Figure 3.13Aiii), but there were some positive cells in the thoracic (Figure 3.14Aiii) and lumbar (Figure 3.15Aii) regions. In the ventral horn, CTB-positive motor neurones were present at every level of the cord (Figure 3.13Aiv, 3.14Aiv and 3.15Aiv). There were CTB-positive cells in the dorsal root ganglia (Figure 3.16A) and these did not colocalise with IB4-positive cell bodies (Figure 3.16B).

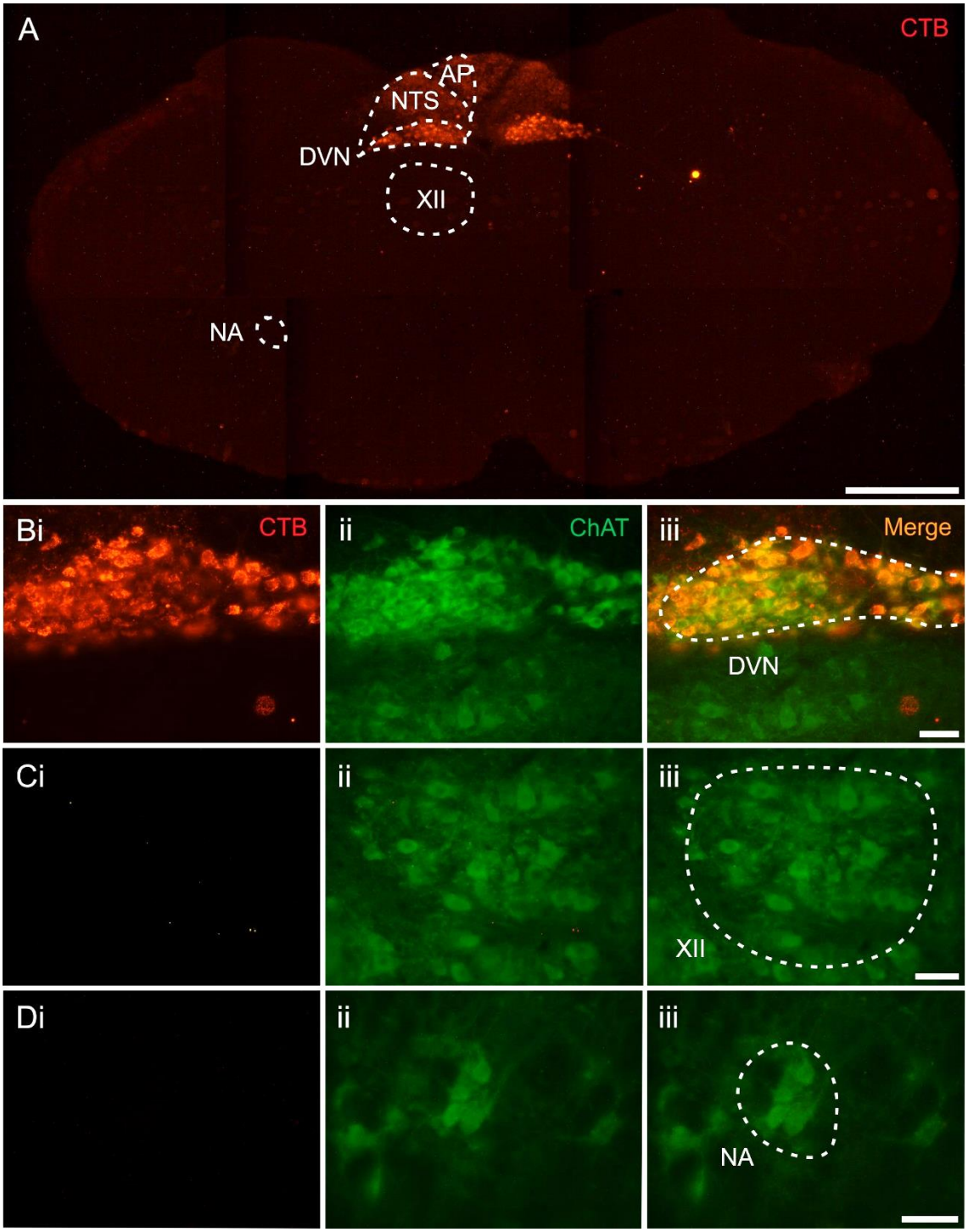

Figure 3.12 CTB labels neurones in the area postrema, nucleus tractus solitarius, and dorsal vagal nucleus following low dose IP injection

Mice were injected IP with 500 µg of CTB and were fixed after three days. Brainstem slices were obtained from removed brains and were then subjected to immunohistochemistry. A) Whole brainstem slice stained with anti-CTB (red). B) The DVN stained with anti-CTB (red, Bi), anti-ChAT (green, Bii) and merged. C) The hypoglossal nucleus stained with anti-CTB (red, CI), anti-ChAT (green, Cii) and merged (Ciii). D) The nucleus ambiguus stained with anti-CTB (red, Di), anti-ChAT (green, Dii) and merged (Diii). Scale bars: A = 500 µm; B-D = 50 µm.

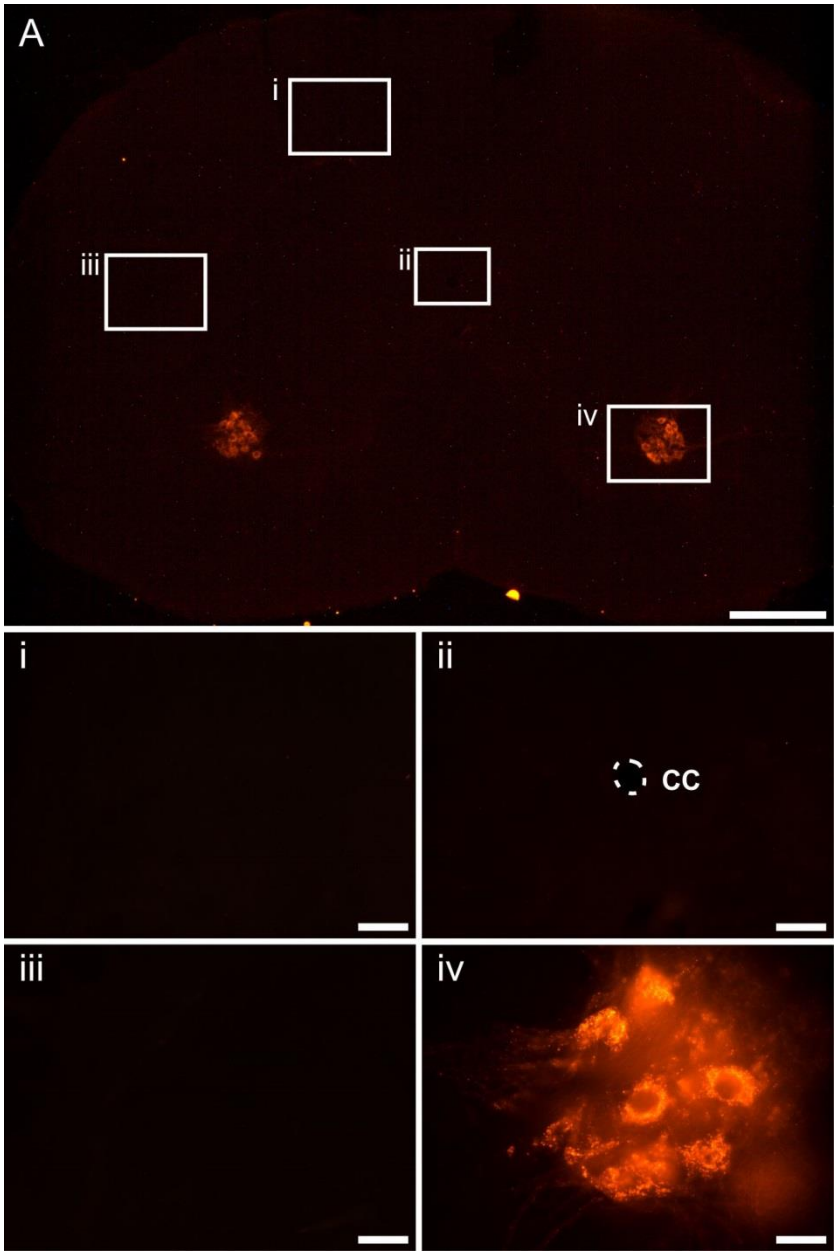

Figure 3.13 CTB labels neurones in the dorsal horn and ventral horn of the cervical spinal cord following low dose IP injection

Mice were injected IP with 500 µg of CTB and were fixed after three days. Slices were obtained from removed spinal cords and were then subjected to immunohistochemistry. A) Cervical spinal cord slice stained with anti-CTB (red) in the dorsal horn (Ai), central canal (Aii) and ventral horn (Aii-iv). Scale bars: A = 250 µm; Ai-iii = 50 µm, Aiv = 25 µm.

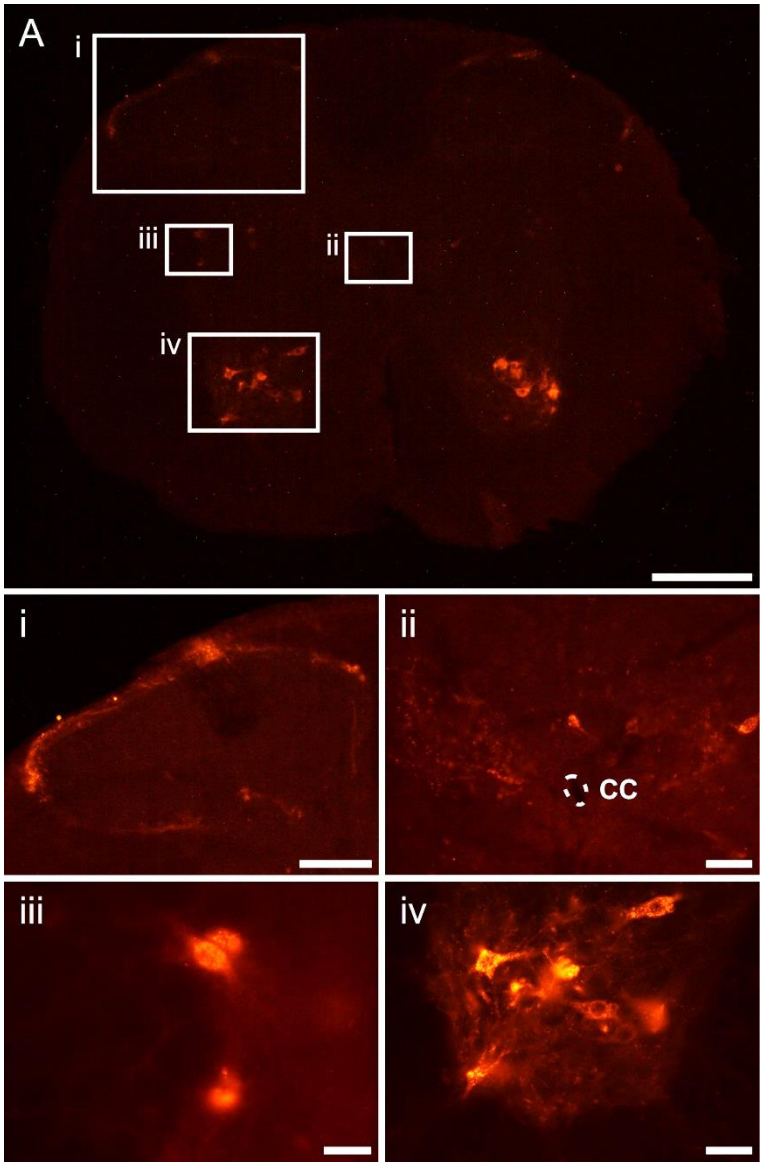

Figure 3.14 CTB labels neurones in the dorsal horn and ventral horn of the thoracic spinal cord following low dose IP injection

Mice were injected IP with 500 µg of CTB and were fixed after three days. Slices were obtained from removed spinal cords and were then subjected to immunohistochemistry. A) Thoracic spinal cord slice stained with anti-CTB (red) in the dorsal horn (Ai), central canal (Aii), IML (Aiii) and ventral horn (Aiv). Scale bars: A = 100 µm; Ai-ii, iv = 50 µm, Aiii = 25 µm.

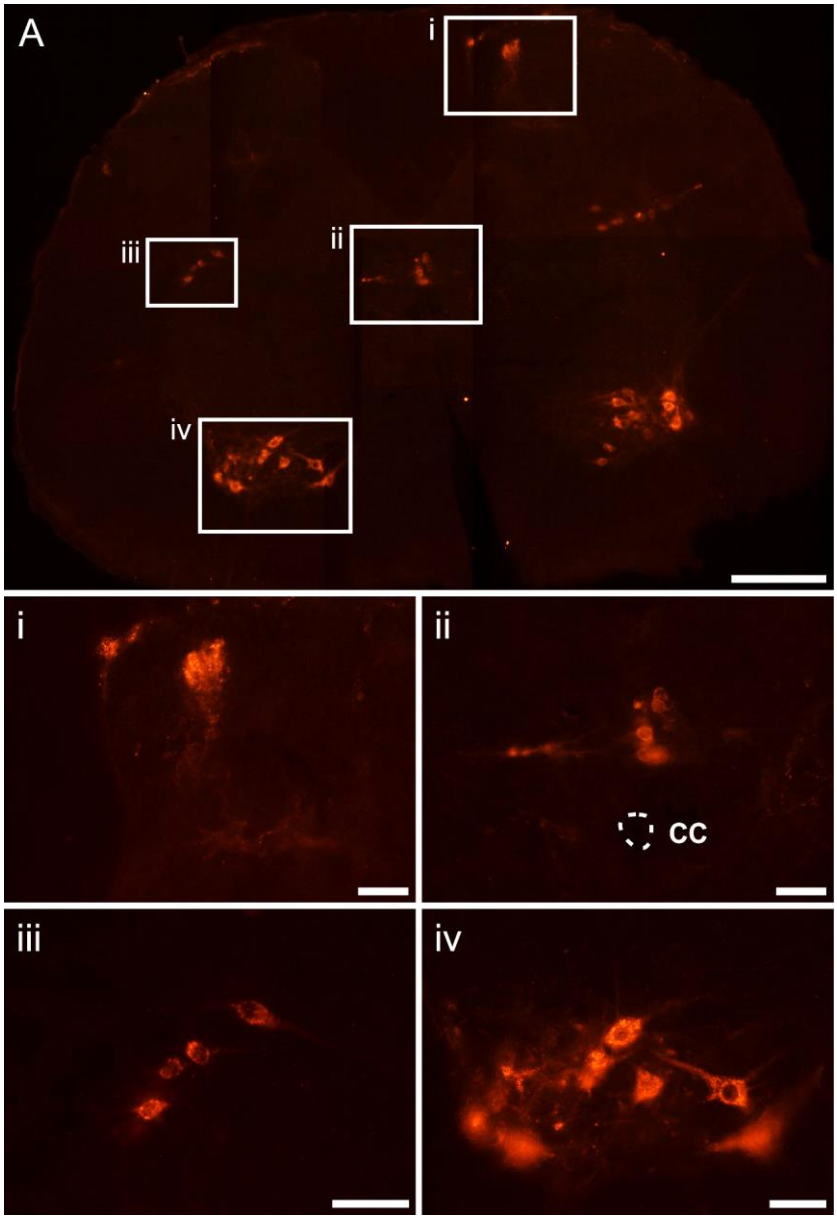

Figure 3.15 CTB labels neurones in the dorsal horn and ventral horn of the lumbar spinal cord following low dose IP injection

Mice were injected IP with 500 µg of CTB and were fixed after three days. Slices were obtained from removed spinal cords and were then subjected to immunohistochemistry. A) Lumbar spinal cord slice stained with anti-CTB (red) in the dorsal horn (Ai), central canal (Aii), IML (Aiii) and ventral horn (Aiv). Scale bars: A = 200 µm; Ai-iv = 50 µm.

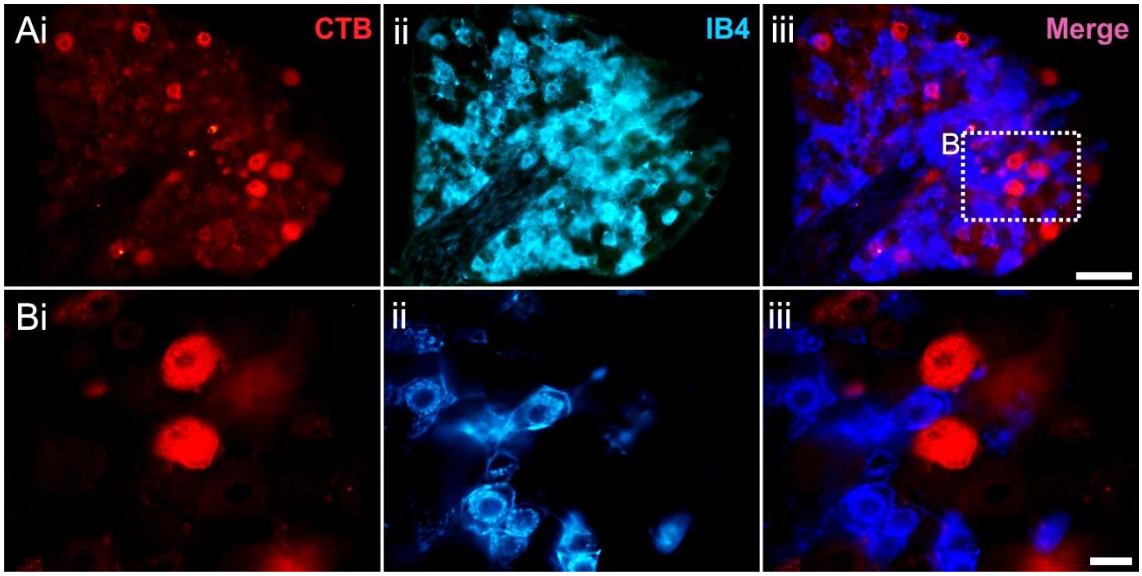

Figure 3.16 CTB does not label IB4-positive cell bodies in the dorsal root ganglia following low dose IP injection

Mice were injected IP with 500 µg of CTB and were fixed after three days. Slices were obtained from removed DRGs and were then subjected to immunohistochemistry. A) Whole DRG slice stained with anti-CTB (red, Ai), isolectin B4 (blue, Aii) and merged (Aiii). B) DRG section stained with anti-CTB (red, Bi), isolectin B4 (blue, Bii) and merged (Biii). Scale bars: A = 100 µm; B = 25 µm.

By counting the number of ChAT-positive cells that were also immunoreactive for CTB it was possible to calculate the proportion of neurones labelled in each area. In the spinal cord there were more CTB-positive cells in every region of the cord with the higher dose of 2000 µg (Figure 3.17A). The biggest difference was in the thoracic region with 73.0 ±4.48% cells labelled with 2000 µg and only 35 ±4.92% labelled with 500 µg ($p=0.00003$). There were significant changes in the cervical region with 55.4 ±4.12% of cells labelled after 2000 µg and 30.3 ±4.75% after 500 µg ($p=0.0001$). The least change was in the lumbar region with 72.9 ±3.18% of cells CTB-positive after 2000 µg, and 49.1 ±7.85% after 500 µg ($p=0.02$). In the brainstem there was no difference in the proportion of DVN cells labelled with CTB (Figure 3.18B), with 87.1 ±4.20% labelled after administration of 2000 µg, and 92.5 ±2.77% after 500 µg ($p=0.30$). In the hypoglossal nucleus there were no neurones labelled at the low dose, and 64.0 ±6.32% of cells were CTB-positive after the high dose ($p=0.00005$). There were significantly fewer cells labelled in the facial motor nucleus with just 20.2 ±10.6% labelled after 500 µg injection and 90.5 ±10.6% after 2000 µg ($p=0.0002$). The nucleus ambiguus also had fewer CTB-positive cells with 78.5 ±11.0% labelled after the high dose, and 21.2 ±10.0% labelled after the lower dose ($p=0.001$).

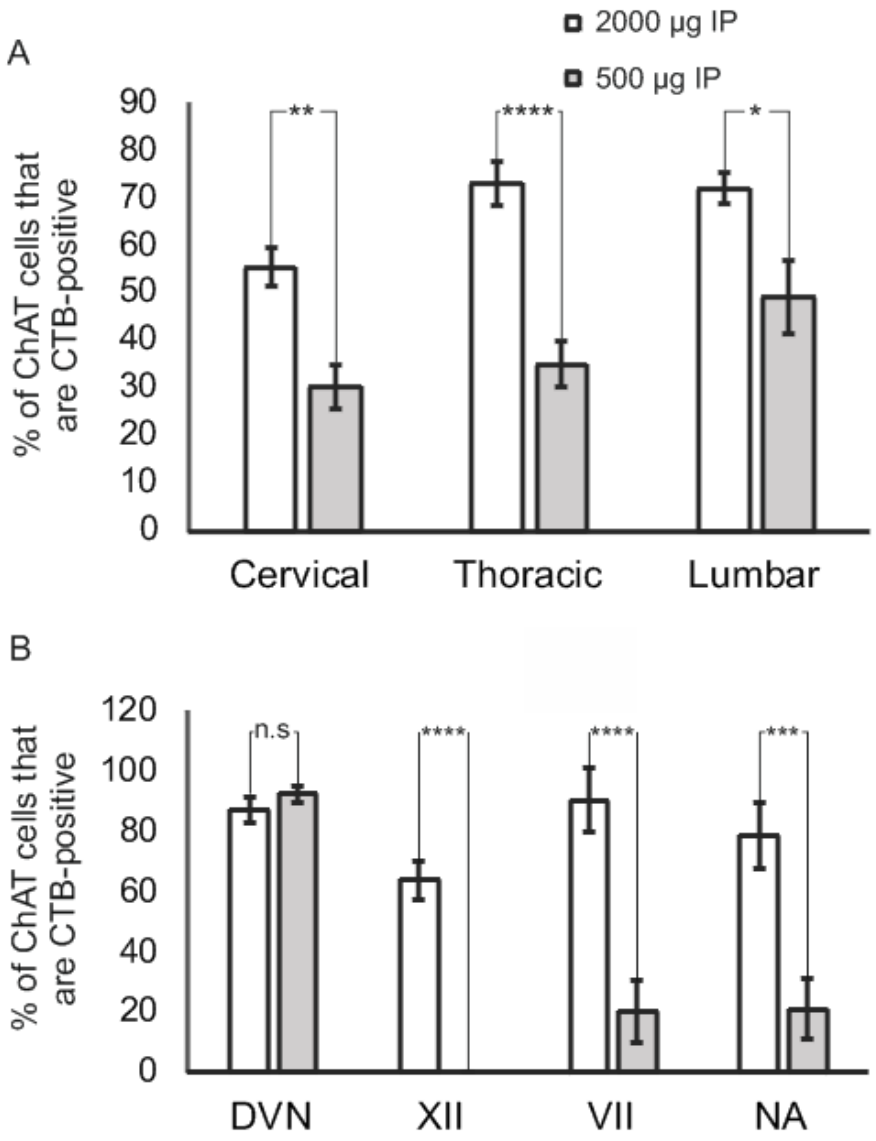

Figure 3.17 A higher proportion of ChAT-positive cells were also CTB-positive in most measured areas of the brainstem and spinal cord after the higher dose delivered IP

The average percentage of CTB labelled cells from the population of ChAT-positive cells ±SEM as measured by immunohistochemistry after IP injection of 2000 µg (white bars) and 500 µg (grey bars) of CTB. A) Comparison of proportion of labelled cells in the spinal cord. B) Comparison of proportion of labelled cells in the brainstem. Results are average of 3 sections from each animal (n=3). Significance measured with Student's unpaired t-test: n.s (not significant), * ($p<0.05$), ** ($p<0.01$), *** ($p<0.001$), **** ($p<0.0001$).

Following IP injection of CTB (500 µg and 2000 µg) the ventral horn was assessed for CTB labelling of alpha and gamma motor neurones. All CTB immunoreactive cells have vGLUT1 terminals in close apposition, suggesting termination of proprioceptive afferents (Figure 3.18A, B) as seen in alpha motor neurones. Most assessed CTB-positive cells were also immunoreactive for NeuN (Figure 3.18C, D) again a marker of alpha motor neurones but of the 73 slices of spinal cord counted, 3 were found to contain one gamma motor neurone each as measured by lack of NeuN staining (Figure 3.18D).

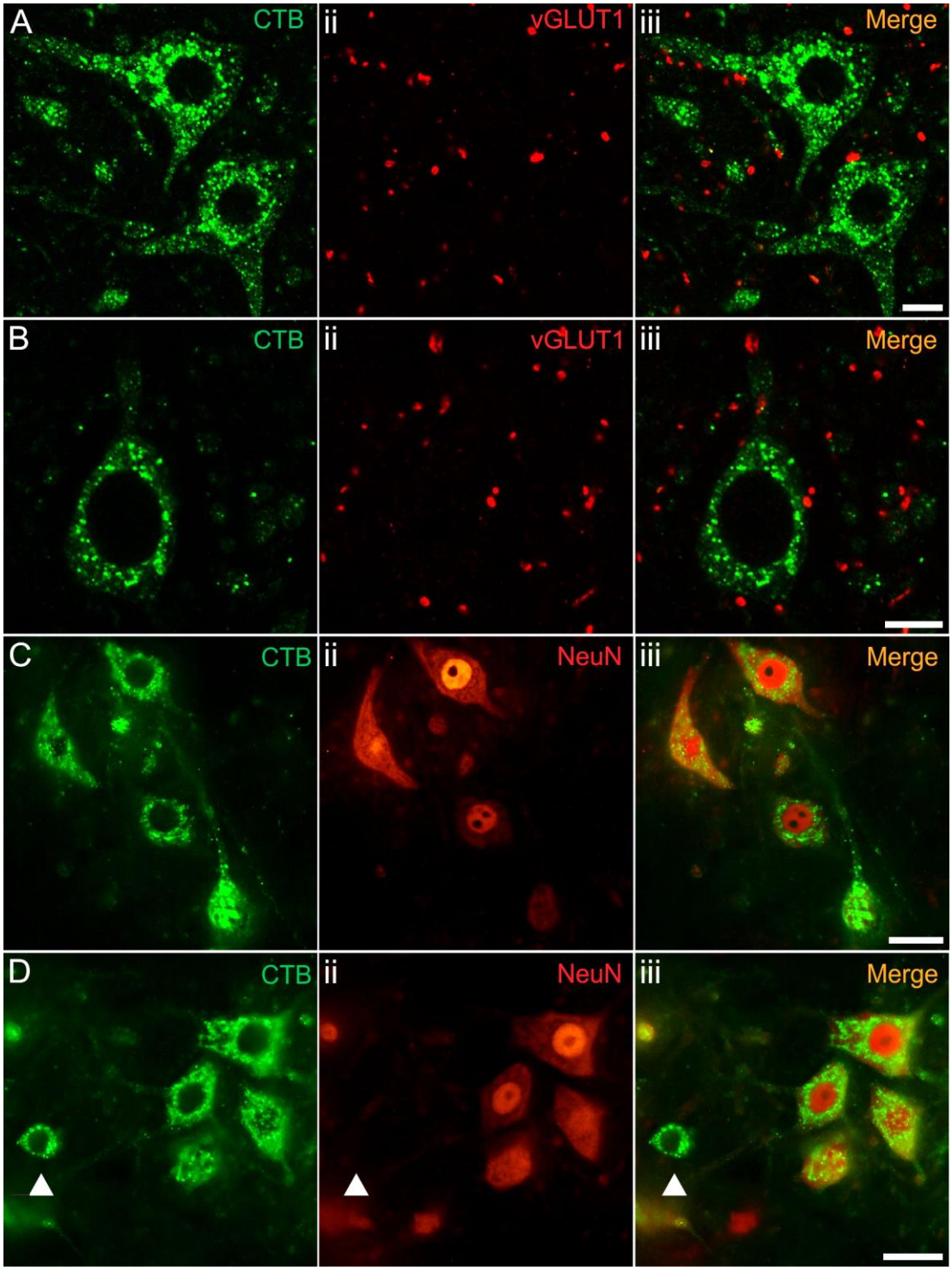

Figure 3.18 CTB predominantly labels alpha motor neurones in the ventral horn of the spinal cord after IP injection

Mice were injected IP with 500 µg (A, C) or 2000 µg (B, D) of CTB and were fixed after three days. Slices were obtained from removed spinal cords and were then subjected to immunohistochemistry. A+B) Ventral horn section stained with anti-CTB (green, Ai+Bi), anti-vGLUT1 (red, Aii+Bii) and merged (Aiii+Biii). C+D) Ventral horn section stained with anti-CTB (green, Ci+Di), anti-NeuN (red, Cii+Dii) and merged (Ciii+Diii). One cell contains staining for CTB without staining for NeuN (arrow, D). Scale bars: A, B = 10 µm; C, D = 25 µm.

The cerebral cortex and cerebellum were not positive for CTB immunoreactivity. Since administration was systemic, other organs were studied to assess for labelling of cells other than neurones. In the kidney there were some small cells labelled but this was primarily autofluorescence (Figure 3.19A). In one animal of the 5 assessed there were labelled cells in the kidney however the type of cell is unknown. Since this only occurred in one animal it is likely that the injection focused CTB directly about the kidney. The liver only had autofluorescent cells (Figure 3.19B). There were CTB-positive fibres in the muscle layer of the small intestine (Figure 3.19C). There was no reactivity for CTB in the heart (Figure 3.19D) or in the olfactory bulb (Figure 3.19E). There were occasional CTB-positive cells in the large intestine and these were not immunoreactive for c-kit, a marker of interstitial cells of Cajal (Figure 3.19Fi-iii).

Figure 3.19 Non-neuronal cells in organs were not labelled with CTB following IP injection

Mice were injected IP with 2000 µg of CTB and were fixed after three days. Slices were obtained from removed organs and were then subjected to immunohistochemistry. A) Section of kidney stained with anti-CTB (red) contains one labelled cell which was found to be autofluorescent. B) Section of liver stained with anti-CTB (red) with a blood vessel (BV) surrounded by autofluorescent cells. C) Section of small intestine (SI) stained with anti-CTB (red). D) Section of heart with the left ventricle (LV) highlighted for reference. E) Section of olfactory bulb (OlfB) stained with anti-CTB (red). F) Section of large intestine (LI) stained with anti-c-kit (red, Fi), anti-CTB (blue, Fii) and merged (Fiii). All autofluorescent cells were identified if they fluoresced under UV light. Scale bars: A, Fi-iii = 25 µm; B, C, E = 50 µm, D = 250 µm.

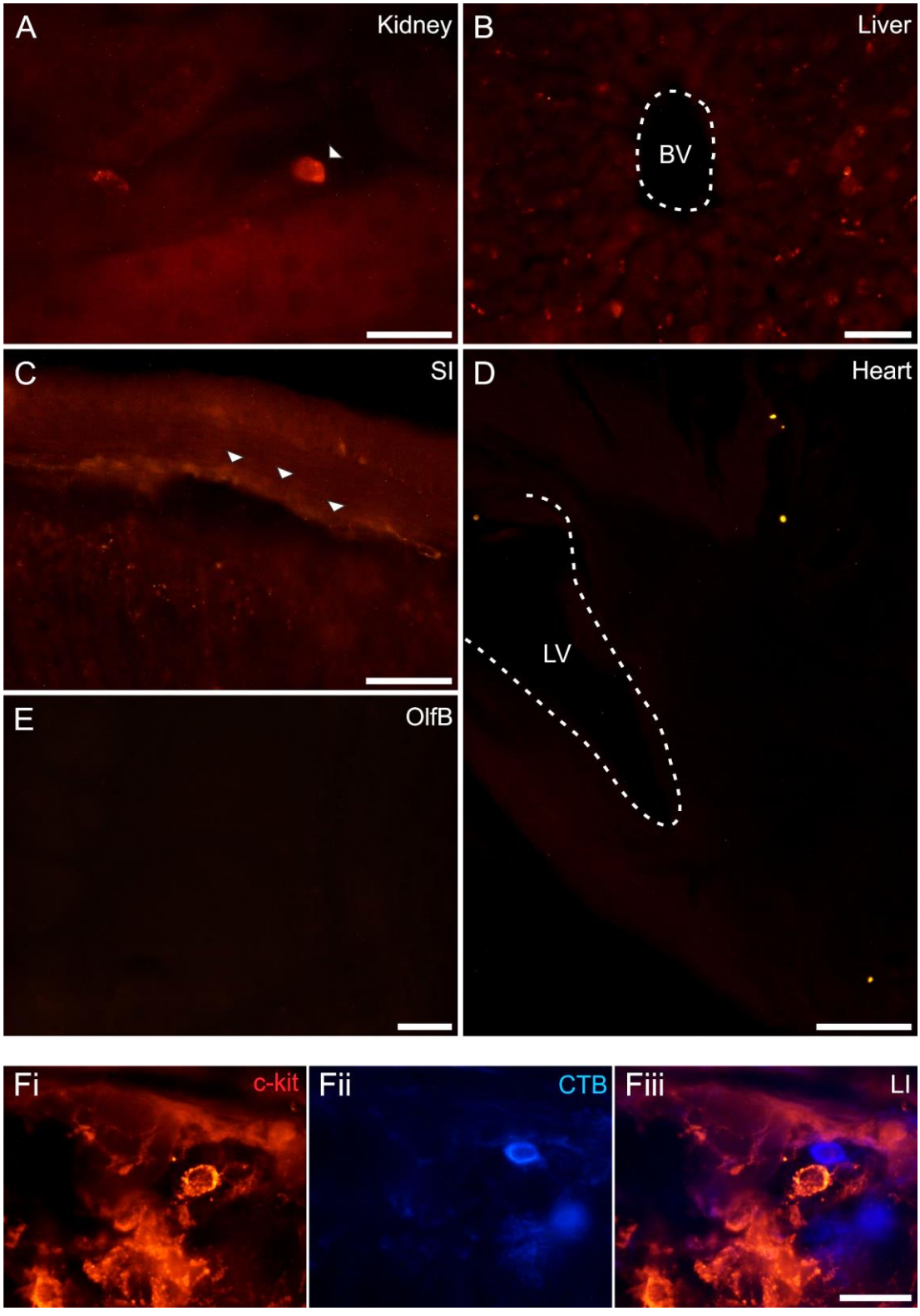
A
Kidney
B
Liver
BV
C
SI
D
Heart
LV
E
OlfB
Fi
c-kit
Fii
CTB
Fiii
LI

3.3.5 Peripheral administration of CTB – intramuscular

Intramuscular administration of 80 µg of CTB to the tongue resulted in intense labelling of the motor neurones of the hypoglossal nucleus (Figure 3.20). There were no other CTB-positive areas found in the brainstem or spinal cord after tongue injections.

Intramuscular administration of 50 µg of CTB to the gastrocnemius resulted in unilateral labelling of neurones in the ventral horn from levels L3-4 (Figure 3.21Aii, Bii). These cells were also positive for ChAT (Figure 3.21Aiii, Biii) indicating that they are motor neurones. The dorsal horn contained CTB-positive afferents at level L3 (Figure 3.21Ai) but not at level L4 (Figure 3.21Bi).

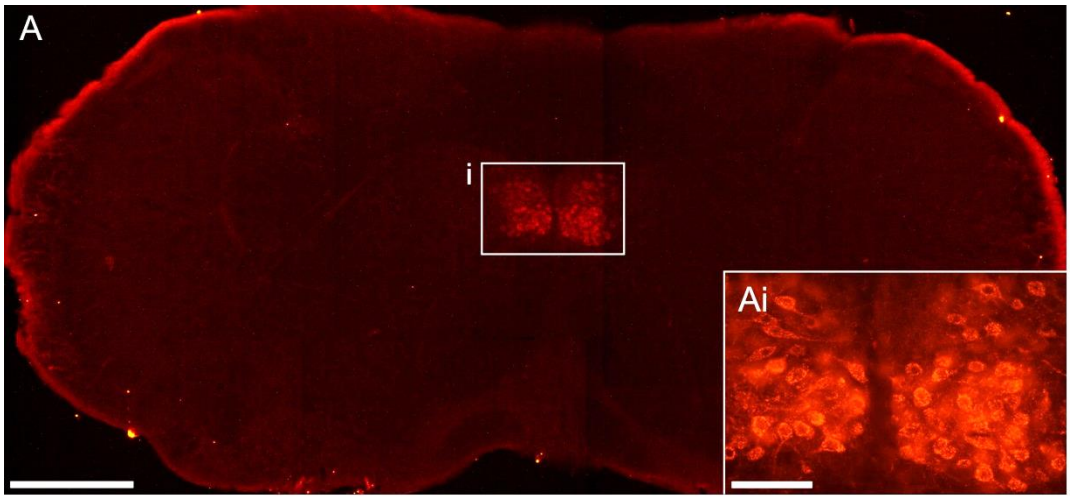

Figure 3.20 CTB labels neurones of the hypoglossal nucleus of the brainstem following tongue injection

Mice were injected with 80 µg of CTB to the tongue and were fixed after three days. Slices were obtained from removed brainstems and were then subjected to immunohistochemistry. A) Whole brainstem slice and hypoglossal nucleus (Ai) stained with anti-CTB (red). Scale bars: A = 500 µm; Ai = 100 µm.

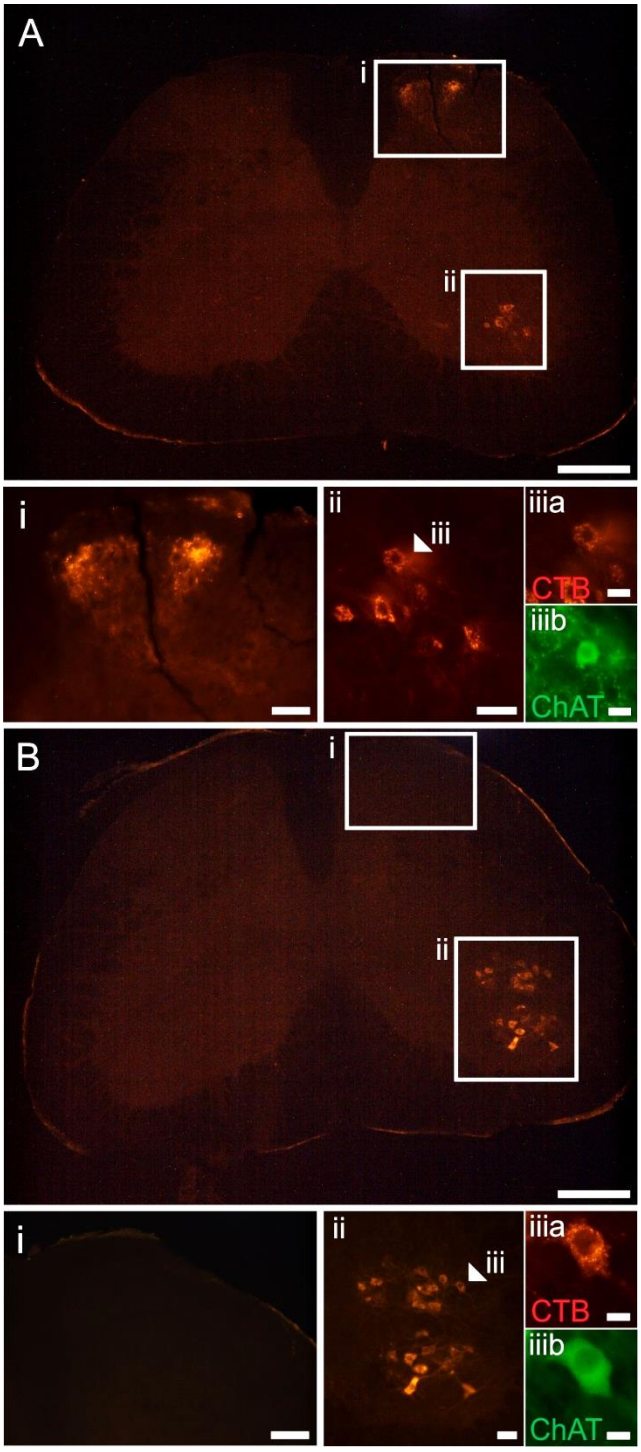

Figure 3.21 CTB labels neurones in the dorsal horn and ventral horn unilaterally after IM injection to the gastrocnemius

Mice were injected IM with 80 µg to the gastrocnemius and were fixed after 4 days. A) Slice from L3 stained with anti-CTB (red) in the dorsal horn (Ai) and ventral horn (Aii), and anti-ChAT (green, Aiiib) in a ventral horn section. B) Slice from L4 stained with anti-CTB (red) in the dorsal horn (Bi) and ventral horn (Bii), and anti-ChAT (green, Biiib) in a ventral horn section. Scale bars: A, B = 250 µm, Ai-ii, Bi-ii = 50 µm, Aiiia-b, Biiia-b = 10 µm.

3.4 Discussion

The experiments carried out in this chapter have elucidated the labelling patterns of LTB and CTB following systemic and central administration. Specifically that:

- Systemic injection of LTB and CTB label neurones in the brainstem and spinal cord with axons in the periphery, the toxins do not enter non-myelinated neurones of the spinal cord.
- There is no difference in the pattern of labelling following IP administration of LTB and CTB.
- Increasing the IP dose of CTB labels an increased number of neurones in the brainstem and spinal cord.
- Injection of CTB into specific muscles results in localised labelling of the neurones innervating the muscle.

3.4.1 Systemic administration of LTB and CTB labels neurones with axons in the peripheral nervous system

After both IP and IV injection of LTB or CTB, at all doses, there was labelling of motor neurones, autonomic preganglionic fibres and primary afferents within the brainstem and spinal cord. IP injections led to the most widespread and consistent labelling, with LTB/CTB-positive cells throughout the whole length of the spinal cord, and labelled cells in the most areas of the brainstem.

Following IP injection of LTB and CTB, the toxins are able to enter any GM1-expressing peripheral neurones. They are endocytosed and once inside the neurone are able to travel to the CNS, bypassing the BBB. The spinal cord contains labelling because while motor neurones have their cell bodies located in the CNS, their axons project out to specific muscles. There are also afferent fibres projecting back to the cord from the muscle which terminate in the dorsal horn. Both sets of neurones have myelinated axons in the periphery and so can endocytose the toxins as GM1 is highly expressed, whereas the non-myelinated C fibres are not able to, as shown by the absence of labelling in IB4-positive afferents. Again, the SPNs in the IML are projecting out from the CNS and so are accessible by the toxins. Motor neurones labelled in the brainstem include those of the facial motor nucleus (cranial nerve VII), hypoglossal nucleus (cranial nerve XII) and the nucleus ambiguus. The facial motor nucleus contains motor neurones that control facial expression (Martin and Lodge, 1977) and the hypoglossal nucleus contains those that innervate the tongue (Sokoloff and Deacon, 1992). The nucleus ambiguus contains motor neurones associated with cranial nerves IX, X and XI, and allows motor innervation of the ipsilateral muscles of

the soft palate, pharynx, larynx and upper oesophagus (Bieger and Hopkins, 1987). The autonomic preganglionic neurones labelled in the brainstem include the DVN, nucleus ambiguus (parasympathetic) and area postrema (sympathetic and vagal terminals). The DVN contains some vagal preganglionic neurones with parasympathetic output to the viscera (Kalia, 1981) as well as efferent fibres supplying the heart and lungs (Donoghue et al., 1981); all of these DVN neurones are predominantly non-myelinated (Agostoni et al., 1957; Nishimura and Oomura, 1987). This suggests these fibres express ganglioside GM1 even though they are not myelinated. One explanation could be that following an IP injection much of the toxin would reach DVN fibres first (i.e. those supplying the abdominal viscera), so even if the expression of GM1 is much lower, it would still be taken up readily.

The nucleus ambiguus gives rise to preganglionic parasympathetic neurones that innervate the heart, as well as the branchial efferent motor fibres of the vagus nerve (McAllen and Spyer, 1978). The area postrema plays a pivotal role in the autonomic functions of the CNS; it is situated where the BBB is leaky and so it senses what is occurring in the blood and is involved in appropriate retching and vomiting responses. The area postrema connects to the NTS and other autonomic control centres in the brainstem (Price et al., 2008). It is also excited by visceral afferents, both sympathetic and vagal. The primary afferents labelled in the brainstem are those of the NTS which contains both myelinated and non-myelinated fibres (Schild et al., 1994; Andresen et al., 2012). The NTS receives afferents from many organs (Kalia, 1981) and can be thought of as the integratory centre for autonomic control.

After IP injections, motor neurones labelled with CTB within the ventral horn were predominantly alpha motor neurones as they were mainly NeuN-positive and had vGLUT1 terminals in close apposition (Eccles et al., 1957). Gamma motor neurones do not express NeuN and are contacted by very few proprioceptive vGLUT1 terminals (Eccles et al., 1960; Friese et al., 2009). Gamma motor neurones constitute around 30% of all the motor neurones; they innervate the intrafusal muscle fibres found in muscle spindles and modulate the sensitivity of the spindles to stretch (Kuffler et al., 1951). Of the 73 spinal cord slices (from five animals) counted only 3 contained a gamma motor neurone, more would be expected to be labelled by CTB; this suggests CTB preferentially enters alpha motor neurones following IP injection.

For IV injections again it is the neurones with axons in the periphery that are able to endocytose the toxins. This is because once in the blood they can travel to the capillaries and access the neurones which are in close apposition. While most of the same areas as IP injection were labelled, it was almost always unilateral in both the

brainstem and spinal cord. This suggests that the LTB was taken up by neurones rapidly before being able to travel further in the blood. After jugular vein injection much of the labelling was in the cervical region, and after femoral injection labelling was predominantly lumbar. There was no LTB-positive labelling in the brainstem after femoral vein injection; whereas jugular injection labelled all the same areas of the brainstem as IP injection, except for the NTS. As the LTB appears to be removed from the blood very quickly by entering neurones it would seem it does not pass any NTS fibres, most of which would be found below the injection site. It is possible that some labelling seen could have resulted from spillage at the injection site, but care was taken to administer the toxin slowly and directly into the veins.

LTB/CTB is able to label the length of a neuron because GM1 is expressed in lipid rafts in the plasma membrane in the cell body, along the axon and upon the dendrites (Ericson and Blomqvist, 1988; Luppi et al., 1990). Toxin that is endocytosed at the terminal can be retrogradely transported to the nucleus by dynein to be recycled (Day et al., 2015). Along with the ability to anterogradely transport this means that the whole length of the neurone is labelled (Angelucci et al., 1996). When injected intraperitoneally the AB_5 toxins may enter blood vessels and the lymph system and then cross into the extracellular space of neurones to label them. This would explain why after injection into the intraperitoneal cavity neurones of the cranial nerves are labelled.

3.4.2 Labelling patterns following IP injection of LTB and CTB are identical

Given the more promiscuous nature of LTB's receptor profile (Fukuta et al., 1988) it was not known whether LTB may enter some additional neuronal populations after systemic administration when compared to CTB. Following IP injection the same areas of the brainstem and spinal cord were immunoreactive for the toxins, the labelling patterns were indistinguishable. This suggests that it is GM1 binding that determines LTB localisation rather than other lower affinity gangliosides it can bind. When assessing labelling within other organs (heart, kidney, liver and gastrointestinal tract) no other cell types were labelled, only autonomic fibres and occasional neuronal cell bodies. There was also no labelling in the cerebellum, forebrain or olfactory bulb. This suggests that the toxins can be used to specifically target neurones of the CNS with axons in the periphery when delivered systemically.

The results of this study predominantly agree with those in the Alisky et al. study where 1500 µg CTB was injected IP in mice. However they saw an increased number of cranial nerve nuclei labelled, as well as hypothalamic neurones (Alisky et al., 2002).

Given that a higher dose of 2000 µg of both LTB and CTB were administered the same results would be expected.

3.4.3 Increasing the dose of IP injection of CTB increases the number of neurones labelled

After injection of a high dose (2000 µg) of CTB there were a higher proportion of cells labelled in the brainstem and spinal cord when compared with a low dose (500 µg). This is likely because the amount of CTB that can be endocytosed by any one neurone will be limited by the GM1 expressed at the cell surface. Once the toxin binds the whole complex with GM1 is endocytosed (Fujinaga et al., 2003), meaning the amount at the cell surface is reduced. Once all the GM1 has been utilised any excess CTB is free to be transported and bind elsewhere. This provides further evidence that the toxin is taken up quickly after administration. In the low dose the CTB is available to fewer neurones as it is taken up rapidly. With a higher dose, along with those same neurones, more are labelled when the excess CTB spreads out, and may even travel in the blood to target other myelinated peripheral neurones.

The only region without a change in proportion of cells labelled was the DVN. This is likely due to the primary region it projects to being the gut, therefore any CTB injected IP would reach these neurones first. For the low dose much of the protein would be endocytosed by the DVN neurones, along with the NTS, but the higher dose saturates this population and is then able to travel in the intraperitoneal cavity and the blood to reach other neurones.

In terms of targeting CTB systemically to deliver another cargo this means if using IP as the delivery route a lower dose might be used if wanting to hit only a small proportion of neurones with axons in the periphery. The dose would need to be increased to target the majority of neurones. More direct injections such as IM will not require such a large dose since there are fewer neurones to target.

3.4.4 IM injection results in localised labelling of the neurones innervating the injected muscle

Injecting CTB into a muscle at a relatively low dose when compared to systemic injections resulted in localised labelling of neurones. For tongue injections, the hypoglossal nucleus was immunoreactive for CTB since this contains the cell bodies of the motor neurones innervating the tongue. Alisky et al. also noted trigeminal afferents, even after 15 µg injections of CTB. Injections to the gastrocnemius labelled cell bodies in the ventral horn from lumbar sections 3-4, the labelling was unilateral and matched to the side of injection. Afferent fibres were labelled in the dorsal horn at L3, but not

more caudally toward L4. The injection dose and volume (50 µg in 5 µL) were quite small and so CTB is likely to have remained in the area it was applied, and any excess was washed away immediately afterward and so couldn't have leaked away. It is possible that the injection sites used happened to be closer to L3 afferent fibres meaning most CTB was taken up by neurones in this area.

The intense and localised labelling of IM injections provides a good test route for any fusion proteins made from the toxins. They also require much less protein than systemic routes, so if conjugate yields are low it should still be possible to test them *in vivo*.

3.4.5 CTB or LTB can target specific subsets of neurones and may be used as delivery vehicles

The ability of CTB and LTB to target specific subsets of neurones when delivered systemically has been proven. The toxins appear to be non-toxic when administered as animals survived all procedures and there were no obvious side effects. This suggests they may provide a safe method of therapeutic delivery in mammals. No large immune response was seen after any route of administration; this was not specifically measured via blood biomarkers but there were no notable changes in animal behaviour suggesting there was not a major systemic immune response. It is possible that repeated administration could result in clearance of the complex before endocytosis by antibodies raised against the toxin subunits. A study with tetanus toxin C (TTC) found that uptake of the protein was not blocked by immunisation against tetanus toxoid (Fishman et al., 2006). The authors suggest that the uptake of the protein by nerve terminals following IM injection is rapid enough to avoid clearance. As already described, CTB and LTB also appear to be taken up very rapidly by cells and so this may prevent an immune response. One strategy to circumvent immunogenicity is to modify the toxin subunit by removing immunodominant epitopes (Cong et al., 1996), though these would need to be tested to check that they have retained their neurotropic properties.

Further evidence for the use of AB_5 toxins to deliver therapeutic cargo is that CTB has been modified before to deliver other proteins (see General Introduction 1.2.6). Considerations must be made as to what would be appropriate to deliver: intracellular targeting, length of time the complex remains inside the cell and whether the complex needs to cross synapses, for example. In terms of targeting, the toxins appear to remain in endosomal compartments following endocytosis; the punctate labelling seen suggests they are within endosomes or lysosomes rather than within the cytoplasm. If this is so, it might be considered to conjugate a protein targeted to lysosomes to treat

lysosomal storage disorders. Delivering the deficient sphingomyelinase that would break down accumulated cholesterol and glycolipids in the lysosomes of those suffering Niemann-Pick disease could be done with CTB (Chang et al., 2005). A targeting motif might be utilised to direct the conjugated protein to a specific intracellular location, or an endosomal escape strategy could be used to release the complex into the cytoplasm (El-Sayed et al., 2009). If a protein is delivered then multiple administrations will be required because the protein will eventually be degraded. Delivery of DNA would mean the cargo can be re-used to make increased amounts of protein; however this would require the complex to be protected from nucleases and other blood components that would destroy the DNA before it was delivered (Al-Dosari and Gao, 2009). If the cargo needs to be delivered to higher order neurones a trans-synaptic portion must be added to the delivery complex, as neither LTB nor CTB were shown to cross synapses in this study.

Given the generalised motor neurone labelling, it might be hypothesised that CTB or LTB could be used as vehicles to target therapeutics to motor neurones for lower motor neurone neuropathies. One such example is amyotrophic lateral sclerosis (ALS) since this causes deterioration of motor neurones and as yet has no successful treatment strategies. As both CTB and LTB would enter primary afferents and autonomic preganglionic neurones any conjugate protein would have to be tested as to whether entrance to off-target neurones was damaging to the other cells. There is a long list of pathways involved in the pathogenesis of ALS, meaning a number of different fusion proteins could be created and tested for therapeutic effect. Once a protocol is in place toxin conjugates can be made with relative ease, providing a useful strategy to quickly target cells with the option to utilise multiple fusion proteins at once.

Conclusion

CTB and LTB offer to be a promising therapeutic tools for delivery of protein or drugs to the CNS when administered at the periphery. The toxin subunits are selectively endocytosed by motor neurones, autonomic preganglionic fibres and primary afferents. Next the toxins need to be modified to be used as delivery vehicles, and the efficacy of these improved such to treat neurological diseases.

Chapter 4

Design and expression of the fusion protein CTB-parvalbumin and its characterisation both *in vitro* and *in vivo*

4.1 Introduction

Cholera toxin B (CTB) is a popular neuronal tracer (Flink and Westman, 1986; Luppi et al., 1987; Ericson and Blomqvist, 1988) and has been used as a delivery vehicle (see General Introduction 1.2.6). A fusion protein of CTB and saporin was found to ablate neurones after direct injection into specific ganglia (Llewellyn-Smith et al., 2000; Lujan et al., 2009). The ability of CTB to target neurones and circumvent the BBB when administered systemically makes it a good candidate for targeted delivery of therapeutic molecules. Specifically, CTB can target motor neurones, autonomic preganglionic neurones and primary afferents (Alisky et al., 2002; Havton and Broman, 2005). With this in mind, we hypothesised that CTB fusion proteins could target motor neurones to potentially improve motor neurone diseases. Amyotrophic lateral sclerosis (ALS) is a progressive disease causing muscle weakness due to deterioration of motor neurones. As of yet there are no successful treatment strategies, with patients usually dying 2-5 years after onset of symptoms (Turner et al., 2013). This presents a major unmet clinical need in the development of therapeutics to treat the disorder.

ALS may be sporadic or familial, and while there are a number of known mutations, common outcomes of many of these are glutamate and calcium excitotoxicity (Jaiswal, 2014; Leal and Gomes, 2015). Some ALS patients have increased glutamate levels in their CSF compared to healthy controls (Spreux-Varoquaux et al., 2002). This could cause excitotoxic motor neurone death via glutamate-induced calcium entry through AMPA receptors and lead to activation of apoptotic pathways. Calcium permeability of AMPA receptors is mediated by the presence of the glutamate receptor 2 (GluR2) subunit (Mishina et al., 1991), those lacking the subunit are more permeable to calcium ions. Motor neurones have relatively low levels of GluR2 (Van Damme et al., 2002) and thus are more prone to calcium overload. In ALS, particularly vulnerable populations of neurones within brainstem and spinal cord are those with low levels of calcium buffer proteins (Alexianu et al., 1994). Parvalbumin and calbindin-D28k are neuronal calcium buffer proteins, they are calcium-free at basal levels but as intracellular calcium increases the ion binds to the proteins to prevent the concentration becoming toxic (Schwaller, 2010). Mitochondria also participate in calcium homeostasis acting to remove cytosolic calcium via a calcium uniporter (Kirichok et al., 2004), this acts as a calcium store where the concentration may reach 50 times that of cytosolic calcium (Nicholls and Scott, 1980).

By increasing the expression of calcium buffer proteins such as parvalbumin it may be possible to prevent the death of motor neurones. This is further supported by a study where SOD1 mutant mice were crossed with a parvalbumin overexpressing mouse line

(Beers et al., 2001). These mice had an increased number of surviving motor neurones, the onset of the disease was delayed (17%) and survival was prolonged (11%). In terms of human life this would make a huge impact for ALS sufferers by delaying onset of symptom worsening, thus improving quality of life.

4.1.1 Summary and objectives

A CTB-parvalbumin fusion protein is hypothesised to enter motor neurones and buffer the calcium overload as seen in ALS. Therefore, in this study, we will design and express a CTB-parvalbumin fusion protein and assess labelling of the spinal cord and brainstem after systemic administration in mice.

Research questions:

1. Can a CTB-parvalbumin fusion protein be expressed using bacteria?
2. Can the fusion protein enter neurones and be detected *in vivo*?
3. Does the fusion protein retain the ability to bind calcium, and is it neuroprotective?

The DNA sequence of the CTB-parvalbumin fusion protein was to be built by assembly PCR, and expressed via *E.coli*. It will be tested in cell culture as well as *in vivo* to test its ability to enter cells and be detected. Isothermal titration calorimetry and calcium imaging will be utilised to assess whether the fusion protein retains calcium binding ability. Also, *ex vivo* experiments in CNS slices will be employed to investigate neuroprotective properties.

The results from this study will provide methodology for expressing CTB fusion proteins in *E.coli*. If the fusion protein is able to enter neurones after systemic administration it will provide further evidence for the use of CTB as a vehicle for targeted delivery of therapeutic cargo.

4.2 Materials and methods

Two different fusion proteins of CTB and parvalbumin were designed: an AB_5 N-terminal parvalbumin fusion protein (AB_5-parv) and a C-terminal CTB fusion protein (CTBparv). Tables of oligonucleotide sequences used in assembly PCR for AB_5-parv can be found in appendix section 8.1 and for CTBparv in section 2.2 (Table 2.1). All molecular biology procedures are described in section 2.2. Protein characterisation techniques are described in General Methods section 2.3.

Cell culture was undertaken as described in General Methods section 2.4. Tracing injections in mice with CTBparv are described in section 2.5.5, see table 4.1 for injection routes tested. All tissue was prepared as described in General Methods section 2.5.6 and 2.5.7 and all antibodies used are listed in table 2.2. Fluorescent images were acquired as described in section 2.6.5.

Route	Dose (µg)	n	Days to perfusion
IP	2000, 1000, 500	3 per dose	3
IP (young)	500	2	2
IM (tongue)	50	3 per dose	1, 4, 7, 13
IM (gastrocnemius)	80	2	4

Table 4.1 Dose, n number and length of time until perfusion for each route of CTBparv injection

4.3 Results

4.3.1 AB_5-parvalbumin N-terminal fusion protein production was not successful

To create an AB_5-parvalbumin fusion protein with the parvalbumin replacing the toxic A1 portion pSAB2.1 (Ross, 2013) was used (see appendix 8.2.1). By using restriction enzymes NdeI and XhoI the MBP-CTA2 portion was removed, to be replaced with parvalbumin-CTA2 built by assembly PCR. The plasmid can then express parv-CTA2 gene fusion and CTB from a polycistronic mRNA (Figure 4.1Ai). Each protein has an LTIIb leader sequence for periplasm targeting; once in the periplasm the two proteins can combine to form an AB_5 fusion protein (Figure 4.1Bi).

Different magnesium concentrations of 1.5, 2 or 4 mM, and a range of melting temperatures (50.0, 53.2, 56.7, 59.9 °C) were used in assembly PCR conditions, as well as the addition of DMSO. In three conditions there appeared to be a product of the expected size, 525 bp (Figure 4.1Aii). However upon attempting to digest, ligate and transform (including using beta-mercaptoethanol) into pSAB2.1 no colonies were grown.

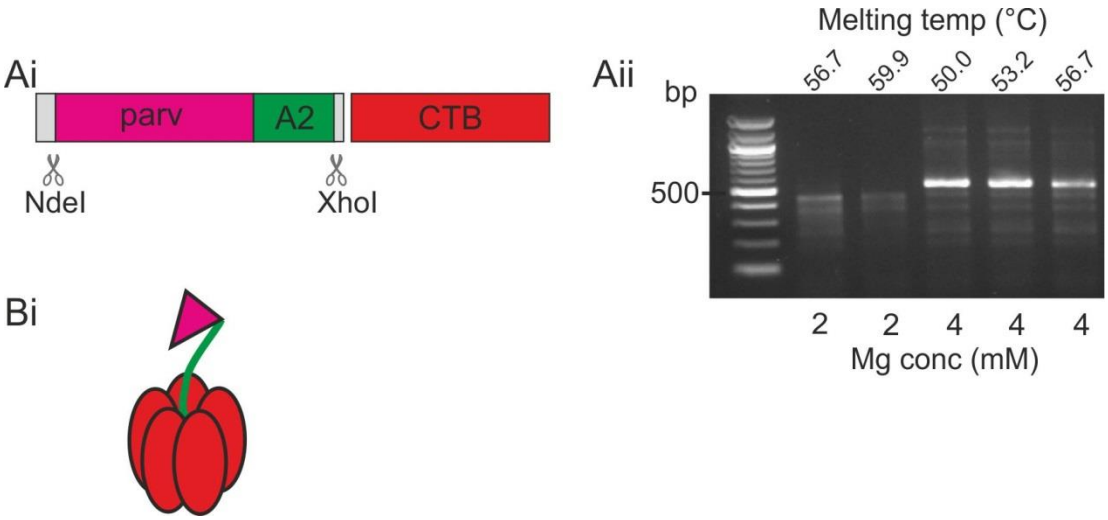

Figure 4.1 N-terminal AB_5-parv fusion protein

The DNA sequence for A2-parv was designed to be built with assembly PCR where, when cut with NdeI and XhoI, the sequence could be ligated into pSAB2.1 containing the sequence for CTB. Ai) Schematic of AB5-parv DNA sequence with restriction sites. Aii) Analysis by agarose gel electrophoresis of assembly PCR products. Bi) Schematic of the expected protein for AB_5-parv: CTB (red), A2 linker (green) and parvalbumin (pink).

4.3.2 A C-terminal CTB-parvalbumin fusion protein (CTBparv) was created, purified and characterised

The C-terminal CTB fusion protein was designed to contain CTB followed by parvalbumin with a glycine and asparagine linker in between (Figure 4.2Ai). The C-terminus of CTB faces away from the GM1 binding face, meaning the parvalbumin should not interfere with endocytosis of the protein. The DNA for CTBparv was assembled using assembly PCR, the whole sequence was 715 bp in length (Figure 4.3). After running PCR products on an agarose gel, a band can be seen around the 700 bp region (Figure 4.2Aii). After digestion with restriction enzymes SphI and PstI the DNA was ligated into pSAB2.2 (see section 8.2.2 for sequence) (Ross, 2013), and the plasmid transformed into XL-10 ultra-competent cells for production of more plasmid. The plasmid was then transformed into C41(DE3) cells for overexpression. The purified protein was expected to be 125 kDa. After SDS-PAGE a band around the expected size can be seen in the elution fractions. The boiled sample contains a band around 25 kDa, the expected size of the fusion protein monomer (Figure 4.2Bii). After further purification via size exclusion chromatography using an S200 column on an ÄKTA fast protein liquid chromatography clean bands can be seen after SDS-PAGE indicating pure protein (Figure 4.2Bii). The complex was sufficiently stable to migrate as a pentamer unless the sample was boiled prior to loading onto the gel. Western blot analysis of purified protein using antibodies against CTB and parvalbumin both detect a protein around 25 kDa, the size of CTBparv monomer suggesting both portions of fusion protein are present (Figure 4.2Biii). A hypothetical schematic of the fusion protein shows the parvalbumin sitting away from the GM1 binding face (Figure 4.2Bi).

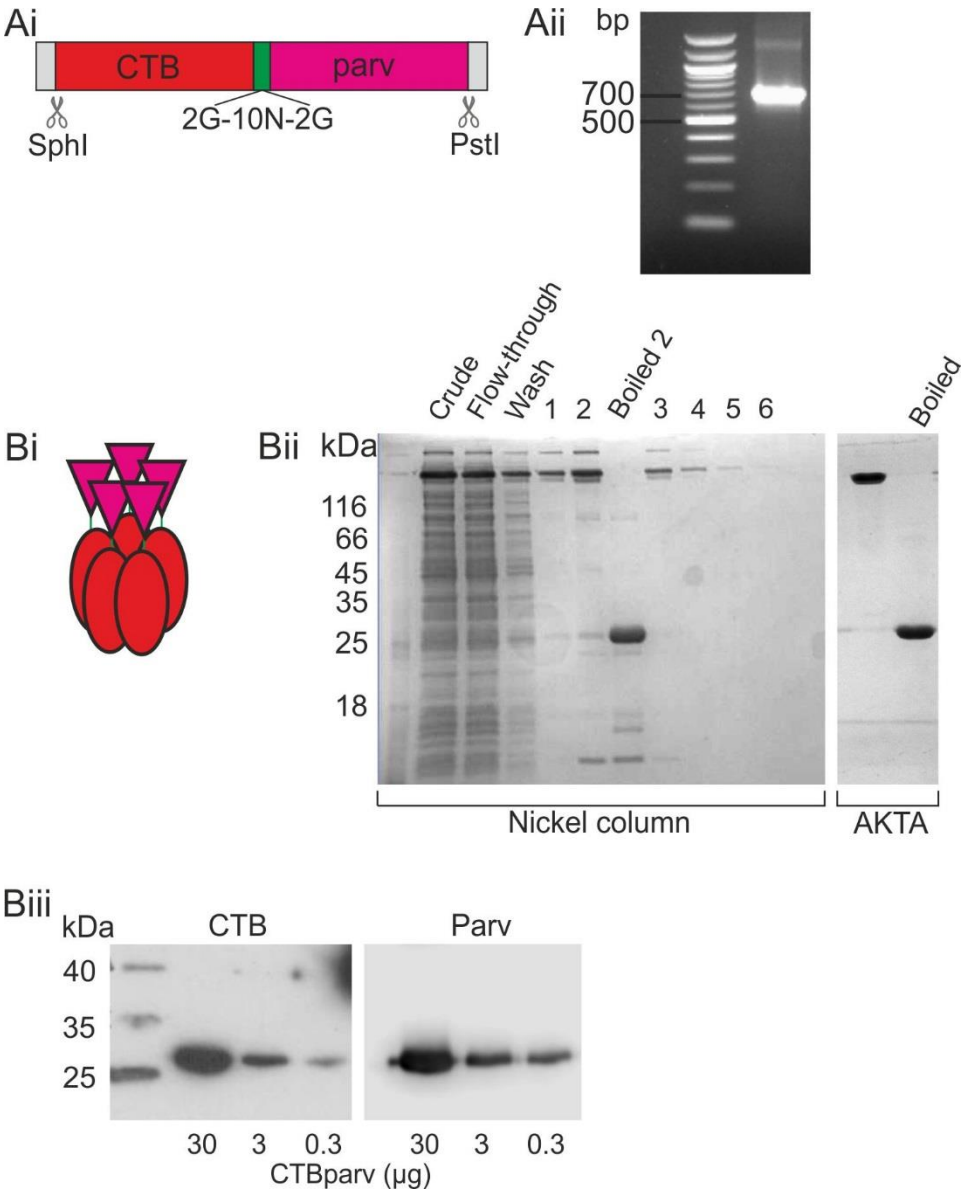

Figure 4.2 C-terminal CTB-parvalbumin fusion protein

The DNA sequence for CTBparv was designed to be built with assembly PCR where, when cut with SphI and PstI, the sequence could be ligated into pSAB2.2 for expression. Ai) Schematic of CTBparv DNA sequence with restriction sites. Aii) Analysis by agarose gel electrophoresis of assembly PCR products. Bi) Schematic of the expected protein for CTBparv: CTB (red), A2 linker (green) and parvalbumin (pink). Bii) SDS-PAGE analysis of nickel-column purified proteins with boiled sample to visualise monomer units; product further purified eluted ÄKTA fast protein liquid chromatography. Biii) Western blot analysis of purified protein probed with anti-CTB and anti-parvalbumin.

CTBparv DNA sequence

CTGTTCAGGCGCATGCAGCTCCTCAAAATATTACTGATTTGTGCGCAGAATACCACAAC
ACACAAATATATACGCTAAATGATAAGATCTTTTCGTATACAGAATCGCTAGCGGGAAAA
AGAGAGATGGCTATCATTACTTTTAAGAATGGTGCAATTTTTCAAGTAGAGGTACCAGGT
AGTCAACATATAGATTCACAAAAAAAAGCGATTGAAAGGATGAAGGATACCCTGAGGAT
TGCATATCTTACTGAAGCTAAAGTCGAAAAGTTATGTGTATGGAATAATAAAACGCCTCA
TGCGATCGCCGCAATTAGTATGGCAAACGGCGGTAATAACAATAACAATAACAATAACA
ATAACGGCGGTATGTCGATGACAGACTTGCTGAACGCTGAGGACATCAAGAAGGCGGT
GGGAGCCTTTAGCGCTACCGACTCCTTCGACCACAAAAAGTTCTTCCAAATGGTCGGC
CTGAAGAAAAAGAGTGCGGATGATGTGAAGAAGGTGTTTCACATGCTGGACAAGGACA
AAAGTGGCTTCATCGAGGAGGATGAGCTGGGATTCATCCTAAAAGGCTTCTCCCCAGA
TGCCAGAGACCTGTCTGCTAAAGAAACCAAGATGCTGATGGCTGCTGGAGACAAAGAT
GGGGACGGCAAAATTGGGGTTGACGAATTCTCCACTCTGGTGGCTGAAAGCTAAGTTT
TCCCTGCAGG

CTBparv amino acid sequence

XVQAHAAPQNITDLCAEYHNTQIYTLNDKIFSYTESLAGKREMAIITFKNGAIFQVEVPGSQHI
DSQKKAIERMKDTLRIAYLTEAKVEKLCVWNNKTPHAIAAISMANGGNNNNNNNNNNGGMS
MTDLLNAEDIKKAVGAFSATDSFDHKKFFQMVGLKKKSADDVKKVFHMLDKDKSGFIEEDE
LGFILKGFSPDARDLSAKETKMLMAAGDKDGDGKIGVDEFSTLVAES*VFPA

Figure 4.3 DNA and amino acid sequences of CTBparv as built by assembly PCR

With CTB (red), linker (green) and parvalbumin (pink). * in amino acid sequence indicates stop codon.

Mass spectrometry analysis of the purified protein revealed the monomer mass to be 25053.24 Da (see appendix 8.3), as expected by the calculated mass of 25053.29 Da. CTBparv was still able to bind its ligand GM1 as measured by ITC (Figure 4.4A) with a dissociation constant (K_d) of 49 nM. ITC was also utilised to assess the calcium binding properties of CTBparv but the results were inconclusive. EDTA was used to remove calcium ions from the fusion protein, and then the chelator dialysed out of solution before ITC. When calcium was added to CTBparv during ITC there looked to be binding as there was a change in differential power (DP) upon each addition, however the change was the same with every injection of calcium and the protein was never saturated (Figure 4.4B). When the instrument detects heat being released in the sample cell, the feedback system compensates by supplying less power to the sample cell heater than to the reference cell heater in order to keep them at the same temperature. The difference in power (DP) supplied to the two cells is the raw data. Integrating the power versus time allows for the measurement of heat released on each injection. CTBparv was passed over an EDTA-agarose gel as another method to remove calcium ions. When calcium was injected in ITC the change in DP was no different to that seen in the control experiment of calcium into buffer (Figure 4.4C); this suggests there was no binding since there was no change in enthalpy. However whether all calcium was removed was not assessed.

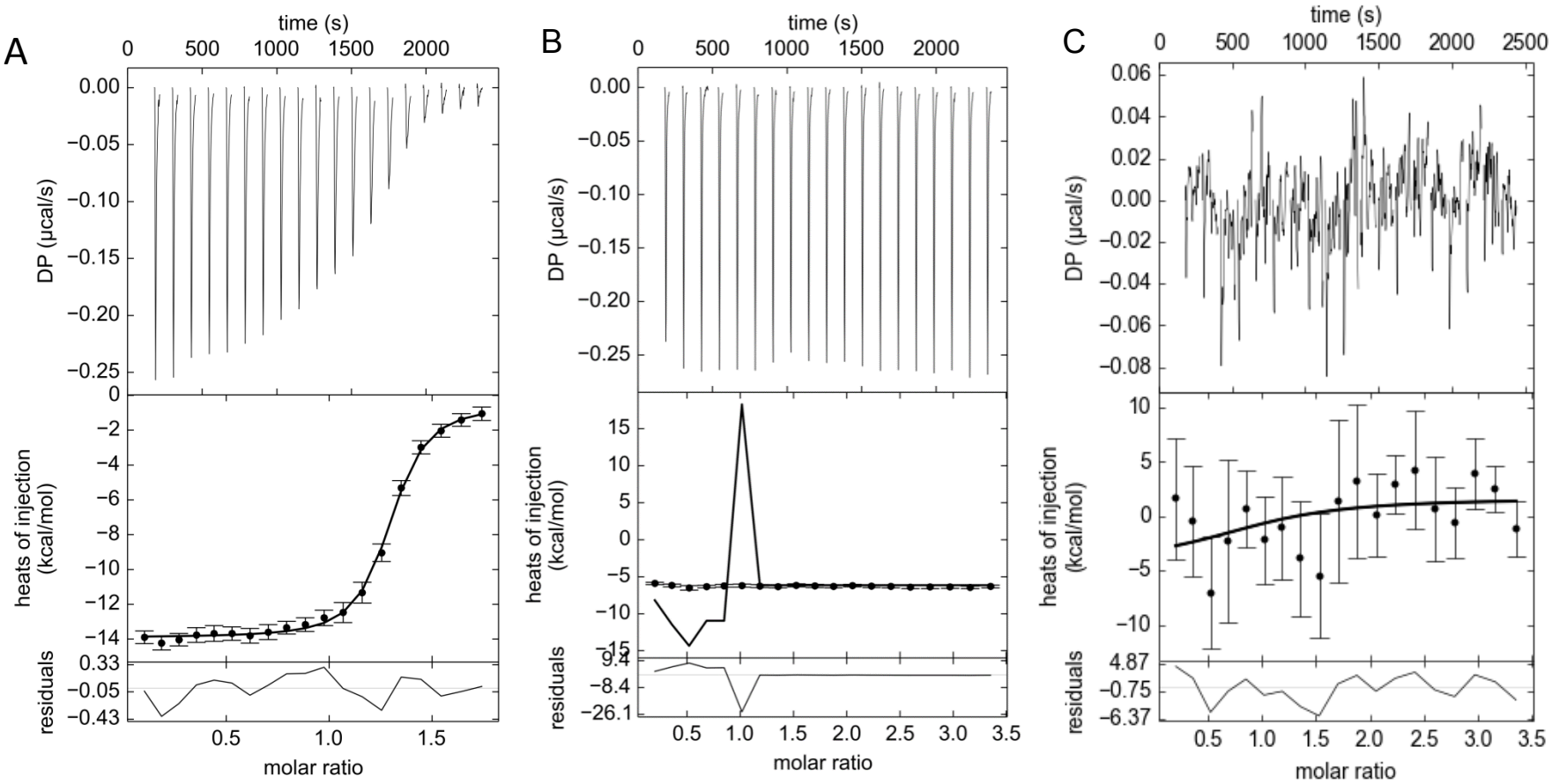

Figure 4.4 Isothermal titration analysis of CTBparv binding either GM1 or calcium

Plots show baseline-adjusted raw trace (upper), the fitted data (centre) and residual error (lower). A) Titration of 88 µM GM1os against 11 µM CTBparv. B) CTBparv was incubated with EDTA to remove calcium ions, titration of142.2 µM calcium chloride against 8.9 µM CTBparv. C) CTBparv was run on an EDTA-agarose column to remove calcium ions, titration of 160 µM calcium chloride against 10 µM CTBparv.

4.3.3 HEK293 cells endocytose CTBparv

HEK293 cells were cultured and incubated with CTB (n=3) or CTBparv (n=3) for 4 hours to assess if the fusion protein could be endocytosed and detected via immunohistochemistry. When incubated with CTBparv and fixed immediately (without acid wash step), immunostaining reveals an outline of parvalbumin around the cells, suggesting it is membrane-bound although some labelling is intracellular (Figure 4.5Ai). This does not wholly colocalise with CTB labelling which is predominantly intracellular (Figure 4.5Aii). Cells can be washed with acetic acid buffer to remove protein that has not been internalised. When the HEK293 cells undergo an acid wash before fixing this excess membrane-bound CTBparv is removed, and both parvalbumin and CTB are immunoreactive intracellularly (n=3) (Figure 4.5Bi-iv). When the cells are incubated with CTB alone without an acid wash, the CTB is clearly intracellular (Figure 4.5Cii-iv). Following an acid wash it becomes much clearer where the CTB can be detected within the cells (n=3). The intense region of staining sitting around a portion of the nucleus is indicative of labelling of the Golgi apparatus (Figure 4.5Div) and the remaining punctate labelling suggests CTB is within endosomes and lysosomes. HEK293 cells do not endogenously express parvalbumin as shown by lack of immunoreactivity for the protein after incubation with just CTB.

HEK293 cells were incubated with CTBparv (2 µg/mL) for 1-24 hours and underwent an acid wash before fixation and immunohistochemistry to determine potential differences in distribution of the fusion protein over time (Figure 4.6). At 1, 2, 4, 8 and 24 hours (n=3 for each time point) immunoreactivity for CTB and parvalbumin is intracellular with colocalisation of each half of the fusion protein throughout the cell (Figure 4.6A-Ei-iv). Over the time course measured the CTB and parvalbumin immunoreactivity does not change throughout the cells, it is punctate in the cytoplasm at all times, but at 8 and 24 hours some puncta are more distinct.

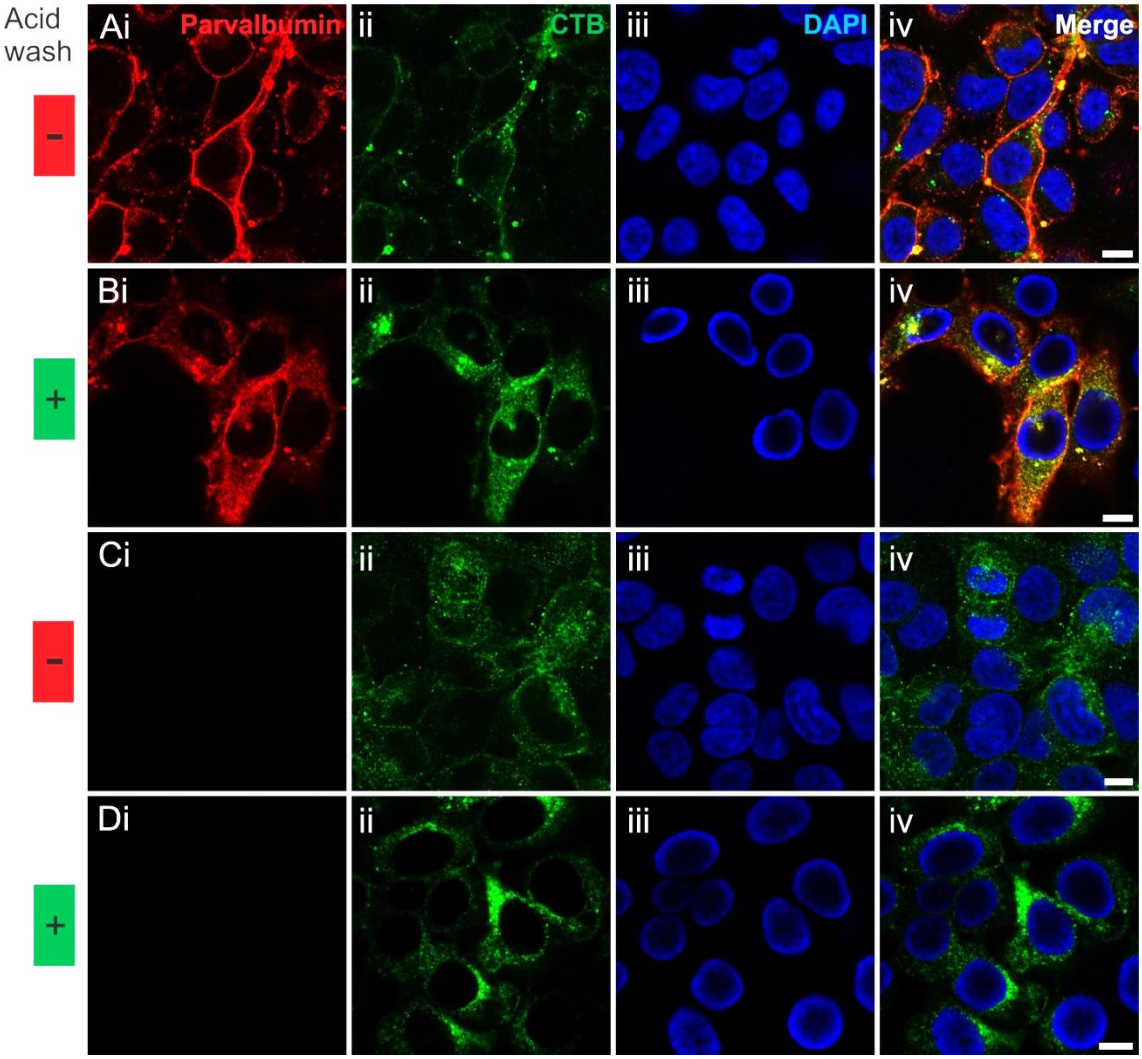

Figure 4.5 CTB and CTBparv label HEK293 cells following incubation

HEK293 cells were incubated with CTB or CTBparv (2 µg/mL) for 4 hours. A) Following incubation with CTB cells were fixed and stained with anti-parvalbumin (red, Ai), anti-CTB (green, Aii), DAPI (blue, Aiii) and merged (Aiv). B) Following incubation with CTB cells underwent an acid wash, were fixed and then stained with anti-parvalbumin (red, Bi), anti-CTB (green, Bii), DAPI (blue, Biii) and merged (Biv). C) Following incubation with CTBparv cells were fixed and stained with anti-parvalbumin (red, Ci), anti-CTB (green, Cii), DAPI (blue, Ciii) and merged (Civ). D) Following incubation with CTBparv cells underwent an acid wash, were fixed and then stained with anti-parvalbumin (red, Di), anti-CTB (green, Dii), DAPI (blue, Diii) and merged (Div). Scale bars: 10 µm.

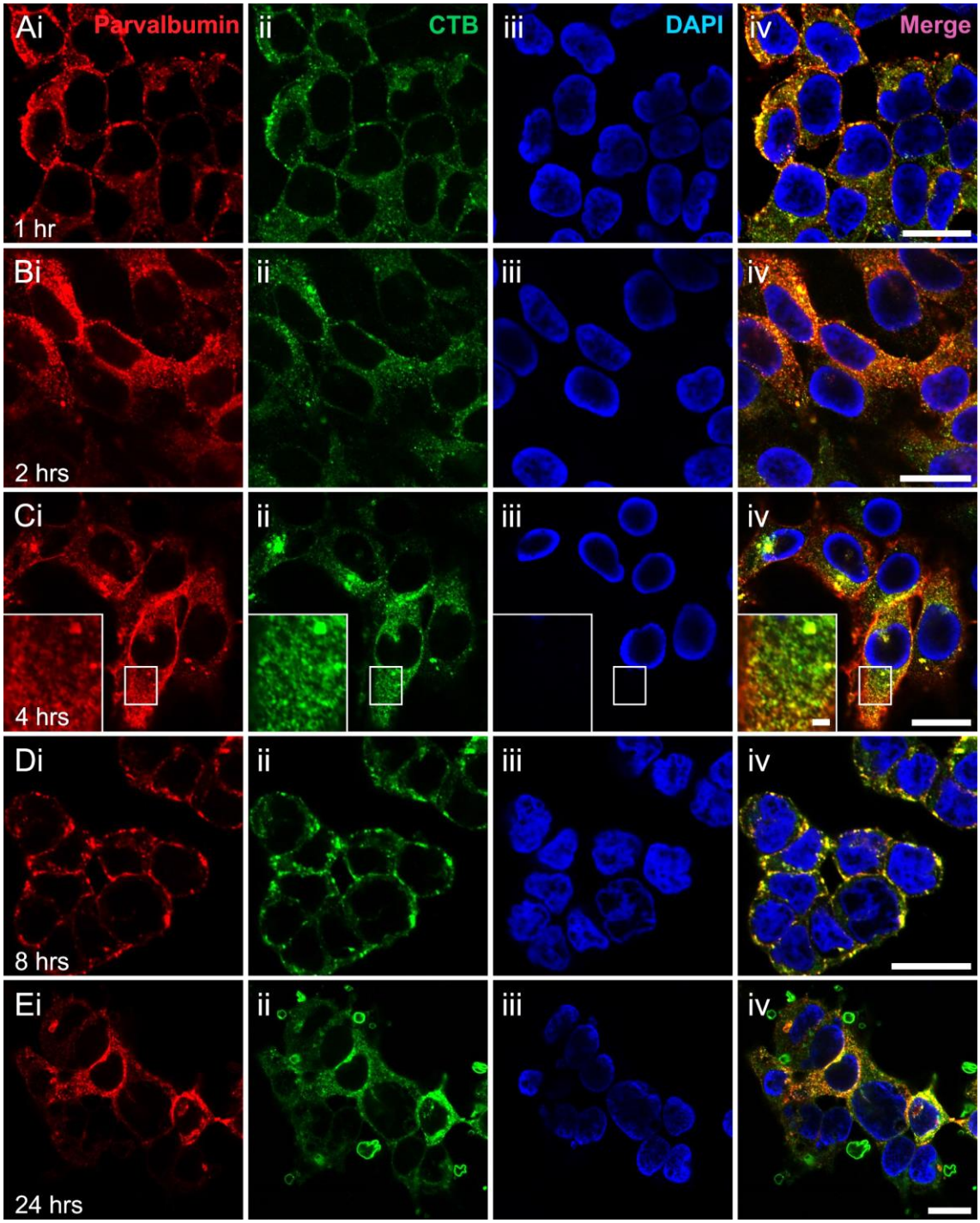

Figure 4.6 HEK293 cells are labelled with CTBparv after 1 and up to 24 hours

HEK293 cells were incubated with CTBparv (2 µg/mL), underwent an acid wash and were then fixed and stained with anti-parvalbumin (red, A-Ei), anti-CTB (green, A-Eii), DAPI (blue, A-Eiii) and merged (A-Eiv). A) HEK293 cells incubated with CTBparv for 1 hour. B) HEK293 cells incubated with CTBparv for 2 hours. C) HEK293 cells incubated with CTBparv for 4 hours with enlarged panels. D) HEK293 cells incubated with CTBparv for 8 hours. E) HEK293 cells incubated with CTBparv for 24 hours. Scale bars: 20 µm; C insert panel = 2 µm.

4.3.4 Cultured dorsal root ganglia are able to endocytose CTBparv

To assess whether neuronal cells would endocytose CTBparv, rat DRG cells were cultured and incubated with 2 µg/mL of the protein for 24 hours. Both CTB and parvalbumin could be detected via immunohistochemistry (Figure 4.7Ai-iii). In the cell body CTB immunoreactivity appeared more punctate compared to parvalbumin which was more intensely stained at the plasma membrane (Figure 4.7Bi-iii). Dendrites were strongly labelled with both CTB and parvalbumin (Figure 4.7Ci-iii) and AiryScan imaging revealed the proteins were predominantly colocalised suggesting the fusion protein was still whole (Figure 4.7Di-iii). Control DRGs were immunolabelled for CTB and parvalbumin; there were no CTB-positive cells, and while some were positive for parvalbumin they were a minority (Figure 4.7Ei-iii).

Figure 4.7 Cultured DRG neurones are labelled following incubation with CTBparv

DRG neurones were incubated with CTBparv (2 µg/mL) for 4 hours, underwent an acid wash, were fixed and then stained with anti-parvalbumin (red, A-Ei), anti-CTB (green, A-Eii) and merged (A-Eiii). A) DRGs incubated with CTBparv and stained for parvalbumin and CTB. B) DRG cell body after incubation with CTBparv stained for parvalbumin and CTB. C) Dendrites after incubation with CTBparv stained for parvalbumin and CTB. D) AiryScan analysis of neurite stained for parvalbumin and CTB. E) Control DRGs with no CTBparv added stained for parvalbumin and CTB. Scale bars: A = 20 µm; B, C = 10 µm; D = 1 µm; E = 25 µm.

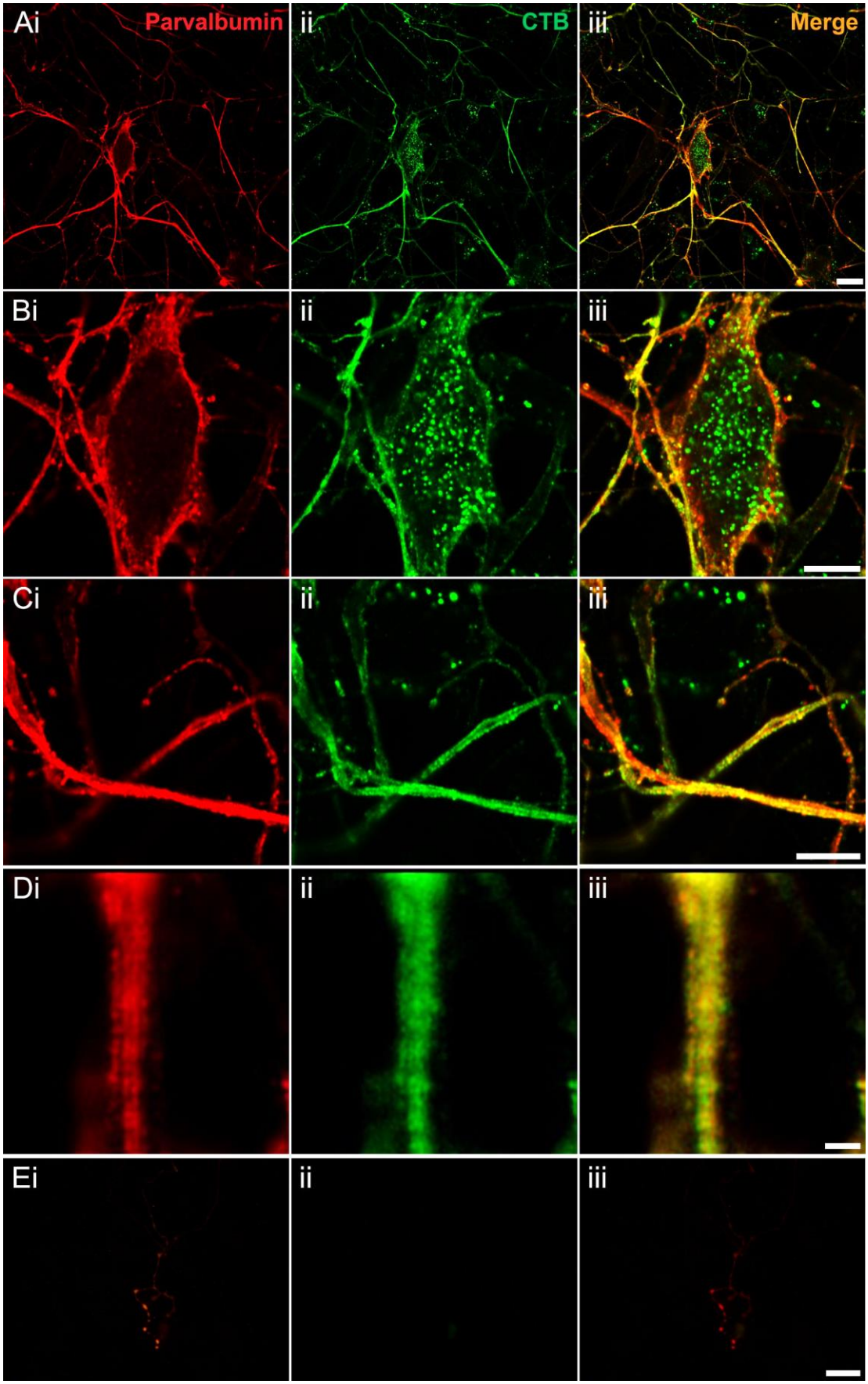
Ai
Parvalbumin
ii
CTB
iii
Merge
Bi
ii
iii
Ci
ii
iii
Di
ii
iii
Ei
ii
iii

4.3.5 CTBparv can be detected in the brainstem following tongue injection

CTBparv was injected IM via the tongue in mice to assess whether the fusion protein could be endocytosed and retrogradely transport *in vivo*. CTBparv was detected in the hypoglossal nucleus one day after tongue injection in mice (n=3) (Figure 4.8Ai-iii). CTB-positive motor neurones are also immunoreactive for parvalbumin (Figure 4.8Bi-iii) however the two proteins are not wholly colocalised within cells (Figure 4.8Ci-iv). Parvalbumin is less punctate than CTB, as well as slightly more membrane-bound. Both proteins partially colocalise with the lysosomal marker LAMP1 (Figure 4.8Civ). Diffuse parvalbumin immunoreactivity in an endogenous parvalbumin-positive cell (Figure 4.8Di) highlights the difference in appearance of exogenously detected parvalbumin which is much more punctate (Figure 4.8Ci). Control mice injected with CTB to the tongue have CTB-positive cells in the hypoglossal, but there is no endogenous parvalbumin detected (Figure 4.8Ei-iii). Hypoglossal cells were immunoreactive for CTBparv in mice sacrificed at 4, 7 and 13 days also (n=3 per dose) (Figure 4.9), occasionally CTB-positive cells were found that were not immunoreactive for parvalbumin (Figure 4.9A).

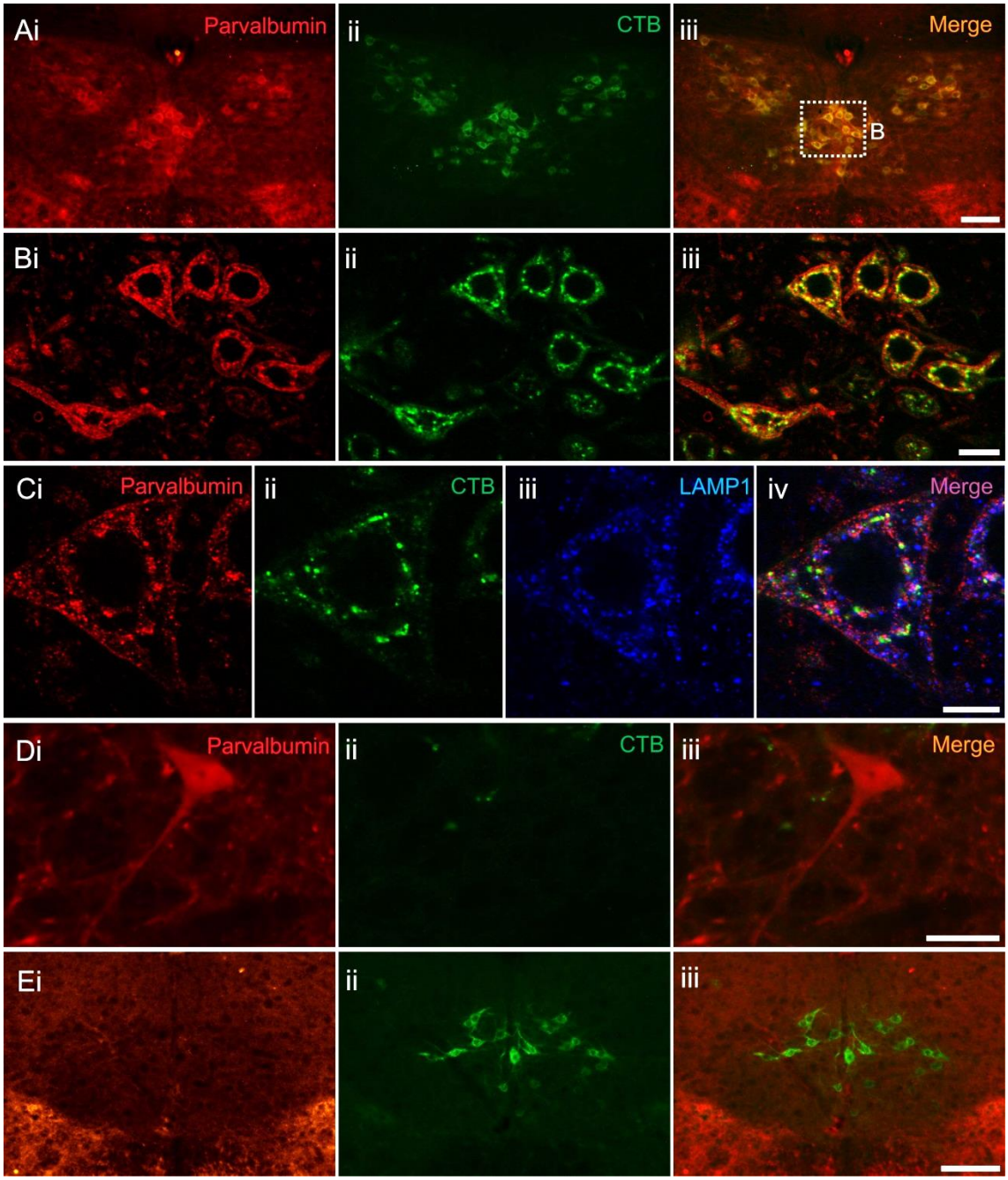

Figure 4.8 CTBparv labels the hypoglossal nucleus of the brainstem following tongue injection

Mice were injected with 50 µg of CTBparv via the tongue and were fixed after one day. Brainstem slices were obtained from removed brains and were then subjected to immunohistochemistry. A-B) The hypoglossal nucleus stained with anti-parvalbumin (red, Ai), anti-CTB (green, Aii) and merged (Aiii). C) Single hypoglossal motor neurones stained with anti-parvalbumin (red, Ci), anti-CTB (green, Cii), anti-LAMP (blue, Ciii) and merged (Civ). D) The reticular thalamic nucleus stained with anti-parvalbumin (red, Di), anti-CTB (green, Dii) and merged (Diii). E) Control CTB tongue injected mouse with hypoglossal nucleus stained with anti-parvalbumin (red, Ei), anti-CTB (green, Eii) and merged (Eiii). Scale bars: A, E = 100 µm; B, D = 20 µm; C = µm.

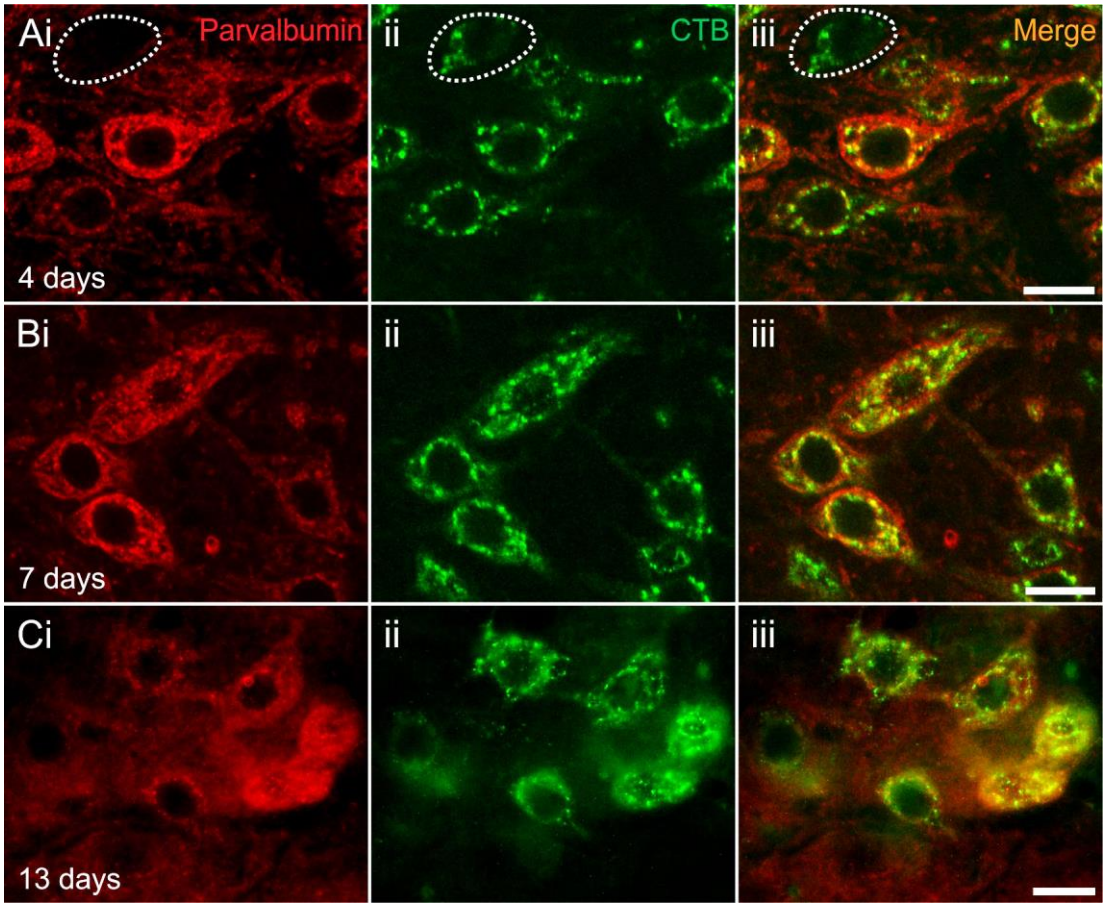

Figure 4.9 CTBparv labels the hypoglossal nucleus of the brainstem following tongue injection after 4, 7 and 13 days

Mice were injected with 50 µg of CTBparv via the tongue and were fixed after 4, 7 or 13 days. Brainstem slices were obtained from removed brains and were then subjected to immunohistochemistry. A-C) The hypoglossal nucleus stained with anti-parvalbumin (red, A-Ci), anti-CTB (green, A-Cii) and merged (A-Ciii). Scale bars = 20 µm.

4.3.6 Parvalbumin could not be detected in motor neurones of the spinal cord after IM injection to the gastrocnemius

CTBparv was injected IM via the gastrocnemius in mice to assess whether the fusion protein could be endocytosed and retrogradely transport *in vivo*. Injections of CTBparv (80 µg) into the gastrocnemius of adult mice (n=2) yielded differing results to those after CTB injection. The dorsal horn from L3-4 was absent of CTB-positive afferents and had only endogenous parvalbumin labelling (Figure 4.10Ai-iii). In a section of spinal cord CTB-positive motor neurones are labelled in the ventral horn but these are not positive for parvalbumin (Figure 4.10Bi-iii), the CTB is clearly punctate within the cell that is absent of parvalbumin (Figure 4.10Ci-iii). In another slice of spinal cord again there are a number of CTB labelled cells in the ventral horn that are not parvalbumin-positive (Figure 4.10Di-iii). One cell is positive for both components of the fusion protein but they do not appear co-localised, rather it is endogenous parvalbumin terminals surrounding the CTB-positive cell (Figure 4.10Ei-iii). It appears that the parvalbumin has been either cleaved and degraded or denatured.

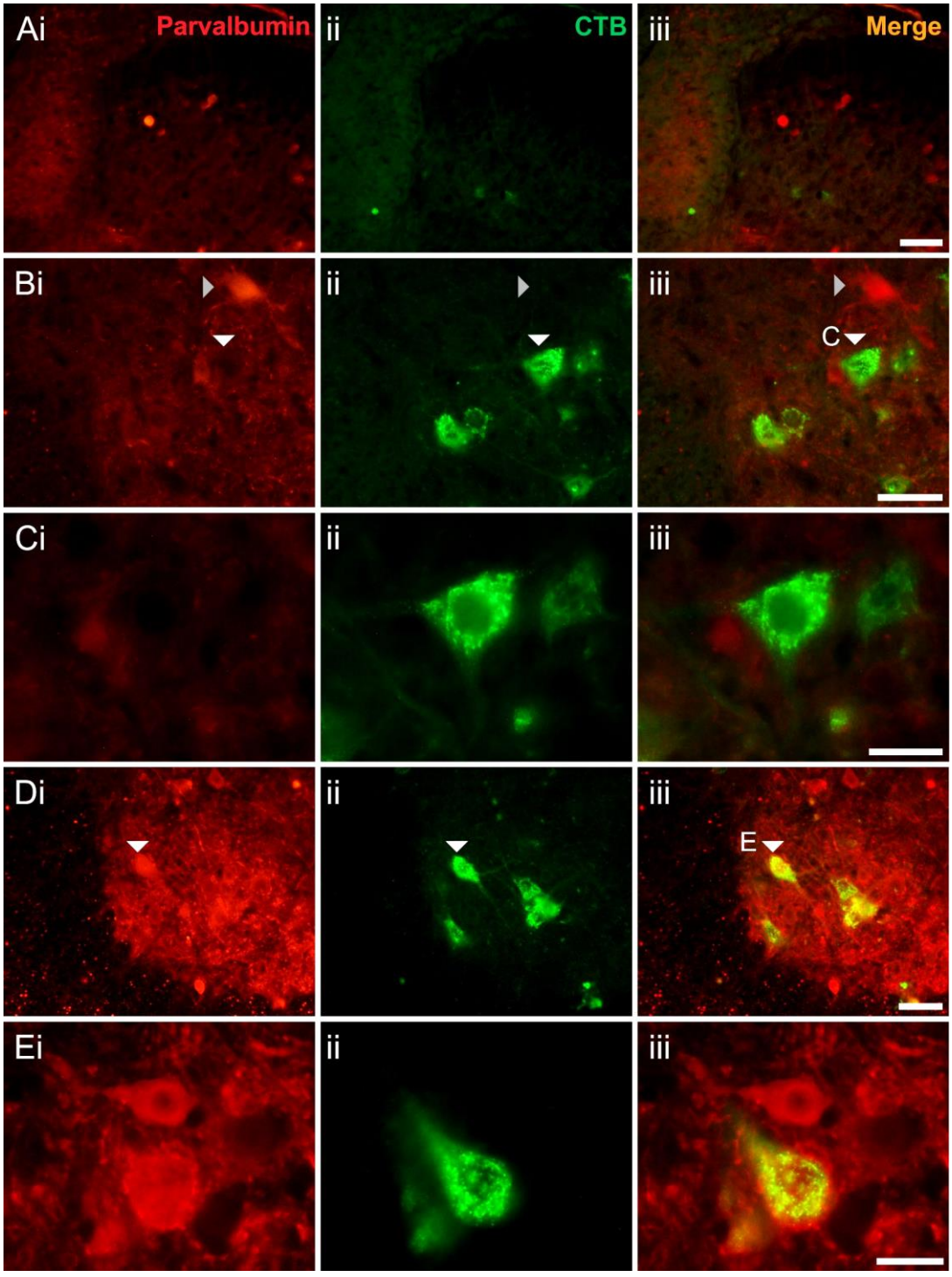

Figure 4.10 Parvalbumin is not detected in the ventral horn of the lumbar spinal cord after IM injection of CTBparv to the gastrocnemius

Mice were injected IM with 80 µg of CTBparv and were fixed after four days. Slices were obtained from removed spinal cords and were then subjected to immunohistochemistry. A) The dorsal horn stained with anti-parvalbumin (red, Ai), anti-CTB (green, Aii) and merged (Aiii). B, D) Ventral horn stained with anti-parvalbumin (red, Bi, Di), anti-CTB (green, Bii, Dii) and merged (Biii. Diii). C, E) Single motor neurones stained with anti-parvalbumin (red, Ci, Ei), anti-CTB (green, Cii, Eii) and merged (Ciii, Eiii). Scale bars: A, B, D = 50 µm; C = 25 µm; E = 20 µm.

4.3.7 After IP injection of CTBparv not all CTB-positive cells are immunoreactive for parvalbumin in the brainstem and spinal cord

CTBparv was injected IP in mice to assess whether the fusion protein could be endocytosed and retrogradely transport *in vivo* following systemic administration. Adult mice receiving IP injections of 2000, 1000 and 500 µg of CTBparv (n=3 per dose) were perfused after 4 days to compare labelling patterns in the brainstem and spinal cord. In the brainstem there was labelling of the DVN with CTB, but not all of these cells were positive for parvalbumin (Figure 4.11Ai-iii). Parvalbumin appears to be enriched at the membrane outlining the neurones, while CTB is intracellular (Figure 4.11Bi-iii). Occasional cells contain intracellular parvalbumin but it is not as punctate as CTB suggesting the fusion protein has been cleaved (Figure 4.11Ci-iii). The NTS, nucleus ambiguus, hypoglossal nucleus and facial motor nucleus were not immunoreactive for CTBparv as they were after IP injection of CTB and LTB. The spinal cord had a similar labelling pattern of CTB immunoreactivity with CTBparv as it did with CTB after IP injection. Afferents were labelled in the dorsal horn, motor neurones in the ventral horn, and SPNs in the central autonomic area (Figure 4.12Aii). The CTB-labelled primary afferents partially colocalise with parvalbumin immunoreactivity but this is likely endogenous parvalbumin (Figure 4.12Bi-iii). There were some CTB immunoreactive cells in the central autonomic area, parvalbumin reactivity was not colocalised within cell bodies but rather as putative fibres of passage or terminals (Figure 4.12Ci-iii). While many motor neurones were CTB-positive, only a few were parvalbumin-positive (Figure 4.12Di-iii). An endogenous parvalbumin cell with diffuse labelling (Figure 4.12Di, white arrow) next to an exogenously labelled CTBparv cell (Figure 4.12Di, grey arrow) highlights the difference in labelling pattern.

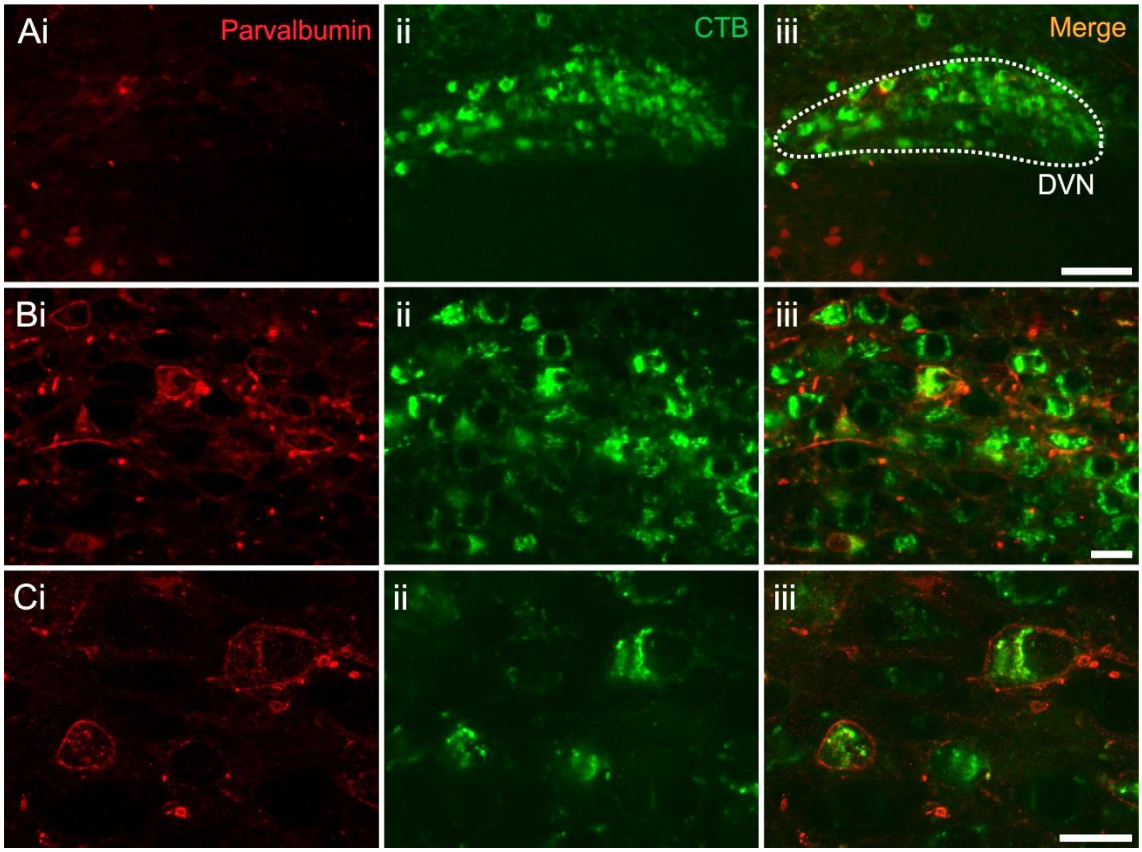

Figure 4.11 The DVN was labelled with CTB, but not parvalbumin after IP injection of CTBparv in adult mice

Mice were injected IP with 1000 µg of CTBparv and were fixed after three days. Brainstem slices were obtained from removed brains and were then subjected to immunohistochemistry. A) The DVN and hypoglossal nucleus stained with anti-parvalbumin (red, Ai), anti-CTB (green, Aii) and merged (Aiii). B-C) DVN stained with anti-parvalbumin (red, B-Ci), anti-CTB (green, B-Cii) and merged (B-Ciii). Scale bars: A = 100 µm; B = 20 µm; C = 10 µm.

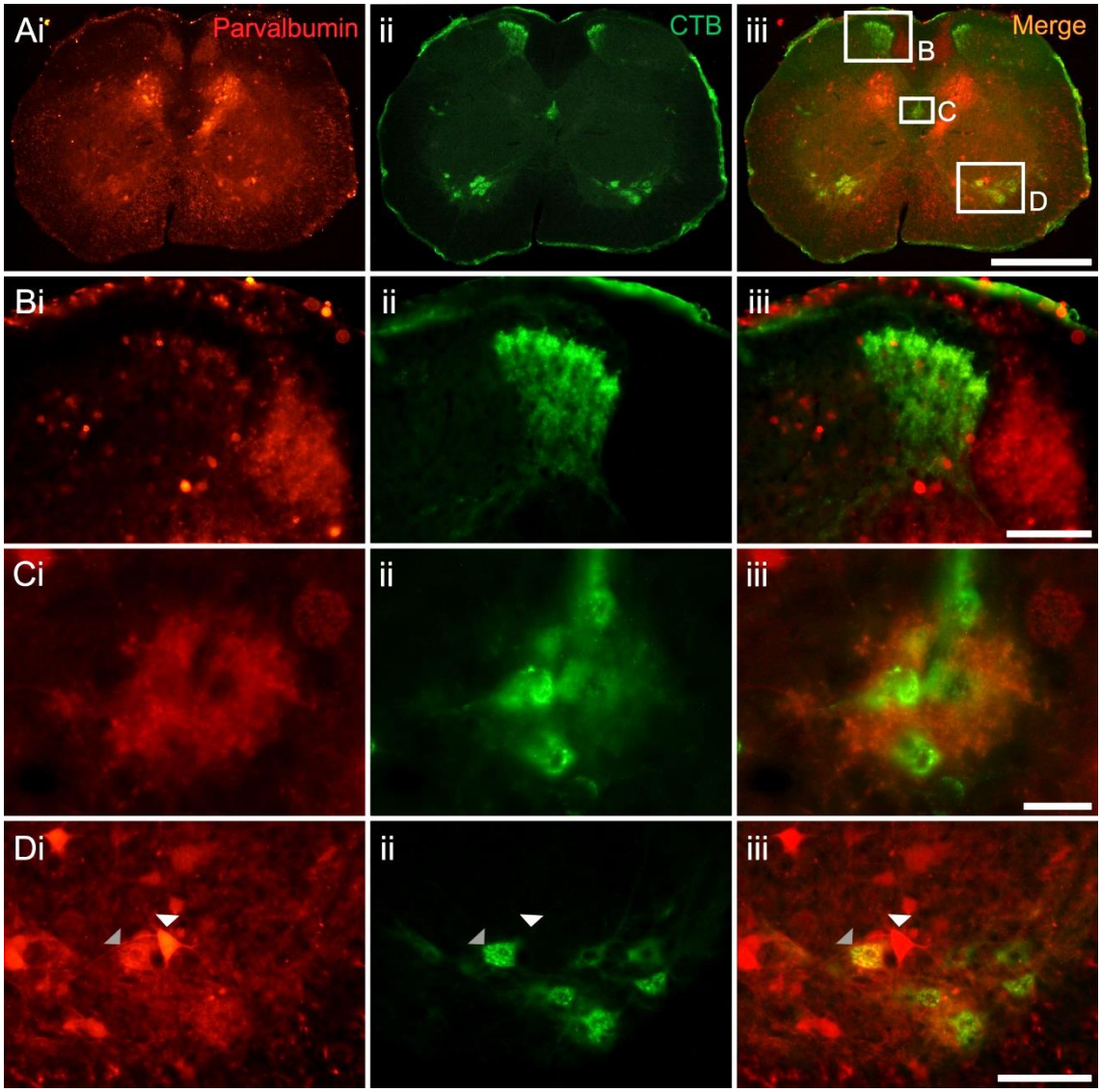

Figure 4.12 Parvalbumin is detected in few cells of the spinal cord after IP injection of CTBparv in adult mice

Mice were injected IP with 1000 µg of CTBparv and were fixed after three days. Slices were obtained from removed spinal cords and were then subjected to immunohistochemistry. A) Whole spinal cord slice stained with anti-parvalbumin (red, Ai), anti-CTB (green, Aii) and merged (Aiii). B) Dorsal horn stained with anti-parvalbumin (red, Bi), anti-CTB (green, Bii) and merged (Biii). C) Central canal area stained with anti-parvalbumin (red, Ci), anti-CTB (green, Cii) and merged (Ciii). D) Ventral horn stained with anti-parvalbumin (red, Di), anti-CTB (green, Dii) and merged (Diii); the white arrow highlights an endogenous parvalbumin cell and the grey arrow highlights and exogenously labelled parvalbumin cell. Scale bars: A = 500 µm; B, D = 100 µm; C = 25 µm.

Young mice receiving IP injection of 500 µg of CTBparv (n=2) were perfused after 2 days to compare labelling in the brainstem and spinal cord. In the brainstem there was labelling of the area postrema, NTS, DVN, hypoglossal nucleus and nucleus ambiguus (Figure 4.13A). The area postrema was strongly labelled with both CTB and parvalbumin, this was colocalised and likely from exogenous application since parvalbumin isn't normally expressed there (Figure 4.13Bi-iii). The DVN of young mice was similar in labelling to adult mice, with CTB-positive cell bodies and predominantly membrane bound parvalbumin (Figure 4.13Ci-iii). The hypoglossal nucleus was immunoreactive for CTB (Figure 4.13Di) and none of these cells were positive for parvalbumin (Figure 4.13Dii-iii). Cells of the nucleus ambiguus were CTB-positive but not all parvalbumin-positive (Figure 4.13Ei-iii). The spinal cord of young CTBparv injected mice provided the most colocalisation of CTB and parvalbumin. CTB immunoreactive cells were located in the dorsal horn, IML and ventral horn (Figure 4.14Ai). CTB-positive primary afferents were also positive for parvalbumin (Figure 4.14Bi-iii). Labelling in the IML was not colocalised with CTB and parvalbumin, the parvalbumin was more membrane bound and outlined the CTB-positive cells (Figure 4.14Ci-iii). Ventral horn motor neurones were CTB-positive, as well as parvalbumin-positive, while the labelling was not completely colocalised the parvalbumin is intracellular (Figure 4.14Di-iii).

Figure 4.13 Parvalbumin is not detected in cell bodies of nuclei in the brainstem after IP injection of CTBparv in young mice

Mice (P14) were injected IP with 500 µg of CTBparv and were fixed after two days. Brainstem slices were obtained from removed brains and were then subjected to immunohistochemistry. A) Whole brainstem slice stained with anti-CTB (green). B) Area postrema stained with anti-CTB (green, Bi), anti-parvalbumin (red, Bii) and merged (Biii). C) DVN stained with anti-CTB (green, Ci), anti-parvalbumin (red, Cii) and merged (Ciii). D) Hypoglossal nucleus stained with anti-CTB (green, Di), anti-parvalbumin (red, Dii) and merged (Diii). E) Nucleus ambiguus stained with anti-CTB (green, Ei), anti-parvalbumin (red, Eii) and merged (Eiii). Scale bars: A = 500 µm; B, C, E = 20 µm; D = 50 µm.

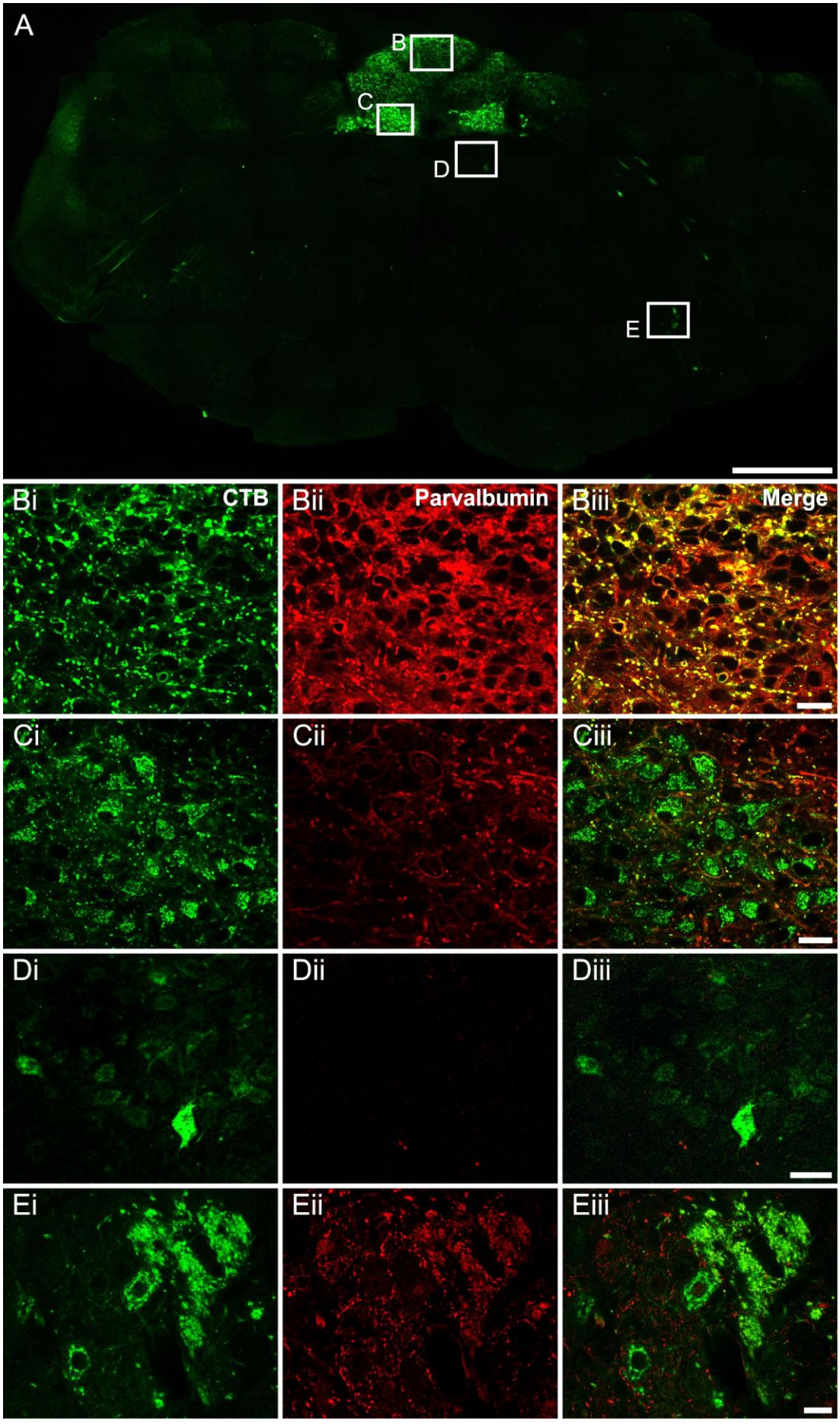
A
B
C
D
E
Bi
CTB
Bii
Parvalbumin
Biii
Merge
Ci
Cii
Ciii
Di
Dii
Diii
Ei
Eii
Eiii

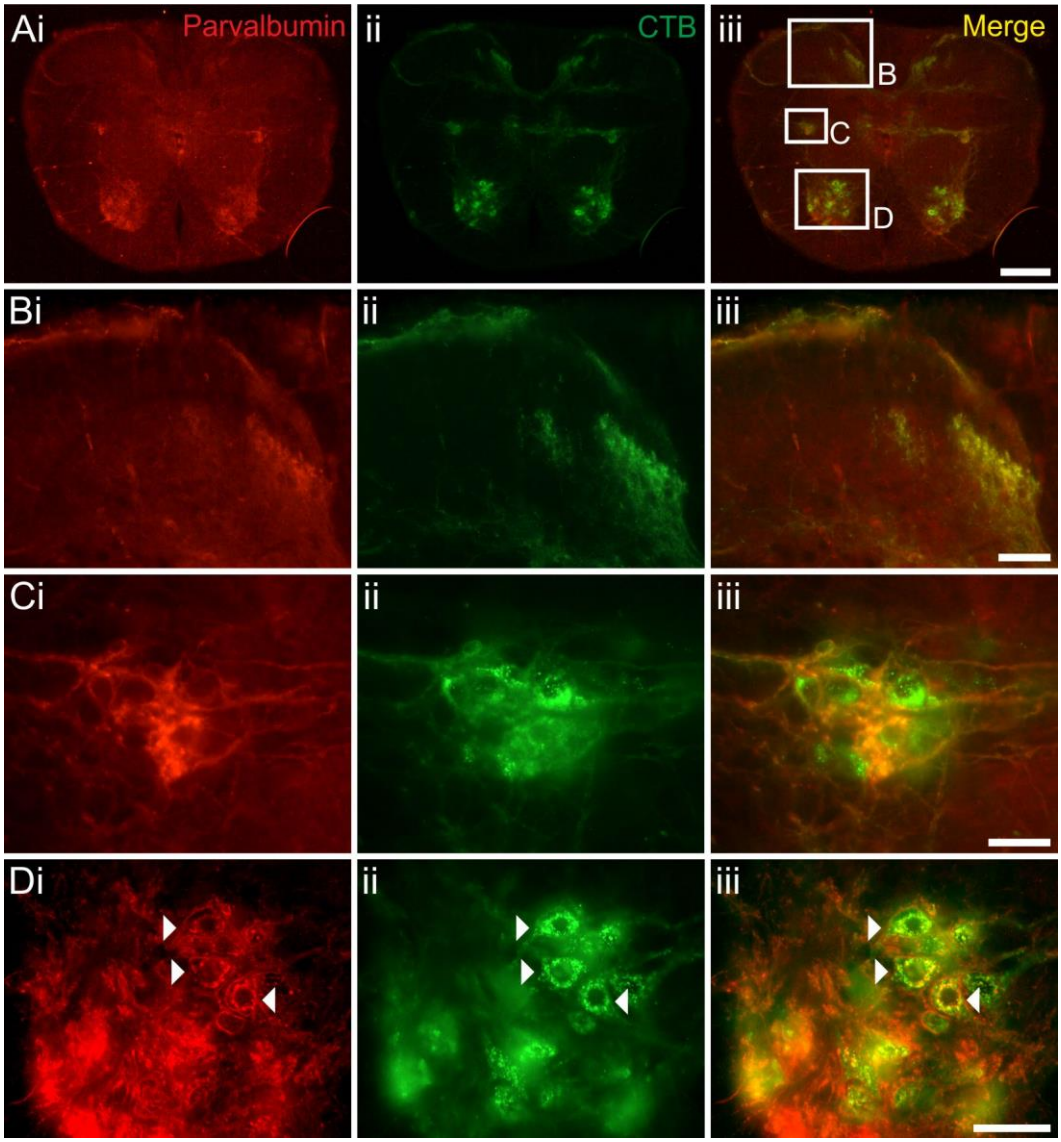

Figure 4.14 The spinal cord is labelled with CTBparv after IP injection in young mice

Mice (P14) were injected IP with 500 µg of CTBparv and were fixed after two days. Slices were obtained from removed spinal cords and were then subjected to immunohistochemistry. A) Whole spinal cord slice stained with anti-parvalbumin (red, Ai), anti-CTB (green, Aii) and merged (Aiii). B) Dorsal horn stained with anti-parvalbumin (red, Bi), anti-CTB (green, Bii) and merged (Biii). C) IML stained with anti-parvalbumin (red, Ci), anti-CTB (green, Cii) and merged (Ciii). D) Ventral horn stained with anti-parvalbumin (red, Di), anti-CTB (green, Dii) and merged (Diii); arrows highlight cells contained both CTB and parvalbumin staining. Scale bars: A = 200 µm; B, D = 50 µm; C = 25 µm.

	IP (young)	IP (adult)	IM (tongue)	IM (gastrocnemius)
Area postrema	CTB +ve, parv +ve	CTB -ve, parv -ve	-	-
Hypoglossal nucleus	CTB +ve, parv -ve	CTB -ve, parv -ve	CTB +ve, parv +ve	-
DVN	CTB +ve, parv +ve	CTB +ve, parv +ve	-	-
NTS	CTB +ve, parv +ve	CTB -ve, parv -ve	-	-
Nucleus ambiguus	CTB +ve, parv -ve	CTB -ve, parv -ve	-	-
Dorsal horn afferents	CTB +ve, parv +ve	CTB +ve, parv -ve	-	CTB -ve, parv -ve
Ventral horn motor neurones	CTB +ve, parv +ve	CTB +ve, some parv +ve	-	CTB +ve, parv -ve

Table 4.2 Localisation of CTB and parvalbumin as measured by immunohistochemistry after injection of CTBparv

+ve denotes immunoreactivity for the named protein, -ve denotes lack of immunoreactivity and – denotes that it would not be expected to be present.

4.4 Discussion

In this chapter a fusion protein of CTB and parvalbumin (CTBparv) was made, characterised and tested.

- CTBparv can bind GM1 and enter cultured cells (HEK293 and DRG).
- CTBparv can be detected *in vivo* after tongue injection in mice.
- Parvalbumin cannot be detected after IP injection of the fusion protein in adult mice, but it can in the spinal cord of young mice.
- The calcium binding properties and potential neuroprotective effects are yet to be fully elucidated.

4.4.1 CTB-parvalbumin fusion protein was purified and characterised

Of the two designed fusion proteins, C-terminal CTBparv was successfully produced while AB_5parv could not be transformed into a plasmid. It was expected that both proteins could be endocytosed and deliver parvalbumin, the difference being that CTB carries 5 parvalbumin proteins and AB_5 can carry just one. Mass spectrometry confirmed that CTBparv was the molecular mass expected, and western blot was positive for both parts of the fusion protein.

Given the DNA sequence was built by assembly PCR, it is feasible that other C-terminal CTB fusion proteins might be assembled in the same way. AB_5 fusion proteins using the heat-labile enterotoxin LTIIa have been made and tested in cell culture; delivering both a reporter protein and a therapeutic cargo (Chen et al., 2015). In this study the genes were purchased and sub-cloned into LTIIa expressing plasmids such that the toxic A1 sequence was replaced. Building genes for expression via assembly PCR using oligonucleotide sequences is much cheaper, and requires only a thermocycler and standard PCR reagents. LTIIa binds preferentially to GD1b (Fukuta et al., 1988), the ganglioside is enriched in neurones (Tettamanti et al., 1973) and so LTIIa may be thought of as a good protein delivery platform for neurones. However LTIIa fusion proteins remain in the periplasm after expression by *E.coli* (Chen et al., 2015), meaning extra steps are required during purification to lyse the cells. CTB fusion proteins are secreted into the growth medium (Reichow et al., 2010) and high yields can be obtained with ammonium sulphate precipitation (CTBparv was produced at 13.7 mg/L).

C-terminal CTB or LTB fusion proteins are good candidates for neuronal targeting due to ease of design, expression and purification with *E.coli* when compared to LT(IIa)B, as proven by the production of CTBparv.

4.4.2 ITC elucidated GM1 binding, but not calcium binding properties of CTBparv

CTBparv was designed with five 12 kDa parvalbumin units on the C-terminal side, while these sit on the opposite side to the GM1 binding face the extra load may have altered affinity. ITC determined a binding affinity of K_d = 49 nM for CTBparv, similar to that of wild-type CTB (K_d = 43 nM, (Turnbull et al., 2004)).

ITC was then utilised to assess calcium binding properties of the fusion protein with inconclusive results. When calcium ions were removed by incubation with EDTA followed by dialysis there was a 10-fold change in differential power (DP) when compared to control, suggesting binding had occurred. However the protein was never saturated and it is possible that binding seen is between calcium and EDTA rather than with CTBparv. To overcome the possibility of some EDTA remaining in solution CTBparv was passed over an EDTA-agarose column to remove any bound calcium ions (Henzl, 2009). The DP change with titration of GM1os into CTBparv was no different to that of the change due to heat of dilution, suggesting the fusion protein does not bind calcium.

Calcium imaging (Eberhard and Erne, 1994), ESI-MS (Troxler et al., 1999) and ITC (Henzl et al., 2003) have been used to measure the calcium and magnesium binding of native parvalbumin. Microscale thermothoresis has been utilised to measure the calcium binding affinity of calbindin (Wienken et al., 2010), a related calcium buffer protein. These methods could be used to assess whether parvalbumin of the fusion protein has retained its ability to buffer calcium.

If CTBparv is not functional, it may be because the protein did not fold properly when generated in bacteria. Codon usage in *E.coli* was taken into account when designing the fusion protein to promote optimal expression. Given that parvalbumin is a eukaryotic protein, it is possible that when produced in a prokaryotic environment the protein is altered. Usually parvalbumin does not undergo post-translational modifications (Fohr et al., 1993) and so this should aid normal production in *E.coli*. The conformation of the fusion protein could be tested with circular dichroism to assess the secondary structure (Kuwajima et al., 1988). Comparison of the fusion protein and endogenous parvalbumin would highlight any differences in alpha-helical structure. Human parvalbumin is not available to purchase however and would be required as a control. It could be produced in *E.coli* or rat parvalbumin could be used since there is a strong structural relationship between the homologues with only 9 conservative amino acid replacements observed (Berchtold, 1989).

While further experiments are required to determine the calcium binding properties of CTBparv, it is possible the protein may have retained functional activity *in vivo*. Given the evidence that CTBparv still bound its entry ligand GM1 *in vitro* testing was utilised to assess cell entry and calcium binding.

4.4.3 CTBparv can enter cultured cells

HEK293 cells have been used to assess retro-translocation of cholera toxin (Moore et al., 2013) meaning the toxin can be endocytosed by the cell line. When either CTB or CTBparv was incubated with HEK293 cells the toxin subunits were detected inside the cells. It is important that cells undergo an acid wash before fixation as following incubation immunohistochemistry reveals a lot of membrane-bound protein. CTBparv may adhere to the plasma membrane via basic amino acid residues such that the GM1-binding face is not aligned with the membrane, this means that the fusion protein cannot be internalised. The brightness of the protein at the membrane makes it difficult to distinguish whether any protein has been endocytosed, especially for parvalbumin. Upon removing this excess protein it is clear that both CTB and parvalbumin can be detected intracellularly. Without the acid wash there is more parvalbumin detected at the membrane than CTB, suggesting that the fusion protein has been cleaved. It is also possible that an excess of CTBparv was used and no more can enter the cells, the fusion protein may then remain bound at the cell surface in such a way that the anti-CTB antibody cannot reach the epitope.

When HEK293 cells were incubated with CTBparv and fixed after different lengths of time there was little difference in intracellular trafficking, with the proteins colocalised within the cells at each time point. CTBparv also successfully entered cultured DRG neurones with both CTB and parvalbumin were clearly colocalised within neurite. There were many CTB-positive puncta that were not immunopositive for parvalbumin within the cell body, suggesting that the fusion protein may have been cleaved. Importantly some parvalbumin could be detected within the cytoplasm meaning cultured DRGs might be used to measure changes in intracellular calcium after incubation with CTBparv. This could be done using whole-cell patch clamp recording in DRGs incubated with CTBparv (Gandini et al., 2014) or via calcium imaging (Savidge et al., 2001). Application of capsaicin induces increases in intracellular calcium (Wood et al., 1988), by comparing these changes with and without CTBparv it may be possible to elucidate the buffering properties of the fusion protein in cultured neurones.

In vitro studies have shown that CTBparv can enter cultured cells and be detected via immunohistochemistry. Further studies are required to assess whether the fusion protein has retained calcium buffering capacity.

4.4.4 IM injection of CTBparv was successful in the tongue, but not in the gastrocnemius

After injection of CTBparv to the tongue the fusion protein was able to retrogradely transport from terminals to cell bodies in the hypoglossal nucleus. CTBparv was detected in the brainstem after just one day and remained detectable for up to two weeks (the maximum duration tested). The proteins were colocalised within cell bodies, but some parvalbumin appeared cytoplasmic compared to the rest of the CTBparv puncta. The glycine-asparagine linker between CTB and parvalbumin was designed such that it is small, flexible and soluble, with no reactive functional groups, therefore it would not be expected for CTBparv to be cleaved between the two proteins. Neurones of the hypoglossal nucleus do not endogenously express parvalbumin, so any detected must have been introduced as the fusion protein. It is possible that the flexible linker is cleaved by a protease during trafficking and the parvalbumin is able to escape to the cytoplasm. While the fusion protein was not designed as such, this would be advantageous as parvalbumin is a cytoplasmic protein (Endo and Onaya, 1988).

Since CTBparv was detected in distinct puncta the labelling was compared with that for the lysosomal marker LAMP1. There was some colocalisation, indicating that some of the fusion protein had been trafficked for degradation. Native cholera toxin is trafficked via the trans-Golgi network to the endoplasmic reticulum (Lencer and Tsai, 2003) and so probing these intracellular compartments for colocalisation may clarify the location of both CTB and parvalbumin within neurones. Electron microscopy (EM) could be utilised to further distinguish intracellular location of the fusion protein as both CTB and parvalbumin have been detected via EM (Ericson and Blomqvist, 1988; Kita, 1994). By using double-labelling both proteins may be visualised in the same cells and location compared to assess if parvalbumin has been cleaved and released.

Following CTBparv injection to the gastrocnemius the spinal cord was assessed for retrograde transport of the fusion protein. CTB was detected in motor neurones of the ventral horn but not within primary afferents of the dorsal horn, as seen with IM injection of the same dose of CTB (see Chapter 3). The extra cargo has altered transport of the toxin as it no longer moves anterogradely. Exogenous parvalbumin was not detected in any CTB-positive cells suggesting it has been cleaved and degraded, or that it has become unfolded and no longer detectable via immunohistochemistry. Both CTB and parvalbumin were detectable in the hypoglossal nucleus up to two weeks after tongue injection, why the parvalbumin is cleared after gastrocnemius injection is unknown. As described previously no specific cleavable linker region was incorporated into the fusion protein and so it was not expected that the parvalbumin would become

separate. It is possible that CTBparv has been trafficked to lysosomes, where the pH is acidic at 4.5-5.0 (Coffey and De Duve, 1968). Parvalbumin functions within the cytoplasm where pH is 7.4 (Roos and Boron, 1981) and so if trafficked to lysosomes the tertiary structure may be denatured such that the epitope is no longer recognisable by the antibody. Repeating the injections and perfusing mice after one day might reveal if parvalbumin is detectable initially and then degraded after a few days in the cell body.

The difference in detection of parvalbumin after IM injection of CTBparv via the tongue or gastrocnemius is curious. This highlights that while cargo can be delivered, the success of delivery and detection may be different between injection routes, and possibly it would also differ depending on the cargo.

4.4.5 The distribution of CTBparv positive neurones following IP injection is different between young and adult mice

CTB entered motor neurones, autonomic preganglionic neurones and primary afferents in the brainstem and spinal cord after IP injection, and it was expected that a fusion protein would label in the same pattern. However after CTBparv injection in adult mice only the DVN of the brainstem was labelled with CTB, and parvalbumin was not colocalised within the cells. CTB was detected as puncta within cell bodies while parvalbumin appeared membrane-bound, forming a distinct outline of the motor neurones. Endogenous parvalbumin is present within processes of the DVN (de Leon et al., 1993) but does not normally form a matrix surrounding the cells as seen after CTBparv injection. As described previously, it seems the fusion protein is being cleaved. Where following gastrocnemius injections it was possible the parvalbumin had become unfolded and thus undetectable, this is not the case for IP injection as the parvalbumin is detected but separate from CTB. Confocal microscopy revealed that some parvalbumin has remained in the cells, however the majority is at the cell surface; whether this is intracellular or extracellular is not known. CTBparv entered the neurones at the terminals or axons, meaning the whole complex was retrogradely transported to the cell body. Either during transportation or once in the cell body the fusion protein is cleaved, and parvalbumin then apparently targeted to membrane or even ejected from the neurone. This was unexpected as there is no specific linker region and parvalbumin does not contain a targeting motif for the plasma membrane. Many membrane proteins contain cysteine residues where modifications for membrane localisation such as palmitoylation occur (Dunphy and Linder, 1998). Parvalbumin does not contain cysteine so it is unlikely to have been tagged for membrane targeting. The parvalbumin may have been cleaved and then tagged as a waste product for expulsion

from the cell via exocytosis. As yet there is no clear explanation as to the separation of CTB and parvalbumin within motor neurones of the DVN.

The spinal cord displayed an identical pattern of labelling for CTB after CTBparv injection when compared to injection of just CTB. CTB-positive cells were found in the motor neurones of the ventral horn, SPNs in the IML and CAA, and afferents in the dorsal horn. Once again though as in the brainstem, most of these cells were not immunoreactive for parvalbumin. CTBparv-positive cells are easily distinguishable from endogenous ones by comparing the labelling within the cells. Endogenous parvalbumin is diffuse throughout the cytoplasm of the cell body, whereas CTBparv is punctate. CTB-positive cells of the IML and CAA were never reactive for parvalbumin after CTBparv injection, but occasional cells were found in the ventral horn. Where in the DVN parvalbumin outlined the neurones, most CTB-reactive cells in the spinal cord are completely absent of parvalbumin. This suggests it has been cleaved and destroyed, or that it has become unfolded and so no longer recognisable by the antibody. Where CTB is detected without parvalbumin it is also plausible that the fusion protein was cleaved before endocytosis. The extra load may have slowed endocytosis of the complex, allowing non-specific extracellular proteins access to it, cleaving the parvalbumin such that CTB enters and traffics alone. The difference in detection of parvalbumin after IP injection in the brainstem and spinal cord remains unexplained, but indicates different processing of the fusion protein dependent on cell type.

When CTBparv was injected IP in young (P16) mice CTB labelling was similar to that seen in CTB IP injections, with positive cells in the area postrema, DVN, hypoglossal nucleus and nucleus ambiguus. However as with adult mice, most cells were not immunoreactive for parvalbumin. The DVN pattern of labelling again featured outlining of the neurones, with only some parvalbumin remaining intracellular. There was no parvalbumin immunoreactivity within the hypoglossal nucleus, and some colocalisation in the nucleus ambiguus. The difference in parvalbumin detection again highlights that CTBparv is processed differently between cell types. The spinal cord of young mice injected with CTBparv contained the most c-localisation between the two parts of the fusion protein. Afferent fibres in the dorsal horn contained CTBparv. Proprioceptive neurones in the dorsal horn were found to degenerate in two mouse models of ALS (SOD1 and TDP43) when assessed with CTB-555 (Vaughan et al., 2015). Delivery of CTBparv in these mice could be used to measure if the fusion protein has any protective effects against degeneration of proprioceptive sensory nerve endings. CTB-positive cell bodies in the IML were not positive for parvalbumin, but the neurites were. This could indicate that it is upon reaching the cell body that CTBparv is cleaved. Motor

neurones of the ventral horn were labelled with parvalbumin intracellularly but some was also detected at the plasma membrane, outlining the cells. It is notable that direct IM injection was not successful in delivering parvalbumin to motor neurones in the spinal cord. Possibly depending where CTBparv enters the neurones, be it terminals or along the axon, it is trafficked differently within the cells.

Along with tongue injections, IP injection of CTBparv in young mice provides evidence of cargo delivery into cells by CTB. Motor neurones are a major target of CTBparv in terms of a therapeutic as introducing the calcium buffering protein could reduce calcium excitotoxic cell death in motor neurones of ALS patients. In this instance the lack of parvalbumin detection in other neurone types is unlikely to affect the potential improvement of motor neurone survival.

One common event following *in vivo* administration is apparent cleavage of the fusion protein; if a specific cleavable linker region was included this could be preferentially cleaved. After internalisation CT is trafficked to the endoplasmic reticulum (ER) via the Golgi apparatus and early endosomes, while CTB is trafficked to lysosomes via the Golgi apparatus (Majoul et al., 1996). A furin linker has been utilised previously in a CTB-GFP fusion protein (Limaye et al., 2006) since the Golgi apparatus (Takahashi et al., 1995), endosomes, plasma membrane and extracellular space (Mayer et al., 2004) are enriched with the enzyme. Furin is a prohormone-proprotein convertase that cleaves protein precursors following basic Arg-Xaa-Lys/Arg-Arg-like motifs (Henrich et al., 2003). If inserted between CTB and parvalbumin in CTBparv it may facilitate intracellular cleavage and release of parvalbumin into the cytosol. Another option is to promote endosomal escape of the fusion protein. This could be achieved by using fusogenic peptides with the ability to disrupt membranes under acidic conditions through pH-conformational changes (Lorieau et al., 2012). A fusogenic peptide (B55, 55 amino acids in length) from a sea urchin (*Strongylocentrotus purpuratus*) was used to deliver IgG in HeLa cells, the antibodies were localised to endosomes but also found throughout the cytoplasm (Niikura et al., 2015). A smaller central version of the fusogenic peptide (B18, 18 amino acids) has been used to deliver single-chain Fv portion of an epidermal growth factor receptor antibody in A431 cells (Niikura et al., 2016). Introducing this peptide sequence to either CTB or parvalbumin could allow the complex escape to the cytosol where parvalbumin can exert its calcium buffering abilities. The shorter sequence would be preferable as it is less likely to hinder activity of the fusion protein. If both a cleavable linker and endosomal escape peptide were engineered into CTBparv it may be possible to deliver cargo to the cytoplasm.

4.4.6 Neuroprotective properties of CTBparv *in vivo* remain unknown

The neuroprotective potential of CTBparv remains to be tested; it could be measured following excitotoxic insult in an acute slice preparation (Cifra et al., 2011). The glutamate re-uptake inhibitor DL-TBOA can be used to block excitatory amino acid transporters (EAAT1, EAAT2, EAAT3, EAAT4 and EAAT5); thereby increasing the concentration of glutamate within synapses and causing glutamate excitotoxicity (Shimamoto et al., 1998; Shigeri et al., 2001). The drug has been used previously to measure the protective effects of riluzole on rat hypoglossal neurones and their protocol could serve as a template for this study (Cifra et al., 2011). Brainstem or spinal cord slices could be incubated with DL-TBOA for 4 hours to induce glutamate excitotoxicity, fixed, re-sectioned, and then immunohistochemistry used to assess cell damage and death. Antibodies against activated caspase-3 would indicate apoptotic cells as the protease acts to initiate the 'death cascade' (Nicholson et al., 1995). Antibodies against activating transcription factor (ATF-3) could also be used, as this has been previously validated as a method to label distressed motor neurones (Nani et al., 2010).

Motor neurones of the hypoglossal nucleus are an early site of motor neurone degeneration in the bulbar form of ALS (DePaul et al., 1988) and thus are a good site to measure potential neuroprotection. Using brainstem slices from tongue injected animals could improve the results since both CTB and parvalbumin were well detected in the hypoglossal nucleus. Aged rodents have thicker skulls and more connective tissue than younger ones and this can delay brain extraction, but assessing adult tissue is more relevant to neurone protection in ALS. Brainstem slices from adult mice have been cultured (Spitzbarth et al., 2015) and so it should be possible to use them in acute slice experiments. It is important to note that neonatal tissue can still clarify the basic mechanisms and possible neuroprotection of motor neurones induced by excitotoxicity.

During acute slice culture experiments there is a certain amount of damage caused via the slicing procedure, inevitably neurones and glia are destroyed at the level of the cutting plain. In the hypoglossal nucleus 35% of neurones and 65% of astrocytes are lost, however after the initial loss the number of hypoglossal neurones remain stable *in vitro* for up to 4 hours (Cifra et al., 2011), this confirms that any further cell loss is induced with excitotoxic drugs.

Rather than using an acute study of slices of CNS tissue, brainstem or spinal cord could be cultured. An excitotoxic model to measure neuroprotection of ventral horn motor neurones has been described where propidium iodide was used to evaluate

glutamate-induced cell death (Gerardo-Nava et al., 2013). Parvalbumin was detected in motor neurones of young mice after CTBparv was administered IP, spinal cord slices cultured from these animals could be measured for potential improved neurone survival. It would also be interesting to culture spinal cord slices and apply CTBparv to the media and then assess which cell type's endocytose the fusion protein. It may be possible to use a model where CTBparv is added to media followed by an excitotoxic insult and neuronal protection compared.

If CTBparv proves neuroprotective in *in vitro* models the next step would be to test in mouse models of ALS (reviewed by Philips and Rothstein (2015)) and assess whether the fusion protein can alter disease progression. There are many experiments that could be carried out, depending on which administration route is used, age of mice, at what point in the disease the mice are, or how often injections are given. Then many parameters may be measured such as changes in motor neurone cell loss, delay in disease onset as measured by behavioural tests and electrophysiological changes in motor neurones. Given that IP injection successfully delivered parvalbumin to motor neurones in young mice this route might be assessed first. Recently IP injection of CTB was found to have an anti-inflammatory effect following ischemia (Zhang et al., 2016) possibly due to its immunomodulatory properties described in general introduction section 1.2.4. Neuroinflammation is another cause of motor neurone cell death in ALS, activated microglia release reactive oxygen species and pro-inflammatory cytokines that further enhance motor neurone stress. CTB was found to inhibit microglia activation by supressing activation of the transcription factor NF-kB and suppressing phosphorylation of ERK1/2, two important mechanisms in production of pro-inflammatory molecules. Delivery of CTBparv could serve a dual purpose of reducing neuroinflammation while also improving calcium buffering capacity and thus reducing excitotoxicity and motor neurone cell death. Intramuscular injections of CTBparv have not yet been tested in young mice. If they successfully deliver both CTB and parvalbumin to motor neurones this route could serve as a good model for measuring changes in motor neurones with the ventral horn of the contralateral side to the injection acting as a control.

While it is known that CTBparv can be detected in hypoglossal motor neurones up to two weeks following tongue injection in adult mice, the length of time the protein remains after other injection routes has not been measured. This would need to be tested to decide how often injections would need to be given. The outcome of multiple injections has not been assessed; it is possible that the complex would be cleared by antibodies or even that antibodies would begin to attack parvalbumin since CTB

behaves as an adjuvant (Stratmann, 2015). To overcome multiple injections, rather than delivering a protein, CTB might be utilised to deliver RNA to neurones.

Conclusion

CTB successfully delivered another protein into neurones after peripheral injection. Future studies should assess the possible neuroprotective effects of CTBparv and elucidate whether the fusion protein maintains calcium buffering capacity. There is scope for the production of other fusion proteins with more sophisticated delivery systems, including cleavable linkers and localisation signals.

Chapter 5
Neuronal tracing with novel CTB conjugates

5.1 Introduction

Cholera toxin B (CTB) has been used extensively as a neuronal tracer; usually detected via fluorescence or DAB immunohistochemistry (Flink and Westman, 1986; Datiche et al., 1995; Luquin et al., 2012), but direct fluorophore conjugates are also available (Fasanella et al., 2008; Conte et al., 2009) as well as CTB-HRP conjugates for detection via peroxidase chemistry (Dederen et al., 1994; Liu et al., 1995). The ability to detect the tracer without the use of antibodies can be advantageous. Direct conjugates do not require an amplification step and so the labelling process is quicker, it may also be cheaper as no antibodies are required. Detecting proteins without immunohistochemistry also means more scope for labelling multiple proteins without cross-reactivity of primary and secondary antibodies.

One method of detecting proteins without using antibodies is to use a chemical reaction such as copper-catalysed azide-alkyne cycloaddition (CuAAC) otherwise known as ‘click chemistry’ (Rostovtsev et al., 2002; Tornoe et al., 2002). The reaction can be conducted under aqueous conditions, at room temperature with pH varying from 4 – 12 and it results in the formation of a triazole from an azide and an alkyne (Figure 5.1A). Click chemistry has been utilised in fixed tissue to detect 5-ethynyl-2′-deoxyuridine (EdU), a thymidine analogue that is incorporated into DNA as cells divide (Salic and Mitchison, 2008). EdU contains an ethynyl group that can be detected with click chemistry using a biotin azide-containing probe (Figure 5.1B). Azide-functionalised amino acids can be incorporated into proteins by using the methionine surrogate azidohomoalanine (Kiick et al., 2002). In methionine-depleted cultures azidohomoalanine is activated by methionyl-tRNA synthetase of methionine auxotroph *Escherichia coli* and replaces methionine in translated proteins. CTB can be synthesised with incorporated azide groups, allowing for detection via click chemistry with a biotinylated alkyne. CTB-azide was created using side-directed mutagenesis to mutate all methionines in CTB to leucine (M37L, M66L, M101L) and then a surface exposed lysine was replaced with methionine (K43M) (Williamson, 2016). This can then be visualised with CuAAC with a biotinylated alkyne followed by a fluorophore- or peroxidase-bound streptavidin.

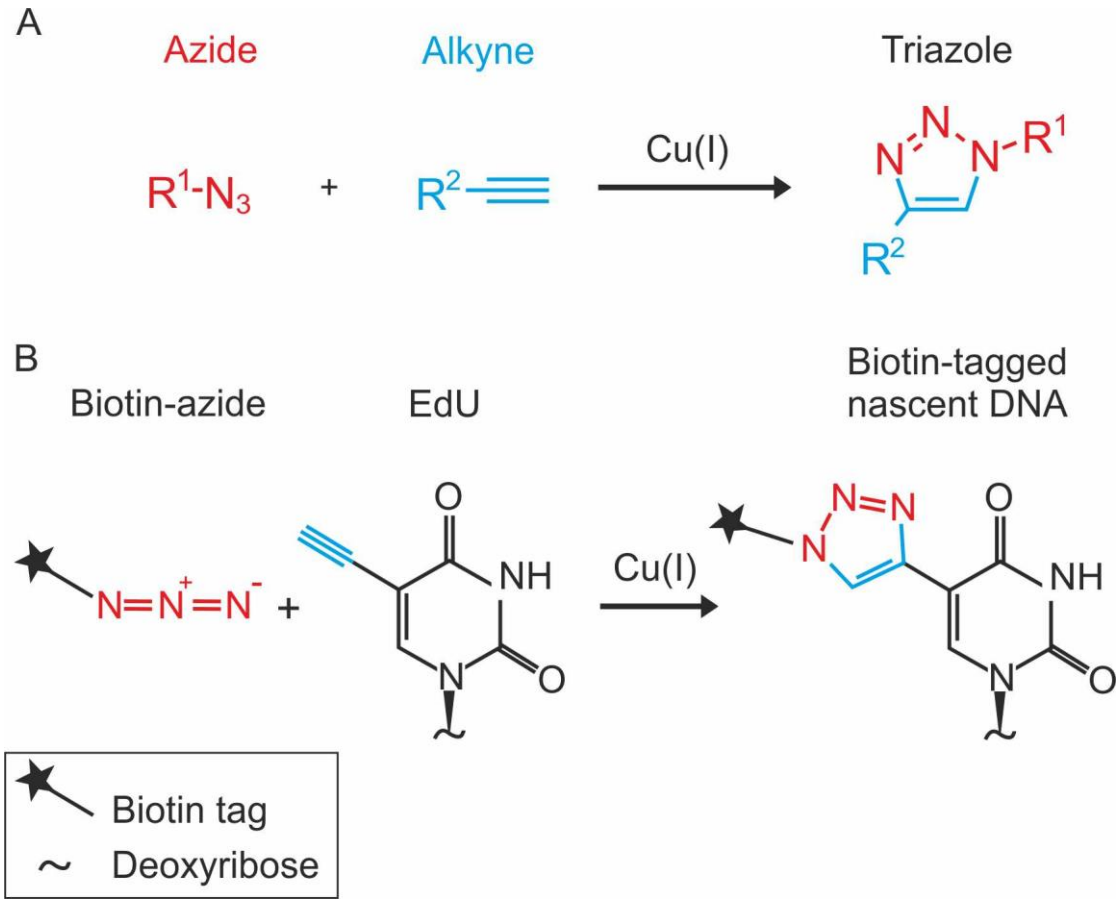

Figure 5.1 A schematic of copper catalysed azide-alkyne cycloaddition (CuAAC).

A) An azide group (red) and an alkyne group (blue) react to form a triazole catalysed by the presence of copper. B) EdU incorporated into nascent DNA is detectable after CuAAC to attach a biotin.

Quantum dots (QDs) coupled to biomolecules have been used as sensitive biological labels (Bruchez et al., 1998; Chan and Nie, 1998). QDs are semi-conducting nanocrystals with unique electronic properties, the unusually high surface-to-volume ratio of them results in fluorescence (Collier et al., 1998). Both founding groups highlighted that QDs would be well suited to cell labelling due to their brightness, chemical stability, photostability and large range of emission spectra. To direct the QDs to specific cells or tissues they must be conjugated to other proteins; for live cell labelling they were conjugated to CTB (Chakraborty et al., 2007). Click chemistry with CTB-azide allows for the addition of up to 5 QDs to CTB on the opposite face to GM1 binding sites. CTB-QD could provide a detection method of CTB as a neuronal tracer without requiring an amplification step with immunohistochemistry.

Avidin is a tetrameric protein found in eukaryotes with the capacity to bind four biotin molecules, and streptavidin is a prokaryotic form of the protein purified from *Streptomyces avidinii* (Green, 1975). The interaction between the proteins and biotin is particularly strong with a dissociation constant of 1×10^{-15} M (Green, 1963). For this reason it was hypothesised that avidin could be used as a central molecule to bring together biotinylated proteins. CTB with biotinlyated A2 linker was made such that it formed an AB_5 complex with the biotin on the N-terminal of A2. When mixed with a fluorescently labelled streptavidin a complex was built where the GM1 binding face of CTB remains free such that the whole complex might be endocytosed and retrogradely transported. Since the streptavidin is already labelled with a fluorophore the complex would not require immunohistochemistry to be detected.

Such methods of conjugation provide great flexibility in the molecules that might be attached and delivered by CTB.

5.1.1 Summary and objectives

Alternate detection methods to immunohistochemistry could be advantageous and this chapter will assess some options utilising the neuronal tracer CTB. If CTB-azide (Figure 5.2A) functions as neuronal tracer detectable via click chemistry it represents a novel detection technique. Quantum dots represent a more photostable alternative to standard fluorophores and so tracing with CTB-QD (Figure 5.2B) will be examined. Alexafluor 555 labelled streptavidin mixed with biotinylated CTB forms a complex with two AB_5 units per streptavidin (Figure 5.2C), whether this would transport in the same way as CTB is unknown. If successful, AB_5-streptavidin-555 presents an opportunity to deliver other biotinylated proteins by mixing them with the complex.

Research questions:

1. Can CTB-azide be detected by click chemistry after injection *in vivo*?
2. Can CTB-azide be conjugated to QDs (CTB-QD) and be used as a neuronal tracer and be detected in fixed tissue?
3. Can an AB_5-strep-555 fusion protein retrogradely transport after peripheral injection?

CTB fusion proteins will be tested by tongue injection, and after fixation the hypoglossal nucleus of the brainstem assessed for the tracers. Immunohistochemistry for CTB will determine whether the complexes have retrogradely transported.

The results from this study will identify novel detection techniques for CTB, and present the potential for innovative delivery methods of other proteins.

5.2 Materials and methods

All tracing studies were carried out in C75Bl/6 mice, see table 5.1 for summary. CTB-azide injections are described in section 2.8, CTB-QD injections are described in section 2.10, and AB_5-Strep-555 injections are described in section 2.9.

Protein	Dose (µg)	Route	n
CTB-azide	50	Tongue	4
CTB-QD	30	Tongue	2
AB_5-strep-555	30	Tongue	2

Table 5.1 Dose of each protein administered and route of injection

All tissue was prepared as described in General Methods section 2.5.6 and 2.5.7 and all antibodies used are listed in table 2.2. Fluorescent images were acquired as described in section 2.6.3. For confocal imaging of CTB-QD, an absorption wavelength under 580 nm and an emission wavelength of 600 nm are used.

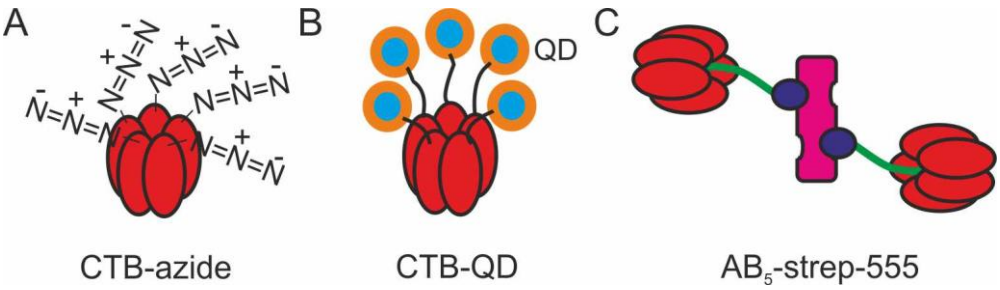

Figure 5.2 Cartoon schematics of CTB-azide, CTB-QD and AB_5-strep-555

A) CTB pentamer (red) with one azide group per monomer. B) CTB pentamer (red) with up to 5 QDs (blue and orange). C) Streptavidin (pink) labelled with Alexafluor-555 with two AB_5-biotin (CTB, red; biotin, purple) units bound.

5.3 Results

5.3.1 CTB-azide can be detected in the hypoglossal nucleus by click chemistry after tongue injection

CTB-azide (provided by Dr D. J. Willaimson) was injected IM via the tongue in mice to assess whether the protein could be endocytosed and retrogradely transport *in vivo* and detected via CuAAC. CTB-azide was detected using click chemistry in PFA-fixed tissue after tongue injection. Immunohistochemistry for CTB reveals the hypoglossal nucleus of the brainstem is labelled (Figure 5.3A, Bi). CuAAC with a biotinylated alkyne, followed by detection with streptavidin-555 reveals CTB-azide in the hypoglossal nucleus (Figure 5.3Bii-iii). Cells were always detected by both immunohistochemistry and click reaction (Figure 5.3C) and labelling within cells was punctate (Figure 5.3D). Control brainstem slices undergoing the click reaction and detection with streptavidin-555 have no positive cells (Figure 5.3E).

Figure 5.3 CTB-azide is detected in the brainstem by CuAAC after tongue injection

Mice were injected IM with 50 µg of CTB-azide to the tongue and were fixed after two days. Brainstem slices were obtained from removed brains and were then subjected to immunohistochemistry and CuAAC. A) Whole brainstem slice stained with anti-CTB (green). B-D) Hypoglossal nucleus stained with anti-CTB (green, B-Di), CuAAC (red, B-Dii) and merged (B-Diii). E) Control brainstem slice from uninjected mouse stained with DAPI (blue, Ei), CuAAC (red, Eii) and merged (Eiii). Scale bars: A = 500 µm; B = 50 µm; C = 25 µm; D = 20 µm; E = 100 µm.

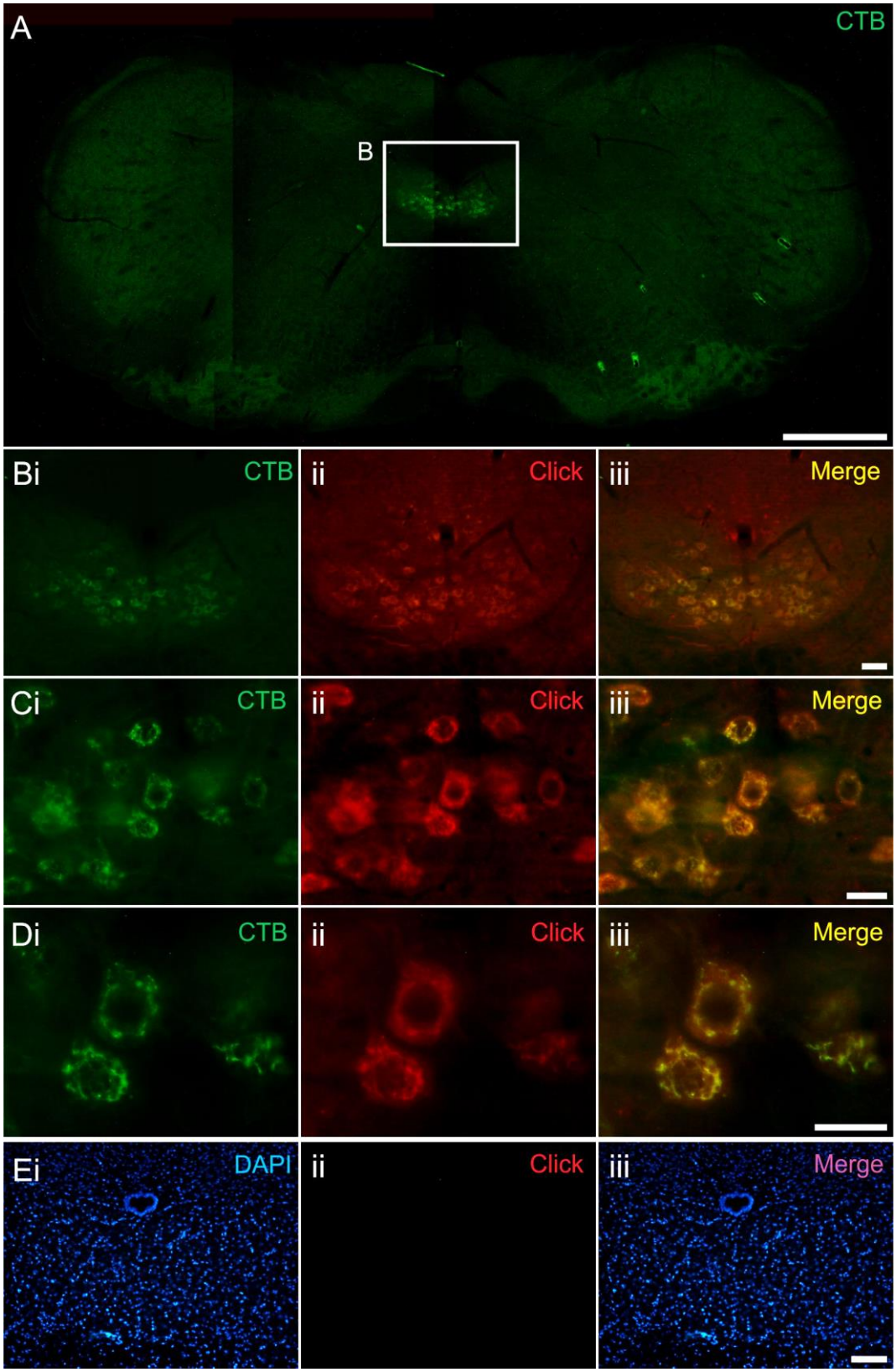
A
CTB
B
Bi
CTB
ii
Click
iii
Merge
Ci
CTB
ii
Click
iii
Merge
Di
CTB
ii
Click
iii
Merge
Ei
DAPI
ii
Click
iii
Merge

5.3.2 QDs were detected in the hypoglossal nucleus after tongue injection of CTB-QD

CTB-QD was injected IM via the tongue in mice to assess whether the protein could be endocytosed and retrogradely transport *in vivo.* After IM injection of CTB-QD, CTB was detected with immunohistochemistry in the hypoglossal nucleus of the brainstem (Figure 5.4A). Some CTB-positive cells are also positive for QDs (Figure 5.4B), yet others are only positive for CTB (Figure 5.4C, dotted outline) or QDs (Figure 5.4C). Mice injected with QD as a control had no CTB or QD detected in the hypoglossal (Figure 5.4D).

Silver enhancement of brainstem slices revealed QDs in neurones of the hypoglossal nucleus after CTB-QD injection (Figure 5.5A). In mice injected with QD there was no QD detected (Figure 5.5B), suggesting they cannot retrogradely transport without CTB. Silver enhanced slices were then prepared for EM where CTB-QD puncta were found to be localised to lysosomes (Figure 5.5C).

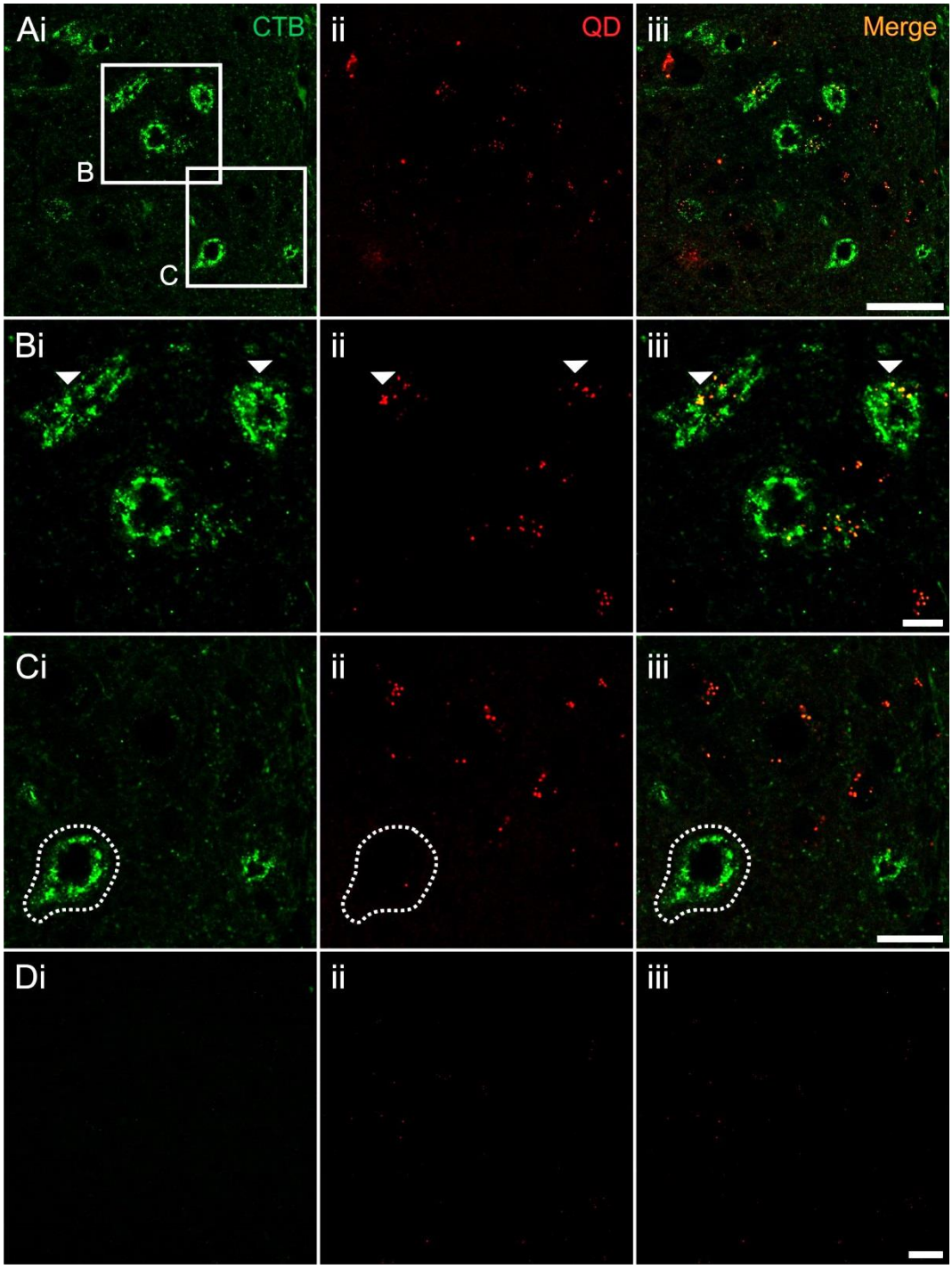

Figure 5.4 CTB-QD can be detected in the brainstem after tongue injection

Mice were injected IM with CTB-QD to the tongue and fixed after three days. Brainstem slices were obtained from removed brains and were then subjected to immunohistochemistry. A-C) Hypoglossal nucleus stained with anti-CTB (green, A-Ci), QD detected (A-Cii) and merged (A-Ciii); arrows highlight colocalised puncta.
D) Control brainstem slice from uninjected mouse stained with anti-CTB (green, Di), QD detected (Dii) and merged (Eiii). Scale bars: A = 50 µm; B = 10 µm; C, D = 20 µm.

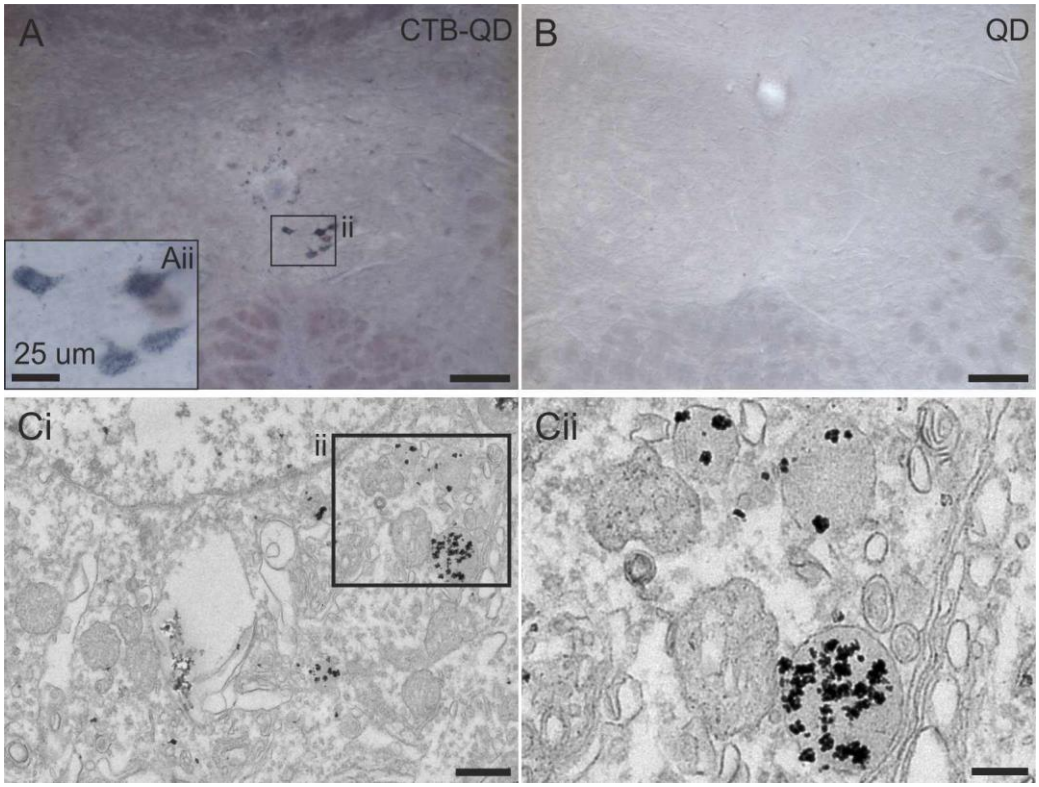

Figure 5.5 CTB-QD can be detected by electron microscopy in the brainstem after tongue injection

Mice were injected IM with CTB-QD to the tongue and fixed after three days. Brainstem slices were obtained from removed brains and were then subjected to silver enhancement and electron microscopy. A) Hypoglossal nucleus having undergone silver enhancement. B) Control brainstem slice from uninjected mouse having undergone silver enhancement. C) Electron microscopy of hypoglossal nucleus cell (Ci) and lysosomes inside that cell (Cii). Scale bars: A, B = 100 µm; Aii = 25 µm; Ci = 0.5 µm; Cii = 0.2 µm.

5.3.3 An AB_5-strep-555 complex can retrogradely transport to the hypoglossal nucleus after tongue injection

AB_5-strep-555 was injected IM via the tongue in mice to assess whether the protein could be endocytosed and retrogradely transport *in vivo.* AB_5-strep-555 was detected in the hypoglossal nucleus, and CTB was detected in the same cells with immunohistochemistry (Figure 5.6A). CTB and strep-555 are colocalised within some of the puncta, but there are also many CTB-positive puncta that are not strep-555 positive (Figure 5.6B). The CTB and strep-555 puncta only partially colocalise with the lysosomal marker LAMP1 (Figure 5.6C) suggesting some of the protein is in other intracellular compartments. Afferent fibres in the cuneate nucleus were CTB-positive but were not labelled with strep-555 (Figure 5.6D) suggesting the CTB had travelled alone. It is possible that there was an excess of CTB when the complex was mixed, otherwise the CTB has been cleaved from strep-555.

Figure 5.6 AB5-strep-555 labels neurones of the brainstem after tongue injection

Mice were injected IM with AB5-strep-555 to the tongue and fixed after three days. Brainstem slices were obtained from removed brains and were then subjected to immunohistochemistry. A-B) Hypoglossal nucleus with AB5-strep-555 (red, A-Bi) stained with anti-CTB (green, A-Bi) and merged (A-Biii). C-D) Hypoglossal nucleus with AB5-strep-555 (red, C-Di) stained with LAMP1 (green, C-Dii) and merged (C-Diii). E) Control brainstem slice from uninjected mouse stained with AB5-strep-555 (red, Ei) stained with anti-CTB (green, Eii) and merged (Eiii). Scale bars: A, E = 20 µm; B, C = 10 µm; D = 2 µm.

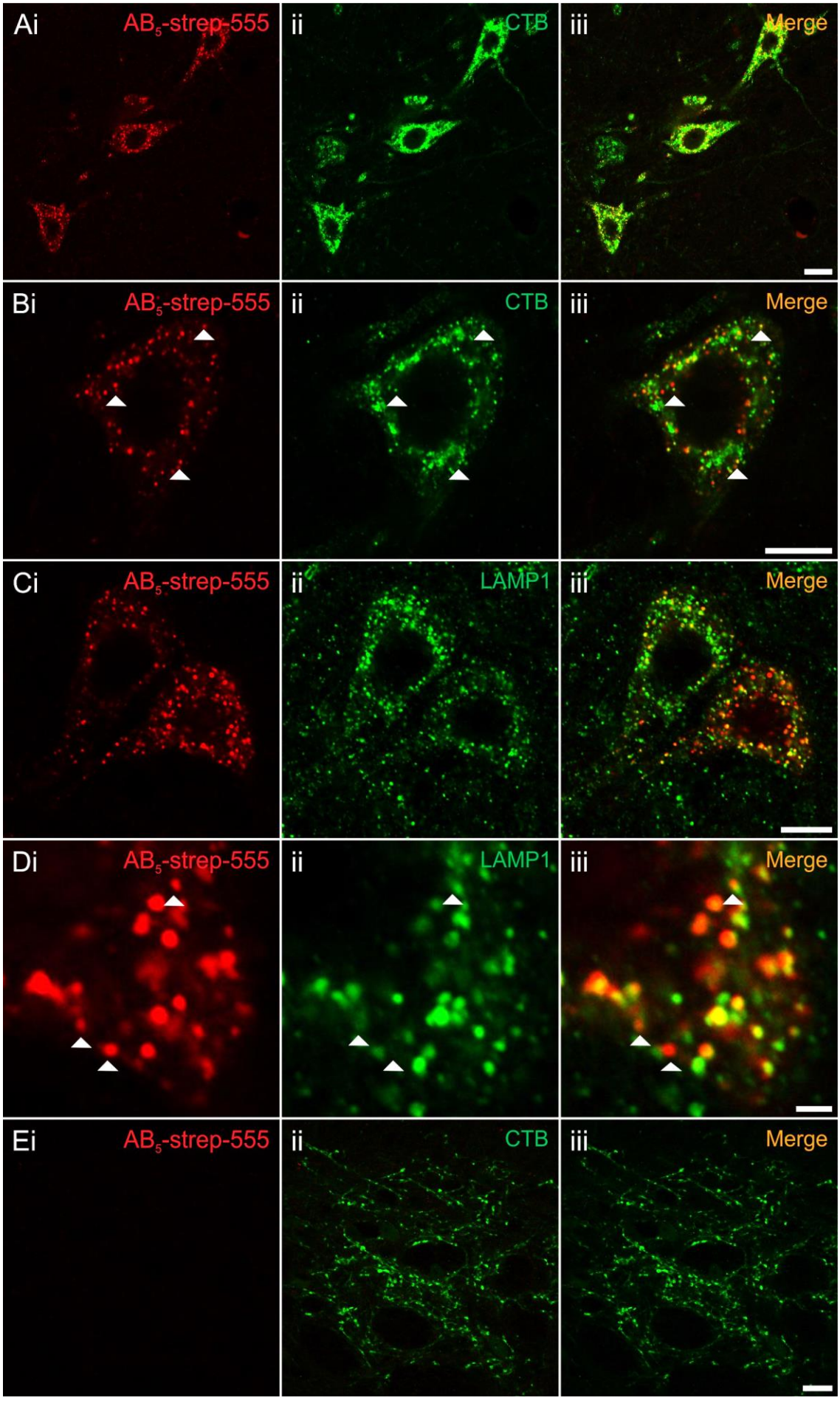
Ai
AB5-strep-555
ii
CTB
iii
Merge
Bi
AB5-strep-555
ii
CTB
iii
Merge
Ci
AB5-strep-555
ii
LAMP1
iii
Merge
Di
AB5-strep-555
ii
LAMP1
iii
Merge
Ei
AB5-strep-555
ii
CTB
iii
Merge

5.4 Discussion

The experiments in this chapter have highlighted novel detection methods for CTB tracers, as well as potential delivery opportunities for other proteins.

- CTB-azide can be detected via a 'click' reaction in fixed tissue.
- QDs were detected in fixed brainstem tissue after tongue injection of CTB-QD.
- AB_5-strep-555 can retrogradely transport after tongue injection, with both strep-555 and CTB detected in the hypoglossal nucleus.

5.4.1 CTB-azide retrogradely transports after IM injection and is detectable via click chemistry

CTB-azide functions as a neuronal tracer, detected in fixed tissue using click chemistry. The CuAAC takes place over an hour, with ascorbic acid serving to reduce copper (II) ions to copper (I) to be used in the catalysis of the reaction at room temperature. This can be followed by immunohistochemistry to identify other proteins within the tissue with less limitation to the primary antibody species that can be used since CTB is detected without antibodies.

CTB-azide might also be exploited for the conjugation of alkyne-containing proteins for delivery to neurones. Using CuAAC might be damaging to protein cargo as copper ions may alter protein structure or remain bound after the reaction, and this could prove damaging upon cell delivery. Strain-promoted alkyne-azide cycloaddition (SPAAC) affords click chemistry without the need for the toxic catalyst (Debets et al., 2010; Jewett and Bertozzi, 2010). Proteins can be engineered to contain alkyne groups by using methionine auxotroph strains of *E.coli* where all methionine residues within the protein can be replaced with alkyne containing 2-amino-5-hexynoic acid (Kiick et al., 2002). Or the alkyne expression can be directed to specific sites within proteins expressed by bacteria and mammalian cells by utilising noncanonical amino acids from orthogonal aminoacyl-tRNA synthetase/tRNA pairs (Wang and Schultz, 2004; Liu and Schultz, 2010; Lang and Chin, 2014); this reduces the chances of the conjugated protein interfering with function. A protein of interest can be designed containing an alkyne, then using SPAAC it may be conjugated to CTB-azide in aqueous solution at room temperature.

SPAAC has been used for rapid labelling of cell-surface proteins in living mammalian cells (Nikic et al., 2015). CTB-azide is internalised and so to use it in live cells a membrane-penetrating dye would be required to visualise the tracer. CTB-azide could be transformed into live cell imaging tool by undergoing a click reaction with an alkyne

containing fluorescent dye, and then being applied to cells for real-time imaging. It could be used to measure axoplasmic transport in neurones, or assess transport of CTB through intracellular compartments. SPAAC with CTB-azide has been successfully used to make CTB-QD, as described in the next section.

CTB-azide presents a useful tool for diversifying CTB as both a tracer and a delivery vehicle due to the ease of directed conjugation via CuAAC and SPAAC.

5.4.2 CTB-QD was detected in hypoglossal motor neurones after tongue injection

After tongue injection of CTB-QD the hypoglossal nucleus of the brainstem was analysed. Immunohistochemistry with antibodies for CTB revealed labelled cell bodies in the hypoglossal nucleus, and many of these were also positive for QD as detected by confocal microscopy. In CTB-labelled neurones the QD puncta colocalised with those of CTB. However there were also CTB immunopositive cells with virtually no detectable QD, as well as QD-positive cells with no CTB. Fixation of CTB-QD containing tissue should not quench QD fluorescence (Knight and Serrano, 2006) so it is unlikely PFA has led to reduced QD detection in some CTB-positive cells. Each CTB pentamer can carry up to 5 QDs; possibly more QDs are required for improved detection via fluorescence. When using immunohistochemistry to detect proteins the signal is greatly amplified when using a polyclonal antibody along with secondary antibodies. The dose injected was relatively low; if the CTB-QD was further concentrated more could be delivered in the maximum injection volume. In cells that are QD-positive but CTB-negative it is not known whether the QD detected is autofluorescence; however it would be unusual to detect it in such clear puncta.

CTB-QD was made using click chemistry with CTB-azide; this allowed for directed addition of the QDs away from the GM1 binding face. QDs can also be conjugated to proteins through the co-ordination of amino acid residues with zinc ions on the QD surface (He et al., 2013). He et al. created a protocol for creation of protein-functionalised QDs using alloyed $Zn_xHg_{1-x}Se$ in a one-step reaction in ambient conditions; the prepared complexes retained capabilities of catalysing reactions and biotargeting. The QDs can co-ordinate with histidine moieties and as such this method could be used to create CTB-QDs since CTB contains histidine residues capable of binding nickel ions (Dertzbaugh and Cox, 1998). The main histidine residue (H13) involved in binding to a nickel resin is located next to the GM1 binding site, as such it may be more appropriate to use site-directed mutagenesis to remove this residue and insert a histidine on the opposite face. QDs bound this way are less likely to alter cell entry mechanisms.

Quantum dots can be detected via silver enhancement, with the QD serving as a nucleation site for deposition of silver. This gives a high contrast signal that is visible using light microscopy. CTB-QD is detected as puncta throughout the cells, and when QD is injected alone it does not retrogradely transport. Silver enhancement is frequently used in electron microscopy (EM), allowing for detection of gold nanoparticles without the need to permeabilise the tissue. In this study CTB-QD was successfully detected via silver enhancement for EM, with puncta localised to lysosomes. CTB-gold has been used as a neuronal tracer for EM (Llewellyn-Smith et al., 1990). CTB-QD could further improve CTB as a tracer for EM as it does not require the need for permeabilisation meaning ultrastructure is maintained. It is detectable via correlated fluorescence, light microscopy and EM and thus provides a much wider scope for possible experiments with tissue.

In this study CTB-QD was used to detect traced neurones in fixed tissue, but Chakraborty et al. (2007) used CTB-QD for live cell labelling in culture. They tested the conjugated protein in an array of stem cell and cancer cell lines, but no neuronal cells. Since CTB enters neurones, CTB-QD could be used to assess retrograde and anterograde axonal transport in cultured neurones. Their photostable nature means that imaging over long periods or with intense exposures is less likely to cause photobleaching when compared to common fluorophores. This would be useful in measuring axoplasmic transport in cultured neurones in real-time, whether this is altered in neurodegenerative disease models, and whether therapeutic molecules can correct any changes. Axonal transport could also be measured *in vivo* with CTB-QD as has been done previously with TTC-555 (Bilsland et al., 2010). This would allow for further interrogation of changes in both retrograde and anterograde transport in mouse models of neurodegenerative diseases and whether these are different when comparing different models of the same disease, for example SOD1 or TDP43 mutants in ALS.

CTB-QD presents a diverse tool for tracing detected both with fluorescence and EM, for use in live and fixed tissue, and for use in extended time-lapse experiments.

5.4.3 A complex of AB_5-strep-555 was used successfully as a neuronal tracer

After tongue injection of AB_5-strep-555 the complex was detected in motor neurones of the hypoglossal nucleus, suggesting it had successfully retrogradely transported from neurone terminals in the tongue to the cell bodies within the brainstem. Immunohistochemistry for CTB reveals that CTB and AB_5-strep-555 puncta are colocalised within cell bodies, although some CTB puncta are not reactive for

strep-555. This could be due to the way the complex was made. The AB_5-biotin and strep-555 were made separately and then mixed, possibly some AB_5 did not complex with the streptavidin leaving an excess in solution; this excess would then be free to transport alone. Size exclusion chromatography could be used to purify the complexed fraction away from non-complexed protein. AB_5-strep-555 colocalised quite strongly with LAMP1 suggesting much of the complex was trafficked to the lysosomes. Some puncta were not colocalised, suggesting a proportion of the complex may reside in endosomes, TGN or the ER; immunohistochemistry with intracellular markers would elucidate this. The cuneate nucleus of the brainstem contained CTB-immunopositive afferent fibres, but was not labelled with AB_5-strep-555. This is again likely due to the way the complex was created, with excess CTB transporting separately to the complex. The cuneate nucleus contains passing fibres of the glossopharyngeal nerve, some of which supply the tongue muscles (Ciriello et al., 1981; Mu and Sanders, 2010). CTB entering terminal glossopharyngeal fibres retrogradely transports to the inferior ganglion, from here it is able to continue transporting in an anterograde manner up via the cuneate nucleus to terminate in the thalamus. It is possible that the AB_5-strep-555 complex was only able to transport in a retrograde direction and so remained within the inferior glossopharyngeal ganglion. Importantly the complex was detectable in the CNS after peripheral delivery.

Streptavidin as a central molecule to bring together biotinylated proteins could be employed to deliver proteins that cannot normally enter cells. The protein to be delivered would need to have biotin attached (Kay et al., 2009), if this was then mixed with streptavidin and AB_5-biotin, a complex could be formed that may retain ability to retrogradely transport. The components would need to be mixed in a proportion such that each streptavidin had at least one AB_5 and one cargo bound. The AB_5-strep-555 complex is around 180 kDa, with two AB_5 units of approximately 58 kDa bound. Each streptavidin homotetramer can bind four biotin molecules, the likely reason only two AB_5-biotins bind this complex is due to their size and structure, with the other two biotin sites being obstructed by CTB. If the cargo was only small protein possibly 3 sites could be used with the final being bound by AB_5-biotin.

Streptavidin can be expressed in bacteria, and recombinant core streptavidin proteins have been designed that show less aggregate formation and have high solubility when compared to native streptavidin (Sano et al., 1995). These core streptavidin proteins have higher accessibility to biotin as steric hindrance is reduced with the terminal regions truncated from the surface of the molecule. They can be easily produced and purified from *E.coli* cultures, and thus would allow laboratories to produce their own

materials for complex formation. Avidin has also been engineered to contain two high and two lower affinity biotin-binding sites (Hytonen et al., 2005). Lower affinity binding sites released biotin within an hour, if biotinylated cargo were bound these may be more likely to be released intracellularly. Another recombinant avidin was modified such that biotin binding was pH-adjustable, with 50% becoming unbound at pH 9 (Marttila et al., 2003). Adjustment such that biotin was released in acidic pH would be useful to release biotinylated cargo once within lysosomes, where some of the complex is targeted in neurones.

Avidins have been modified plenty (Laitinen et al., 2007), and represent a versatile tool for protein conjugation via avidin-biotin technology. A complex of AB_5-streptavidin mixed with a biotinylated therapeutic cargo holds promise as a novel delivery mechanism in neurones.

Conclusion

CTB has the potential to be engineered for non-antibody mediated detection and for the delivery of cargo. CTB-azide can be developed to create interchangeable conjugated proteins via click chemistry; it could deliver multiple cargo at once, or cargo along with a reporter dye. This has been proven with CTB-QDs produced from CTB-azide; the QDs were detectable after injection *in vivo*. Biotinylated CTB in the form of an AB_5 holotoxin has the potential for creating further interchangeable delivery complexes with strepatavidin and biotinylated cargo. There is a wide scope of opportunity for delivery with CTB conjugates with the prospect of creating a CTB toolbox where proteins of interest might be easily ‘clicked’ on.

Chapter 6
Tracing of peripheral neuronal networks using viruses expressing synapse-crossing proteins

6.1 Introduction

Proteins with the ability to cross neuronal synapses are useful tools for elucidating networks in the brain and spinal cord as synapsing neurones can be labelled. When a trans-synaptic tracer is used alone it is difficult to distinguish first order neurones from any further labelled ones. Using viruses expressing a fluorescent dye in first order neurones, and then producing a synapse-crossing protein to label connecting neurones means it is possible to differentiate first and second order neurones. With these properties it is possible to map circuits within the CNS, or deliver therapeutic proteins to higher order neurones after peripheral administration. For example, the components of neuronal circuitry may be elucidated following peripheral injection to a muscle; the first order motor neurones would express the reporter protein and higher order neurones traced with trans-synaptic protein. The types of neurones within the circuit can be assessed using immunohistochemistry, elucidation of such networks will allow for modulation of higher order neurones to probe effects in disease. Such a system might also be used to deliver therapeutic molecules to higher order neurones if created as fusion proteins with a trans-synaptic protein to be expressed by a virus.

Wheat germ agglutinin (WGA) is a plant lectin with the ability to enter neurones and then escape them to be taken up by neighbouring neurones, being transported both retrogradely and anterogradely (Gerfen et al., 1982). For this reason WGA has been widely used as a tracer of neural circuits, either as the native protein delivered exogenously (Schwanzel-Fukuda et al., 1984; Arbab et al., 1986; Holstege, 1987), expressed in transgenic mice (Yoshihara et al., 1999; Sugita and Shiba, 2005), or delivered via a virus (Braz et al., 2002; Kinoshita et al., 2002). Viral tracing studies have employed expression of a WGA and Cre recombinase fusion protein; this allows for tracing of neuronal network connections in Cre-dependent transgenic animals as well as the possibility of inducing topological transgene expression (Gompf et al., 2015; Libbrecht et al., 2016; Sanders and Jaeger, 2016).

Adeno-associated viruses (AAVs) are often used as delivery vectors due to their low immunogenicity, lack of toxicity and ability to provide long-lasting gene expression. Delivered systemically, AAVs tend to transduce the heart and liver predominantly, but AAV8 and AAV9 are able to express in the brain (Zincarelli et al., 2008). Direct injection of AAVs into DRG neurones was successful for gene delivery, with AAV5 yielding the highest transduction rates (Mason et al., 2010). By injecting an AAV expressing WGA-Cre in one brain region, and one expressing a Cre-dependent opsin in another, it was possible to activate distant gene expression in only the neurones connected to the primary injection area (Gradinaru et al., 2010). Where the WGA-Cre was expressed it

was able to trans-synaptically transport and enter connected neurones; when these neurones contain a floxed opsin the delivered Cre recombinase allows for opsin expression. When light of the relevant wavelength is applied neuronal activity can be measured, confirming transgene expression. This provides rationale that delivery of AAVs with WGA-Cre to peripheral neurones could then allow for genetic manipulation of neurones within the CNS.

Tetanus toxin fragment C (TTC), part of the toxin produced by *Clostridium tetani*, is another protein with the ability to cross synapses. TTC can target therapeutic molecules to motor neurones to be retrogradely transported from the periphery since it binds pre-synaptic motor neurone terminals (Toivonen et al., 2010). Canine adenovirus (CAV-2) expressing GFP-TTC was injected into the striatum and after 1 month GFP was detected in the ventral thalamus, control injections of virus expressing just GFP had no trans-synaptic transfer (Kissa et al., 2002). CAV-2 vectors, much like AAV vectors, are powerful tools for gene delivery due to their negligible immunogenicity. CAV-2 preferentially transduces neurones due to their selective use of coxsackievirus and adenovirus receptor (CAR) located on the pre-synaptic terminal of neurones (Junyent and Kremer, 2015). Their widespread distribution via retrograde axonal transport and long duration of expression make CAV-2 vectors good candidates for targeted delivery to the CNS.

6.1.1 Summary and objectives

Combining neurone transducing viruses that have the ability to retrogradely transport and express trans-synaptic proteins gives us a useful tool for elucidating neuronal networks. It may also be possible to deliver therapeutic molecules to higher order neurones after delivery in the periphery.

Research questions:

- Can neurones be transduced from the periphery to study neuronal circuits?
- Is there a difference in transduction efficiency between AAV2 and CAV-2?
- Is there a difference in transduction efficiency between rats and mice?

Rats and mice will be injected intramuscularly and directly into nerves and ganglia, to assess whether the viruses can transduce neurones following injections at axonal sites. After fixation, tissue will undergo immunohistochemistry to detect trans-synaptic proteins both in the innervating area, and in known projecting areas.

The results of this study will elucidate whether AAV2 or CAV-2 vectors can be applied to the peripheral nervous system (PNS) to transduce neurones within the CNS. It has

the potential to open up new avenues for study of neuroanatomical analysis of PNS-CNS circuits, as well as the potential for novel delivery methods of therapeutics for neurological diseases.

6.2 Materials and methods

AAV2 containing pAAV-EF1a-mCherry-IRES-WGA-Cre (UNC Gene Therapy Vector Core) was tested *in vivo* as described in General Methods section 2.11.2. Injection routes and species used are listed in table 6.1.

Route	Species
Tongue	mouse
Nodose ganglion	rat
4V	mouse
Intranasal	rat

Table 6.1 Injection routes for AAVs, tested serotypes listed with species

CAV-2 expressing GFP-TTC and a CAV-2 reporter expressing DsRed were tested *in vivo* as described in General Methods section 2.11.3. Injection routes, serotypes and species used are listed in table 6.2.

Route	Species
Gastrocnemius	rat
Tongue	mouse
Nodose ganglion	rat
SCG	rat
Sciatic nerve	rat
Peroneal nerve	mouse
Adrenal gland	mouse
Intranasal	rat

Table 6.2 Injection routes for CAV-2 listed with species tested

Both viruses were also tested in cell culture for infection efficiency as described in section 2.11.4.

6.3 Results

6.3.1 CAV-2 and AAV2 vectors successfully express in cultured 911 cells

Viruses were tested in 911 cells to assess transduction efficiency. Both CAV-2 vectors successfully transduced 911 cells after incubation for 24 hours. CAV2-GFP-TTC at 3.7 x 10^{11} VG effectively expressed GFP, immunohistochemistry detected TTC and the signals were colocalised (Figure 6.1Ai-iii). CAV2-DsRed transduced 911 cells at 5.7 x 10^{7} VG, and there was no GFP signal detected, as expected. AAV2-mCherry-WGA-Cre transduced 911 cells after incubation for 24 hours with 2.7 x10^{10} virus molecules/mL. This provided rationale to test the viruses *in vivo*.

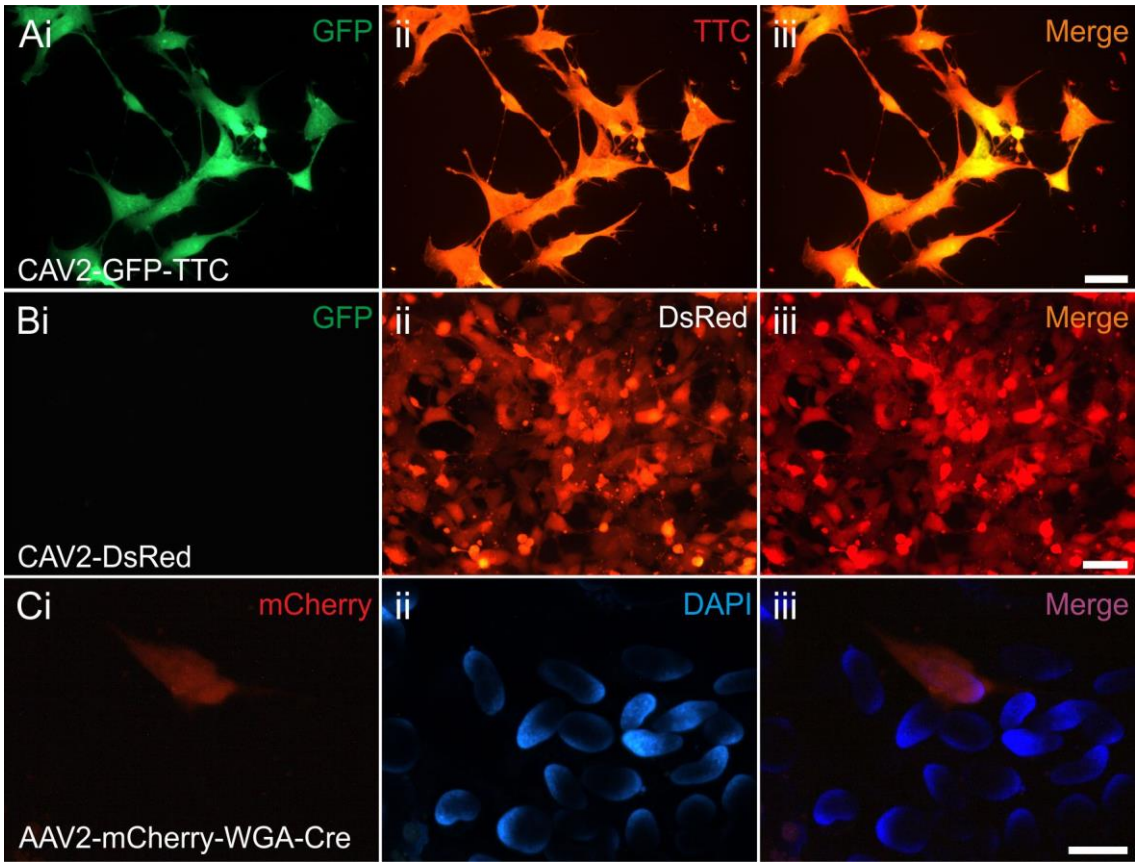

Figure 6.1 CAV-2 and AAV2 transduce 911 cells

Cells were incubated with virus for 24 hours, fixed and some underwent immunohistochemistry. A) Following infection with 3.7 x 10^{11} VG of CAV2-GFP-TTC cells were assessed for GFP expression (green, Ai), stained with anti-TTC (red, Aii) and merged (Aiii). B) Following infection with 5.7 x 10^{7} VG of CAV2-DsRed cells were assessed for GFP expression (green, Bi), DsRed expression (red, Bii) and merged (Biii). C) Following infection with 2.7 x10^{10} virus molecules/mL of AAV2-mCherry-WGA-Cre cells were assessed for expression of mCherry (red, Ci), DAPI (blue, Cii) and merged (Ciii). Scale bars: A, C = 50 µm; B = 100 µm.

6.3.2 CAV2-GFP-TTC transduced few neurones in the dorsal vagal nucleus after nodose ganglion injection in rats

CAV2 vectors were administered via various peripheral routes in rats to assess transduction. Nodose ganglion injection of CAV2-GFP-TTC transduced neurones of the DVN after 4 weeks; however there were only 3 GFP-positive cells found. The cells were located in both caudal (Figure 6.2Ai) and rostral (Figure 6.2Bi) brainstem regions, and labelling was diffuse throughout the cells (Figure 6.2Aii, Bii). There were no GFP-positive cells in the nucleus ambiguus or afferents in the NTS. Subsequent brainstem slices probed with anti-TTC were not immunoreactive for the toxin subunit, suggesting it have been degraded.

Following dual IM injection of CAV2-GFP-TTC and CAV2-DsRed to the gastrocnemius there were no transduced cells in the spinal cord from L4-6 (Figure 6.3Ai-iv). The ventral horn was clearly absent of DsRed or GFP-positive motor neurones (Figure 6.3Bi-iv). Direct injection to the sciatic nerve did not transduce any cells in the spinal cord, and no reporter-positive cells or fibres were detected in the sciatic nerve. Injection of the superior cervical ganglia (SCG) with CAV2-GFP-TTC yielded no GFP-positive cells in the DVN or NTS. Intranasal application of CAV2-GFP-TTC did not transduce cells of the olfactory bulb.

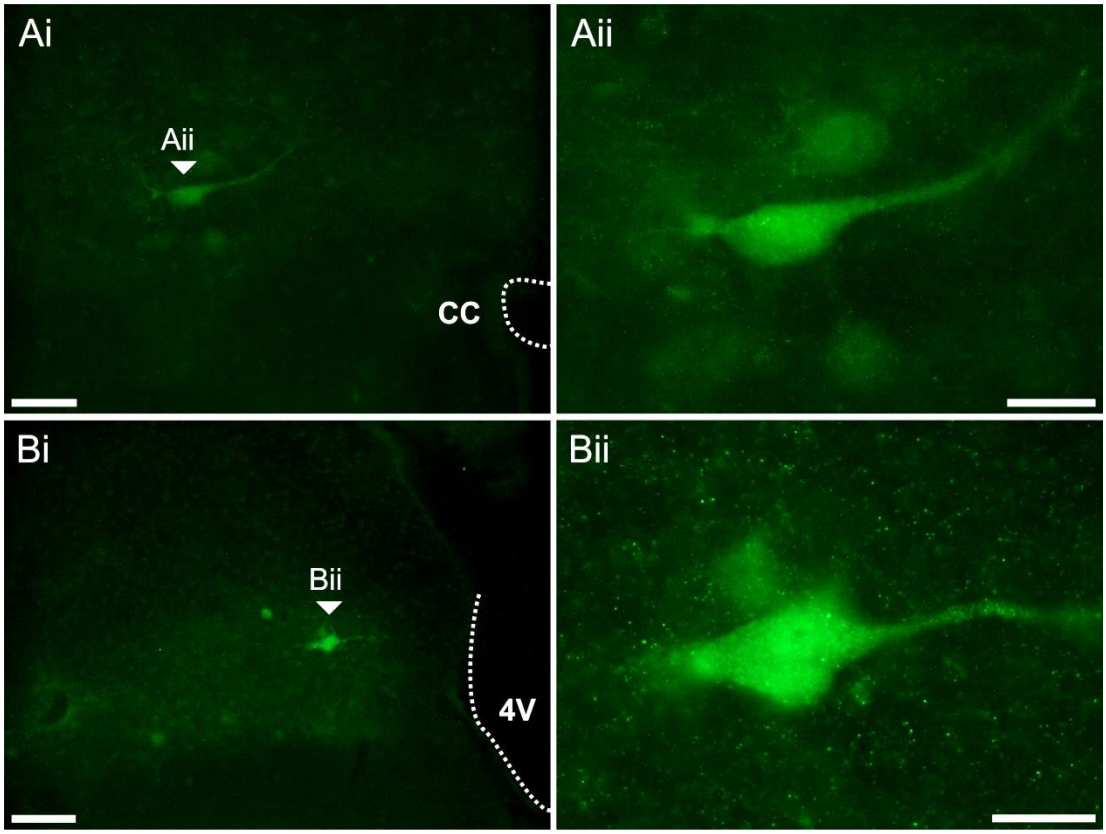

Figure 6.2 CAV2-GFP-TTC transduces few neurones in the DVN following nodose ganglion injection in rat

A rat was injected with 3.7 x 10^{13} VG CAV2-GFP-TTC to the nodose ganglion and fixed after four weeks. A) Caudal brainstem section assessed for GFP expression. B) Rostral brainstem section assessed for GFP expression. Scale bars: Ai = 50 µm; Aii, Bii = 25 µm; Bi = 100 µm.

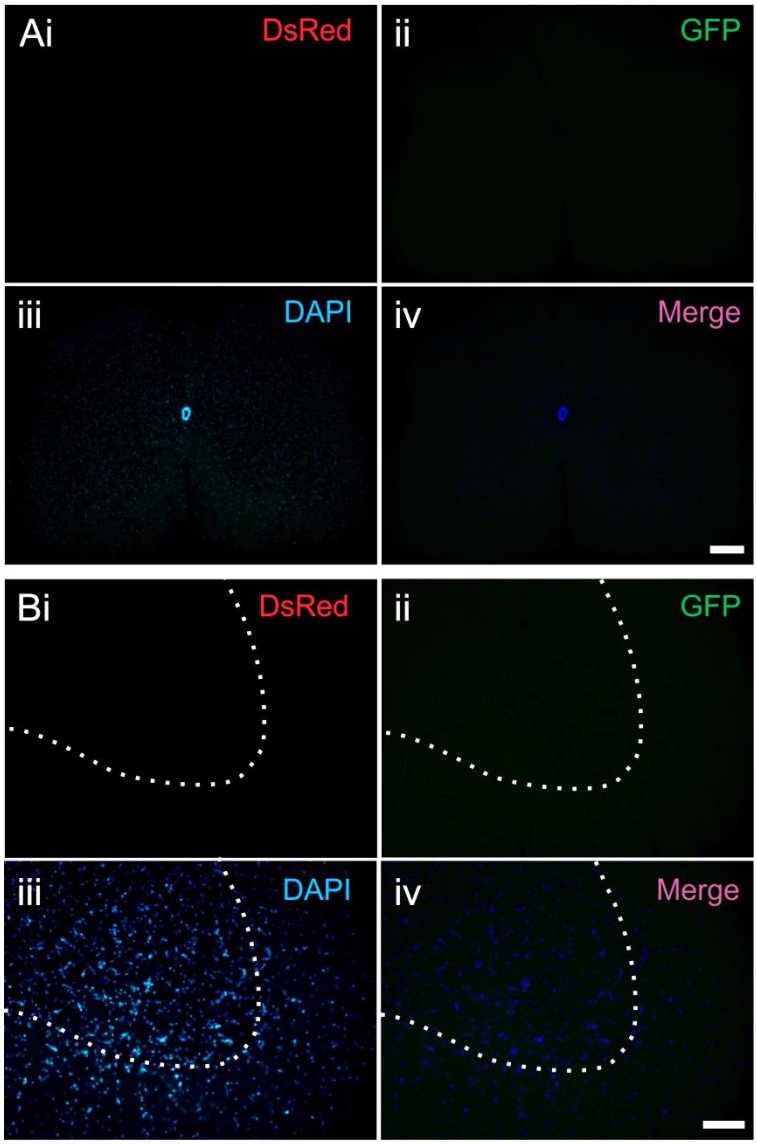

Figure 6.3 Intramuscular injection of CAV2-DsRed and CAV2-GFP-TTC to the gastrocnemius failed to transduce neurones in the lumbar region of the spinal cord in rat

Rats were injected with 3.7 x 10^{13} VG CAV2-GFP-TTC and 5.7 x 10^{9} VG CAV2-DsRed to the gastrocnemius and fixed after four or five weeks. A+B) Whole spinal cord slice (A) and ventral horn (B) from L4 assessed for DsRed expression (red, A-Bi), GFP expression (green, A-Bii), DAPI (blue, A-Biii) and merged (A-Biv). Scale bars: A = 200 µm; B = 100 µm.

6.3.3 CAV-2 viruses did not successfully transduce neurones via any route used in mice

Tongue injections of both viruses were unable to transduce neurones as the hypoglossal nucleus in the brainstem was absent of GFP and DsRed after 3 and 4 weeks. Injections directly to the peroneal nerve did not transduce neurones as neither reporter protein was expressed in the spinal cord. Adrenal gland injections of both viruses yielded no GFP or DsRed-positive SPNs in the thoracic region of the spinal cord (Parker et al., 1993).

6.3.4 AAV2 did not successfully transduce neurones via any injection route in mice or rats

AAV2 was administered via various routes in mice and rats to assess transduction. In mice, no neurones were transduced by any AAV2 via any route tested as no mCherry was detected and immunohistochemistry for WGA was negative. Injections of AAV2 to the tongue yielded no labelling of the hypoglossal nucleus of the brainstem. Central injections to the fourth ventricle did not transduce cells at the site of injection within the CNS.

In rats, intranasal administration of AAV2 did not transduce neurones of the olfactory bulb. Injections of AAV2 to the nodose ganglion did not transduce neurones of the DVN or NTS as no mCherry was detected and immunohistochemistry for WGA was negative.

6.4 Discussion

This study provides evidence of the difficulties in targeting peripheral neurones for trans-synaptic tracing into the CNS with AAV and CAV-2.

- CAV-2 vectors did not transduce neurones in mice after injection into the tongue, peroneal nerve or adrenal gland.
- CAV-2 vectors did not transduce neurones in rats after injection into the gastrocnemius, SCG or sciatic nerve, or after intranasal administration.
- CAV2-GFP-TTC transduced only a few neurones of the DVN after injection to the nodose ganglion in rats.
- AAV2 did not transduce neurones in mice after peripheral injections to the tongue or following central injections to the fourth ventricle.
- Injection of AAV2 to the nodose ganglion in rats did not transduce neurones; intranasal administration was also unsuccessful.

6.4.1 CAV-2 vectors do not transduce neurones after peripheral administration in rats and mice by most routes tested

The ability of CAV-2 vectors to transduce cells and express reporter proteins was proven in cell culture, but the vectors did not successfully transduce neurones in adult rats or mice as they have been reported to in previous studies (Soudais et al., 2001; Soudais et al., 2004). Intramuscular injections to the tongue and gastrocnemius require infection of neurone terminals at the neuromuscular junction (NMJ), and then retrograde transport of the virus to the cell body. The receptor for CAV-2, CAR, is not expressed at the NMJ, but it can be detected on the neurites of innervating motor neurones (Soudais et al., 2001). IM injections to the gastrocnemius of P4 mice resulted in successful transduction of motor neurones but not skeletal muscle after 3 weeks (Soudais et al., 2001). The difference in results following gastrocnemius injection could be down to down-regulation of CAR expression following neuronal differentiation (Honda et al., 2000). Analysis of mRNA and protein expression of CAR from whole brain samples showed a significant decrease from P7 to P21; however care should be taken when extrapolating this result to the PNS where changes in CAR expression during development have not been tested.

Direct injections to nerves and SCG were also unsuccessful; there were no GFP or DsRed-positive cell bodies in the CNS, or fibres in the nerve itself. It is not known whether the viruses were unable to infect, unable to retrogradely transport, or if they failed to transduce neurones once at the cell body. Injections of CAV2-GFP directly into the striatum selectively transduced neurones (Soudais et al., 2001). These injections introduced 2×10^9 VG, whereas in this study direct injection to nerves and ganglia introduced 3.7×10^{13} VG. Possibly the titre was too high and caused the death of neurones. However no ill effects were noted in mice and neurones were still detectable in the innervating nuclei. Injection of CAV2-GFP-TTC into the nodose ganglion of a rat transduced just three cells in the DVN after 4 weeks. It is possible that GFP-TTC was expressed by neurones but cleared by the time the rat was perfused. Soudais et al (2001) report GFP being detected up to 8 weeks following injection, however the fusion protein of GFP-TTC could be directed to lysosomes and behave differently to just GFP as expressed in their study.

Intranasal administration of CAV2-GFP-TTC failed to transduce neurones of the olfactory bulb after 4 weeks. Soudais et al (2001) detected GFP positive olfactory neurones two weeks after administration. This difference could be attributed to the administration technique they used, where CAV2-GFP was administered to the

ethmoid labyrinth. This is much deeper into the nasal cavity than our administration, and so possibly the virus remained at the epithelium.

CAV-2 vectors have been shown to transduce motor neurones in culture, where the virus is able to move in both retrograde and anterograde directions along the axon by utilising kinesin-1 and cytoplasmic dynein motor activities (Bru et al., 2010). This would be useful for targeting degenerative motor neurone diseases as lower motor neurones could be transduced. It is possible in this study that the neurones were successfully transduced because they were cultured from rat E13.5 embryos, and so likely to express higher levels of CAR.

CAV-2 has many favourable characteristics making it a good candidate for neuronal tracing and delivery: neural tropism, retrograde transport, negligible immunogenicity and long lasting gene expression (Junyent and Kremer, 2015). However in adult mice and rats in my studies, neuronal transduction following peripheral administration has not been successful. There is a lack of evidence in the literature to support the peripheral retrograde transport of CAV-2 vectors; while IM injection in P4 mice resulted in transduction of innervating motor neurones, all evidence of retrograde transport in adult neurones comes from central administration (Soudais et al., 2001). CAV-2 may therefore be better suited to targeting neurones in young rodents, or used in administration directly to the CNS.

6.4.2 AAV2 does not transduce neurones in rats and mice via all routes tested

AAV2 as tested in this study did not successfully transduce neurones following either central or peripheral injection in rats or mice. Injections to the nodose ganglion in rats did not transduce cells of the DVN or NTS with mCherry or WGA-Cre.

AAV2 was tested via intramuscular (tongue), central (fourth ventricle), direct nerve (nodose) and intranasal injections. AAV2 has been used previously to target motor neurones by retrograde transport after injection to the quadriceps in mice (Kaspar et al., 2003). For GFP expression in ChAT-positive motor neurones in the lumbar region of the spinal cord a dose of 1×10^{10} viral particles was required. The tongue injections in this study used 2.7×10^{9} viral particles, possibly this titre was not high enough for transgene expression. Kasper et al. (2003) then delivered insulin-like growth factor-1 (IGF-1) in an ALS mouse model; this prolonged life expectancy and delayed progression of the disease. Clearly AAV2 can be used to target motor neurones from the periphery, but more titres need to be tested with AAV2 (pAAV-EF1a-mCherry-IRES-WGA-Cre).

AAV2 binds heparin sulphate proteoglycan (HSPG) to attach to cells (Summerford and Samulski, 1998) and only recently the protein receptor (AAVR) for cell entry was elucidated (Pillay et al., 2016). AAVR serves as a critical host factor for AAV serotypes 1, 5, 6, 8 and 9 also, as AAVR knockout cells were resistant to AAV infection. The cell entry ligands for serotypes other than AAV2 remain relatively unknown. Cellular binding of AAV1 and AAV6 is mediated by sialylated glycoproteins (Wu et al., 2006), AAV5 vectors require an N-linked sialic acid (Walters et al., 2001) and AAV4 requires an O-linked sialic acid (Kaludov et al., 2001). HSPGs are abundant on neuronal plasma membranes (Hsueh et al., 1998) and sialylated glycoproteins are also ubiquitously expressed on cell surfaces, therefore it is likely that an unknown protein receptor mediates the entry of each AAV serotype giving the altered tropism between them. Since these receptors are unknown it cannot be determined yet which serotype is most appropriate for administration to neuromuscular junctions in adult mice for retrograde transport and transduction.

Injection of AAV2 into the corticospinal tract (CST) proved to be an effective approach for selectively targeting corticospinal motor neurones, the vector was able to retrogradely transduce cells from the spinal cord to be detected in the motor cortex (Jara et al., 2012). AAV2 has also been shown to be capable of anterograde axonal transport after injection to rat striatum (Ciesielska et al., 2011). Central injection of AAV2 into the fourth ventricle did not successfully transduce cells at the injection site, or elsewhere in the brain of mice. While a similar titre was used to Jara et al. (2012), their injection was directly into the spinal cord, whereas into the fourth ventricle the viral dose is diluted by the CSF. Direct injections to the nodose ganglion failed to transduce neurones of the NTS. AAV2 and AAV2/8 successfully transduced neurones in guinea pigs 4 weeks after injection to the nodose ganglion (Kollarik et al., 2010). In the same study, direct injection to the cervical oesophageal wall transduced nodose ganglion neurones with GFP detected in the NTS also. Titres injected by Kollarik et al. were 10 times as high as those used in this study. Systemic administration of AAV2 via tail vein injections resulted in low transgene expression and slow onset compared to other serotypes, and most expression was detected in the upper abdominal and hindlimb regions (Zincarelli et al., 2008). This suggests systemic administration is unable to effectively target neurones, and so more direct routes are required.

AAV2 is able to target neurones, transport in both anterograde and retrograde directions, and has a proven safety profile in phase 1 and 2 clinical trials (Fiandaca et al., 2008; Bowles et al., 2012) making it a good candidate for targeting motor neurones

in neurodegenerative diseases for therapeutic transgene expression. However the route used must be carefully considered and a variety of titres tested.

This study looked at just one serotype of AAV, but 11 naturally occurring serotypes have been described (Choi et al., 2005). Many of these have been tested for neurotropism and ability to retrogradely transport from the periphery. Tongue injection of AAV9 in wild-type and dystrophic mice successfully transduced hypoglossal neurones, though this was only 30% as efficient as CTB (ElMallah et al., 2012). AAV vectors can be pseudotyped with the capsid proteins from other serotypes to alter their tropism. Intramuscular injections of AAV2/1 and AAV2/2 transduced spinal motor neurones unilaterally and halted progression of neuropathology in peripheral nerves by transgene expression of the deficient Spg7 gene (Pirozzi et al., 2006). A rate limiting step in AAV transduction is the second-strand synthesis stage (Ferrari et al., 1996); the single-strand DNA (ssDNA) released from viral uncoating must be converted to double-stranded DNA (dsDNA), only then can replication and transcription occur. Rather than containing single-stranded DNA, self-complementary AAVs (scAAVs) are packaged with two strands as a single DNA molecule. Upon infection the dsDNA is ready for immediate replication and transcription. scAAV vectors have half the transgene capacity of single-stranded AAVs but are more efficient at transducing various tissues (McCarty et al., 2001). IM and sciatic nerve injection of scAAV1 transduced motor neurones in the spinal cord by retrogradely transporting (Hollis et al., 2008). AAV6 has also been shown to target motor neurones for transduction after IM injection to the gastrocnemius in primates (Towne et al., 2010). IV delivery of AAV6 in an ALS mouse model transduced motor neurones at all levels of the spinal cord and brainstem, though skeletal muscle, heart and liver tissue were also transduced (Towne et al., 2008). The study aimed to deliver shRNAs to silence mutant SOD1, and while AAV6 did transduce spinal motor neurones disease progression was not halted compared to disease controls.

Peripheral administration of AAV represents an efficient method of targeting lower motor neurones for long-term transgene expression since it is much less invasive than central delivery. However off-target transduction in other tissues following systemic administration means more targeted delivery routes such as IM are more appropriate. Successful selective transgene expression could deliver therapeutic molecules to treat motor neurone diseases such as ALS and spinal muscular atrophy. Currently more research is needed to make delivery more specific to motor neurones and to ensure retrograde transport.

6.4.3 Viruses need to be re-targeted to peripheral neurones for increased transduction efficiency

One strategy for increasing transduction efficiency and improving neurotropism of the viruses is by re-targeting them with proteins known to enter neurones. Adenoviral vectors were coated with TTC to improve neuronal cell entry (Schneider et al., 2000). Two methods were employed to attach the toxin fragment to the virus, either TTC-poly-L-lysine conjugates that can electrostatically bind the virus surface, or the Fab fragment of a neutralising anti-knob antibody covalently bound to TTC. Tongue injection of the TTC-antibody conjugated adenovirus was able to transduce neurones of the hypoglossal nucleus, though the number of transduced cells was no different to the control group treated with the unmodified virus. There were markedly fewer infected muscle and connective tissue cells at the injection site in mice that were administered retargeted vector suggesting the TTC had made the tropism more selective for neurones. It may be possible to coat viruses with CTB in a similar manner to target viruses to motor neurones after intramuscular injection, as well as to SPNs and primary afferents after systemic administration. CTB-azide as described in chapter 5 could be used to conjugate the toxin to an antibody against a viral coat protein via click chemistry. Then upon mixing with the virus it would be coated in the toxin ready for delivery.

Lentiviral vectors have been pseudotyped with rabies virus glycoprotein (rabies-G) to improve neurotropism and retrograde transport (Mazarakis et al., 2001). Peripheral delivery of the pseudotyped virus via gastrocnemius injection transduced motor neurones of the lumbar spinal cord selectively, compared to control virus injections that only expressed the transgene in muscle cells surrounding the injection site. Chimeric pseudotyped viruses have also been produced by replacing the cytoplasmic tail of rabies-G with that of vesicular stomatitis virus G protein (VSV-G) (Carpentier et al., 2012). This resulted in more rabies-G being incorporated in each vector particle and in neuronal cell culture the vectors possessed higher biological activity. When tested *in vivo* via striatum injections the hybrid vector had a lower rate of neuronal transduction when compared to rabies-G pseudotyped vectors. CAV-2 has been pseudotyped with rabies-G for use as a vaccine, providing protective immunity against rabies in mice (Li et al., 2006; Tordo et al., 2008). Neither of these studies assessed the spinal cord for entry of the virus following IM injection, but there were no clinical signs of immune response. This suggests rabies-G pseudotyped CAV-2 vectors could be used to safely target peripheral neurones for retrograde transport and transgene expression.

The promoter used to express the transgene can affect transduction efficiency. Generally a cytomegalovirus (CMV) promoter is used due to their strong transcriptional ability, but transduction could be improved by using a neuronal promoter for the transgene, restricting expression to specific subpopulations. Expression of VSV-G pseudotyped lentiviral vectors was restricted to certain types of neurones depending on the promoter used (Delzor et al., 2012). Hippocampal injections of the lentivirus with Dlx5/6 promoter transduced neurones with GFP reporter expressed at very high levels but only in a very small subset of cells.

There is a lot of scope for vectors to be re-targeted via pseudotyping, or to increase their retrograde transport and transduction efficiency. By implementing these ideas with viruses tested in this chapter it may be possible to transduce neurones after peripheral application.

6.4.4 Wheat-germ agglutinin could be used to target neurones from the periphery

AAV vectors were utilised to target peripheral neurones for central transgene expression of WGA-Cre, a protein with the ability to cross synapses and take cargo with it (Broadwell and Balin, 1985). Instead of using a virus, WGA could be utilised alone to deliver cargo to neurones, either to trace networks or deliver therapeutics. Intrapleural injection of WGA-Alexa 488 labelled the phrenic nerve and intercostal motor nuclei. The lectin was then trans-synaptically transported to the rostral ventral respiratory group (rVRG) containing the neurones responsible for the descending drive to phrenic neurones during inspiration, as well as to select cells of the nucleus ambiguus (Goshgarian and Buttry, 2014; Buttry and Goshgarian, 2015).

One downside to using WGA alone is the lack of selectivity when compared with WGA-Cre. Viruses expressing WGA-Cre can express transgenes only in neurones with floxed genes, thus limiting expression to specific cell types or to a specific area. However if widespread neuronal delivery is required the lectin would prove useful. WGA is a good candidate vehicle for delivery of other proteins trans-synaptically from the periphery, but its structural complexity means high yields of recombinant protein cannot be made in bacterial expression systems. Recently high-level expression and purification of WGA was achieved using a baculovirus expression system (Urtasun N, 2015). It may be possible to use this system to make fusion proteins; otherwise chemical conjugation would be required.

Conclusion

The efficient delivery and long-term expression of therapeutic genes in spinal motor neurones after peripheral delivery opens up the possibility for the treatment of neurodegenerative diseases. This is challenging as viruses must be neurotropic, infect at the terminals, retrogradely transport and express the transgene to sufficient levels within the neurones. The viruses tested in this study could be pseudotyped to better target them to neurones, and more titres tested to achieve improved transduction rates.

Chapter 7
General Discussion

7.1 Summary

Techniques to circumvent the BBB are highly desired, both as experimental tools in neuroscience and as therapeutics for neurodegenerative diseases; bacterial toxins and viruses have shown promising results as vehicles capable of this task. There were two main aims of this study. The first was to assess the ability of bacterial toxins and virally delivered sugar-binding proteins to enter neurones. The second was to develop these vehicles for neuronal tracing and the delivery of other molecules.

The hypotheses and aims as set out in chapter 1 have been addressed in this thesis.

1. LTB will have a similar pattern of labelling in the CNS as CTB after systemic administration in mice.

The labelling patterns of the CNS were studied after systemic injection of both CTB and LTB; in general, motor neurones, autonomic preganglionic neurones and primary afferents of the brainstem and spinal cord could be targeted after peripheral administration. The labelling pattern between the two toxin subunits was indistinguishable. The toxin subunits circumvented the BBB by entering neurones within the peripheral nervous system and retrogradely travelling into the CNS.

2. Bacterial toxins may be utilised to deliver a functional protein to neurones either by direct or systemic administration of engineered fusion proteins.

The labelling patterns following peripheral administration led to the hypothesis that CTB might be utilised to deliver the calcium binding protein parvalbumin to lower motor neurones in an attempt to improve their calcium buffering capacity and prevent excitotoxicity as seen in motor neurone diseases. The fusion protein CTBparv was designed and expressed by *E.coli* and could be detected in the CNS after tongue injection in adult mice, and after IP injection in young mice. Following IP and IM (gastrocnemius) injection of CTBparv in adult mice CTB was detected in neurones of the CNS but parvalbumin was absent in most cells, suggesting it may have been cleaved or degraded.

3. CTB may be engineered for methods of detection other than immunohistochemistry.

Engineered variants of CTB including CTB-azide and AB_5-biotin were able to enter neurones after tongue injection and were detected in the hypoglossal nucleus. Click chemistry was used to detect CTB-azide after injection; it was also used to conjugate quantum dots to CTB for detection via correlated light, fluorescence and electron

microscopy. AB_5-biotin bound to fluorescent streptavidin was delivered via tongue injection, the whole complex was able to enter and retrogradely transport in hypoglossal motor neurones for detection.

4. AAV and CAV-2 vectors may be used to transduce neurones via peripheral delivery.

Administration of CAV-2 vectors expressing DsRed or GFP-TTC proved mostly ineffective at transducing neurones from the periphery in rats and mice. AAV2 expressing mCherry and WGA-Cre did not successfully transduce neurones in rats or mice after peripheral administration. It is hoped that pseudo-typing their viral coats may improve selective targeting and transduction with CAV-2 and AAVs.

The data in these studies suggest that virulence factors can be repurposed as experimental tools for elucidating mechanisms in neuroscience, and as potential therapeutic delivery vehicles.

7.2 Engineered variants of CTB can be detected *in vivo* and are capable of delivering protein cargo

CTB successfully delivered a protein cargo of parvalbumin created as a genetic fusion protein. CTB modified to contain an azide group could be detected by copper-catalysed alkyne-azide cycloaddition, and further modification to attach quantum dots also proved successful as a detection method.

7.2.1 CTB is a potential vehicle for the delivery of therapeutic molecules to neurones

CTBparv was successfully delivered and detected *in vivo* by several injection routes, it was most successful following tongue injections in mice. Direct injections to the gastrocnemius (n=2) failed to deliver parvalbumin to the innervating spinal motor neurones, and only CTB was detected. This would be a preferred route for treatment of ALS as deteriorating muscles could be specifically targeted and a lower dose could be used. Possibly a different protein may be trafficked in a different manner and be able to reach the cell body within the CNS, or if the DNA or RNA for parvalbumin could be delivered this would enhance protein expression and reduce the need for regular injections. The length of time that any delivered protein would remain within cells before degradation is unknown. However if CTBparv did function as a therapeutic for ALS, given that there is only one other treatment, patients would likely take repeated injections if it meant an improved quality of life and slowed disease progression.

Another neurological issue that might be targeted with CTBparv is spinal cord injury (SCI). Following SCI there are a number of secondary mechanisms that lead to progressive degeneration of cells in the spinal cord, one such event is glutamate excitotoxicity (Liu et al., 1991). Glutamate is released from lysed and necrotic cells following SCI, and this leads to an increased activation of glutamate receptors among neurones and glia and thus increased calcium influx via NMDA and AMPA receptors (MacDermott et al., 1986; Agrawal and Fehlings, 1997). Cytosolic calcium concentration is further increased via a feed-forward mechanism of calcium-mediated calcium release from intracellular calcium stores due to NMDA receptor activation (Sattler and Tymianski, 2000). Delivery of a calcium-binding protein such as parvalbumin may act to sequester calcium ions and buffer the intracellular levels to decrease activation of apoptotic mechanisms. Systemic administration of CTBparv could be tested as this has the opportunity to target neurones along the length of the spinal cord; IP injection in adult mice did not successfully deliver the exogenous protein to motor neurones but when translated to humans the delivery pattern could be altered. Of note IP administration requires a high dose and would only target neurones with axons in the periphery, as such interneurones and glial cells would not be targeted. CTBparv could be delivered centrally via intrathecal injection to target all neurones at the injury site and prevent the spread of secondary damage. Central delivery may reduce the opportunity of CTB fusion proteins to be cleaved by extracellular proteases as the toxin would be taken up very quickly at the site of administration unlike in systemic routes where it must travel before reaching neurones to be endocytosed.

Tongue injection of CTBparv was by far the most successful route of administration with parvalbumin detected in hypoglossal neurones after 1 day and up to the maximum measured 13 days. Therefore CTB could be used to target disorders involving the hypoglossal nucleus such as obstructive sleep apnea (Remmers et al., 1978; Horner, 2012). Obstructive sleep apnea is a common breathing disorder that affects approximately 2-4% of the worldwide population (West et al., 2009); the disorder is characterised by repeated episodes of upper airway collapse. Hypoglossal motor neurones innervate the tongue muscles and exert a critical role in maintaining airway patency (Horner, 2012). Inactivity of the hypoglossal nucleus decreases pharyngeal muscle tone, increases airway resistance and induces the closure of the upper airway (Horner, 2007). Patients with obstructive sleep apnea have closure of the upper airway during sleep as the excitability of hypoglossal motor neurones is insufficient to keep it open. The most common treatment strategy is continuous positive airway pressure but this has poor patient compliance due to discomfort (Weaver and Grunstein, 2008). CTB might be used to target an agent to hypoglossal motor neurones to increase their

activity during sleep. *In vivo* studies have shown that histamine can increase hypoglossal nucleus activity and modulate genioglossus muscle activity (Bastedo et al., 2009; Neuzeret et al., 2009). Histamine causes depolarisation of hypoglossal motor neurones via activation of phospholipase C (PLC) (Liu et al., 2016). Histamine binds to the metabotropic receptor H_1R, triggering $G_{q/11}$ and activating the second messenger pathway to release calcium via inositol-1,4,5-trisphosphate production (Haas et al., 2008). Targeting this intracellular signalling pathway with a CTB fusion protein may provide a novel therapeutic avenue for obstructive sleep apnea. While tongue injections would be uncomfortable a numbing agent could be used before administration, topical administration might also be utilised if enough motor neurones can be accessed by this route.

CTB fusion proteins have been produced in plant material for oral delivery for use as adjuvants (Stratmann, 2015) and to deliver exogenous proteins (Limaye et al., 2006; Kohli et al., 2014). This presents a route of administration with high patient compliance as there is little pain or discomfort when compared to injections. Delivering therapeutic cargo to the CNS with CTB via this route would be a highly desired treatment strategy. Kohli et al (2014) delivered myelin basic protein to the brain after oral administration of the bioencapsulated fusion protein (CTB-MBP) in mice. The authors suggest MBP was cleaved from CTB and able to enter the bloodstream where it then entered the CNS. Targeting the released protein to its site of action may be difficult as the authors do not suggest a mechanism for this. If CTB were used to deliver a targeted protein or drug into the bloodstream following oral delivery this would be useful. One step further than this would be to transform bacteria that are resident to the gastrointestinal tract microbiome with a plasmid for the production of a CTB fusion protein. By introducing these transformed bacteria to the gut the therapeutic protein could be produced and leaked into the bloodstream or even target cells within the gastrointestinal tract. One caveat in such a system would be control of expression levels, but different promoters could be tested for variation in protein expression and the most appropriate one used for each delivered protein.

CTB has the potential to deliver a wide range of proteins and drugs, and by altering the delivery route different populations of cells might be targeted. As well as treating neurological disorders, any organ could be targeted if CTB can release its cargo into the bloodstream before entering neurones.

7.2.2 Protein conjugation methods that might be utilised with CTB

The scope for proteins that may be delivered with cholera or heat-labile enterotoxins is vast. Fusion proteins may be produced as genetic fusions, as chemical conjugates or

via generation of recombinant proteins with site-specific enzymes to ligate them. CTBparv was produced as a genetic fusion protein, with the DNA sequence built via assembly PCR and ligated into a CTB expressing plasmid (pSAB2.2). This presents the opportunity to make other fusion proteins using the same method providing that the protein of interest (POI) can be produced in a bacterial expression system.

As discussed in chapter 5, CTB-azide might be utilised for site-specific conjugation of proteins containing an alkyne via strain-promoted alkyne-azide cycloaddition (SPAAC). Other site-specific modifications of toxins can be used to conjugate detection molecules such as fluorophores or other proteins for delivery. Sortase-mediated ligation with a depsipeptide substrate can be used for N-terminal modification of proteins (Williamson et al., 2012). Sortase A catalyses the reversible attachment of virulence factors to the cell walls of Gram positive bacteria by C-terminal modification of proteins at an LPXTG recognition sequence (Ton-That et al., 1999), using a depsipeptide as the substrate prevents the reverse reaction. For N-terminal labelling of proteins with sortase A only a single N-terminal glycine is required (Huang et al., 2003). The N-terminal of CTB is close to the GM1 binding site and thus is not an appropriate location for conjugation of molecules as this would likely hinder endocytosis of the protein. AB_5 toxins could be engineered to contain a glycine residue at the N-terminus of the A2 linker region, this would allow essentially for the toxic A1 portion to be replaced by another protein. CTB could be engineered to contain an LPXTG motif at the C-terminus (facing away from the GM1 binding face). Sortase would cleave the motif between the threonine and glycine residues to facilitate the attachment of an exogenously added oligoglycine peptide modified with the functional group of interest, be it a fluorophore, biotin or a protein (Guimaraes et al., 2013).

Attachment of biotin via sortase to any POI could be used to form a complex with AB_5-biotin and streptavidin for targeted delivery to neurones. Using streptavidin as a central connective piece to click on an array of biotinylated proteins forms a versatile tool where any POI that can be biotinylated may be targeted to neurones. By using a fluorescently labelled streptavidin the delivery can be easily monitored.

7.2.3 CTB could be used to deliver RNA and DNA to neurones

Non-viral gene delivery vectors can introduce transgenes encoding therapeutic proteins into target cells with an improved safety profile when compared to their viral counterparts. CTB could be used to deliver RNA to neurones to potentially upregulate expression of a POI, or siRNA could be delivered to knockdown a POI. Systemic delivery of RNA is technically challenging as it is highly susceptible to degradation by ribonucleases (RNases) in the blood. Producing phosphorothiate-containing RNAs is

one way to protect delivered RNA from RNase and improve stability *in vivo* (Ueda et al., 1991). Phosphorothioate antisense oligodeoxynucleotide was efficiently transfected into the nuclei of skeletal muscle without a carrier following IP injection (Takeshima et al., 2005). By conjugating phosphorothioate RNA or DNA to CTB it may be specifically targeted to peripheral neurones. Such a complex would likely be targeted to endosomes or lysosomes and so a cleavable linker region could be introduced to allow the RNA to reach the cytosol. The resulting CTB-phosphorothioate RNA would be resistant to RNase after systemic administration and thus have an increased half-life compared to standard RNA, while retaining its functional capability.

DNA has been delivered with CTB in both undifferentiated and differentiated PC12 cells via polyplexes formed of a conjugate of CTB and poly-D-lysine (K_{100}) along with cDNA (Barrett et al., 2004). Transfection of NGF-differentiated PC12 cells with CTB-K_{100} containing pCMV-DNA_{LacZ} resulted in a 133-fold increase in levels of LacZ expression when compared to untargeted K_{100} polyplexes. The CTB used in this study was not designed to contain a classical nuclear localisation signal, but the authors suggest basic residues within the sequence may facilitate the nuclear localisation of CTB-K_{100} polyplexes for transduction. As yet DNA has not been delivered *in vivo* by CTB, but the polyplexes could be tested for transgene expression following systemic administration.

Another method of transgene delivery to neurones is via neurotropic nanoparticles carrying encapsulated DNA. Polyethylenimine (PEI) nanoparticles have been functionalised with PEGylated TTC to target them to peripheral neurones for retrograde transport and delivery of DNA; this was successful in primary cultured dissociated DRGs where GFP expression was detected after administration (Oliveira et al., 2010). The performance of the nanoparticles *in vivo* was then evaluated for their ability to target neurons after footpad injection in rats (Lopes et al., 2016). They were able to mediate the transfection and protein expression in 56% and 64% of L4 and L5 DRG neurones at 5 days post-injection, respectively. Animals presented moderate swelling in their footpads within the first hours after administration, but 24 hours later they had regained normal appearance and the rats showed normal use of the limb. This suggests neurotropic nanoparticles have a good safety profile footpads were not sensitised nor was there a large inflammatory response. CTB could be conjugated to the nanoparticles in an attempt to spatially limit transgene expression following peripheral administration. Intramuscular injection of CTB-coated nanoparticles could deliver DNA to motor neurones or intravenous administration may target motor neurones, autonomic preganglionic and primary afferents as CTB alone does. After

addition of polyethylene glycol (PEG) to CTB on the non-GM1 binding face the methods of Oliveira et al. (2010) could be followed to create the nanoparticle.

7.2.4 CTB-azide is a versatile tool for neuronal tracing and delivery

In this study CTB-azide has been used as a neuronal tracer detectable via CuAAC and modification of CTB-azide via SPAAC allowed for the creation of CTB-QD. CTB-azide could just as easily be utilised for the production of fluorophore or biotin tagged CTB via click chemistry and there is also the opportunity to 'click on' other alkyne-containing proteins.

Recently click chemistry has been utilised for the correlated light, fluorescence and EM imaging of metabolically tagged non-protein biomolecules (Ngo et al., 2016). Azide-functionalised dyes that are capable of photo-oxidising DAB were metabolically tagged to biomolecules in fixed cells. This meant that dye-labelled biomolecules could be visualised by fluorescence microscopy, and following reaction with DAB the precipitate could be viewed via EM. To visualise DNA, cells were incubated with the alkyne-containing thymidine analogue EdU that is incorporated into DNA during replication (Salic and Mitchison, 2008). To visualise newly synthesised RNA, cells were incubated with 5-ethynyl-uridine, an alkyne-containing uridine analogue that is selectively incorporated into RNA (Jao and Salic, 2008). CTB-azide could be used in a similar way but with alkyne-functionalised dyes used to detect it, this would allow for tracing of neurones and detection at EM for assessment of the types of neurones labelled. CTB-QD made via CTB-azide can be used as a tracer for detection via correlated light, fluorescence and electron microscopy. Quantum dots are visible via confocal microscopy and following silver intensification may be viewed via light and EM without the need for membrane permeabilisation. This means that ultrastructure is maintained when compared to CTB detection methods where membrane permeabilisation agents such as Triton X-100 are required.

7.3 Neurotropic viral vectors for transduction of neurones from the periphery

Techniques to target neurones via peripheral administration are highly desired; they present an easier mode of drug delivery in the treatment of neurodegenerative disorders when compared to central administration which is far more invasive.

7.3.1 Viruses could be retargeted with CTB to target delivery to neurone subpopulations

One method of retargeting viruses is to conjugate antibody fragments against viral knob proteins to a ligand such that the virus particle may be coated. Adenovirus serotype 5 (Ad5) was directed to platelet-derived growth factor (PDGF) receptor expressing cells; a single chain antibody fragment raised against the adenoviral knob protein was attached to a PDGF peptide sequence that targets the receptor as a genetic fusion protein produced in a bacterial expression system (Schoemaker et al., 2008). When the Ad5 and antibody fusion protein were mixed, the virus was coated with PDGF receptor binding peptide. Adenoviral gene transfer was enhanced in 3T3 fibroblasts and primary activated rat stellate cells, and reduced in primary rat hepatocytes. In chronic liver damage hepatic activated stellate cells are crucial to disease progression and improving targeting to them and reducing tropism to hepatocytes opens up new possibilities for the treatment of liver fibrosis. The retargeting of viruses via fusion proteins with viral coat antibodies might be utilised with CTB to better target them to neurones.

CAV-2 and AAVs were not successful in transducing neurones via IM or direct nerve and ganglia injections. Bringing together data from each chapter, viruses could be better targeted to peripheral neurones by conjugating CTB to their viral coat. CTB targets motor neurones, autonomic preganglionic neurones and primary afferents after systemic injection, and targets innervating motor neurones as well as afferent fibres following IM injection. CTB can be engineered to deliver cargo to neurones as shown with CTBparv. CTB-azide may be modified via click chemistry to add the Fab fragment of an antibody raised against a viral coat protein (Figure 7.1A). Mixing this complex with the virus should then coat the virus surface with CTB (Figure 7.1B). Application of the recombinant virus is hypothesised to enter neurones after peripheral administration and retrogradely transport to the cell body within the CNS, here the virus can uncoat and transduce. Initial proof-of-principle studies should look to deliver a reporter molecule such as GFP. Eventually this method might be used to deliver parvalbumin to motor neurones. Expression of the exogenous protein via viral-mediated delivery may be longer lasting than introduction of protein itself as a fusion, if so this would mean that repeated administration could be reduced.

By coating viruses that are already neurotropic transduction rates may be increased since the vectors can already be expressed in central neurones and would likely transduce peripheral neurones if they could gain entry and retrogradely transport. CTB could be used to retarget AAVs, CAV-2, herpes simplex virus 1 and lentiviruses to give

a wide range of transgene carrying capacity dependent on the material to be delivered. Coating the virus may also reduce immunogenicity associated with viral gene therapy as the virus should be endocytosed quickly and viral coat proteins may be harder to recognise by the immune system since CTB may hinder detection.

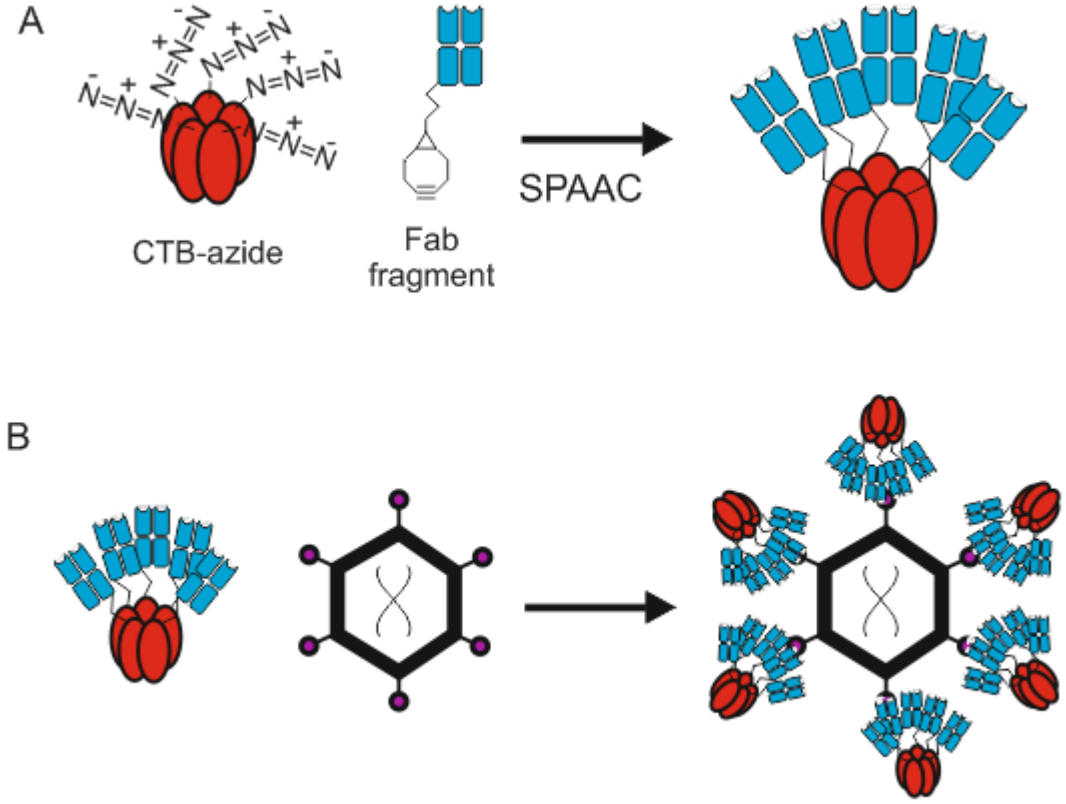

Figure 7.1 Retargeting viruses with CTB

A) CTB-azide can be reacted with an alkyne containing Fab fragment of an antibody raised against a viral coat protein via strain-promoted azide-alkyne cycloaddition (SPAAC). B) The resulting complex can be mixed with AAV and the Fab binds to the viral coat protein, covering the virus with CTB.

7.4 Crossing the blood-brain barrier to target neurones

The BBB serves to protect the CNS by preventing the entrance of unwanted particles. It is composed of endothelial cells that allow the passive transfer of small, lipophilic molecules between the blood and brain parenchyma but are impermeable to larger, more hydrophobic molecules. For this reason many therapeutic agents are poorly delivered to the CNS and ways to improve entry are highly desired.

7.4.1 Hyperosmolar agents

Hyperosmolar agents increase the permeability of the BBB by temporarily increasing osmotic pressure in the blood; this creates space between the tight junctions between the endothelial cells. By loosening the tight junctions, drugs that normally wouldn't fit through can pass into the CSF after IV administration. One such agent is the sugar alcohol mannitol which acts to reversibly disrupt the BBB and allow entrance of foreign molecules. IV injection via the internal carotid artery of mannitol 5 minutes before or after administration of the dye Evans blue was found to give optimal entrance of the marker to the CNS (Cosolo et al., 1989). Transgene delivery to the CNS was increased ten-fold when SV40 viral vectors were administered intravenously 20 minutes after IP injection of mannitol in mice (Louboutin et al., 2010). The majority of transgene expressing cells were neurones, occasional microglia were detected and no astrocytes were transduced. Transgene expression was widely distributed in the cortex of mice that received mannitol, with immunopositive cells detected in the cingulate, piriform, motor, somatosensory and visual cortices as well as in along the length of the spinal cord in both dorsal and ventral horns.

Agents could be targeted to central neurones using CTB, either as fusion proteins or as retargeted viral vectors. This would allow for the targeting of peripheral and central neurones simultaneously following systemic delivery with mannitol, and should limit glial targeting. Such a therapy would be useful in the treatment of motor neurone diseases where both upper and lower motor neurones are affected; usually the upper motor neurones are protected by the BBB so mannitol could provide access. CTB is hypothesised to target the cargo to neurones rather than glial cells once in the CNS.

7.4.2 Microbubbles

Microbubbles along with focused ultrasound to target their delivery have been used to facilitate transport of cargo across the BBB. Microbubbles are formed of lipid or polymer shells, are under 10 μm, and contain an inert gas core. Ultrasound delivery of the biologically inert microbubbles is based on the principle that those within the target volume become 'acoustically activated' by acoustic cavitation (Choi et al., 2011). This

causes the microbubbles to expand and contract with acoustic pressure rarefaction and compression over several cycles; direct interaction with microvessel walls allows for transient opening of tight junctions (Caskey et al., 2007). Repeated opening of the BBB in rhesus macaques was found to be safe and efficacious as behaviour was not altered and no tissue damage was detected; this suggests microbubbles could be used as a non-invasive targeted drug delivery method (McDannold et al., 2012). Scanning ultrasound has also been used with microbubbles to target the whole CNS where it was found to reduce amyloid plaque burden in an AD mouse model (Leinenga and Gotz, 2015). The treatment was found to induce microglial activation which was able to clear plaques and improve cognition in mice. Short hairpin RNA encapsulated within microbubbles was delivered to cultured ovarian cancer cells to inhibit survivin gene expression (Zhang et al., 2015). The expression of survivin mRNA was increased, proliferation rates were reduced and apoptosis increased suggesting delivery was successful. Liposomes containing the reporter molecule indocyanine green were attached to the surface of microbubbles and delivered via IV injection in mice. This doubled indocyanine green deposition when compared to co-delivery of microbubbles and liposomes that were not attached (Cool et al., 2013).

Using focused ultrasound with microbubbles, unlike mannitol, means that the BBB can be opened only in the target area such that therapeutic molecules can be directed to their site of action and the entrance to non-specific sites is reduced. It might be used to open the BBB around the motor cortex to target upper motor neurones with CTB carrying therapeutics. Since CTB enters neurones rapidly it would need to be delivered intravenously close to the target and the ultrasound activation co-ordinated to ensure maximum delivery to targeted neurones. There is also scope to coat microbubbles that encapsulate a drug or vector with CTB to target them to neurones, where sonication would then release the contents into the cells. CTB-coated liposomes might be conjugated to microbubbles for increased directed delivery of cargo as evidenced by Cool et al. (2013).

7.4.3 Transferrin receptor-mediated transcytosis

The transferrin receptor (TfR) mediates receptor-mediated transcytosis of transferrin-bound iron across endothelial cells of the BBB (Pardridge et al., 1987). It has been shown that modulating the affinity of anti-TfR antibodies or using a peptide as a transferrin receptor ligand can improve the delivery of exogenous molecules across the BBB (Staquicini et al., 2011; Yu et al., 2011). Anti-TfR antibodies that bind with high affinity remain associated with the BBB, whereas low affinity variants are released from endothelial cells of the BBB to enter the CNS (Yu et al., 2011). This led to the creation

of a bi-specific antibody, in which one arm contained a low affinity variant of anti-TfR and the other carried a Fab fragment that binds with high affinity to β-secretase (BACE1), the enzyme required for processing amyloid precursor protein into Aβ. After a single systemic dose the Aβ plaque burden in AD mouse brains was reduced. Conjugating a single chain Fab fragment of a monoclonal anti-TfR antibody to the C-terminal of an anti-Aβ monoclonal antibody was tested for its ability to deliver the exogenous antibody across the BBB (Niewoehner et al., 2014). This led to enhanced *in vivo* potency of the antibody and increased plaque reduction when compared to the monoclonal anti-Aβ alone, this suggests that TfR binding leads to increased brain penetration.

If the single chain Fab fragment of monoclonal anti-TfR was conjugated to a CTB fusion protein, this could take the complex across the BBB and target it to neuronal cells. It might also be possible to create an aptamer capable of binding the transferrin receptor; this short sequence would be less likely to hinder the transport of CTB. It would be interesting to compare the intracellular transport of a TfR-binding CTB complex; CTB remains within cells after endocytosis while low affinity TfR-binding molecules undergo trancytosis and release. It is possible that after systemic delivery such a complex could target peripheral neurones where CTB binds and initiates endocytosis, but also to target cargo past the BBB and into the CSF via TfR binding. This could allow for targeting of both the PNS and CNS and would be a highly desirable therapeutic vehicle.

7.5 Conclusions

These studies confirm the use of modified CTB as both a neuronal tracer and a delivery vehicle, as well as the potential use of LTB as well since it also targets neurones. With modified toxin subunits such as CTB-biotin and CTB-azide it is possible that a protein toolbox could be created with ease in which a POI is simply ‘clicked’ on for delivery. While CAV-2 and AAV vectors failed to transduce neurones from the periphery future studies should look to retarget them for retrograde transport in neurones using bacterial toxin subunits. This thesis validates the use of bacterial toxin subunits for future clinically relevant studies, as well as for use as experimental tools in neuroscience.

Chapter 8
Appendix

8.1 AB_5parv oligonucleotide sequences

Building the DNA sequence for an N-terminal fusion protein of CTA2 and parvalbumin was attempted via assembly PCR. The sequence would then be ligated into pSAB2.1 after cutting with NdeI and XhoI such that an AB_5 fusion would be produced.

Nomenclature	Sequence (5' – 3′)
PVCTA FT	ATTTCACATATGGGATCC
PVCTA-1 (with NdeI)	ATTTCACATATGGGATCCGAAAACCTGTACTTTCAGGGTGGCGGTATGTCG
PVCTA-2	CCACCGCCTTCTTGATGTCCTCAGCGTTCAGCAAGTCTGTGATCGACATACCGCCACC
PVCTA-3	ATCAAGAAGGCGGTGGGAGCCTTTAGCGCTACCGACTCCTTCGACCACAAAAAGTTCTTC
PVCTA-4	TCTTCACATCATCCGCACTCTTTTTCTTCAGGCCGACCATTTGGAAGAACTTTTTGTGGTC
PVCTA-5	TGCGGATGATGTGAAGAAGGTGTTTCACATGCTGGACAAGGACAAAAGTGGCTTCATCGA
PVCTA-6	TCTGGGGAGAAGCCTTTTAGGATGAATCCCAGCTCATCCTCCTCGATGAAGCCACTTTTG
PVCTA-7	AAGGCTTCTCCCCAGATGCCAGAGACCTGTCTGCTAAAGAAACCAAGATGCTGATGGCTG
PVCTA-8	AATTCGTCAACCCCAATTTTGCCGTCCCCATCTTTGTCTCCAGCAGCCATCAGCATCTTG
PVCTA-9	AATTGGGGTTGACGAATTCTCCACTCTGGTGGCTGAAAGCGGAGGTGGCGATGAAAAAACC
PVCTA-10	ACTTTAGATTGGTATTCGTCAAGGAATTTTACACCATGACTTTGGGTTTTTTCATCGCCAC
PVCTA-11	ACGAATACCAATCTAAAGTTAAAAGACAAATATTTTCAGGCTATCAATCTGATATTGATACA
PVCTA-12 (with XhoI)	ATTCACCTCGAGGTCATAATTCATCCTTAATTCTATTATGTGTATCAATATCAGATTGAT
PVCTA-RT	GAATTCACCTCGAGGTC

Table 8.1 N-terminal CTA2-parvalbumin fusion protein oligonucleotide sequences and primers, restriction enzyme sites highlighted

8.2 Plasmids

Maps of plasmids used in the synthesis of AB_5parv and CTBparv created using SnapGene. The genes encoding the proteins CTB, MBP and CTA2 are highlighted in red, blue and green respectively in the full sequences.

8.2.1 pSAB2.1

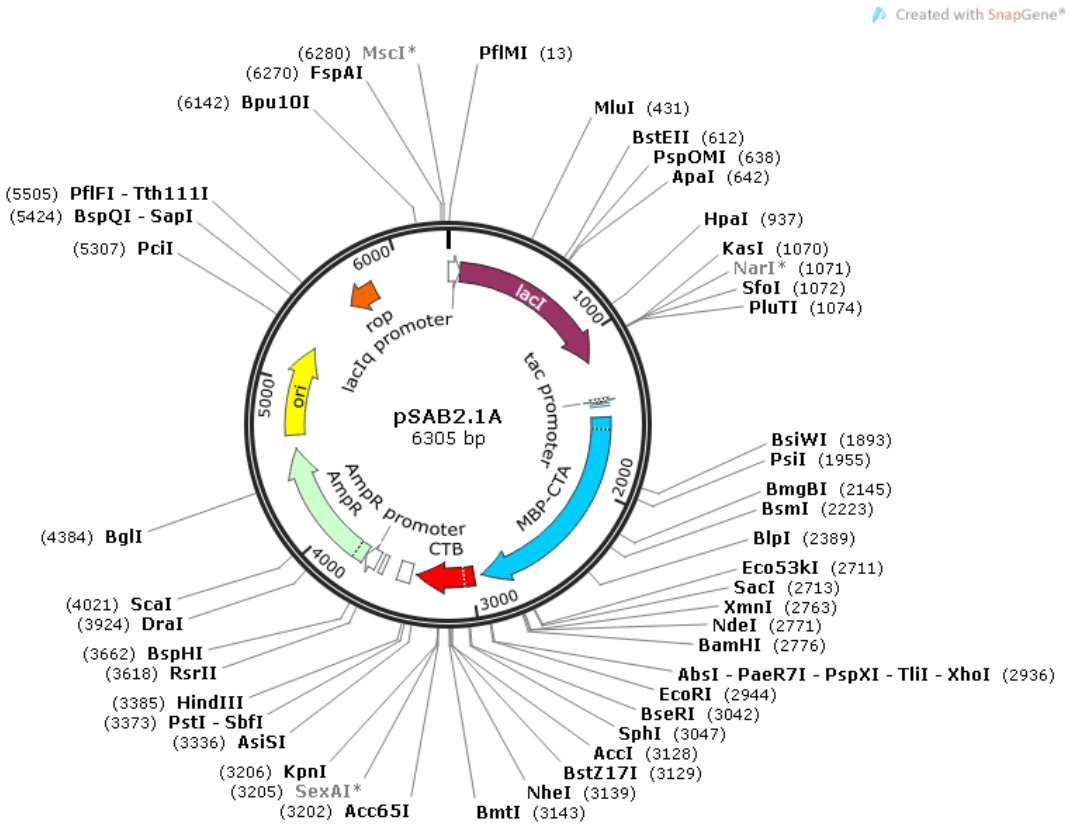

Figure 8.1 Plasmid map for pSAB2.1

The pSAB2.1 plasmid expresses the MBP-CTA2 gene fusion and CTB from a single polycistronic mRNA, with the LTIIB efficient periplasmic targeting leader sequence. It is derived from pMAL-p5X obtained from Genscript and was prepared by Dr James Ross.

Full sequence:

CCGACACCATCGAATGGTGCAAAACCTTTCGCGGTATGGCATGATAGCGCCCGG
AAGAGAGTCAATTCAGGGTGGTGAATGTGAAACCAGTAACGTTATACGATGTCGC
AGAGTATGCCGGTGTCTCTTATCAGACCGTTTCCCGCGTGGTGAACCAGGCCAGC
CACGTTTCTGCGAAAACGCGGGAAAAAGTGGAAGCGGCGATGGCGGAGCTGAAT
TACATTCCCAACCGCGTGGCACAACAACTGGCGGGCAAACAGTCGTTGCTGATTG
GCGTTGCCACCTCCAGTCTGGCCCTGCACGCGCCGTCGCAAATTGTCGCGGCGA
TTAAATCTCGCGCCGATCAACTGGGTGCCAGCGTGGTGGTGTCGATGGTAGAAC
GAAGCGGCGTCGAAGCCTGTAAAGCGGCGGTGCACAATCTTCTCGCGCAACGCG
TCAGTGGGCTGATCATTAACTATCCGCTGGATGACCAGGATGCCATTGCTGTGGA
AGCTGCCTGCACTAATGTTCCGGCGTTATTTCTTGATGTCTCTGACCAGACACCCA
TCAACAGTATTATTTTCTCCCATGAAGACGGTACGCGACTGGGCGTGGAGCATCT
GGTCGCATTGGGTCACCAGCAAATCGCGCTGTTAGCGGGCCCATTAAGTTCTGTC
TCGGCGCGTCTGCGTCTGGCTGGCTGGCATAAATATCTCACTCGCAATCAAATTC
AGCCGATAGCGGAACGGGAAGGCGACTGGAGTGCCATGTCCGGTTTTCAACAAA
CCATGCAAATGCTGAATGAGGGCATCGTTCCCACTGCGATGCTGGTTGCCAACGA
TCAGATGGCGCTGGGCGCAATGCGCGCCATTACCGAGTCCGGGCTGCGCGTTG
GTGCGGATATTTCGGTAGTGGGATACGACGATACCGAAGACAGCTCATGTTATAT
CCCGCCGTTAACCACCATCAAACAGGATTTTCGCCTGCTGGGGCAAACCAGCGTG
GACCGCTTGCTGCAACTCTCTCAGGGCCAGGCGGTGAAGGGCAATCAGCTGTTG
CCCGTCTCACTGGTGAAAAGAAAAACCACCCTGGCGCCCAATACGCAAACCGCCT
CTCCCCGCGCGTTGGCCGATTCATTAATGCAGCTGGCACGACAGGTTTCCCGACT
GGAAAGCGGGCAGTGAGCGCAACGCAATTAATGTAAGTTAGCTCACTCATTAGGC
ACAATTCTCATGTTTGACAGCTTATCATCGACTGCACGGTGCACCAATGCTTCTGG
CGTCAGGCAGCCATCGGAAGCTGTGGTATGGCTGTGCAGGTCGTAAATCACTGC
ATAATTCGTGTCGCTCAAGGCGCACTCCCGTTCTGGATAATGTTTTTTGCGCCGAC
ATCATAACGGTTCTGGCAAATATTCTGAAATGAGCTGTTGACAATTAATCATCGGC
TCGTATAATGTGTGGAATTGTGAGCGGATAACAATTTCACACAGGAAACAGCCAGT
CCGTTTAGGTGTTTTCACGAGCAATTGACCAACAAGGACCATAGATTATGAAAATA
AAAACAGGTGCACGCATCCTCGCATTATCCGCATTAACGACGATGATGTTTTCCG
CCTCGGCTCTCGCCAAAATCGAAGAAGGTAAACTGGTAATCTGGATTAACGGCGA
TAAAGGCTATAACGGTCTCGCTGAAGTCGGTAAGAAATTCGAGAAAGATACCGGA
ATTAAAGTCACCGTTGAGCATCCGGATAAACTGGAAGAGAAATTCCCACAGGTTG
CGGCAACTGGCGATGGCCCTGACATTATCTTCTGGGCACACGACCGCTTTGGTG
GCTACGCTCAATCTGGCCTGTTGGCTGAAATCACCCCGGACAAAGCGTTCCAGGA
CAAGCTGTATCCGTTTACCTGGGATGCCGTACGTTACAACGGCAAGCTGATTGCT
TACCCGATCGCTGTTGAAGCGTTATCGCTGATTTATAACAAAGATCTGCTGCCGAA

CCCGCCAAAAACCTGGGAAGAGATCCCGGCGCTGGATAAAGAACTGAAAGCGAA
AGGTAAGAGCGCGCTGATGTTCAACCTGCAAGAACCGTACTTCACCTGGCCGCTG
ATTGCTGCTGACGGGGGTTATGCGTTCAAGTATGAAAACGGCAAGTACGACATTA
AAGACGTGGGCGTGGATAACGCTGGCGCGAAAGCGGGTCTGACCTTCCTGGTTG
ACCTGATTAAAAACAAACACATGAATGCAGACACCGATTACTCCATCGCAGAAGCT
GCCTTTAATAAAGGCGAAACAGCGATGACCATCAACGGCCCGTGGGCATGGTCC
AACATCGACACCAGCAAAGTGAATTATGGTGTAACGGTACTGCCGACCTTCAAGG
GTCAACCATCCAAACCGTTCGTTGGCGTGCTGAGCGCAGGTATTAACGCCGCCA
GTCCGAACAAAGAGCTGGCAAAAGAGTTCCTCGAAAACTATCTGCTGACTGATGA
AGGTCTGGAAGCGGTTAATAAAGACAAACCGCTGGGTGCCGTAGCGCTGAAGTC
TTACGAGGAAGAGTTGGTGAAAGATCCGCGTATTGCCGCCACTATGGAAAACGCC
CAGAAAGGTGAAATCATGCCGAACATCCCGCAGATGTCCGCTTTCTGGTATGCCG
TGCGTACTGCGGTGATCAACGCCGCCAGCGGTCGTCAGACTGTCGATGAAGCCC
TGAAAGACGCGCAGACTAATTCGAGCTCGAACAACAACAACAATAACAATAACAAC
AACCTCGGGATCGAGGGAAGGATTTCACATATGgatccgaaaacctgtactttcagggtggcgg
tgatgaaaaaacccaaagtcatggtgtaaaattccttgacgaataccaatctaaagttaaaagacaaatattttcaggcta
tcaatctgatattgatacacataatagaattaaggatgaattatgaCCTCGAGGTGAATTCACGAGCAATT
GACCAACAAGGACCATAGATTATGAGCTTTAAGAAAATTATCAAGGCATTTGTTAT
CATGGCTGCTTTGGTATCTGTTCAGGCGCATGCAGCTCCTCAAAATATTACTGATT
TGTGCGCAGAATACCACAACACACAAATATATACGCTAAATGATAAGATCTTTTCG
TATACAGAATCGCTAGCGGGAAAAAGAGAGATGGCTATCATTACTTTTAAGAATGG
TGCAATTTTTCAAGTAGAGGTACCAGGTAGTCAACATATAGATTCACAAAAAAAAG
CGATTGAAAGGATGAAGGATACCCTGAGGATTGCATATCTTACTGAAGCTAAAGTC
GAAAAGTTATGTGTATGGAATAATAAAACGCCTCATGCGATCGCCGCAATTAGTAT
GGCAAACTAAGTTTTCCCTGCAGGTAATTAAATAAGCTTCAAATAAAACGAAAGGC
TCAGTCGAAAGACTGGGCCTTTCGTTTTATCTGTTGTTTGTCGGTGAACGCTCTCC
TGAGTAGGACAAATCCGCCGGGAGCGGATTTGAACGTTGCGAAGCAACGGCCCG
GAGGGTGGCGGGCAGGACGCCCGCCATAAACTGCCAGGCATCAAATTAAGCAGA
AGGCCATCCTGACGGATGGCCTTTTTGCGTTTCTACAAACTCTTTCGGTCCGTTGT
TTATTTTTCTAAATACATTCAAATATGTATCCGCTCATGAGACAATAACCCTGATAA
ATGCTTCAATAATATTGAAAAAGGAAGAGTATGAGTATTCAACATTTCCGTGTCGC
CCTTATTCCCTTTTTTGCGGCATTTTGCCTTCCTGTTTTTGCTCACCCAGAAACGCT
GGTGAAAGTAAAAGATGCTGAAGATCAGTTGGGTGCACGAGTGGGTTACATCGAA
CTGGATCTCAACAGCGGTAAGATCCTTGAGAGTTTTCGCCCCGAAGAACGTTTCC
CAATGATGAGCACTTTTAAAGTTCTGCTATGTGGCGCGGTATTATCCCGTGTTGAC
GCCGGGCAAGAGCAACTCGGTCGCCGCATACACTATTCTCAGAATGACTTGGTTG
AGTACTCACCAGTCACAGAAAAGCATCTTACGGATGGCATGACAGTAAGAGAATT

ATGCAGTGCTGCCATAACCATGAGTGATAACACTGCGGCCAACTTACTTCTGACA
ACGATCGGAGGACCGAAGGAGCTAACCGCTTTTTTGCACAACATGGGGGATCATG
TAACTCGCCTTGATCGTTGGGAACCGGAGCTGAATGAAGCCATACCAAACGACGA
GCGTGACACCACGATGCCTGTAGCAATGGCAACAACGTTGCGCAAACTATTAACT
GGCGAACTACTTACTCTAGCTTCCCGGCAACAATTAATAGACTGGATGGAGGCGG
ATAAAGTTGCAGGACCACTTCTGCGCTCGGCCCTTCCGGCTGGCTGGTTTATTGC
TGATAAATCTGGAGCCGGTGAGCGTGGGTCTCGCGGTATCATTGCAGCACTGGG
GCCAGATGGTAAGCCCTCCCGTATCGTAGTTATCTACACGACGGGGAGTCAGGC
AACTATGGATGAACGAAATAGACAGATCGCTGAGATAGGTGCCTCACTGATTAAG
CATTGGTAACTGTCAGACCAAGTTTACTCATATATACTTTAGATTGATTTCCTTAGG
ACTGAGCGTCAACCCCGTAGAAAAGATCAAAGGATCTTCTTGAGATCCTTTTTTTC
TGCGCGTAATCTGCTGCTTGCAAACAAAAAAACCACCGCTACCAGCGGTGGTTTG
TTTGCCGGATCAAGAGCTACCAACTCTTTTTCCGAAGGTAACTGGCTTCAGCAGA
GCGCAGATACCAAATACTGTCCTTCTAGTGTAGCCGTAGTTAGGCCACCACTTCA
AGAACTCTGTAGCACCGCCTACATACCTCGCTCTGCTAATCCTGTTACCAGTGGC
TGCTGCCAGTGGCGATAAGTCGTGTCTTACCGGGTTGGACTCAAGACGATAGTTA
CCGGATAAGGCGCAGCGGTCGGGCTGAACGGGGGGTTCGTGCACACAGCCCAG
CTTGGAGCGAACGACCTACACCGAACTGAGATACCTACAGCGTGAGCTATGAGAA
AGCGCCACGCTTCCCGAAGGGAGAAAGGCGGACAGGTATCCGGTAAGCGGCAG
GGTCGGAACAGGAGAGCGCACGAGGGAGCTTCCAGGGGGAAACGCCTGGTATC
TTTATAGTCCTGTCGGGTTTCGCCACCTCTGACTTGAGCGTCGATTTTTGTGATGC
TCGTCAGGGGGGCGGAGCCTATGGAAAAACGCCAGCAACGCGGCCTTTTTACGG
TTCCTGGCCTTTTGCTGGCCTTTTGCTCACATGTTCTTTCCTGCGTTATCCCCTGA
TTCTGTGGATAACCGTATTACCGCCTTTGAGTGAGCTGATACCGCTCGCCGCAGC
CGAACGACCGAGCGCAGCGAGTCAGTGAGCGAGGAAGCGGAAGAGCGCCTGAT
GCGGTATTTTCTCCTTACGCATCTGTGCGGTATTTCACACCGCATATAAGGTGCAC
TGTGACTGGGTCATGGCTGCGCCCCGACACCCGCCAACACCCGCTGACGCGCCC
TGACGGGCTTGTCTGCTCCCGGCATCCGCTTACAGACAAGCTGTGACCGTCTCC
GGGAGCTGCATGTGTCAGAGGTTTTCACCGTCATCACCGAAACGCGCGAGGCAG
CTGCGGTAAAGCTCATCAGCGTGGTCGTGCAGCGATTCACAGATGTCTGCCTGTT
CATCCGCGTCCAGCTCGTTGAGTTTCTCCAGAAGCGTTAATGTCTGGCTTCTGATA
AAGCGGGCCATGTTAAGGGCGGTTTTTTCCTGTTTGGTCACTGATGCCTCCGTGT
AAGGGGGATTTCTGTTCATGGGGGTAATGATACCGATGAAACGAGAGAGGATGCT
CACGATACGGGTTACTGATGATGAACATGCCCGGTTACTGGAACGTTGTGAGGGT
AAACAACTGGCGGTATGGATGCGGCGGGACCAGAGAAAAATCACTCAGGGTCAA
TGCCAGCGCTTCGTTAATACAGATGTAGGTGTTCCACAGGGTAGCCAGCAGCATC
CTGCGATGCAGATCCGGAACATAATGGTGCAGGGCGCTGACTTCCGCGTTTCCA

GACTTTACGAAACACGGAAACCGAAGACCATTCATGTTGTTGCTCAGGTCGCAGA
CGTTTTGCAGCAGCAGTCGCTTCACGTTCGCTCGCGTATCGGTGATTCATTCTGC
TAACCAGTAAGGCAACCCCGCCAGCCTAGCCGGGTCCTCAACGACAGGAGCACG
ATCATGCGCACCCGTGGCCAGGACCCAACGCTGCCCGAAATT

8.2.2 pSAB2.2

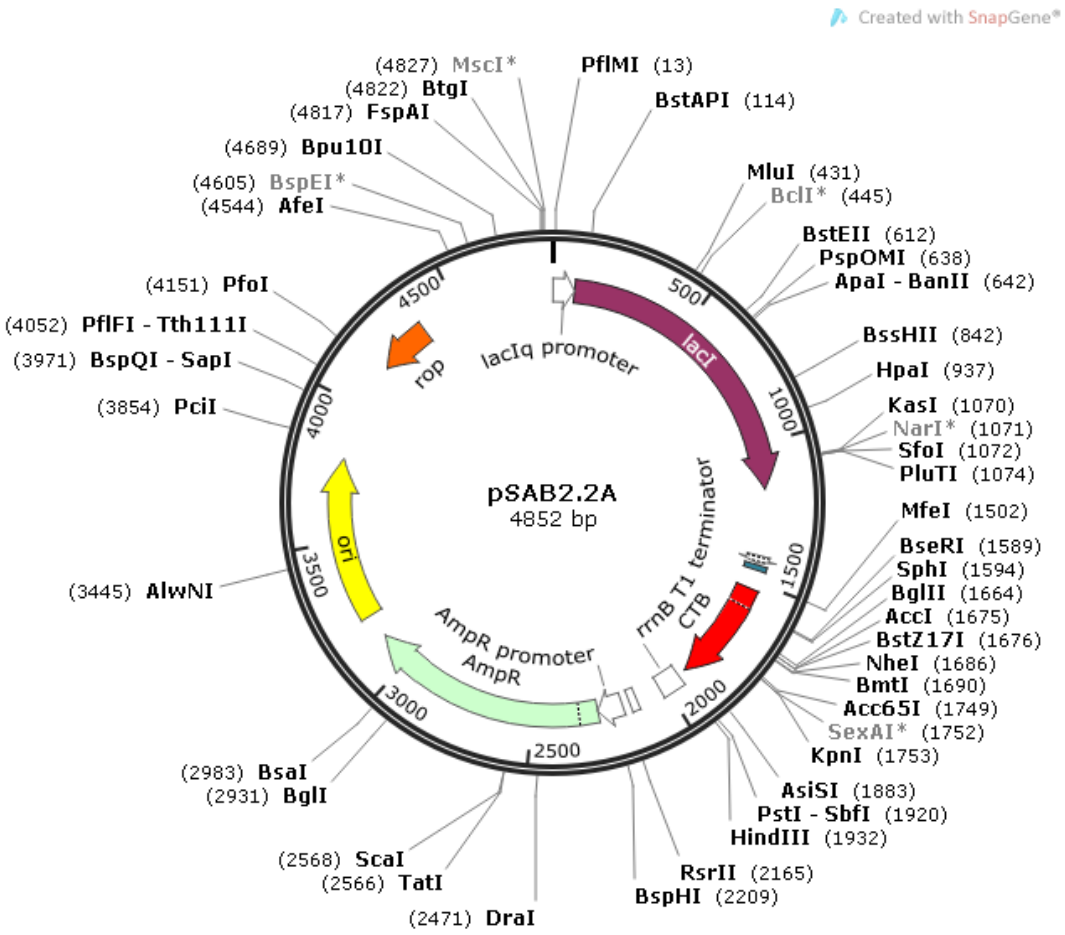

Figure 8.2 Plasmid map for pSAB2.2

The pSAB2.2 plasmid expresses CTB from a single mRNA. It is derived from pMAL-p5X obtained from Genscript. An MBP-CTA2 fusion was introduced along with the gene for CTB, with the LTIIB efficient periplasmic targeting leader sequence. This resulted in plasmid pSAB2.1. The MBP-CTA2 gene was then removed to produce plasmid pSAB2.2 containing only the CTB gene (preparation of the plasmid performed by Dr James Ross).

Full sequence:

CCGACACCATCGAATGGTGCAAAACCTTTCGCGGTATGGCATGATAGCGCCCGG
AAGAGAGTCAATTCAGGGTGGTGAATGTGAAACCAGTAACGTTATACGATGTCGC
AGAGTATGCCGGTGTCTCTTATCAGACCGTTTCCCGCGTGGTGAACCAGGCCAGC
CACGTTTCTGCGAAAACGCGGGAAAAAGTGGAAGCGGCGATGGCGGAGCTGAAT
TACATTCCCAACCGCGTGGCACAACAACTGGCGGGCAAACAGTCGTTGCTGATTG
GCGTTGCCACCTCCAGTCTGGCCCTGCACGCGCCGTCGCAAATTGTCGCGGCGA
TTAAATCTCGCGCCGATCAACTGGGTGCCAGCGTGGTGGTGTCGATGGTAGAAC

GAAGCGGCGTCGAAGCCTGTAAAGCGGCGGTGCACAATCTTCTCGCGCAACGCG
TCAGTGGGCTGATCATTAACTATCCGCTGGATGACCAGGATGCCATTGCTGTGGA
AGCTGCCTGCACTAATGTTCCGGCGTTATTTCTTGATGTCTCTGACCAGACACCCA
TCAACAGTATTATTTTCTCCCATGAAGACGGTACGCGACTGGGCGTGGAGCATCT
GGTCGCATTGGGTCACCAGCAAATCGCGCTGTTAGCGGGCCCATTAAGTTCTGTC
TCGGCGCGTCTGCGTCTGGCTGGCTGGCATAAATATCTCACTCGCAATCAAATTC
AGCCGATAGCGGAACGGGAAGGCGACTGGAGTGCCATGTCCGGTTTTCAACAAA
CCATGCAAATGCTGAATGAGGGCATCGTTCCCACTGCGATGCTGGTTGCCAACGA
TCAGATGGCGCTGGGCGCAATGCGCGCCATTACCGAGTCCGGGCTGCGCGTTG
GTGCGGATATTTCGGTAGTGGGATACGACGATACCGAAGACAGCTCATGTTATAT
CCCGCCGTTAACCACCATCAAACAGGATTTTCGCCTGCTGGGGCAAACCAGCGTG
GACCGCTTGCTGCAACTCTCTCAGGGCCAGGCGGTGAAGGGCAATCAGCTGTTG
CCCGTCTCACTGGTGAAAAGAAAAACCACCCTGGCGCCCAATACGCAAACCGCCT
CTCCCCGCGCGTTGGCCGATTCATTAATGCAGCTGGCACGACAGGTTTCCCGACT
GGAAAGCGGGCAGTGAGCGCAACGCAATTAATGTAAGTTAGCTCACTCATTAGGC
ACAATTCTCATGTTTGACAGCTTATCATCGACTGCACGGTGCACCAATGCTTCTGG
CGTCAGGCAGCCATCGGAAGCTGTGGTATGGCTGTGCAGGTCGTAAATCACTGC
ATAATTCGTGTCGCTCAAGGCGCACTCCCGTTCTGGATAATGTTTTTTGCGCCGAC
ATCATAACGGTTCTGGCAAATATTCTGAAATGAGCTGTTGACAATTAATCATCGGC
TCGTATAATGTGTGGAATTGTGAGCGGATAACAATTTCACACAGGAAACAGCCAGT
CCGTTTAGGTGTTTTCACGAGCAATTGACCAACAAGGACCATAGATTATGAGCTTT
AAGAAAATTATCAAGGCATTTGTTATCATGGCTGCTTTGGTATCTGTTCAGGCGCA
TGCAGCTCCTCAAAATATTACTGATTTGTGCGCAGAATACCACAACACACAAATAT
ATACGCTAAATGATAAGATCTTTTCGTATACAGAATCGCTAGCGGGAAAAAGAGAG
ATGGCTATCATTACTTTTAAGAATGGTGCAATTTTTCAAGTAGAGGTACCAGGTAG
TCAACATATAGATTCACAAAAAAAAGCGATTGAAAGGATGAAGGATACCCTGAGGA
TTGCATATCTTACTGAAGCTAAAGTCGAAAAGTTATGTGTATGGAATAATAAAACG
CCTCATGCGATCGCCGCAATTAGTATGGCAAACTAAGTTTTCCCTGCAGGTAATTA
AATAAGCTTCAAATAAAACGAAAGGCTCAGTCGAAAGACTGGGCCTTTCGTTTTAT
CTGTTGTTTGTCGGTGAACGCTCTCCTGAGTAGGACAAATCCGCCGGGAGCGGAT
TTGAACGTTGCGAAGCAACGGCCCGGAGGGTGGCGGGCAGGACGCCCGCCATA
AACTGCCAGGCATCAAATTAAGCAGAAGGCCATCCTGACGGATGGCCTTTTTGCG
TTTCTACAAACTCTTTCGGTCCGTTGTTTATTTTTCTAAATACATTCAAATATGTATC
CGCTCATGAGACAATAACCCTGATAAATGCTTCAATAATATTGAAAAAGGAAGAGT
ATGAGTATTCAACATTTCCGTGTCGCCCTTATTCCCTTTTTTGCGGCATTTTGCCTT
CCTGTTTTTGCTCACCCAGAAACGCTGGTGAAAGTAAAAGATGCTGAAGATCAGTT
GGGTGCACGAGTGGGTTACATCGAACTGGATCTCAACAGCGGTAAGATCCTTGAG

AGTTTTCGCCCCGAAGAACGTTTCCCAATGATGAGCACTTTTAAAGTTCTGCTATG
TGGCGCGGTATTATCCCGTGTTGACGCCGGGCAAGAGCAACTCGGTCGCCGCAT
ACACTATTCTCAGAATGACTTGGTTGAGTACTCACCAGTCACAGAAAAGCATCTTA
CGGATGGCATGACAGTAAGAGAATTATGCAGTGCTGCCATAACCATGAGTGATAA
CACTGCGGCCAACTTACTTCTGACAACGATCGGAGGACCGAAGGAGCTAACCGC
TTTTTTGCACAACATGGGGGATCATGTAACTCGCCTTGATCGTTGGGAACCGGAG
CTGAATGAAGCCATACCAAACGACGAGCGTGACACCACGATGCCTGTAGCAATGG
CAACAACGTTGCGCAAACTATTAACTGGCGAACTACTTACTCTAGCTTCCCGGCAA
CAATTAATAGACTGGATGGAGGCGGATAAAGTTGCAGGACCACTTCTGCGCTCGG
CCCTTCCGGCTGGCTGGTTTATTGCTGATAAATCTGGAGCCGGTGAGCGTGGGTC
TCGCGGTATCATTGCAGCACTGGGGCCAGATGGTAAGCCCTCCCGTATCGTAGTT
ATCTACACGACGGGGAGTCAGGCAACTATGGATGAACGAAATAGACAGATCGCTG
AGATAGGTGCCTCACTGATTAAGCATTGGTAACTGTCAGACCAAGTTTACTCATAT
ATACTTTAGATTGATTTCCTTAGGACTGAGCGTCAACCCCGTAGAAAAGATCAAAG
GATCTTCTTGAGATCCTTTTTTTCTGCGCGTAATCTGCTGCTTGCAAACAAAAAAAC
CACCGCTACCAGCGGTGGTTTGTTTGCCGGATCAAGAGCTACCAACTCTTTTTCC
GAAGGTAACTGGCTTCAGCAGAGCGCAGATACCAAATACTGTCCTTCTAGTGTAG
CCGTAGTTAGGCCACCACTTCAAGAACTCTGTAGCACCGCCTACATACCTCGCTC
TGCTAATCCTGTTACCAGTGGCTGCTGCCAGTGGCGATAAGTCGTGTCTTACCGG
GTTGGACTCAAGACGATAGTTACCGGATAAGGCGCAGCGGTCGGGCTGAACGGG
GGGTTCGTGCACACAGCCCAGCTTGGAGCGAACGACCTACACCGAACTGAGATA
CCTACAGCGTGAGCTATGAGAAAGCGCCACGCTTCCCGAAGGGAGAAAGGCGGA
CAGGTATCCGGTAAGCGGCAGGGTCGGAACAGGAGAGCGCACGAGGGAGCTTC
CAGGGGGAAACGCCTGGTATCTTTATAGTCCTGTCGGGTTTCGCCACCTCTGACT
TGAGCGTCGATTTTTGTGATGCTCGTCAGGGGGGCGGAGCCTATGGAAAAACGC
CAGCAACGCGGCCTTTTTACGGTTCCTGGCCTTTTGCTGGCCTTTTGCTCACATGT
TCTTTCCTGCGTTATCCCCTGATTCTGTGGATAACCGTATTACCGCCTTTGAGTGA
GCTGATACCGCTCGCCGCAGCCGAACGACCGAGCGCAGCGAGTCAGTGAGCGA
GGAAGCGGAAGAGCGCCTGATGCGGTATTTTCTCCTTACGCATCTGTGCGGTATT
TCACACCGCATATAAGGTGCACTGTGACTGGGTCATGGCTGCGCCCCGACACCC
GCCAACACCCGCTGACGCGCCCTGACGGGCTTGTCTGCTCCCGGCATCCGCTTA
CAGACAAGCTGTGACCGTCTCCGGGAGCTGCATGTGTCAGAGGTTTTCACCGTCA
TCACCGAAACGCGCGAGGCAGCTGCGGTAAAGCTCATCAGCGTGGTCGTGCAGC
GATTCACAGATGTCTGCCTGTTCATCCGCGTCCAGCTCGTTGAGTTTCTCCAGAA
GCGTTAATGTCTGGCTTCTGATAAAGCGGGCCATGTTAAGGGCGGTTTTTTCCTG
TTTGGTCACTGATGCCTCCGTGTAAGGGGGATTTCTGTTCATGGGGGTAATGATA
CCGATGAAACGAGAGAGGATGCTCACGATACGGGTTACTGATGATGAACATGCCC

GGTTACTGGAACGTTGTGAGGGTAAACAACTGGCGGTATGGATGCGGCGGGACC
AGAGAAAAATCACTCAGGGTCAATGCCAGCGCTTCGTTAATACAGATGTAGGTGT
TCCACAGGGTAGCCAGCAGCATCCTGCGATGCAGATCCGGAACATAATGGTGCA
GGGCGCTGACTTCCGCGTTTCCAGACTTTACGAAACACGGAAACCGAAGACCATT
CATGTTGTTGCTCAGGTCGCAGACGTTTTGCAGCAGCAGTCGCTTCACGTTCGCT
CGCGTATCGGTGATTCATTCTGCTAACCAGTAAGGCAACCCCGCCAGCCTAGCCG
GGTCCTCAACGACAGGAGCACGATCATGCGCACCCGTGGCCAGGACCCAACGCT
GCCCGAAATT

8.3 Mass spectrometry

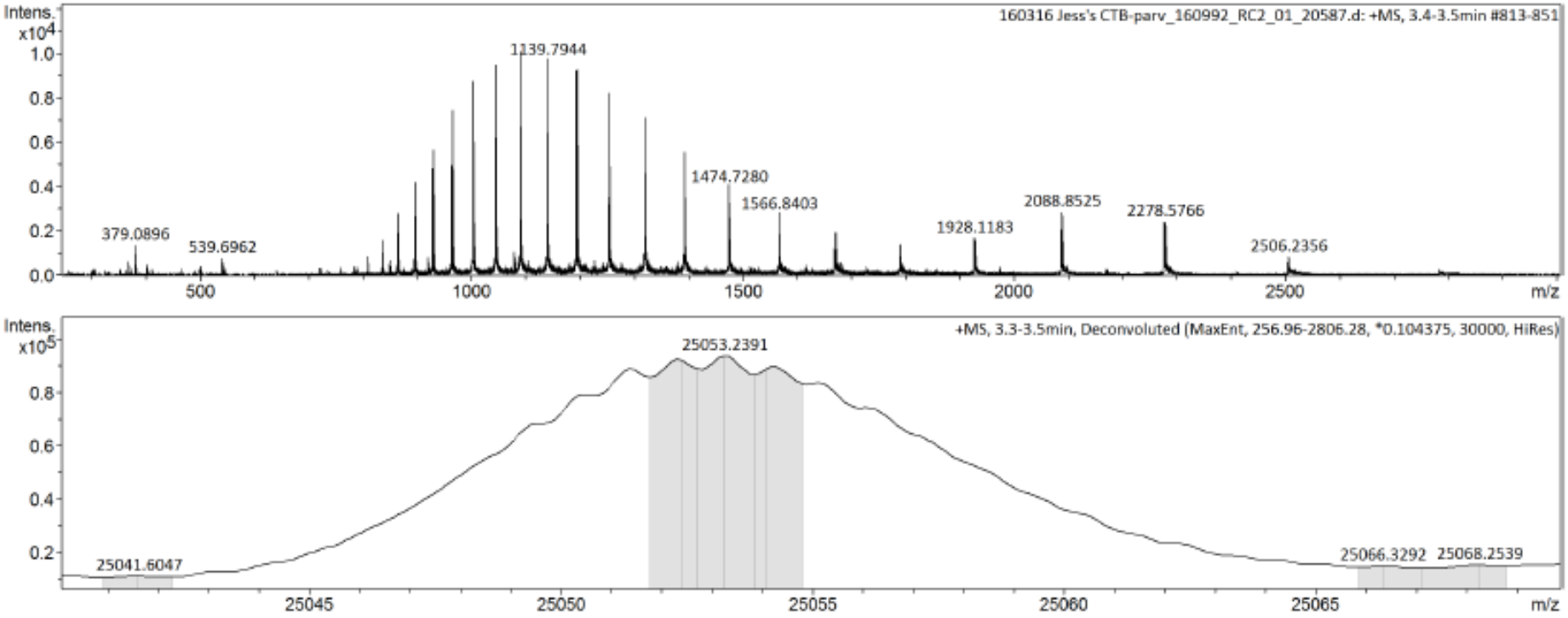

Figure 8.3 Mass spectrometry readout for CTBparv

Mass spectrometry analysis of the purified protein revealed the monomer mass to be 25053.24 Da, as expected by the mass calculated of 25053.29 Da.

References

Agostoni E, Chinnock JE, De Daly MB, Murray JG (1957) Functional and histological studies of the vagus nerve and its branches to the heart, lungs and abdominal viscera in the cat. The Journal of physiology 135:182-205.

Agrawal SK, Fehlings MG (1997) Role of NMDA and non-NMDA ionotropic glutamate receptors in traumatic spinal cord axonal injury. The Journal of neuroscience : the official journal of the Society for Neuroscience 17:1055-1063.

Airaksinen MS, Eilers J, Garaschuk O, Thoenen H, Konnerth A, Meyer M (1997) Ataxia and altered dendritic calcium signaling in mice carrying a targeted null mutation of the calbindin D28k gene. Proceedings of the National Academy of Sciences of the United States of America 94:1488-1493.

Al-Dosari MS, Gao X (2009) Nonviral gene delivery: principle, limitations, and recent progress. The AAPS journal 11:671-681.

Alexianu ME, Ho BK, Mohamed AH, La Bella V, Smith RG, Appel SH (1994) The role of calcium-binding proteins in selective motoneuron vulnerability in amyotrophic lateral sclerosis. Annals of neurology 36:846-858.

Alisky JM, van de Wetering CI, Davidson BL (2002) Widespread dispersal of cholera toxin subunit b to brain and spinal cord neurons following systemic delivery. Experimental neurology 178:139-146.

Aman AT, Fraser S, Merritt EA, Rodigherio C, Kenny M, Ahn M, Hol WG, Williams NA, Lencer WI, Hirst TR (2001) A mutant cholera toxin B subunit that binds GM1-ganglioside but lacks immunomodulatory or toxic activity. Proceedings of the National Academy of Sciences of the United States of America 98:8536-8541.

Andresen MC, Hofmann ME, Fawley JA (2012) The unsilent majority-TRPV1 drives "spontaneous" transmission of unmyelinated primary afferents within cardiorespiratory NTS. American journal of physiology Regulatory, integrative and comparative physiology 303:R1207-1216.

Angelucci A, Clasca F, Sur M (1996) Anterograde axonal tracing with the subunit B of cholera toxin: a highly sensitive immunohistochemical protocol for revealing fine axonal morphology in adult and neonatal brains. Journal of neuroscience methods 65:101-112.

Antonucci F, Rossi C, Gianfranceschi L, Rossetto O, Caleo M (2008) Long-distance retrograde effects of botulinum neurotoxin A. The Journal of neuroscience : the official journal of the Society for Neuroscience 28:3689-3696.

Araye A, Goudet A, Barbier J, Pichard S, Baron B, England P, Perez J, Zinn-Justin S, Chenal A, Gillet D (2016) The Translocation Domain of Botulinum Neurotoxin A Moderates the Propensity of the Catalytic Domain to Interact with Membranes at Acidic pH. PloS one 11:e0153401.

Arbab MA, Wiklund L, Svendgaard NA (1986) Origin and distribution of cerebral vascular innervation from superior cervical, trigeminal and spinal ganglia investigated with retrograde and anterograde WGA-HRP tracing in the rat. Neuroscience 19:695-708.

Ariza L, Gimenez-Llort L, Cubizolle A, Pages G, Garcia-Lareu B, Serratrice N, Cots D, Thwaite R, Chillon M, Kremer EJ, Bosch A (2014) Central nervous system delivery of helper-dependent canine adenovirus corrects neuropathology and behavior in mucopolysaccharidosis type VII mice. Human gene therapy 25:199-211.

Arnold ES, Ling SC, Huelga SC, Lagier-Tourenne C, Polymenidou M, Ditsworth D, Kordasiewicz HB, McAlonis-Downes M, Platoshyn O, Parone PA, Da Cruz S, Clutario KM, Swing D, Tessarollo L, Marsala M, Shaw CE, Yeo GW, Cleveland DW (2013) ALS-linked TDP-43 mutations produce aberrant RNA splicing and adult-onset motor neuron disease without aggregation or loss of nuclear TDP-

43. Proceedings of the National Academy of Sciences of the United States of America 110:E736-745.
Arnon SS, Schechter R, Inglesby TV, Henderson DA, Bartlett JG, Ascher MS, Eitzen E, Fine AD, Hauer J, Layton M, Lillibridge S, Osterholm MT, O'Toole T, Parker G, Perl TM, Russell PK, Swerdlow DL, Tonat K, Working Group on Civilian B (2001) Botulinum toxin as a biological weapon: medical and public health management. Jama 285:1059-1070.
Bade S, Rummel A, Reisinger C, Karnath T, Ahnert-Hilger G, Bigalke H, Binz T (2004) Botulinum neurotoxin type D enables cytosolic delivery of enzymatically active cargo proteins to neurones via unfolded translocation intermediates. Journal of neurochemistry 91:1461-1472.
Barinka F, Druga R (2010) Calretinin expression in the mammalian neocortex: a review. Physiological research / Academia Scientiarum Bohemoslovaca 59:665-677.
Barrett LB, Berry M, Ying WB, Hodgkin MN, Seymour LW, Gonzalez AM, Read ML, Baird A, Logan A (2004) CTb targeted non-viral cDNA delivery enhances transgene expression in neurons. The journal of gene medicine 6:429-438.
Basso M, Massignan T, Samengo G, Cheroni C, De Biasi S, Salmona M, Bendotti C, Bonetto V (2006) Insoluble mutant SOD1 is partly oligoubiquitinated in amyotrophic lateral sclerosis mice. The Journal of biological chemistry 281:33325-33335.
Bastedo T, Chan E, Park E, Liu H, Horner RL (2009) Modulation of genioglossus muscle activity across sleep-wake states by histamine at the hypoglossal motor pool. Sleep 32:1313-1324.
Beccia MR, Sauge-Merle S, Lemaire D, Bremond N, Pardoux R, Blangy S, Guilbaud P, Berthomieu C (2015) Thermodynamics of Calcium binding to the Calmodulin N-terminal domain to evaluate site-specific affinity constants and cooperativity. Journal of biological inorganic chemistry : JBIC : a publication of the Society of Biological Inorganic Chemistry 20:905-919.
Beddoe T, Paton AW, Le Nours J, Rossjohn J, Paton JC (2010) Structure, biological functions and applications of the AB5 toxins. Trends in biochemical sciences 35:411-418.
Beers DR, Ho BK, Siklos L, Alexianu ME, Mosier DR, Mohamed AH, Otsuka Y, Kozovska ME, McAlhany RE, Smith RG, Appel SH (2001) Parvalbumin overexpression alters immune-mediated increases in intracellular calcium, and delays disease onset in a transgenic model of familial amyotrophic lateral sclerosis. Journal of neurochemistry 79:499-509.
Bellido T, Huening M, Raval-Pandya M, Manolagas SC, Christakos S (2000) Calbindin-D28k is expressed in osteoblastic cells and suppresses their apoptosis by inhibiting caspase-3 activity. The Journal of biological chemistry 275:26328-26332.
Bendotti C, Marino M, Cheroni C, Fontana E, Crippa V, Poletti A, De Biasi S (2012) Dysfunction of constitutive and inducible ubiquitin-proteasome system in amyotrophic lateral sclerosis: implication for protein aggregation and immune response. Progress in neurobiology 97:101-126.
Benkhelifa-Ziyyat S, Besse A, Roda M, Duque S, Astord S, Carcenac R, Marais T, Barkats M (2013) Intramuscular scAAV9-SMN injection mediates widespread gene delivery to the spinal cord and decreases disease severity in SMA mice. Molecular therapy : the journal of the American Society of Gene Therapy 21:282-290.
Bennett MK, Calakos N, Scheller RH (1992) Syntaxin: a synaptic protein implicated in docking of synaptic vesicles at presynaptic active zones. Science 257:255-259.
Berchtold MW (1989) Parvalbumin genes from human and rat are identical in intron/exon organization and contain highly homologous regulatory elements and coding sequences. Journal of molecular biology 210:417-427.

Bercsenyi K, Schmieg N, Bryson JB, Wallace M, Caccin P, Golding M, Zanotti G, Greensmith L, Nischt R, Schiavo G (2014) Tetanus toxin entry. Nidogens are therapeutic targets for the prevention of tetanus. Science 346:1118-1123.

Berggard T, Szczepankiewicz O, Thulin E, Linse S (2002a) Myo-inositol monophosphatase is an activated target of calbindin D28k. The Journal of biological chemistry 277:41954-41959.

Berggard T, Miron S, Onnerfjord P, Thulin E, Akerfeldt KS, Enghild JJ, Akke M, Linse S (2002b) Calbindin D28k exhibits properties characteristic of a Ca2+ sensor. The Journal of biological chemistry 277:16662-16672.

Bergvall M, Melendy T, Archambault J (2013) The E1 proteins. Virology 445:35-56.

Bernardi KM, Forster ML, Lencer WI, Tsai B (2008) Derlin-1 facilitates the retro-translocation of cholera toxin. Molecular biology of the cell 19:877-884.

Bharati K, Ganguly NK (2011) Cholera toxin: a paradigm of a multifunctional protein. The Indian journal of medical research 133:179-187.

Bhidayasiri R, Truong DD (2005) Expanding use of botulinum toxin. Journal of the neurological sciences 235:1-9.

Bieger D, Hopkins DA (1987) Viscerotopic representation of the upper alimentary tract in the medulla oblongata in the rat: the nucleus ambiguus. The Journal of comparative neurology 262:546-562.

Bilsland LG, Sahai E, Kelly G, Golding M, Greensmith L, Schiavo G (2010) Deficits in axonal transport precede ALS symptoms in vivo. Proceedings of the National Academy of Sciences of the United States of America 107:20523-20528.

Blasi J, Chapman ER, Yamasaki S, Binz T, Niemann H, Jahn R (1993a) Botulinum neurotoxin C1 blocks neurotransmitter release by means of cleaving HPC-1/syntaxin. The EMBO journal 12:4821-4828.

Blasi J, Chapman ER, Link E, Binz T, Yamasaki S, De Camilli P, Sudhof TC, Niemann H, Jahn R (1993b) Botulinum neurotoxin A selectively cleaves the synaptic protein SNAP-25. Nature 365:160-163.

Boender AJ, de Jong JW, Boekhoudt L, Luijendijk MC, van der Plasse G, Adan RA (2014) Combined use of the canine adenovirus-2 and DREADD-technology to activate specific neural pathways in vivo. PloS one 9:e95392.

Boggs JM (2006) Myelin basic protein: a multifunctional protein. Cellular and molecular life sciences : CMLS 63:1945-1961.

Boillee S, Yamanaka K, Lobsiger CS, Copeland NG, Jenkins NA, Kassiotis G, Kollias G, Cleveland DW (2006) Onset and progression in inherited ALS determined by motor neurons and microglia. Science 312:1389-1392.

Bomba-Warczak E, Vevea JD, Brittain JM, Figueroa-Bernier A, Tepp WH, Johnson EA, Yeh FL, Chapman ER (2016) Interneuronal Transfer and Distal Action of Tetanus Toxin and Botulinum Neurotoxins A and D in Central Neurons. Cell reports 16:1974-1987.

Bories C, Amendola J, Lamotte d'Incamps B, Durand J (2007) Early electrophysiological abnormalities in lumbar motoneurons in a transgenic mouse model of amyotrophic lateral sclerosis. The European journal of neuroscience 25:451-459.

Borke JL, Caride A, Verma AK, Penniston JT, Kumar R (1989) Plasma membrane calcium pump and 28-kDa calcium binding protein in cells of rat kidney distal tubules. The American journal of physiology 257:F842-849.

Bowles DE, McPhee SW, Li C, Gray SJ, Samulski JJ, Camp AS, Li J, Wang B, Monahan PE, Rabinowitz JE, Grieger JC, Govindasamy L, Agbandje-McKenna M, Xiao X, Samulski RJ (2012) Phase 1 gene therapy for Duchenne muscular dystrophy using a translational optimized AAV vector. Molecular therapy : the journal of the American Society of Gene Therapy 20:443-455.

Braz JM, Rico B, Basbaum AI (2002) Transneuronal tracing of diverse CNS circuits by Cre-mediated induction of wheat germ agglutinin in transgenic mice. Proceedings of the National Academy of Sciences of the United States of America 99:15148-15153.

Broadwell RD, Balin BJ (1985) Endocytic and exocytic pathways of the neuronal secretory process and trans-synaptic transfer of wheat germ agglutinin-horseradish peroxidase in vivo. The Journal of comparative neurology 242:632-650.

Brooks VB, Curtis DR, Eccles JC (1957) The action of tetanus toxin on the inhibition of motoneurones. The Journal of physiology 135:655-672.

Bru T, Salinas S, Kremer EJ (2010) An update on canine adenovirus type 2 and its vectors. Viruses 2:2134-2153.

Bruchez M, Jr., Moronne M, Gin P, Weiss S, Alivisatos AP (1998) Semiconductor nanocrystals as fluorescent biological labels. Science 281:2013-2016.

Bruijn LI, Becher MW, Lee MK, Anderson KL, Jenkins NA, Copeland NG, Sisodia SS, Rothstein JD, Borchelt DR, Price DL, Cleveland DW (1997) ALS-linked SOD1 mutant G85R mediates damage to astrocytes and promotes rapidly progressive disease with SOD1-containing inclusions. Neuron 18:327-338.

Burger C, Gorbatyuk OS, Velardo MJ, Peden CS, Williams P, Zolotukhin S, Reier PJ, Mandel RJ, Muzyczka N (2004) Recombinant AAV viral vectors pseudotyped with viral capsids from serotypes 1, 2, and 5 display differential efficiency and cell tropism after delivery to different regions of the central nervous system. Molecular therapy : the journal of the American Society of Gene Therapy 10:302-317.

Burkart V, Kim YE, Hartmann B, Ghiea I, Syldath U, Kauer M, Fingberg W, Hanifi-Moghaddam P, Muller S, Kolb H (2002) Cholera toxin B pretreatment of macrophages and monocytes diminishes their proinflammatory responsiveness to lipopolysaccharide. Journal of immunology 168:1730-1737.

Buttry JL, Goshgarian HG (2015) WGA-Alexa transsynaptic labeling in the phrenic motor system of adult rats: Intrapleural injection versus intradiaphragmatic injection. Journal of neuroscience methods 241:137-145.

Byres E, Paton AW, Paton JC, Lofling JC, Smith DF, Wilce MC, Talbot UM, Chong DC, Yu H, Huang S, Chen X, Varki NM, Varki A, Rossjohn J, Beddoe T (2008) Incorporation of a non-human glycan mediates human susceptibility to a bacterial toxin. Nature 456:648-652.

Carlesi C, Pasquali L, Piazza S, Lo Gerfo A, Caldarazzo Ienco E, Alessi R, Fornai F, Siciliano G (2011) Strategies for clinical approach to neurodegeneration in Amyotrophic lateral sclerosis. Archives italiennes de biologie 149:151-167.

Carlton E, Teng Q, Federici T, Yang J, Riley J, Boulis NM (2008) Fusion of the tetanus toxin C fragment binding domain and Bcl-xL for protection of peripheral nerve neurons. Neurosurgery 63:1175-1182; discussion 1182-1174.

Carpentier DC, Vevis K, Trabalza A, Georgiadis C, Ellison SM, Asfahani RI, Mazarakis ND (2012) Enhanced pseudotyping efficiency of HIV-1 lentiviral vectors by a rabies/vesicular stomatitis virus chimeric envelope glycoprotein. Gene therapy 19:761-774.

Carter ME, Soden ME, Zweifel LS, Palmiter RD (2013) Genetic identification of a neural circuit that suppresses appetite. Nature 503:111-114.

Caskey CF, Stieger SM, Qin S, Dayton PA, Ferrara KW (2007) Direct observations of ultrasound microbubble contrast agent interaction with the microvessel wall. The Journal of the Acoustical Society of America 122:1191-1200.

Castle MJ, Gershenson ZT, Giles AR, Holzbaur EL, Wolfe JH (2014) Adeno-associated virus serotypes 1, 8, and 9 share conserved mechanisms for anterograde and retrograde axonal transport. Human gene therapy 25:705-720.

Cates MS, Teodoro ML, Phillips GN, Jr. (2002) Molecular mechanisms of calcium and magnesium binding to parvalbumin. Biophysical journal 82:1133-1146.

Cats EA, Jacobs BC, Yuki N, Tio-Gillen AP, Piepers S, Franssen H, van Asseldonk JT, van den Berg LH, van der Pol WL (2010) Multifocal motor neuropathy: association of anti-GM1 IgM antibodies with clinical features. Neurology 75:1961-1967.

Cavallo G, Iavarone C, Tubaro E (1993) Preparation and characterization of four new variously deacetylated lysogangliosides, breakdown products of GM1. Carbohydrate research 248:251-265.
Celio MR (1990) Calbindin D-28k and parvalbumin in the rat nervous system. Neuroscience 35:375-475.
Celio MR, Heizmann CW (1982) Calcium-binding protein parvalbumin is associated with fast contracting muscle fibres. Nature 297:504-506.
Chaib-Oukadour I, Gil C, Aguilera J (2004) The C-terminal domain of the heavy chain of tetanus toxin rescues cerebellar granule neurones from apoptotic death: involvement of phosphatidylinositol 3-kinase and mitogen-activated protein kinase pathways. Journal of neurochemistry 90:1227-1236.
Chakraborty SK, Fitzpatrick JA, Phillippi JA, Andreko S, Waggoner AS, Bruchez MP, Ballou B (2007) Cholera toxin B conjugated quantum dots for live cell labeling. Nano letters 7:2618-2626.
Chan WC, Nie S (1998) Quantum dot bioconjugates for ultrasensitive nonisotopic detection. Science 281:2016-2018.
Chang J, Baloh RH, Milbrandt J (2009) The NIMA-family kinase Nek3 regulates microtubule acetylation in neurons. Journal of cell science 122:2274-2282.
Chang TY, Reid PC, Sugii S, Ohgami N, Cruz JC, Chang CC (2005) Niemann-Pick type C disease and intracellular cholesterol trafficking. The Journal of biological chemistry 280:20917-20920.
Chattopadhyaya R, Meador WE, Means AR, Quiocho FA (1992) Calmodulin structure refined at 1.7 A resolution. Journal of molecular biology 228:1177-1192.
Chen C, Fu Z, Kim JJ, Barbieri JT, Baldwin MR (2009) Gangliosides as high affinity receptors for tetanus neurotoxin. The Journal of biological chemistry 284:26569-26577.
Chen C, Przedpelski A, Tepp WH, Pellett S, Johnson EA, Barbieri JT (2015) Heat-Labile Enterotoxin IIa, a Platform To Deliver Heterologous Proteins into Neurons. mBio 6:e00734.
Chen P, Li J, Barnes J, Kokkonen GC, Lee JC, Liu Y (2002) Restraint of proinflammatory cytokine biosynthesis by mitogen-activated protein kinase phosphatase-1 in lipopolysaccharide-stimulated macrophages. Journal of immunology 169:6408-6416.
Chen S, Zhang X, Song L, Le W (2012) Autophagy dysregulation in amyotrophic lateral sclerosis. Brain pathology 22:110-116.
Cherington M (1998) Clinical spectrum of botulism. Muscle & nerve 21:701-710.
Cheung WT, Richards DE, Rogers JH (1993) Calcium binding by chick calretinin and rat calbindin D28k synthesised in bacteria. European journal of biochemistry / FEBS 215:401-410.
Chian RJ, Li J, Ay I, Celia SA, Kashi BB, Tamrazian E, Matthews JC, Bronson RT, Rossomando A, Pepinsky RB, Fishman PS, Brown RH, Jr., Francis JW (2009) IGF-1:tetanus toxin fragment C fusion protein improves delivery of IGF-1 to spinal cord but fails to prolong survival of ALS mice. Brain research 1287:1-19.
Chin D, Means AR (2000) Calmodulin: a prototypical calcium sensor. Trends in cell biology 10:322-328.
Chinnapen DJ, Hsieh WT, te Welscher YM, Saslowsky DE, Kaoutzani L, Brandsma E, D'Auria L, Park H, Wagner JS, Drake KR, Kang M, Benjamin T, Ullman MD, Costello CE, Kenworthy AK, Baumgart T, Massol RH, Lencer WI (2012) Lipid sorting by ceramide structure from plasma membrane to ER for the cholera toxin receptor ganglioside GM1. Developmental cell 23:573-586.
Choi JJ, Selert K, Vlachos F, Wong A, Konofagou EE (2011) Noninvasive and localized neuronal delivery using short ultrasonic pulses and microbubbles. Proceedings of the National Academy of Sciences of the United States of America 108:16539-16544.
Choi VW, McCarty DM, Samulski RJ (2005) AAV hybrid serotypes: improved vectors for gene delivery. Current gene therapy 5:299-310.

Christakos S, Gabrielides C, Rhoten WB (1989) Vitamin D-dependent calcium binding proteins: chemistry, distribution, functional considerations, and molecular biology. Endocrine reviews 10:3-26.

Chung YH, Joo KM, Nam RH, Cho MH, Kim DJ, Lee WB, Cha CI (2005) Decreased expression of calretinin in the cerebral cortex and hippocampus of SOD1G93A transgenic mice. Brain research 1035:105-109.

Ciesielska A, Mittermeyer G, Hadaczek P, Kells AP, Forsayeth J, Bankiewicz KS (2011) Anterograde axonal transport of AAV2-GDNF in rat basal ganglia. Molecular therapy : the journal of the American Society of Gene Therapy 19:922-927.

Cifra A, Nani F, Nistri A (2011) Riluzole is a potent drug to protect neonatal rat hypoglossal motoneurons in vitro from excitotoxicity due to glutamate uptake block. The European journal of neuroscience 33:899-913.

Ciriello J, Hrycyshyn AW, Calaresu FR (1981) Glossopharyngeal and vagal afferent projections to the brain stem of the cat: a horseradish peroxidase study. Journal of the autonomic nervous system 4:63-79.

Ciriza J, Moreno-Igoa M, Calvo AC, Yague G, Palacio J, Miana-Mena FJ, Munoz MJ, Zaragoza P, Brulet P, Osta R (2008) A genetic fusion GDNF-C fragment of tetanus toxin prolongs survival in a symptomatic mouse ALS model. Restorative neurology and neuroscience 26:459-465.

Coffey JW, De Duve C (1968) Digestive activity of lysosomes. I. The digestion of proteins by extracts of rat liver lysosomes. The Journal of biological chemistry 243:3255-3263.

Cohen S, Aizer A, Shav-Tal Y, Yanai A, Motro B (2013) Nek7 kinase accelerates microtubule dynamic instability. Biochimica et biophysica acta 1833:1104-1113.

Collier CP, Vossmeyer T, Heath JR (1998) Nanocrystal superlattices. Annual review of physical chemistry 49:371-404.

Collin T, Chat M, Lucas MG, Moreno H, Racay P, Schwaller B, Marty A, Llano I (2005) Developmental changes in parvalbumin regulate presynaptic Ca2+ signaling. The Journal of neuroscience : the official journal of the Society for Neuroscience 25:96-107.

Cong Y, Bowdon HR, Elson CO (1996) Identification of an immunodominant T cell epitope on cholera toxin. European journal of immunology 26:2587-2594.

Conte WL, Kamishina H, Reep RL (2009) Multiple neuroanatomical tract-tracing using fluorescent Alexa Fluor conjugates of cholera toxin subunit B in rats. Nature protocols 4:1157-1166.

Cool SK, Geers B, Roels S, Stremersch S, Vanderperren K, Saunders JH, De Smedt SC, Demeester J, Sanders NN (2013) Coupling of drug containing liposomes to microbubbles improves ultrasound triggered drug delivery in mice. Journal of controlled release : official journal of the Controlled Release Society 172:885-893.

Cosolo WC, Martinello P, Louis WJ, Christophidis N (1989) Blood-brain barrier disruption using mannitol: time course and electron microscopy studies. The American journal of physiology 256:R443-447.

Dallas WS, Falkow S (1980) Amino acid sequence homology between cholera toxin and Escherichia coli heat-labile toxin. Nature 288:499-501.

Datiche F, Luppi PH, Cattarelli M (1995) Serotonergic and non-serotonergic projections from the raphe nuclei to the piriform cortex in the rat: a cholera toxin B subunit (CTb) and 5-HT immunohistochemical study. Brain research 671:27-37.

Davletov B, Bajohrs M, Binz T (2005) Beyond BOTOX: advantages and limitations of individual botulinum neurotoxins. Trends in neurosciences 28:446-452.

Day CA, Baetz NW, Copeland CA, Kraft LJ, Han B, Tiwari A, Drake KR, De Luca H, Chinnapen DJ, Davidson MW, Holmes RK, Jobling MG, Schroer TA, Lencer WI, Kenworthy AK (2015) Microtubule motors power plasma membrane tubulation in clathrin-independent endocytosis. Traffic 16:572-590.

Daya S, Berns KI (2008) Gene therapy using adeno-associated virus vectors. Clinical microbiology reviews 21:583-593.

De Haan L, Hirst TR (2004) Cholera toxin: a paradigm for multi-functional engagement of cellular mechanisms (Review). Molecular membrane biology 21:77-92.

de Leon M, Covenas R, Narvaez JA, Aguirre JA, Gonzalez-Baron S (1993) Distribution of parvalbumin immunoreactivity in the cat brain stem. Brain research bulletin 32:639-646.

Debets MF, van der Doelen CW, Rutjes FP, van Delft FL (2010) Azide: a unique dipole for metal-free bioorthogonal ligations. Chembiochem : a European journal of chemical biology 11:1168-1184.

Debono MW, Le Guern J, Canton T, Doble A, Pradier L (1993) Inhibition by riluzole of electrophysiological responses mediated by rat kainate and NMDA receptors expressed in Xenopus oocytes. European journal of pharmacology 235:283-289.

Dederen PJ, Gribnau AA, Curfs MH (1994) Retrograde neuronal tracing with cholera toxin B subunit: comparison of three different visualization methods. The Histochemical journal 26:856-862.

Deinhardt K, Salinas S, Verastegui C, Watson R, Worth D, Hanrahan S, Bucci C, Schiavo G (2006) Rab5 and Rab7 control endocytic sorting along the axonal retrograde transport pathway. Neuron 52:293-305.

Deisseroth K, Heist EK, Tsien RW (1998) Translocation of calmodulin to the nucleus supports CREB phosphorylation in hippocampal neurons. Nature 392:198-202.

DeJesus-Hernandez M et al. (2011) Expanded GGGGCC hexanucleotide repeat in noncoding region of C9ORF72 causes chromosome 9p-linked FTD and ALS. Neuron 72:245-256.

Delzor A, Dufour N, Petit F, Guillermier M, Houitte D, Auregan G, Brouillet E, Hantraye P, Deglon N (2012) Restricted transgene expression in the brain with cell-type specific neuronal promoters. Human gene therapy methods 23:242-254.

DeMarco ML, Woods RJ (2009) Atomic-resolution conformational analysis of the GM3 ganglioside in a lipid bilayer and its implications for ganglioside-protein recognition at membrane surfaces. Glycobiology 19:344-355.

DePaul R, Abbs JH, Caligiuri M, Gracco VL, Brooks BR (1988) Hypoglossal, trigeminal, and facial motoneuron involvement in amyotrophic lateral sclerosis. Neurology 38:281-283.

Dertzbaugh MT, Cox LM (1998) The affinity of cholera toxin for Ni2+ ion. Protein engineering 11:577-581.

Dewey CM, Cenik B, Sephton CF, Johnson BA, Herz J, Yu G (2012) TDP-43 aggregation in neurodegeneration: are stress granules the key? Brain research 1462:16-25.

Dobi A, Margolis EB, Wang HL, Harvey BK, Morales M (2010) Glutamatergic and nonglutamatergic neurons of the ventral tegmental area establish local synaptic contacts with dopaminergic and nondopaminergic neurons. The Journal of neuroscience : the official journal of the Society for Neuroscience 30:218-229.

Dolly O (2003) Synaptic transmission: inhibition of neurotransmitter release by botulinum toxins. Headache 43 Suppl 1:S16-24.

Dong M, Yeh F, Tepp WH, Dean C, Johnson EA, Janz R, Chapman ER (2006) SV2 is the protein receptor for botulinum neurotoxin A. Science 312:592-596.

Donoghue S, Fox RE, Kidd C, Koley BN (1981) The distribution in the cat brain stem of neurones activated by vagal nonmyelinated fibres from the heart and lungs. Quarterly journal of experimental physiology 66:391-404.

Dormann D, Rodde R, Edbauer D, Bentmann E, Fischer I, Hruscha A, Than ME, Mackenzie IR, Capell A, Schmid B, Neumann M, Haass C (2010) ALS-associated fused in sarcoma (FUS) mutations disrupt Transportin-mediated nuclear import. The EMBO journal 29:2841-2857.

Dunphy JT, Linder ME (1998) Signalling functions of protein palmitoylation. Biochimica et biophysica acta 1436:245-261.

Dutheil N, Shi F, Dupressoir T, Linden RM (2000) Adeno-associated virus site-specifically integrates into a muscle-specific DNA region. Proceedings of the National Academy of Sciences of the United States of America 97:4862-4866.
Eberhard M, Erne P (1994) Calcium and magnesium binding to rat parvalbumin. European journal of biochemistry / FEBS 222:21-26.
Eccles JC, Eccles RM, Lundberg A (1957) The convergence of monosynaptic excitatory afferents on to many different species of alpha motoneurones. The Journal of physiology 137:22-50.
Eccles JC, Eccles RM, Iggo A, Lundberg A (1960) Electrophysiological studies on gamma motoneurones. Acta physiologica Scandinavica 50:32-40.
Ehehalt R, Keller P, Haass C, Thiele C, Simons K (2003) Amyloidogenic processing of the Alzheimer beta-amyloid precursor protein depends on lipid rafts. The Journal of cell biology 160:113-123.
Ekstrand MI, Nectow AR, Knight ZA, Latcha KN, Pomeranz LE, Friedman JM (2014) Molecular profiling of neurons based on connectivity. Cell 157:1230-1242.
El-Sayed A, Futaki S, Harashima H (2009) Delivery of macromolecules using arginine-rich cell-penetrating peptides: ways to overcome endosomal entrapment. The AAPS journal 11:13-22.
Elliott JL, Snider WD (1995) Parvalbumin is a marker of ALS-resistant motor neurons. Neuroreport 6:449-452.
ElMallah MK, Falk DJ, Lane MA, Conlon TJ, Lee KZ, Shafi NI, Reier PJ, Byrne BJ, Fuller DD (2012) Retrograde gene delivery to hypoglossal motoneurons using adeno-associated virus serotype 9. Human gene therapy methods 23:148-156.
Endo T, Onaya T (1988) Immunohistochemical localization of parvalbumin in rat and monkey autonomic ganglia. Journal of neurocytology 17:73-77.
Engelhardt J, Appel SH (1990a) Motor neuron reactivity of sera from animals with autoimmune models of motor neuron destruction. Journal of the neurological sciences 96:333-352.
Engelhardt JI, Appel SH (1990b) IgG reactivity in the spinal cord and motor cortex in amyotrophic lateral sclerosis. Archives of neurology 47:1210-1216.
Engelhardt JI, Siklos L, Komuves L, Smith RG, Appel SH (1995) Antibodies to calcium channels from ALS patients passively transferred to mice selectively increase intracellular calcium and induce ultrastructural changes in motoneurons. Synapse 20:185-199.
Ericson H, Blomqvist A (1988) Tracing of neuronal connections with cholera toxin subunit B: light and electron microscopic immunohistochemistry using monoclonal antibodies. Journal of neuroscience methods 24:225-235.
Evangelisti E, Wright D, Zampagni M, Cascella R, Bagnoli S, Relini A, Nichino D, Scartabelli T, Nacmias B, Sorbi S, Cecchi C (2012) Lipid Rafts Mediate Amyloid-induced Calcium Dyshomeostasis and Oxidative Stress in Alzheimer's Disease. Current Alzheimer research.
Faas GC, Schwaller B, Vergara JL, Mody I (2007) Resolving the fast kinetics of cooperative binding: Ca2+ buffering by calretinin. PLoS biology 5:e311.
Fahandejsaadi A, Leung E, Rahaii R, Bu J, Geula C (2004) Calbindin-D28K, parvalbumin and calretinin in primate lower motor neurons. Neuroreport 15:443-448.
Fallaux FJ, Kranenburg O, Cramer SJ, Houweling A, Van Ormondt H, Hoeben RC, Van Der Eb AJ (1996) Characterization of 911: a new helper cell line for the titration and propagation of early region 1-deleted adenoviral vectors. Human gene therapy 7:215-222.
Fan E, Merritt EA, Verlinde CL, Hol WG (2000) AB(5) toxins: structures and inhibitor design. Current opinion in structural biology 10:680-686.
Farg MA, Sundaramoorthy V, Sultana JM, Yang S, Atkinson RA, Levina V, Halloran MA, Gleeson PA, Blair IP, Soo KY, King AE, Atkin JD (2014) C9ORF72, implicated in amytrophic lateral sclerosis and frontotemporal dementia, regulates endosomal trafficking. Human molecular genetics 23:3579-3595.

Fasanella KE, Christianson JA, Chanthaphavong RS, Davis BM (2008) Distribution and neurochemical identification of pancreatic afferents in the mouse. The Journal of comparative neurology 509:42-52.
Feasby TE, Gilbert JJ, Brown WF, Bolton CF, Hahn AF, Koopman WF, Zochodne DW (1986) An acute axonal form of Guillain-Barre polyneuropathy. Brain : a journal of neurology 109 (Pt 6):1115-1126.
Feng Y, Jadhav AP, Rodighiero C, Fujinaga Y, Kirchhausen T, Lencer WI (2004) Retrograde transport of cholera toxin from the plasma membrane to the endoplasmic reticulum requires the trans-Golgi network but not the Golgi apparatus in Exo2-treated cells. EMBO reports 5:596-601.
Ferrari E et al. (2013) Synthetic self-assembling clostridial chimera for modulation of sensory functions. Bioconjugate chemistry 24:1750-1759.
Ferrari FK, Samulski T, Shenk T, Samulski RJ (1996) Second-strand synthesis is a rate-limiting step for efficient transduction by recombinant adeno-associated virus vectors. Journal of virology 70:3227-3234.
Ferrari FK, Xiao X, McCarty D, Samulski RJ (1997) New developments in the generation of Ad-free, high-titer rAAV gene therapy vectors. Nature medicine 3:1295-1297.
Fiandaca M, Forsayeth J, Bankiewicz K (2008) Current status of gene therapy trials for Parkinson's disease. Experimental neurology 209:51-57.
Figueiredo DM, Hallewell RA, Chen LL, Fairweather NF, Dougan G, Savitt JM, Parks DA, Fishman PS (1997) Delivery of recombinant tetanus-superoxide dismutase proteins to central nervous system neurons by retrograde axonal transport. Experimental neurology 145:546-554.
Finkelstein RA, LoSpalluto JJ (1969) Pathogenesis of experimental cholera. Preparation and isolation of choleragen and choleragenoid. The Journal of experimental medicine 130:185-202.
Fischer LR, Culver DG, Tennant P, Davis AA, Wang M, Castellano-Sanchez A, Khan J, Polak MA, Glass JD (2004) Amyotrophic lateral sclerosis is a distal axonopathy: evidence in mice and man. Experimental neurology 185:232-240.
Fishman PS, Matthews CC, Parks DA, Box M, Fairweather NF (2006) Immunization does not interfere with uptake and transport by motor neurons of the binding fragment of tetanus toxin. Journal of neuroscience research 83:1540-1543.
Flink R, Westman J (1986) Different neuron populations in the feline lateral cervical nucleus: a light and electron microscopic study with the retrograde axonal transport technique. The Journal of comparative neurology 250:265-281.
Fohr UG, Weber BR, Muntener M, Staudenmann W, Hughes GJ, Frutiger S, Banville D, Schafer BW, Heizmann CW (1993) Human alpha and beta parvalbumins. Structure and tissue-specific expression. European journal of biochemistry / FEBS 215:719-727.
Foster KA (2005) A new wrinkle on pain relief: re-engineering clostridial neurotoxins for analgesics. Drug discovery today 10:563-569.
Fotinou C, Emsley P, Black I, Ando H, Ishida H, Kiso M, Sinha KA, Fairweather NF, Isaacs NW (2001) The crystal structure of tetanus toxin Hc fragment complexed with a synthetic GT1b analogue suggests cross-linking between ganglioside receptors and the toxin. The Journal of biological chemistry 276:32274-32281.
Foust KD, Nurre E, Montgomery CL, Hernandez A, Chan CM, Kaspar BK (2009) Intravascular AAV9 preferentially targets neonatal neurons and adult astrocytes. Nature biotechnology 27:59-65.
Fratta P, Mizielinska S, Nicoll AJ, Zloh M, Fisher EM, Parkinson G, Isaacs AM (2012) C9orf72 hexanucleotide repeat associated with amyotrophic lateral sclerosis and frontotemporal dementia forms RNA G-quadruplexes. Scientific reports 2:1016.
Friese A, Kaltschmidt JA, Ladle DR, Sigrist M, Jessell TM, Arber S (2009) Gamma and alpha motor neurons distinguished by expression of transcription factor Err3.

Proceedings of the National Academy of Sciences of the United States of America 106:13588-13593.
Fujinaga Y, Wolf AA, Rodighiero C, Wheeler H, Tsai B, Allen L, Jobling MG, Rapoport T, Holmes RK, Lencer WI (2003) Gangliosides that associate with lipid rafts mediate transport of cholera and related toxins from the plasma membrane to endoplasmic reticulm. Molecular biology of the cell 14:4783-4793.
Fukuta S, Magnani JL, Twiddy EM, Holmes RK, Ginsburg V (1988) Comparison of the carbohydrate-binding specificities of cholera toxin and Escherichia coli heat-labile enterotoxins LTh-I, LT-IIa, and LT-IIb. Infection and immunity 56:1748-1753.
Gall D, Roussel C, Susa I, D'Angelo E, Rossi P, Bearzatto B, Galas MC, Blum D, Schurmans S, Schiffmann SN (2003) Altered neuronal excitability in cerebellar granule cells of mice lacking calretinin. The Journal of neuroscience : the official journal of the Society for Neuroscience 23:9320-9327.
Gandini MA, Sandoval A, Felix R (2014) Whole-cell patch-clamp recordings of Ca2+ currents from isolated neonatal mouse dorsal root ganglion (DRG) neurons. Cold Spring Harbor protocols 2014:389-395.
Garrity MM, Gibbons SJ, Smyrk TC, Vanderwinden JM, Gomez-Pinilla PJ, Nehra A, Borg M, Farrugia G (2009) Diagnostic challenges of motility disorders: optimal detection of CD117+ interstitial cells of Cajal. Histopathology 54:286-294.
Gerardo-Nava J, Mayorenko, II, Grehl T, Steinbusch HW, Weis J, Brook GA (2013) Differential pattern of neuroprotection in lumbar, cervical and thoracic spinal cord segments in an organotypic rat model of glutamate-induced excitotoxicity. Journal of chemical neuroanatomy 53:11-17.
Gerfen CR, O'Leary DD, Cowan WM (1982) A note on the transneuronal transport of wheat germ agglutinin-conjugated horseradish peroxidase in the avian and rodent visual systems. Experimental brain research 48:443-448.
Glogau RG (2002) Review of the use of botulinum toxin for hyperhidrosis and cosmetic purposes. The Clinical journal of pain 18:S191-197.
Gompf HS, Budygin EA, Fuller PM, Bass CE (2015) Targeted genetic manipulations of neuronal subtypes using promoter-specific combinatorial AAVs in wild-type animals. Frontiers in behavioral neuroscience 9:152.
Gong Z, Long X, Pan L, Le Y, Liu Q, Wang S, Guo J, Xiao B, Zhou M, Mei D (2009) Cloning, expression, purification and characterization of the cholera toxin B subunit and triple glutamic acid decarboxylase epitopes fusion protein in Escherichia coli. Protein expression and purification 66:191-197.
Goodnough MC, Oyler G, Fishman PS, Johnson EA, Neale EA, Keller JE, Tepp WH, Clark M, Hartz S, Adler M (2002) Development of a delivery vehicle for intracellular transport of botulinum neurotoxin antagonists. FEBS letters 513:163-168.
Goshgarian HG, Buttry JL (2014) The pattern and extent of retrograde transsynaptic transport of WGA-Alexa 488 in the phrenic motor system is dependent upon the site of application. Journal of neuroscience methods 222:156-164.
Gradinaru V, Zhang F, Ramakrishnan C, Mattis J, Prakash R, Diester I, Goshen I, Thompson KR, Deisseroth K (2010) Molecular and cellular approaches for diversifying and extending optogenetics. Cell 141:154-165.
Gramsbergen A, J IJ-P, Meek MF (2000) Sciatic nerve transection in the adult rat: abnormal EMG patterns during locomotion by aberrant innervation of hindleg muscles. Experimental neurology 161:183-193.
Green NM (1963) Avidin. 1. The Use of (14-C)Biotin for Kinetic Studies and for Assay. The Biochemical journal 89:585-591.
Green NM (1975) Avidin. Advances in protein chemistry 29:85-133.
Groves P, Palczewska M (2001) Cation binding properties of calretinin, an EF-hand calcium-binding protein. Acta biochimica Polonica 48:113-119.

Guimaraes CP, Witte MD, Theile CS, Bozkurt G, Kundrat L, Blom AE, Ploegh HL (2013) Site-specific C-terminal and internal loop labeling of proteins using sortase-mediated reactions. Nature protocols 8:1787-1799.

Haas HL, Sergeeva OA, Selbach O (2008) Histamine in the nervous system. Physiological reviews 88:1183-1241.

Hack NJ, Wride MC, Charters KM, Kater SB, Parks TN (2000) Developmental changes in the subcellular localization of calretinin. The Journal of neuroscience : the official journal of the Society for Neuroscience 20:RC67.

Hafer-Macko C, Hsieh ST, Li CY, Ho TW, Sheikh K, Cornblath DR, McKhann GM, Asbury AK, Griffin JW (1996) Acute motor axonal neuropathy: an antibody-mediated attack on axolemma. Annals of neurology 40:635-644.

Hakomori S, Handa K, Iwabuchi K, Yamamura S, Prinetti A (1998) New insights in glycosphingolipid function: "glycosignaling domain," a cell surface assembly of glycosphingolipids with signal transducer molecules,involved in cell adhesion coupled with signaling. Glycobiology 8:xi-xix.

Hall ED, Oostveen JA, Gurney ME (1998) Relationship of microglial and astrocytic activation to disease onset and progression in a transgenic model of familial ALS. Glia 23:249-256.

Haner M, Henzl MT, Raissouni B, Birnbaum ER (1984) Synthesis of a new chelating gel: removal of Ca2+ ions from parvalbumin. Analytical biochemistry 138:229-234.

Harding TC, Dickinson PJ, Roberts BN, Yendluri S, Gonzalez-Edick M, Lecouteur RA, Jooss KU (2006) Enhanced gene transfer efficiency in the murine striatum and an orthotopic glioblastoma tumor model, using AAV-7- and AAV-8-pseudotyped vectors. Human gene therapy 17:807-820.

Havton LA, Broman J (2005) Systemic administration of cholera toxin B subunit conjugated to horseradish peroxidase in the adult rat labels preganglionic autonomic neurons, motoneurons, and select primary afferents for light and electron microscopic studies. Journal of neuroscience methods 149:101-109.

Hayashi S, Amari M, Okamoto K (2013) Loss of calretinin- and parvalbumin-immunoreactive axons in anterolateral columns beyond the corticospinal tracts of amyotrophic lateral sclerosis spinal cords. Journal of the neurological sciences 331:61-66.

He X, Gao L, Ma N (2013) One-step instant synthesis of protein-conjugated quantum dots at room temperature. Scientific reports 3:2825.

Heckmann M, Ceballos-Baumann AO, Plewig G, Hyperhidrosis Study G (2001) Botulinum toxin A for axillary hyperhidrosis (excessive sweating). The New England journal of medicine 344:488-493.

Henrich S, Cameron A, Bourenkov GP, Kiefersauer R, Huber R, Lindberg I, Bode W, Than ME (2003) The crystal structure of the proprotein processing proteinase furin explains its stringent specificity. Nature structural biology 10:520-526.

Henzl MT (2009) Characterization of parvalbumin and polcalcin divalent ion binding by isothermal titration calorimetry. Methods in enzymology 455:259-297.

Henzl MT, Tanner JJ (2008) Solution structure of Ca2+-free rat alpha-parvalbumin. Protein science : a publication of the Protein Society 17:431-438.

Henzl MT, Larson JD, Agah S (2003) Estimation of parvalbumin Ca(2+)- and Mg(2+)-binding constants by global least-squares analysis of isothermal titration calorimetry data. Analytical biochemistry 319:216-233.

Hirakawa N, Morimoto M, Totoki T (1993) Sympathetic innervation of the young canine heart using antero- and retrograde axonal tracer methods. Brain research bulletin 31:673-680.

Hirst TR, Sanchez J, Kaper JB, Hardy SJ, Holmgren J (1984) Mechanism of toxin secretion by Vibrio cholerae investigated in strains harboring plasmids that encode heat-labile enterotoxins of Escherichia coli. Proceedings of the National Academy of Sciences of the United States of America 81:7752-7756.

Hnasko TS, Perez FA, Scouras AD, Stoll EA, Gale SD, Luquet S, Phillips PE, Kremer EJ, Palmiter RD (2006) Cre recombinase-mediated restoration of nigrostriatal dopamine in dopamine-deficient mice reverses hypophagia and bradykinesia. Proceedings of the National Academy of Sciences of the United States of America 103:8858-8863.

Ho BK, Alexianu ME, Colom LV, Mohamed AH, Serrano F, Appel SH (1996) Expression of calbindin-D28K in motoneuron hybrid cells after retroviral infection with calbindin-D28K cDNA prevents amyotrophic lateral sclerosis IgG-mediated cytotoxicity. Proceedings of the National Academy of Sciences of the United States of America 93:6796-6801.

Ho TW, Mishu B, Li CY, Gao CY, Cornblath DR, Griffin JW, Asbury AK, Blaser MJ, McKhann GM (1995) Guillain-Barre syndrome in northern China. Relationship to Campylobacter jejuni infection and anti-glycolipid antibodies. Brain : a journal of neurology 118 (Pt 3):597-605.

Hollis ER, 2nd, Kadoya K, Hirsch M, Samulski RJ, Tuszynski MH (2008) Efficient retrograde neuronal transduction utilizing self-complementary AAV1. Molecular therapy : the journal of the American Society of Gene Therapy 16:296-301.

Holmgren J, Lonnroth I, Svennerholm L (1973) Tissue receptor for cholera exotoxin: postulated structure from studies with GM1 ganglioside and related glycolipids. Infection and immunity 8:208-214.

Holmgren J, Lonnroth I, Mansson J, Svennerholm L (1975) Interaction of cholera toxin and membrane GM1 ganglioside of small intestine. Proceedings of the National Academy of Sciences of the United States of America 72:2520-2524.

Holmgren J, Adamsson J, Anjuere F, Clemens J, Czerkinsky C, Eriksson K, Flach CF, George-Chandy A, Harandi AM, Lebens M, Lehner T, Lindblad M, Nygren E, Raghavan S, Sanchez J, Stanford M, Sun JB, Svennerholm AM, Tengvall S (2005) Mucosal adjuvants and anti-infection and anti-immunopathology vaccines based on cholera toxin, cholera toxin B subunit and CpG DNA. Immunology letters 97:181-188.

Holstege JC (1987) Brainstem projections to lumbar motoneurons in rat--II. An ultrastructural study by means of the anterograde transport of wheat germ agglutinin coupled to horseradish peroxidase and using the tetramethyl benzidine reaction. Neuroscience 21:369-376.

Honda T, Saitoh H, Masuko M, Katagiri-Abe T, Tominaga K, Kozakai I, Kobayashi K, Kumanishi T, Watanabe YG, Odani S, Kuwano R (2000) The coxsackievirus-adenovirus receptor protein as a cell adhesion molecule in the developing mouse brain. Brain research Molecular brain research 77:19-28.

Horner RL (2007) Respiratory motor activity: influence of neuromodulators and implications for sleep disordered breathing. Canadian journal of physiology and pharmacology 85:155-165.

Horner RL (2012) Neural control of the upper airway: integrative physiological mechanisms and relevance for sleep disordered breathing. Comprehensive Physiology 2:479-535.

Hsueh YP, Yang FC, Kharazia V, Naisbitt S, Cohen AR, Weinberg RJ, Sheng M (1998) Direct interaction of CASK/LIN-2 and syndecan heparan sulfate proteoglycan and their overlapping distribution in neuronal synapses. The Journal of cell biology 142:139-151.

Hu JH, Zhang H, Wagey R, Krieger C, Pelech SL (2003) Protein kinase and protein phosphatase expression in amyotrophic lateral sclerosis spinal cord. Journal of neurochemistry 85:432-442.

Huang X, Aulabaugh A, Ding W, Kapoor B, Alksne L, Tabei K, Ellestad G (2003) Kinetic mechanism of Staphylococcus aureus sortase SrtA. Biochemistry 42:11307-11315.

Hytonen VP, Nordlund HR, Horha J, Nyholm TK, Hyre DE, Kulomaa T, Porkka EJ, Marttila AT, Stayton PS, Laitinen OH, Kulomaa MS (2005) Dual-affinity avidin molecules. Proteins 61:597-607.

Ichikawa N, Iwabuchi K, Kurihara H, Ishii K, Kobayashi T, Sasaki T, Hattori N, Mizuno Y, Hozumi K, Yamada Y, Arikawa-Hirasawa E (2009) Binding of laminin-1 to monosialoganglioside GM1 in lipid rafts is crucial for neurite outgrowth. Journal of cell science 122:289-299.

Iglesias-Bartolome R, Trenchi A, Comin R, Moyano AL, Nores GA, Daniotti JL (2009) Differential endocytic trafficking of neuropathy-associated antibodies to GM1 ganglioside and cholera toxin in epithelial and neural cells. Biochimica et biophysica acta 1788:2526-2540.

Ikeda K, Yamaguchi T, Fukunaga S, Hoshino M, Matsuzaki K (2011) Mechanism of amyloid beta-protein aggregation mediated by GM1 ganglioside clusters. Biochemistry 50:6433-6440.

Illa I, Ortiz N, Gallard E, Juarez C, Grau JM, Dalakas MC (1995) Acute axonal Guillain-Barre syndrome with IgG antibodies against motor axons following parenteral gangliosides. Annals of neurology 38:218-224.

Jaiswal MK (2014) Selective vulnerability of motoneuron and perturbed mitochondrial calcium homeostasis in amyotrophic lateral sclerosis: implications for motoneurons specific calcium dysregulation. Molecular and cellular therapies 2:26.

Jalabert M, Bourdy R, Courtin J, Veinante P, Manzoni OJ, Barrot M, Georges F (2011) Neuronal circuits underlying acute morphine action on dopamine neurons. Proceedings of the National Academy of Sciences of the United States of America 108:16446-16450.

Jao CY, Salic A (2008) Exploring RNA transcription and turnover in vivo by using click chemistry. Proceedings of the National Academy of Sciences of the United States of America 105:15779-15784.

Jara JH, Villa SR, Khan NA, Bohn MC, Ozdinler PH (2012) AAV2 mediated retrograde transduction of corticospinal motor neurons reveals initial and selective apical dendrite degeneration in ALS. Neurobiology of disease 47:174-183.

Jewett JC, Bertozzi CR (2010) Cu-free click cycloaddition reactions in chemical biology. Chemical Society reviews 39:1272-1279.

Johnson EA (1999) Clostridial toxins as therapeutic agents: benefits of nature's most toxic proteins. Annual review of microbiology 53:551-575.

Junyent F, Kremer EJ (2015) CAV-2--why a canine virus is a neurobiologist's best friend. Current opinion in pharmacology 24:86-93.

Kaji R, Kimura J (1999) Facts and fallacies on anti-GM1 antibodies: physiology of motor neuropathies. Brain : a journal of neurology 122 (Pt 5):797-798.

Kalia M (1981) Brain stem localization of vagal preganglionic neurons. Journal of the autonomic nervous system 3:451-481.

Kaludov N, Brown KE, Walters RW, Zabner J, Chiorini JA (2001) Adeno-associated virus serotype 4 (AAV4) and AAV5 both require sialic acid binding for hemagglutination and efficient transduction but differ in sialic acid linkage specificity. Journal of virology 75:6884-6893.

Kanning KC, Kaplan A, Henderson CE (2010) Motor neuron diversity in development and disease. Annual review of neuroscience 33:409-440.

Kaspar BK, Llado J, Sherkat N, Rothstein JD, Gage FH (2003) Retrograde viral delivery of IGF-1 prolongs survival in a mouse ALS model. Science 301:839-842.

Kay BK, Thai S, Volgina VV (2009) High-throughput biotinylation of proteins. Methods in molecular biology 498:185-196.

Keller S, Vargas C, Zhao H, Piszczek G, Brautigam CA, Schuck P (2012) High-precision isothermal titration calorimetry with automated peak-shape analysis. Analytical chemistry 84:5066-5073.

Kenna KP et al. (2016) NEK1 variants confer susceptibility to amyotrophic lateral sclerosis. Nature genetics.

Kibbe WA (2007) OligoCalc: an online oligonucleotide properties calculator. Nucleic acids research 35:W43-46.

Kiernan MC, Vucic S, Cheah BC, Turner MR, Eisen A, Hardiman O, Burrell JR, Zoing MC (2011) Amyotrophic lateral sclerosis. Lancet 377:942-955.
Kiick KL, Saxon E, Tirrell DA, Bertozzi CR (2002) Incorporation of azides into recombinant proteins for chemoselective modification by the Staudinger ligation. Proceedings of the National Academy of Sciences of the United States of America 99:19-24.
Kim SU, Moretto G, Lee V, Yu RK (1986) Neuroimmunology of gangliosides in human neurons and glial cells in culture. Journal of neuroscience research 15:303-321.
Kimura N, Yanagisawa K (2007) Endosomal accumulation of GM1 ganglioside-bound amyloid beta-protein in neurons of aged monkey brains. Neuroreport 18:1669-1673.
Kinoshita N, Mizuno T, Yoshihara Y (2002) Adenovirus-mediated WGA gene delivery for transsynaptic labeling of mouse olfactory pathways. Chemical senses 27:215-223.
Kirichok Y, Krapivinsky G, Clapham DE (2004) The mitochondrial calcium uniporter is a highly selective ion channel. Nature 427:360-364.
Kirkham M, Fujita A, Chadda R, Nixon SJ, Kurzchalia TV, Sharma DK, Pagano RE, Hancock JF, Mayor S, Parton RG (2005) Ultrastructural identification of uncoated caveolin-independent early endocytic vehicles. The Journal of cell biology 168:465-476.
Kissa K, Mordelet E, Soudais C, Kremer EJ, Demeneix BA, Brulet P, Coen L (2002) In vivo neuronal tracing with GFP-TTC gene delivery. Molecular and cellular neurosciences 20:627-637.
Kita H (1994) Parvalbumin-immunopositive neurons in rat globus pallidus: a light and electron microscopic study. Brain research 657:31-41.
Klein RL, Dayton RD, Leidenheimer NJ, Jansen K, Golde TE, Zweig RM (2006) Efficient neuronal gene transfer with AAV8 leads to neurotoxic levels of tau or green fluorescent proteins. Molecular therapy : the journal of the American Society of Gene Therapy 13:517-527.
Klein RL, Meyer EM, Peel AL, Zolotukhin S, Meyers C, Muzyczka N, King MA (1998) Neuron-specific transduction in the rat septohippocampal or nigrostriatal pathway by recombinant adeno-associated virus vectors. Experimental neurology 150:183-194.
Klevit RE (1983) Spectroscopic analyses of calmodulin and its interactions. Methods in enzymology 102:82-104.
Klonjkowski B, Gilardi-Hebenstreit P, Hadchouel J, Randrianarison V, Boutin S, Yeh P, Perricaudet M, Kremer EJ (1997) A recombinant E1-deleted canine adenoviral vector capable of transduction and expression of a transgene in human-derived cells and in vivo. Human gene therapy 8:2103-2115.
Knight VB, Serrano EE (2006) Tissue and species differences in the application of quantum dots as probes for biomolecular targets in the inner ear and kidney. IEEE transactions on nanobioscience 5:251-262.
Kohli N, Westerveld DR, Ayache AC, Verma A, Shil P, Prasad T, Zhu P, Chan SL, Li Q, Daniell H (2014) Oral delivery of bioencapsulated proteins across blood-brain and blood-retinal barriers. Molecular therapy : the journal of the American Society of Gene Therapy 22:535-546.
Kojetin DJ, Venters RA, Kordys DR, Thompson RJ, Kumar R, Cavanagh J (2006) Structure, binding interface and hydrophobic transitions of Ca2+-loaded calbindin-D(28K). Nature structural & molecular biology 13:641-647.
Kollarik M, Carr MJ, Ru F, Ring CJ, Hart VJ, Murdock P, Myers AC, Muroi Y, Undem BJ (2010) Transgene expression and effective gene silencing in vagal afferent neurons in vivo using recombinant adeno-associated virus vectors. The Journal of physiology 588:4303-4315.
Kordys DR, Bobay BG, Thompson RJ, Venters RA, Cavanagh J (2007) Peptide binding proclivities of calcium loaded calbindin-D28k. FEBS letters 581:4778-4782.

Kozireski-Chuback D, Wu G, Ledeen RW (1999) Developmental appearance of nuclear GM1 in neurons of the central and peripheral nervous systems. Brain research Developmental brain research 115:201-208.
Kremer EJ, Boutin S, Chillon M, Danos O (2000) Canine adenovirus vectors: an alternative for adenovirus-mediated gene transfer. Journal of virology 74:505-512.
Kretsinger RH, Nockolds CE (1973) Carp muscle calcium-binding protein. II. Structure determination and general description. The Journal of biological chemistry 248:3313-3326.
Kreutz F, Frozza RL, Breier AC, de Oliveira VA, Horn AP, Pettenuzzo LF, Netto CA, Salbego CG, Trindade VM (2011) Amyloid-beta induced toxicity involves ganglioside expression and is sensitive to GM1 neuroprotective action. Neurochemistry international 59:648-655.
Kuffler SW, Hunt CC, Quilliam JP (1951) Function of medullated small-nerve fibers in mammalian ventral roots; efferent muscle spindle innervation. Journal of neurophysiology 14:29-54.
Kunzelmann K, Mall M (2002) Electrolyte transport in the mammalian colon: mechanisms and implications for disease. Physiological reviews 82:245-289.
Kuwajima K, Sakuraoka A, Fueki S, Yoneyama M, Sugai S (1988) Folding of carp parvalbumin studied by equilibrium and kinetic circular dichroism spectra. Biochemistry 27:7419-7428.
Kuznicki J, Strauss KI, Jacobowitz DM (1995) Conformational changes and calcium binding by calretinin and its recombinant fragments containing different sets of EF hand motifs. Biochemistry 34:15389-15394.
Kwak S, Kawahara Y (2005) Deficient RNA editing of GluR2 and neuronal death in amyotropic lateral sclerosis. Journal of molecular medicine 83:110-120.
Kwiatkowski TJ, Jr. et al. (2009) Mutations in the FUS/TLS gene on chromosome 16 cause familial amyotrophic lateral sclerosis. Science 323:1205-1208.
Kwon KC, Nityanandam R, New JS, Daniell H (2013) Oral delivery of bioencapsulated exendin-4 expressed in chloroplasts lowers blood glucose level in mice and stimulates insulin secretion in beta-TC6 cells. Plant biotechnology journal 11:77-86.
Lagier-Tourenne C et al. (2012) Divergent roles of ALS-linked proteins FUS/TLS and TDP-43 intersect in processing long pre-mRNAs. Nature neuroscience 15:1488-1497.
Laitinen OH, Nordlund HR, Hytonen VP, Kulomaa MS (2007) Brave new (strept)avidins in biotechnology. Trends in biotechnology 25:269-277.
Lang K, Chin JW (2014) Cellular incorporation of unnatural amino acids and bioorthogonal labeling of proteins. Chemical reviews 114:4764-4806.
Leal SS, Gomes CM (2015) Calcium dysregulation links ALS defective proteins and motor neuron selective vulnerability. Frontiers in cellular neuroscience 9:225.
Lebens M, Johansson S, Osek J, Lindblad M, Holmgren J (1993) Large-scale production of Vibrio cholerae toxin B subunit for use in oral vaccines. Bio/technology 11:1574-1578.
Ledeen R, Wu G (2007) GM1 in the nuclear envelope regulates nuclear calcium through association with a nuclear sodium-calcium exchanger. Journal of neurochemistry 103:126-134.
Ledeen RW, Wu G, Lu ZH, Kozireski-Chuback D, Fang Y (1998) The role of GM1 and other gangliosides in neuronal differentiation. Overview and new finding. Annals of the New York Academy of Sciences 845:161-175.
Lee EB, Lee VM, Trojanowski JQ (2012) Gains or losses: molecular mechanisms of TDP43-mediated neurodegeneration. Nature reviews Neuroscience 13:38-50.
Lee JH, Gleeson JG (2010) The role of primary cilia in neuronal function. Neurobiology of disease 38:167-172.

Lee SH, Schwaller B, Neher E (2000a) Kinetics of Ca2+ binding to parvalbumin in bovine chromaffin cells: implications for [Ca2+] transients of neuronal dendrites. The Journal of physiology 525 Pt 2:419-432.

Lee SH, Rosenmund C, Schwaller B, Neher E (2000b) Differences in Ca2+ buffering properties between excitatory and inhibitory hippocampal neurons from the rat. The Journal of physiology 525 Pt 2:405-418.

Leinenga G, Gotz J (2015) Scanning ultrasound removes amyloid-beta and restores memory in an Alzheimer's disease mouse model. Science translational medicine 7:278ra233.

Lemmens R, Moore MJ, Al-Chalabi A, Brown RH, Jr., Robberecht W (2010) RNA metabolism and the pathogenesis of motor neuron diseases. Trends in neurosciences 33:249-258.

Lencer WI, Tsai B (2003) The intracellular voyage of cholera toxin: going retro. Trends in biochemical sciences 28:639-645.

Lencer WI, Constable C, Moe S, Jobling MG, Webb HM, Ruston S, Madara JL, Hirst TR, Holmes RK (1995) Targeting of cholera toxin and Escherichia coli heat labile toxin in polarized epithelia: role of COOH-terminal KDEL. The Journal of cell biology 131:951-962.

Levine TP, Daniels RD, Gatta AT, Wong LH, Hayes MJ (2013) The product of C9orf72, a gene strongly implicated in neurodegeneration, is structurally related to DENN Rab-GEFs. Bioinformatics 29:499-503.

Lewis DJ, Huo Z, Barnett S, Kromann I, Giemza R, Galiza E, Woodrow M, Thierry-Carstensen B, Andersen P, Novicki D, Del Giudice G, Rappuoli R (2009) Transient facial nerve paralysis (Bell's palsy) following intranasal delivery of a genetically detoxified mutant of Escherichia coli heat labile toxin. PloS one 4:e6999.

Li J, Faber M, Papaneri A, Faber ML, McGettigan JP, Schnell MJ, Dietzschold B (2006) A single immunization with a recombinant canine adenovirus expressing the rabies virus G protein confers protective immunity against rabies in mice. Virology 356:147-154.

Li S, Wei Z, Chen J, Chen Y, Lv Z, Yu W, Meng Q, Jin Y (2014) Oral administration of a fusion protein between the cholera toxin B subunit and the 42-amino acid isoform of amyloid-beta peptide produced in silkworm pupae protects against Alzheimer's disease in mice. PloS one 9:e113585.

Libbrecht S, Van den Haute C, Malinouskaya L, Gijsbers R, Baekelandt V (2016) Evaluation of WGA-Cre-dependent topological transgene expression in the rodent brain. Brain structure & function.

Lillo P, Hodges JR (2009) Frontotemporal dementia and motor neurone disease: overlapping clinic-pathological disorders. Journal of clinical neuroscience : official journal of the Neurosurgical Society of Australasia 16:1131-1135.

Limaye A, Koya V, Samsam M, Daniell H (2006) Receptor-mediated oral delivery of a bioencapsulated green fluorescent protein expressed in transgenic chloroplasts into the mouse circulatory system. FASEB journal : official publication of the Federation of American Societies for Experimental Biology 20:959-961.

Lin H, Zhai J, Schlaepfer WW (2005) RNA-binding protein is involved in aggregation of light neurofilament protein and is implicated in the pathogenesis of motor neuron degeneration. Human molecular genetics 14:3643-3659.

Linden RM, Ward P, Giraud C, Winocour E, Berns KI (1996) Site-specific integration by adeno-associated virus. Proceedings of the National Academy of Sciences of the United States of America 93:11288-11294.

Lindh B, Aldskogius H, Hokfelt T (1989) Simultaneous immunohistochemical demonstration of intra-axonally transported markers and neuropeptides in the peripheral nervous system of the guinea pig. Histochemistry 92:367-376.

Liu CC, Schultz PG (2010) Adding new chemistries to the genetic code. Annual review of biochemistry 79:413-444.

Liu D, Thangnipon W, McAdoo DJ (1991) Excitatory amino acids rise to toxic levels upon impact injury to the rat spinal cord. Brain research 547:344-348.

Liu H, Llewellyn-Smith IJ, Basbaum AI (1995) Co-injection of wheat germ agglutinin-HRP and choleragenoid-HRP into the sciatic nerve of the rat blocks transganglionic transport. The journal of histochemistry and cytochemistry : official journal of the Histochemistry Society 43:489-495.

Liu ZL, Wu X, Luo YJ, Wang L, Qu WM, Li SQ, Huang ZL (2016) Signaling mechanism underlying the histamine-modulated action of hypoglossal motoneurons. Journal of neurochemistry 137:277-286.

Llewellyn-Smith IJ, Minson JB, Wright AP, Hodgson AJ (1990) Cholera toxin B-gold, a retrograde tracer that can be used in light and electron microscopic immunocytochemical studies. The Journal of comparative neurology 294:179-191.

Llewellyn-Smith IJ, Martin CL, Arnolda LF, Minson JB (1999) Retrogradely transported CTB-saporin kills sympathetic preganglionic neurons. Neuroreport 10:307-312.

Llewellyn-Smith IJ, Martin CL, Arnolda LF, Minson JB (2000) Tracer-toxins: cholera toxin B-saporin as a model. Journal of neuroscience methods 103:83-90.

Logroscino G, Traynor BJ, Hardiman O, Chio A, Couratier P, Mitchell JD, Swingler RJ, Beghi E, Eurals (2008) Descriptive epidemiology of amyotrophic lateral sclerosis: new evidence and unsolved issues. Journal of neurology, neurosurgery, and psychiatry 79:6-11.

Logroscino G, Traynor BJ, Hardiman O, Chio A, Mitchell D, Swingler RJ, Millul A, Benn E, Beghi E, Eurals (2010) Incidence of amyotrophic lateral sclerosis in Europe. Journal of neurology, neurosurgery, and psychiatry 81:385-390.

Lopes CD, Oliveira H, Estevao I, Pires LR, Pego AP (2016) In vivo targeted gene delivery to peripheral neurons mediated by neurotropic poly(ethylene imine)-based nanoparticles. International journal of nanomedicine 11:2675-2683.

Lorieau JL, Louis JM, Schwieters CD, Bax A (2012) pH-triggered, activated-state conformations of the influenza hemagglutinin fusion peptide revealed by NMR. Proceedings of the National Academy of Sciences of the United States of America 109:19994-19999.

Louboutin JP, Chekmasova AA, Marusich E, Chowdhury JR, Strayer DS (2010) Efficient CNS gene delivery by intravenous injection. Nature methods 7:905-907.

Lujan HL, Palani G, Peduzzi JD, DiCarlo SE (2010) Targeted ablation of mesenteric projecting sympathetic neurons reduces the hemodynamic response to pain in conscious, spinal cord-transected rats. American journal of physiology Regulatory, integrative and comparative physiology 298:R1358-1365.

Lujan HL, Palani G, Chen Y, Peduzzi JD, Dicarlo SE (2009) Targeted ablation of cardiac sympathetic neurons reduces resting, reflex and exercise-induced sympathetic activation in conscious rats. American journal of physiology Heart and circulatory physiology 296:H1305-1311.

Luppi PH, Fort P, Jouvet M (1990) Iontophoretic application of unconjugated cholera toxin B subunit (CTb) combined with immunohistochemistry of neurochemical substances: a method for transmitter identification of retrogradely labeled neurons. Brain research 534:209-224.

Luppi PH, Sakai K, Salvert D, Fort P, Jouvet M (1987) Peptidergic hypothalamic afferents to the cat nucleus raphe pallidus as revealed by a double immunostaining technique using unconjugated cholera toxin as a retrograde tracer. Brain research 402:339-345.

Luquin N, Sierra S, Rico AJ, Gomez-Bautista V, Roda E, Conte-Perales L, Franco R, McCormick P, Labandeira-Garcia JL, Lanciego JL (2012) Unmasking adenosine 2A receptors (A2ARs) in monkey basal ganglia output neurons using cholera toxin subunit B (CTB). Neurobiology of disease 47:347-357.

Lutz W, Frank EM, Craig TA, Thompson R, Venters RA, Kojetin D, Cavanagh J, Kumar R (2003) Calbindin D28K interacts with Ran-binding protein M: identification of

interacting domains by NMR spectroscopy. Biochemical and biophysical research communications 303:1186-1192.
Ma Y (2016) Recent advances in nontoxic Escherichia coli heat-labile toxin and its derivative adjuvants. Expert review of vaccines:1-11.
MacDermott AB, Mayer ML, Westbrook GL, Smith SJ, Barker JL (1986) NMDA-receptor activation increases cytoplasmic calcium concentration in cultured spinal cord neurones. Nature 321:519-522.
MacKenzie CR, Hirama T, Lee KK, Altman E, Young NM (1997) Quantitative analysis of bacterial toxin affinity and specificity for glycolipid receptors by surface plasmon resonance. The Journal of biological chemistry 272:5533-5538.
Majoul IV, Bastiaens PI, Soling HD (1996) Transport of an external Lys-Asp-Glu-Leu (KDEL) protein from the plasma membrane to the endoplasmic reticulum: studies with cholera toxin in Vero cells. The Journal of cell biology 133:777-789.
Majounie E et al. (2012) Frequency of the C9orf72 hexanucleotide repeat expansion in patients with amyotrophic lateral sclerosis and frontotemporal dementia: a cross-sectional study. The Lancet Neurology 11:323-330.
Mangione AS, Obara I, Maiaru M, Geranton SM, Tassorelli C, Ferrari E, Leese C, Davletov B, Hunt SP (2016) Nonparalytic botulinum molecules for the control of pain. Pain 157:1045-1055.
Marconi S, De Toni L, Lovato L, Tedeschi E, Gaetti L, Acler M, Bonetti B (2005) Expression of gangliosides on glial and neuronal cells in normal and pathological adult human brain. Journal of neuroimmunology 170:115-121.
Martin MR, Lodge D (1977) Morphology of the facial nucleus of the rat. Brain research 123:1-12.
Marttila AT, Hytonen VP, Laitinen OH, Bayer EA, Wilchek M, Kulomaa MS (2003) Mutation of the important Tyr-33 residue of chicken avidin: functional and structural consequences. The Biochemical journal 369:249-254.
Mason MR, Ehlert EM, Eggers R, Pool CW, Hermening S, Huseinovic A, Timmermans E, Blits B, Verhaagen J (2010) Comparison of AAV serotypes for gene delivery to dorsal root ganglion neurons. Molecular therapy : the journal of the American Society of Gene Therapy 18:715-724.
Matlack KE, Mothes W, Rapoport TA (1998) Protein translocation: tunnel vision. Cell 92:381-390.
Matsushita M, Ragnarson B, Grant G (1991) Topographic relationship between sagittal Purkinje cell bands revealed by a monoclonal antibody to zebrin I and spinocerebellar projections arising from the central cervical nucleus in the rat. Experimental brain research 84:133-141.
Mattson MP, Rychlik B, Chu C, Christakos S (1991) Evidence for calcium-reducing and excito-protective roles for the calcium-binding protein calbindin-D28k in cultured hippocampal neurons. Neuron 6:41-51.
Mayer G, Boileau G, Bendayan M (2004) The proprotein convertase furin colocalizes with caveolin-1 in the Golgi apparatus and endosomes of hepatocytes. Cell and tissue research 316:55-63.
Mazarakis ND, Azzouz M, Rohll JB, Ellard FM, Wilkes FJ, Olsen AL, Carter EE, Barber RD, Baban DF, Kingsman SM, Kingsman AJ, O'Malley K, Mitrophanous KA (2001) Rabies virus glycoprotein pseudotyping of lentiviral vectors enables retrograde axonal transport and access to the nervous system after peripheral delivery. Human molecular genetics 10:2109-2121.
McAllen RM, Spyer KM (1978) Two types of vagal preganglionic motoneurones projecting to the heart and lungs. The Journal of physiology 282:353-364.
McCarty DM, Monahan PE, Samulski RJ (2001) Self-complementary recombinant adeno-associated virus (scAAV) vectors promote efficient transduction independently of DNA synthesis. Gene therapy 8:1248-1254.
McDannold N, Arvanitis CD, Vykhodtseva N, Livingstone MS (2012) Temporary disruption of the blood-brain barrier by use of ultrasound and microbubbles:

safety and efficacy evaluation in rhesus macaques. Cancer research 72:3652-3663.
Merritt EA, Hol WG (1995) AB5 toxins. Current opinion in structural biology 5:165-171.
Merritt EA, Sixma TK, Kalk KH, van Zanten BA, Hol WG (1994a) Galactose-binding site in Escherichia coli heat-labile enterotoxin (LT) and cholera toxin (CT). Molecular microbiology 13:745-753.
Merritt EA, Sarfaty S, van den Akker F, L'Hoir C, Martial JA, Hol WG (1994b) Crystal structure of cholera toxin B-pentamer bound to receptor GM1 pentasaccharide. Protein science : a publication of the Protein Society 3:166-175.
Meunier FA, Lisk G, Sesardic D, Dolly JO (2003) Dynamics of motor nerve terminal remodeling unveiled using SNARE-cleaving botulinum toxins: the extent and duration are dictated by the sites of SNAP-25 truncation. Molecular and cellular neurosciences 22:454-466.
Miller TM, Kaspar BK, Kops GJ, Yamanaka K, Christian LJ, Gage FH, Cleveland DW (2005) Virus-delivered small RNA silencing sustains strength in amyotrophic lateral sclerosis. Annals of neurology 57:773-776.
Mishina M, Sakimura K, Mori H, Kushiya E, Harabayashi M, Uchino S, Nagahari K (1991) A single amino acid residue determines the Ca2+ permeability of AMPA-selective glutamate receptor channels. Biochemical and biophysical research communications 180:813-821.
Mobius W, Herzog V, Sandhoff K, Schwarzmann G (1999) Gangliosides are transported from the plasma membrane to intralysosomal membranes as revealed by immuno-electron microscopy. Bioscience reports 19:307-316.
Montecucco C, Schiavo G, Dasgupta BR (1989) Effect of pH on the interaction of botulinum neurotoxins A, B and E with liposomes. The Biochemical journal 259:47-53.
Moore P, He K, Tsai B (2013) Establishment of an in vitro transport assay that reveals mechanistic differences in cytosolic events controlling cholera toxin and T-cell receptor alpha retro-translocation. PloS one 8:e75801.
Mosier DR, Baldelli P, Delbono O, Smith RG, Alexianu ME, Appel SH, Stefani E (1995) Amyotrophic lateral sclerosis immunoglobulins increase Ca2+ currents in a motoneuron cell line. Annals of neurology 37:102-109.
Moss J, Richardson SH (1978) Activation of adenylate cyclase by heat-labile Escherichia coli enterotoxin. Evidence for ADP-ribosyltransferase activity similar to that of choleragen. The Journal of clinical investigation 62:281-285.
Mu L, Sanders I (2010) Human tongue neuroanatomy: Nerve supply and motor endplates. Clinical anatomy 23:777-791.
Mullen RJ, Buck CR, Smith AM (1992) NeuN, a neuronal specific nuclear protein in vertebrates. Development 116:201-211.
Muller M, Felmy F, Schwaller B, Schneggenburger R (2007) Parvalbumin is a mobile presynaptic Ca2+ buffer in the calyx of Held that accelerates the decay of Ca2+ and short-term facilitation. The Journal of neuroscience : the official journal of the Society for Neuroscience 27:2261-2271.
Mutoh T, Tokuda A, Miyadai T, Hamaguchi M, Fujiki N (1995) Ganglioside GM1 binds to the Trk protein and regulates receptor function. Proceedings of the National Academy of Sciences of the United States of America 92:5087-5091.
Nagy D, Kato T, Kushner PD (1994) Reactive astrocytes are widespread in the cortical gray matter of amyotrophic lateral sclerosis. Journal of neuroscience research 38:336-347.
Nani F, Cifra A, Nistri A (2010) Transient oxidative stress evokes early changes in the functional properties of neonatal rat hypoglossal motoneurons in vitro. The European journal of neuroscience 31:951-966.
Neumann M, Sampathu DM, Kwong LK, Truax AC, Micsenyi MC, Chou TT, Bruce J, Schuck T, Grossman M, Clark CM, McCluskey LF, Miller BL, Masliah E, Mackenzie IR, Feldman H, Feiden W, Kretzschmar HA, Trojanowski JQ, Lee

VM (2006) Ubiquitinated TDP-43 in frontotemporal lobar degeneration and amyotrophic lateral sclerosis. Science 314:130-133.
Neuzeret PC, Sakai K, Gormand F, Petitjean T, Buda C, Sastre JP, Parrot S, Guidon G, Lin JS (2009) Application of histamine or serotonin to the hypoglossal nucleus increases genioglossus muscle activity across the wake-sleep cycle. Journal of sleep research 18:113-121.
Ngo JT, Adams SR, Deerinck TJ, Boassa D, Rodriguez-Rivera F, Palida SF, Bertozzi CR, Ellisman MH, Tsien RY (2016) Click-EM for imaging metabolically tagged nonprotein biomolecules. Nature chemical biology 12:459-465.
Nicholls DG, Scott ID (1980) The regulation of brain mitochondrial calcium-ion transport. The role of ATP in the discrimination between kinetic and membrane-potential-dependent calcium-ion efflux mechanisms. The Biochemical journal 186:833-839.
Nichols NL, Vinit S, Bauernschmidt L, Mitchell GS (2015) Respiratory function after selective respiratory motor neuron death from intrapleural CTB-saporin injections. Experimental neurology 267:18-29.
Nicholson DW, Ali A, Thornberry NA, Vaillancourt JP, Ding CK, Gallant M, Gareau Y, Griffin PR, Labelle M, Lazebnik YA, et al. (1995) Identification and inhibition of the ICE/CED-3 protease necessary for mammalian apoptosis. Nature 376:37-43.
Niewoehner J, Bohrmann B, Collin L, Urich E, Sade H, Maier P, Rueger P, Stracke JO, Lau W, Tissot AC, Loetscher H, Ghosh A, Freskgard PO (2014) Increased brain penetration and potency of a therapeutic antibody using a monovalent molecular shuttle. Neuron 81:49-60.
Niikura K, Horisawa K, Doi N (2015) A fusogenic peptide from a sea urchin fertilization protein promotes intracellular delivery of biomacromolecules by facilitating endosomal escape. Journal of controlled release : official journal of the Controlled Release Society 212:85-93.
Niikura K, Horisawa K, Doi N (2016) Endosomal escape efficiency of fusogenic B18 and B55 peptides fused with anti-EGFR single chain Fv as estimated by nuclear translocation. Journal of biochemistry 159:123-132.
Nikic I, Kang JH, Girona GE, Aramburu IV, Lemke EA (2015) Labeling proteins on live mammalian cells using click chemistry. Nature protocols 10:780-791.
Nishiki T, Tokuyama Y, Kamata Y, Nemoto Y, Yoshida A, Sato K, Sekiguchi M, Takahashi M, Kozaki S (1996) The high-affinity binding of Clostridium botulinum type B neurotoxin to synaptotagmin II associated with gangliosides GT1b/GD1a. FEBS letters 378:253-257.
Nishimoto Y, Koga M, Kamijo M, Hirata K, Yuki N (2004) Immunoglobulin improves a model of acute motor axonal neuropathy by preventing axonal degeneration. Neurology 62:1939-1944.
Nishimura H, Oomura Y (1987) Effects of hypothalamic stimulation on activity of dorsomedial medulla neurons that respond to subdiaphragmatic vagal stimulation. Journal of neurophysiology 58:655-675.
Nishio M, Fukumoto S, Furukawa K, Ichimura A, Miyazaki H, Kusunoki S, Urano T, Furukawa K (2004) Overexpressed GM1 suppresses nerve growth factor (NGF) signals by modulating the intracellular localization of NGF receptors and membrane fluidity in PC12 cells. The Journal of biological chemistry 279:33368-33378.
Noel G, Tham DK, Moukhles H (2009) Interdependence of laminin-mediated clustering of lipid rafts and the dystrophin complex in astrocytes. The Journal of biological chemistry 284:19694-19704.
Northrup RS, Fauci AS (1972) Adjuvant effect of cholera enterotoxin on the immune response of the mouse to sheep red blood cells. The Journal of infectious diseases 125:672-673.
O'Hanlon GM, Paterson GJ, Wilson G, Doyle D, McHardie P, Willison HJ (1996) Anti-GM1 ganglioside antibodies cloned from autoimmune neuropathy patients show

diverse binding patterns in the rodent nervous system. Journal of neuropathology and experimental neurology 55:184-195.
Odagiri K, Katoh H, Kawashima H, Tanaka T, Ohtani H, Saotome M, Urushida T, Satoh H, Hayashi H (2009) Local control of mitochondrial membrane potential, permeability transition pore and reactive oxygen species by calcium and calmodulin in rat ventricular myocytes. Journal of molecular and cellular cardiology 46:989-997.
Ogawa-Goto K, Funamoto N, Ohta Y, Abe T, Nagashima K (1992) Myelin gangliosides of human peripheral nervous system: an enrichment of GM1 in the motor nerve myelin isolated from cauda equina. Journal of neurochemistry 59:1844-1849.
Olinger E, Schwaller B, Loffing J, Gailly P, Devuyst O (2012) Parvalbumin: calcium and magnesium buffering in the distal nephron. Nephrology, dialysis, transplantation : official publication of the European Dialysis and Transplant Association - European Renal Association 27:3988-3994.
Oliveira AL, Hydling F, Olsson E, Shi T, Edwards RH, Fujiyama F, Kaneko T, Hokfelt T, Cullheim S, Meister B (2003) Cellular localization of three vesicular glutamate transporter mRNAs and proteins in rat spinal cord and dorsal root ganglia. Synapse 50:117-129.
Oliveira H, Fernandez R, Pires LR, Martins MC, Simoes S, Barbosa MA, Pego AP (2010) Targeted gene delivery into peripheral sensorial neurons mediated by self-assembled vectors composed of poly(ethylene imine) and tetanus toxin fragment c. Journal of controlled release : official journal of the Controlled Release Society 143:350-358.
Orlandi PA, Fishman PH (1998) Filipin-dependent inhibition of cholera toxin: evidence for toxin internalization and activation through caveolae-like domains. The Journal of cell biology 141:905-915.
Ou SH, Wu F, Harrich D, Garcia-Martinez LF, Gaynor RB (1995) Cloning and characterization of a novel cellular protein, TDP-43, that binds to human immunodeficiency virus type 1 TAR DNA sequence motifs. Journal of virology 69:3584-3596.
Oudega M, Varon S, Hagg T (1994) Distribution of corticospinal motor neurons in the postnatal rat: quantitative evidence for massive collateral elimination and modest cell death. The Journal of comparative neurology 347:115-126.
Oyler GA, Higgins GA, Hart RA, Battenberg E, Billingsley M, Bloom FE, Wilson MC (1989) The identification of a novel synaptosomal-associated protein, SNAP-25, differentially expressed by neuronal subpopulations. The Journal of cell biology 109:3039-3052.
Paillard F (1997) Advantages of non-human adenoviruses versus human adenoviruses. Human gene therapy 8:2007-2009.
Papadeas ST, Kraig SE, O'Banion C, Lepore AC, Maragakis NJ (2011) Astrocytes carrying the superoxide dismutase 1 (SOD1G93A) mutation induce wild-type motor neuron degeneration in vivo. Proceedings of the National Academy of Sciences of the United States of America 108:17803-17808.
Paparounas K, O'Hanlon GM, O'Leary CP, Rowan EG, Willison HJ (1999) Anti-ganglioside antibodies can bind peripheral nerve nodes of Ranvier and activate the complement cascade without inducing acute conduction block in vitro. Brain : a journal of neurology 122 (Pt 5):807-816.
Pardridge WM, Eisenberg J, Yang J (1987) Human blood-brain barrier transferrin receptor. Metabolism: clinical and experimental 36:892-895.
Parker TL, Kesse WK, Mohamed AA, Afework M (1993) The innervation of the mammalian adrenal gland. Journal of anatomy 183 (Pt 2):265-276.
Pellizzari R, Rossetto O, Schiavo G, Montecucco C (1999) Tetanus and botulinum neurotoxins: mechanism of action and therapeutic uses. Philosophical transactions of the Royal Society of London Series B, Biological sciences 354:259-268.

Pepper DS (1994) Some alternative coupling chemistries for affinity chromatography. Molecular biotechnology 2:157-178.
Philips T, Robberecht W (2011) Neuroinflammation in amyotrophic lateral sclerosis: role of glial activation in motor neuron disease. The Lancet Neurology 10:253-263.
Philips T, Rothstein JD (2015) Rodent Models of Amyotrophic Lateral Sclerosis. Current protocols in pharmacology / editorial board, SJ Enna 69:5 67 61-21.
Pickett CL, Twiddy EM, Coker C, Holmes RK (1989) Cloning, nucleotide sequence, and hybridization studies of the type IIb heat-labile enterotoxin gene of Escherichia coli. Journal of bacteriology 171:4945-4952.
Picklo MJ, Wiley RG, Lappi DA, Robertson D (1994) Noradrenergic lesioning with an anti-dopamine beta-hydroxylase immunotoxin. Brain research 666:195-200.
Pillay S, Meyer NL, Puschnik AS, Davulcu O, Diep J, Ishikawa Y, Jae LT, Wosen JE, Nagamine CM, Chapman MS, Carette JE (2016) An essential receptor for adeno-associated virus infection. Nature 530:108-112.
Pirazzini M, Rossetto O, Bolognese P, Shone CC, Montecucco C (2011) Double anchorage to the membrane and intact inter-chain disulfide bond are required for the low pH induced entry of tetanus and botulinum neurotoxins into neurons. Cellular microbiology 13:1731-1743.
Pirozzi M, Quattrini A, Andolfi G, Dina G, Malaguti MC, Auricchio A, Rugarli EI (2006) Intramuscular viral delivery of paraplegin rescues peripheral axonopathy in a model of hereditary spastic paraplegia. The Journal of clinical investigation 116:202-208.
Porath J (1992) Immobilized metal ion affinity chromatography. Protein expression and purification 3:263-281.
Prendergast J, Umanah GK, Yoo SW, Lagerlof O, Motari MG, Cole RN, Huganir RL, Dawson TM, Dawson VL, Schnaar RL (2014) Ganglioside regulation of AMPA receptor trafficking. The Journal of neuroscience : the official journal of the Society for Neuroscience 34:13246-13258.
Price CJ, Hoyda TD, Ferguson AV (2008) The area postrema: a brain monitor and integrator of systemic autonomic state. The Neuroscientist : a review journal bringing neurobiology, neurology and psychiatry 14:182-194.
Prinetti A, Chigorno V, Mauri L, Loberto N, Sonnino S (2007) Modulation of cell functions by glycosphingolipid metabolic remodeling in the plasma membrane. Journal of neurochemistry 103 Suppl 1:113-125.
Rabin SJ, Mocchetti I (1995) GM1 Ganglioside Activates the High-Affinity Nerve Growth Factor Receptor trkA. Journal of neurochemistry 65:347-354.
Ralph GS, Radcliffe PA, Day DM, Carthy JM, Leroux MA, Lee DC, Wong LF, Bilsland LG, Greensmith L, Kingsman SM, Mitrophanous KA, Mazarakis ND, Azzouz M (2005) Silencing mutant SOD1 using RNAi protects against neurodegeneration and extends survival in an ALS model. Nature medicine 11:429-433.
Reichow SL, Korotkov KV, Hol WG, Gonen T (2010) Structure of the cholera toxin secretion channel in its closed state. Nature structural & molecular biology 17:1226-1232.
Reilly MP, McKenzie SE (2002) Mechanisms of action of IVIg: physiology of Fc receptors. Vox sanguinis 83 Suppl 1:57-63.
Remmers JE, deGroot WJ, Sauerland EK, Anch AM (1978) Pathogenesis of upper airway occlusion during sleep. Journal of applied physiology: respiratory, environmental and exercise physiology 44:931-938.
Renton AE et al. (2011) A hexanucleotide repeat expansion in C9ORF72 is the cause of chromosome 9p21-linked ALS-FTD. Neuron 72:257-268.
Restani L, Antonucci F, Gianfranceschi L, Rossi C, Rossetto O, Caleo M (2011) Evidence for anterograde transport and transcytosis of botulinum neurotoxin A (BoNT/A). The Journal of neuroscience : the official journal of the Society for Neuroscience 31:15650-15659.

Ringholz GM, Appel SH, Bradshaw M, Cooke NA, Mosnik DM, Schulz PE (2005) Prevalence and patterns of cognitive impairment in sporadic ALS. Neurology 65:586-590.
Robberecht W, Philips T (2013) The changing scene of amyotrophic lateral sclerosis. Nature reviews Neuroscience 14:248-264.
Rogers JH (1987) Calretinin: a gene for a novel calcium-binding protein expressed principally in neurons. The Journal of cell biology 105:1343-1353.
Roos A, Boron WF (1981) Intracellular pH. Physiological reviews 61:296-434.
Rosen DR, Siddique T, Patterson D, Figlewicz DA, Sapp P, Hentati A, Donaldson D, Goto J, O'Regan JP, Deng HX, et al. (1993) Mutations in Cu/Zn superoxide dismutase gene are associated with familial amyotrophic lateral sclerosis. Nature 362:59-62.
Ross J (2013) PhD Thesis. In: University of Leeds.
Rossetto O, Caccin P, Rigoni M, Tonello F, Bortoletto N, Stevens RC, Montecucco C (2001) Active-site mutagenesis of tetanus neurotoxin implicates TYR-375 and GLU-271 in metalloproteolytic activity. Toxicon : official journal of the International Society on Toxinology 39:1151-1159.
Rostovtsev VV, Green LG, Fokin VV, Sharpless KB (2002) A stepwise huisgen cycloaddition process: copper(I)-catalyzed regioselective "ligation" of azides and terminal alkynes. Angewandte Chemie 41:2596-2599.
Rothstein JD, Martin LJ, Kuncl RW (1992) Decreased glutamate transport by the brain and spinal cord in amyotrophic lateral sclerosis. The New England journal of medicine 326:1464-1468.
Ruhlman T, Ahangari R, Devine A, Samsam M, Daniell H (2007) Expression of cholera toxin B-proinsulin fusion protein in lettuce and tobacco chloroplasts--oral administration protects against development of insulitis in non-obese diabetic mice. Plant biotechnology journal 5:495-510.
Rummel A, Bade S, Alves J, Bigalke H, Binz T (2003) Two carbohydrate binding sites in the H(CC)-domain of tetanus neurotoxin are required for toxicity. Journal of molecular biology 326:835-847.
Rummel A, Karnath T, Henke T, Bigalke H, Binz T (2004) Synaptotagmins I and II act as nerve cell receptors for botulinum neurotoxin G. The Journal of biological chemistry 279:30865-30870.
Rydzanicz R, Zhao XS, Johnson PE (2005) Assembly PCR oligo maker: a tool for designing oligodeoxynucleotides for constructing long DNA molecules for RNA production. Nucleic acids research 33:W521-525.
Salic A, Mitchison TJ (2008) A chemical method for fast and sensitive detection of DNA synthesis in vivo. Proceedings of the National Academy of Sciences of the United States of America 105:2415-2420.
Salinas S, Bilsland LG, Henaff D, Weston AE, Keriel A, Schiavo G, Kremer EJ (2009) CAR-associated vesicular transport of an adenovirus in motor neuron axons. PLoS pathogens 5:e1000442.
Sama RR, Ward CL, Bosco DA (2014) Functions of FUS/TLS from DNA repair to stress response: implications for ALS. ASN neuro 6.
Samulski RJ, Berns KI, Tan M, Muzyczka N (1982) Cloning of adeno-associated virus into pBR322: rescue of intact virus from the recombinant plasmid in human cells. Proceedings of the National Academy of Sciences of the United States of America 79:2077-2081.
Sanchez J, Holmgren J (2005) Virulence factors, pathogenesis and vaccine protection in cholera and ETEC diarrhea. Current opinion in immunology 17:388-398.
Sanchez J, Holmgren J (2008) Cholera toxin structure, gene regulation and pathophysiological and immunological aspects. Cellular and molecular life sciences : CMLS 65:1347-1360.
Sanders TH, Jaeger D (2016) Optogenetic stimulation of cortico-subthalamic projections is sufficient to ameliorate bradykinesia in 6-ohda lesioned mice. Neurobiology of disease 95:225-237.

Sanger F, Coulson AR (1975) A rapid method for determining sequences in DNA by primed synthesis with DNA polymerase. Journal of molecular biology 94:441-448.

Sanger F, Nicklen S, Coulson AR (1977) DNA sequencing with chain-terminating inhibitors. Proceedings of the National Academy of Sciences of the United States of America 74:5463-5467.

Sano T, Pandori MW, Chen X, Smith CL, Cantor CR (1995) Recombinant core streptavidins. A minimum-sized core streptavidin has enhanced structural stability and higher accessibility to biotinylated macromolecules. The Journal of biological chemistry 270:28204-28209.

Sasaki S (2011) Autophagy in spinal cord motor neurons in sporadic amyotrophic lateral sclerosis. Journal of neuropathology and experimental neurology 70:349-359.

Sattler R, Tymianski M (2000) Molecular mechanisms of calcium-dependent excitotoxicity. Journal of molecular medicine 78:3-13.

Savidge JR, Ranasinghe SP, Rang HP (2001) Comparison of intracellular calcium signals evoked by heat and capsaicin in cultured rat dorsal root ganglion neurons and in a cell line expressing the rat vanilloid receptor, VR1. Neuroscience 102:177-184.

Saxena S, Caroni P (2011) Selective neuronal vulnerability in neurodegenerative diseases: from stressor thresholds to degeneration. Neuron 71:35-48.

Schengrund CL, DasGupta BR, Ringler NJ (1991) Binding of botulinum and tetanus neurotoxins to ganglioside GT1b and derivatives thereof. Journal of neurochemistry 57:1024-1032.

Schepelmann K, Winter Y, Spottke AE, Claus D, Grothe C, Schroder R, Heuss D, Vielhaber S, Mylius V, Kiefer R, Schrank B, Oertel WH, Dodel R (2010) Socioeconomic burden of amyotrophic lateral sclerosis, myasthenia gravis and facioscapulohumeral muscular dystrophy. Journal of neurology 257:15-23.

Schiavo G, Matteoli M, Montecucco C (2000) Neurotoxins affecting neuroexocytosis. Physiological reviews 80:717-766.

Schiavo G, Rossetto O, Benfenati F, Poulain B, Montecucco C (1994a) Tetanus and botulinum neurotoxins are zinc proteases specific for components of the neuroexocytosis apparatus. Annals of the New York Academy of Sciences 710:65-75.

Schiavo G, Poulain B, Rossetto O, Benfenati F, Tauc L, Montecucco C (1992) Tetanus toxin is a zinc protein and its inhibition of neurotransmitter release and protease activity depend on zinc. The EMBO journal 11:3577-3583.

Schiavo G, Santucci A, Dasgupta BR, Mehta PP, Jontes J, Benfenati F, Wilson MC, Montecucco C (1993) Botulinum neurotoxins serotypes A and E cleave SNAP-25 at distinct COOH-terminal peptide bonds. FEBS letters 335:99-103.

Schiavo G, Malizio C, Trimble WS, Polverino de Laureto P, Milan G, Sugiyama H, Johnson EA, Montecucco C (1994b) Botulinum G neurotoxin cleaves VAMP/synaptobrevin at a single Ala-Ala peptide bond. The Journal of biological chemistry 269:20213-20216.

Schiffmann SN, Cheron G, Lohof A, d'Alcantara P, Meyer M, Parmentier M, Schurmans S (1999) Impaired motor coordination and Purkinje cell excitability in mice lacking calretinin. Proceedings of the National Academy of Sciences of the United States of America 96:5257-5262.

Schild JH, Clark JW, Hay M, Mendelowitz D, Andresen MC, Kunze DL (1994) A- and C-type rat nodose sensory neurons: model interpretations of dynamic discharge characteristics. Journal of neurophysiology 71:2338-2358.

Schmidt H, Arendt O, Brown EB, Schwaller B, Eilers J (2007) Parvalbumin is freely mobile in axons, somata and nuclei of cerebellar Purkinje neurones. Journal of neurochemistry 100:727-735.

Schmitz A, Herrgen H, Winkeler A, Herzog V (2000) Cholera toxin is exported from microsomes by the Sec61p complex. The Journal of cell biology 148:1203-1212.

Schnaar RL (2016) Gangliosides of the vertebrate nervous system. Journal of molecular biology.

Schnaar RL, Gerardy-Schahn R, Hildebrandt H (2014) Sialic acids in the brain: gangliosides and polysialic acid in nervous system development, stability, disease, and regeneration. Physiological reviews 94:461-518.

Schneider H, Groves M, Muhle C, Reynolds PN, Knight A, Themis M, Carvajal J, Scaravilli F, Curiel DT, Fairweather NF, Coutelle C (2000) Retargeting of adenoviral vectors to neurons using the Hc fragment of tetanus toxin. Gene therapy 7:1584-1592.

Schneider JS, Sendek S, Daskalakis C, Cambi F (2010) GM1 ganglioside in Parkinson's disease: Results of a five year open study. Journal of the neurological sciences 292:45-51.

Schneider JS, Gollomp SM, Sendek S, Colcher A, Cambi F, Du W (2013) A randomized, controlled, delayed start trial of GM1 ganglioside in treated Parkinson's disease patients. Journal of the neurological sciences 324:140-148.

Schoemaker MH, Rots MG, Beljaars L, Ypma AY, Jansen PL, Poelstra K, Moshage H, Haisma HJ (2008) PDGF-receptor beta-targeted adenovirus redirects gene transfer from hepatocytes to activated stellate cells. Molecular pharmaceutics 5:399-406.

Schwab ME, Suda K, Thoenen H (1979) Selective retrograde transsynaptic transfer of a protein, tetanus toxin, subsequent to its retrograde axonal transport. The Journal of cell biology 82:798-810.

Schwaller B (2010) Cytosolic Ca2+ buffers. Cold Spring Harbor perspectives in biology 2:a004051.

Schwaller B, Meyer M, Schiffmann S (2002) 'New' functions for 'old' proteins: the role of the calcium-binding proteins calbindin D-28k, calretinin and parvalbumin, in cerebellar physiology. Studies with knockout mice. Cerebellum 1:241-258.

Schwaller B, Durussel I, Jermann D, Herrmann B, Cox JA (1997) Comparison of the Ca2+-binding properties of human recombinant calretinin-22k and calretinin. The Journal of biological chemistry 272:29663-29671.

Schwanzel-Fukuda M, Morrell JI, Pfaff DW (1984) Localization of forebrain neurons which project directly to the medulla and spinal cord of the rat by retrograde tracing with wheat germ agglutinin. The Journal of comparative neurology 226:1-20.

Sears CL, Kaper JB (1996) Enteric bacterial toxins: mechanisms of action and linkage to intestinal secretion. Microbiological reviews 60:167-215.

Shalom O, Shalva N, Altschuler Y, Motro B (2008) The mammalian Nek1 kinase is involved in primary cilium formation. FEBS letters 582:1465-1470.

Sheikh KA, Deerinck TJ, Ellisman MH, Griffin JW (1999) The distribution of ganglioside-like moieties in peripheral nerves. Brain : a journal of neurology 122 (Pt 3):449-460.

Shigeri Y, Shimamoto K, Yasuda-Kamatani Y, Seal RP, Yumoto N, Nakajima T, Amara SG (2001) Effects of threo-beta-hydroxyaspartate derivatives on excitatory amino acid transporters (EAAT4 and EAAT5). Journal of neurochemistry 79:297-302.

Shimamoto K, Lebrun B, Yasuda-Kamatani Y, Sakaitani M, Shigeri Y, Yumoto N, Nakajima T (1998) DL-threo-beta-benzyloxyaspartate, a potent blocker of excitatory amino acid transporters. Molecular pharmacology 53:195-201.

Sim WS (2011) Application of botulinum toxin in pain management. The Korean journal of pain 24:1-6.

Simons K, Sampaio JL (2011) Membrane organization and lipid rafts. Cold Spring Harbor perspectives in biology 3:a004697.

Simpson LL (2004) Identification of the major steps in botulinum toxin action. Annual review of pharmacology and toxicology 44:167-193.

Sinclair D, Abba K, Zaman K, Qadri F, Graves PM (2011) Oral vaccines for preventing cholera. The Cochrane database of systematic reviews:CD008603.

Smith HO, Hutchison CA, 3rd, Pfannkoch C, Venter JC (2003) Generating a synthetic genome by whole genome assembly: phiX174 bacteriophage from synthetic oligonucleotides. Proceedings of the National Academy of Sciences of the United States of America 100:15440-15445.

Smits HH, Gloudemans AK, van Nimwegen M, Willart MA, Soullie T, Muskens F, de Jong EC, Boon L, Pilette C, Johansen FE, Hoogsteden HC, Hammad H, Lambrecht BN (2009) Cholera toxin B suppresses allergic inflammation through induction of secretory IgA. Mucosal immunology 2:331-339.

Sokoloff AJ, Deacon TW (1992) Musculotopic organization of the hypoglossal nucleus in the cynomolgus monkey, Macaca fascicularis. The Journal of comparative neurology 324:81-93.

Sonnino S, Mauri L, Chigorno V, Prinetti A (2007) Gangliosides as components of lipid membrane domains. Glycobiology 17:1R-13R.

Sooy K, Schermerhorn T, Noda M, Surana M, Rhoten WB, Meyer M, Fleischer N, Sharp GW, Christakos S (1999) Calbindin-D(28k) controls [Ca(2+)](i) and insulin release. Evidence obtained from calbindin-d(28k) knockout mice and beta cell lines. The Journal of biological chemistry 274:34343-34349.

Soudais C, Skander N, Kremer EJ (2004) Long-term in vivo transduction of neurons throughout the rat CNS using novel helper-dependent CAV-2 vectors. FASEB journal : official publication of the Federation of American Societies for Experimental Biology 18:391-393.

Soudais C, Laplace-Builhe C, Kissa K, Kremer EJ (2001) Preferential transduction of neurons by canine adenovirus vectors and their efficient retrograde transport in vivo. FASEB journal : official publication of the Federation of American Societies for Experimental Biology 15:2283-2285.

Soudais C, Boutin S, Hong SS, Chillon M, Danos O, Bergelson JM, Boulanger P, Kremer EJ (2000) Canine adenovirus type 2 attachment and internalization: coxsackievirus-adenovirus receptor, alternative receptors, and an RGD-independent pathway. Journal of virology 74:10639-10649.

Spitzbarth I, Cana A, Hahn K, Hansmann F, Baumgartner W (2015) Associated occurrence of p75 neurotrophin receptor expressing aldynoglia and microglia/macrophages in long term organotypic murine brain slice cultures. Brain research 1595:29-42.

Spreux-Varoquaux O, Bensimon G, Lacomblez L, Salachas F, Pradat PF, Le Forestier N, Marouan A, Dib M, Meininger V (2002) Glutamate levels in cerebrospinal fluid in amyotrophic lateral sclerosis: a reappraisal using a new HPLC method with coulometric detection in a large cohort of patients. Journal of the neurological sciences 193:73-78.

Spruill MM, Kuncl RW (2015) Calbindin-D28K is increased in the ventral horn of spinal cord by neuroprotective factors for motor neurons. Journal of neuroscience research 93:1184-1191.

Srivastava A, Lusby EW, Berns KI (1983) Nucleotide sequence and organization of the adeno-associated virus 2 genome. Journal of virology 45:555-564.

Staquicini FI et al. (2011) Systemic combinatorial peptide selection yields a non-canonical iron-mimicry mechanism for targeting tumors in a mouse model of human glioblastoma. The Journal of clinical investigation 121:161-173.

Stoeckel K, Schwab M, Thoenen H (1977) Role of gangliosides in the uptake and retrograde axonal transport of cholera and tetanus toxin as compared to nerve growth factor and wheat germ agglutinin. Brain research 132:273-285.

Stratmann T (2015) Cholera Toxin Subunit B as Adjuvant--An Accelerator in Protective Immunity and a Break in Autoimmunity. Vaccines 3:579-596.

Sugita M, Shiba Y (2005) Genetic tracing shows segregation of taste neuronal circuitries for bitter and sweet. Science 309:781-785.

Summerford C, Samulski RJ (1998) Membrane-associated heparan sulfate proteoglycan is a receptor for adeno-associated virus type 2 virions. Journal of virology 72:1438-1445.

Susuki K, Rasband MN, Tohyama K, Koibuchi K, Okamoto S, Funakoshi K, Hirata K, Baba H, Yuki N (2007) Anti-GM1 antibodies cause complement-mediated disruption of sodium channel clusters in peripheral motor nerve fibers. The Journal of neuroscience : the official journal of the Society for Neuroscience 27:3956-3967.

Svennerholm L, Bostrom K, Fredman P, Mansson JE, Rosengren B, Rynmark BM (1989) Human brain gangliosides: developmental changes from early fetal stage to advanced age. Biochimica et biophysica acta 1005:109-117.

Svennerholm L, Brane G, Karlsson I, Lekman A, Ramstrom I, Wikkelso C (2002) Alzheimer disease - effect of continuous intracerebroventricular treatment with GM1 ganglioside and a systematic activation programme. Dementia and geriatric cognitive disorders 14:128-136.

Swindells MB, Ikura M (1996) Pre-formation of the semi-open conformation by the apo-calmodulin C-terminal domain and implications binding IQ-motifs. Nature structural biology 3:501-504.

Takahashi S, Nakagawa T, Banno T, Watanabe T, Murakami K, Nakayama K (1995) Localization of furin to the trans-Golgi network and recycling from the cell surface involves Ser and Tyr residues within the cytoplasmic domain. The Journal of biological chemistry 270:28397-28401.

Takano K, Kirchner F, Gremmelt A, Matsuda M, Ozutsumi N, Sugimoto N (1989) Blocking effects of tetanus toxin and its fragment [A-B] on the excitatory and inhibitory synapses of the spinal motoneurone of the cat. Toxicon : official journal of the International Society on Toxinology 27:385-392.

Takeshima Y, Yagi M, Wada H, Matsuo M (2005) Intraperitoneal administration of phosphorothioate antisense oligodeoxynucleotide against splicing enhancer sequence induced exon skipping in dystrophin mRNA expressed in mdx skeletal muscle. Brain & development 27:488-493.

Tarsy D, Simon DK (2006) Dystonia. The New England journal of medicine 355:818-829.

Tettamanti G, Bonali F, Marchesini S, Zambotti V (1973) A new procedure for the extraction, purification and fractionation of brain gangliosides. Biochimica et biophysica acta 296:160-170.

Thalmann O et al. (2013) Complete mitochondrial genomes of ancient canids suggest a European origin of domestic dogs. Science 342:871-874.

Tidow H, Nissen P (2013) Structural diversity of calmodulin binding to its target sites. The FEBS journal 280:5551-5565.

Tinker JK, Erbe JL, Holmes RK (2005) Characterization of fluorescent chimeras of cholera toxin and Escherichia coli heat-labile enterotoxins produced by use of the twin arginine translocation system. Infection and immunity 73:3627-3635.

Toivonen JM, Olivan S, Osta R (2010) Tetanus toxin C-fragment: the courier and the cure? Toxins 2:2622-2644.

Ton-That H, Liu G, Mazmanian SK, Faull KF, Schneewind O (1999) Purification and characterization of sortase, the transpeptidase that cleaves surface proteins of Staphylococcus aureus at the LPXTG motif. Proceedings of the National Academy of Sciences of the United States of America 96:12424-12429.

Tordo N, Foumier A, Jallet C, Szelechowski M, Klonjkowski B, Eloit M (2008) Canine adenovirus based rabies vaccines. Developments in biologicals 131:467-476.

Torgersen ML, Skretting G, van Deurs B, Sandvig K (2001) Internalization of cholera toxin by different endocytic mechanisms. Journal of cell science 114:3737-3747.

Tornoe CW, Christensen C, Meldal M (2002) Peptidotriazoles on solid phase: [1,2,3]-triazoles by regiospecific copper(i)-catalyzed 1,3-dipolar cycloadditions of terminal alkynes to azides. The Journal of organic chemistry 67:3057-3064.

Towne C, Raoul C, Schneider BL, Aebischer P (2008) Systemic AAV6 delivery mediating RNA interference against SOD1: neuromuscular transduction does not alter disease progression in fALS mice. Molecular therapy : the journal of the American Society of Gene Therapy 16:1018-1025.

Towne C, Schneider BL, Kieran D, Redmond DE, Jr., Aebischer P (2010) Efficient transduction of non-human primate motor neurons after intramuscular delivery of recombinant AAV serotype 6. Gene therapy 17:141-146.

Troost D, Sillevis Smitt PA, de Jong JM, Swaab DF (1992) Neurofilament and glial alterations in the cerebral cortex in amyotrophic lateral sclerosis. Acta neuropathologica 84:664-673.

Troxler H, Kuster T, Rhyner JA, Gehrig P, Heizmann CW (1999) Electrospray ionization mass spectrometry: analysis of the Ca2+-binding properties of human recombinant alpha-parvalbumin and nine mutant proteins. Analytical biochemistry 268:64-71.

Tsai B, Rodighiero C, Lencer WI, Rapoport TA (2001) Protein disulfide isomerase acts as a redox-dependent chaperone to unfold cholera toxin. Cell 104:937-948.

Turnbull WB, Precious BL, Homans SW (2004) Dissecting the cholera toxin-ganglioside GM1 interaction by isothermal titration calorimetry. Journal of the American Chemical Society 126:1047-1054.

Turner AK, Stephens JC, Beavis JC, Greenwood J, Gewert C, Randall R, Freeman D, Darsley MJ (2011) Generation and characterization of a live attenuated enterotoxigenic Escherichia coli combination vaccine expressing six colonization factors and heat-labile toxin subunit B. Clinical and vaccine immunology : CVI 18:2128-2135.

Turner MR, Hardiman O, Benatar M, Brooks BR, Chio A, de Carvalho M, Ince PG, Lin C, Miller RG, Mitsumoto H, Nicholson G, Ravits J, Shaw PJ, Swash M, Talbot K, Traynor BJ, Van den Berg LH, Veldink JH, Vucic S, Kiernan MC (2013) Controversies and priorities in amyotrophic lateral sclerosis. The Lancet Neurology 12:310-322.

Ueda A, Shima S, Miyashita T, Ito S, Ueda M, Kusunoki S, Asakura K, Mutoh T (2010) Anti-GM1 antibodies affect the integrity of lipid rafts. Molecular and cellular neurosciences 45:355-362.

Ueda T, Tohda H, Chikazumi N, Eckstein F, Watanabe K (1991) Phosphorothioate-containing RNAs show mRNA activity in the prokaryotic translation systems in vitro. Nucleic acids research 19:547-552.

Urtasun N MFB, Osvaldo Cascone, , Federico J. Wolman, María V. Miranda (2015) High-level expression and purification of recombinant wheat germ agglutinin in Rachiplusia nu larvae. Process Biochemistry 50:40-47.

Vajn K, Viljetic B, Degmecic IV, Schnaar RL, Heffer M (2013) Differential distribution of major brain gangliosides in the adult mouse central nervous system. PloS one 8:e75720.

Van Damme P, Van Den Bosch L, Van Houtte E, Callewaert G, Robberecht W (2002) GluR2-dependent properties of AMPA receptors determine the selective vulnerability of motor neurons to excitotoxicity. Journal of neurophysiology 88:1279-1287.

van de Haar HJ, Burgmans S, Jansen JF, van Osch MJ, van Buchem MA, Muller M, Hofman PA, Verhey FR, Backes WH (2016) Blood-Brain Barrier Leakage in Patients with Early Alzheimer Disease. Radiology:152244.

van den Akker F, Sarfaty S, Twiddy EM, Connell TD, Holmes RK, Hol WG (1996) Crystal structure of a new heat-labile enterotoxin, LT-IIb. Structure 4:665-678.

Van den Berg LH, Franssen H, Wokke JH (1998) The long-term effect of intravenous immunoglobulin treatment in multifocal motor neuropathy. Brain : a journal of neurology 121 (Pt 3):421-428.

Van Den Bosch L, Schwaller B, Vleminckx V, Meijers B, Stork S, Ruehlicke T, Van Houtte E, Klaassen H, Celio MR, Missiaen L, Robberecht W, Berchtold MW (2002) Protective effect of parvalbumin on excitotoxic motor neuron death. Experimental neurology 174:150-161.

van Zundert B, Peuscher MH, Hynynen M, Chen A, Neve RL, Brown RH, Jr., Constantine-Paton M, Bellingham MC (2008) Neonatal neuronal circuitry shows hyperexcitable disturbance in a mouse model of the adult-onset neurodegenerative disease amyotrophic lateral sclerosis. The Journal of neuroscience : the official journal of the Society for Neuroscience 28:10864-10874.

Vance C et al. (2009) Mutations in FUS, an RNA processing protein, cause familial amyotrophic lateral sclerosis type 6. Science 323:1208-1211.

Vanden Broeck D, Horvath C, De Wolf MJ (2007) Vibrio cholerae: cholera toxin. The international journal of biochemistry & cell biology 39:1771-1775.

Vanselow BK, Keller BU (2000) Calcium dynamics and buffering in oculomotor neurones from mouse that are particularly resistant during amyotrophic lateral sclerosis (ALS)-related motoneurone disease. The Journal of physiology 525 Pt 2:433-445.

Vaughan SK, Kemp Z, Hatzipetros T, Vieira F, Valdez G (2015) Degeneration of proprioceptive sensory nerve endings in mice harboring amyotrophic lateral sclerosis-causing mutations. The Journal of comparative neurology 523:2477-2494.

Venters RA, Benson LM, Craig TA, Bagu J, Paul KH, Kordys DR, Thompson R, Naylor S, Kumar R, Cavanagh J (2003) The effects of Ca(2+) binding on the conformation of calbindin D(28K): a nuclear magnetic resonance and microelectrospray mass spectrometry study. Analytical biochemistry 317:59-66.

Vogler C, Levy B, Kyle JW, Sly WS, Williamson J, Whyte MP (1994) Mucopolysaccharidosis VII: postmortem biochemical and pathological findings in a young adult with beta-glucuronidase deficiency. Modern pathology : an official journal of the United States and Canadian Academy of Pathology, Inc 7:132-137.

Waddell T, Head S, Petric M, Cohen A, Lingwood C (1988) Globotriosyl ceramide is specifically recognized by the Escherichia coli verocytotoxin 2. Biochemical and biophysical research communications 152:674-679.

Walters RW, Yi SM, Keshavjee S, Brown KE, Welsh MJ, Chiorini JA, Zabner J (2001) Binding of adeno-associated virus type 5 to 2,3-linked sialic acid is required for gene transfer. The Journal of biological chemistry 276:20610-20616.

Wang L, Schultz PG (2004) Expanding the genetic code. Angewandte Chemie 44:34-66.

Wang SJ, Wang KY, Wang WC (2004) Mechanisms underlying the riluzole inhibition of glutamate release from rat cerebral cortex nerve terminals (synaptosomes). Neuroscience 125:191-201.

Weaver TE, Grunstein RR (2008) Adherence to continuous positive airway pressure therapy: the challenge to effective treatment. Proceedings of the American Thoracic Society 5:173-178.

Weinberg MS, Samulski RJ, McCown TJ (2013) Adeno-associated virus (AAV) gene therapy for neurological disease. Neuropharmacology 69:82-88.

Weinberg MS, Blake BL, Samulski RJ, McCown TJ (2011) The influence of epileptic neuropathology and prior peripheral immunity on CNS transduction by rAAV2 and rAAV5. Gene therapy 18:961-968.

Weinberg T, Solish N, Murray C (2014) Botulinum neurotoxin treatment of palmar and plantar hyperhidrosis. Dermatologic clinics 32:505-515.

West SD, McBeath HA, Stradling JR (2009) Obstructive sleep apnoea in adults. Bmj 338:b1165.

Wienken CJ, Baaske P, Rothbauer U, Braun D, Duhr S (2010) Protein-binding assays in biological liquids using microscale thermophoresis. Nature communications 1:100.

Williamson DJ (2016) In: University of Leeds.

Williamson DJ, Fascione MA, Webb ME, Turnbull WB (2012) Efficient N-terminal labeling of proteins by use of sortase. Angewandte Chemie 51:9377-9380.

Williamson TL, Cleveland DW (1999) Slowing of axonal transport is a very early event in the toxicity of ALS-linked SOD1 mutants to motor neurons. Nature neuroscience 2:50-56.

Wold WS, Toth K (2013) Adenovirus vectors for gene therapy, vaccination and cancer gene therapy. Current gene therapy 13:421-433.

Won TB, Quan SH, Kim DY, Rhee CS, Lee CH (2009) Immunostimulatory sequence oligdeoxynucleotide/cholera toxin B conjugate: a novel allergen-independent intranasal vaccine for allergic rhinitis. Annals of allergy, asthma & immunology : official publication of the American College of Allergy, Asthma, & Immunology 102:314-322.

Wong WS, Rosoff PM (1996) Pharmacology of pertussis toxin B-oligomer. Canadian journal of physiology and pharmacology 74:559-564.

Wood JN, Winter J, James IF, Rang HP, Yeats J, Bevan S (1988) Capsaicin-induced ion fluxes in dorsal root ganglion cells in culture. The Journal of neuroscience : the official journal of the Society for Neuroscience 8:3208-3220.

Wu G, Lu ZH, Ledeen RW (1995) GM1 ganglioside in the nuclear membrane modulates nuclear calcium homeostasis during neurite outgrowth. Journal of neurochemistry 65:1419-1422.

Wu G, Xie X, Lu ZH, Ledeen RW (2009) Sodium-calcium exchanger complexed with GM1 ganglioside in nuclear membrane transfers calcium from nucleoplasm to endoplasmic reticulum. Proceedings of the National Academy of Sciences of the United States of America 106:10829-10834.

Wu G, Lu ZH, Kulkarni N, Ledeen RW (2012) Deficiency of ganglioside GM1 correlates with Parkinson's disease in mice and humans. Journal of neuroscience research 90:1997-2008.

Wu G, Lu ZH, Wang J, Wang Y, Xie X, Meyenhofer MF, Ledeen RW (2005) Enhanced susceptibility to kainate-induced seizures, neuronal apoptosis, and death in mice lacking gangliotetraose gangliosides: protection with LIGA 20, a membrane-permeant analog of GM1. The Journal of neuroscience : the official journal of the Society for Neuroscience 25:11014-11022.

Wu Z, Miller E, Agbandje-McKenna M, Samulski RJ (2006) Alpha2,3 and alpha2,6 N-linked sialic acids facilitate efficient binding and transduction by adeno-associated virus types 1 and 6. Journal of virology 80:9093-9103.

Xie X, Wu G, Lu ZH, Ledeen RW (2002) Potentiation of a sodium-calcium exchanger in the nuclear envelope by nuclear GM1 ganglioside. Journal of neurochemistry 81:1185-1195.

Xie X, Wu G, Lu ZH, Rohowsky-Kochan C, Ledeen RW (2004) Presence of sodium-calcium exchanger/GM1 complex in the nuclear envelope of non-neural cells: nature of exchanger-GM1 interaction. Neurochemical research 29:2135-2146.

Xiong AS, Peng RH, Zhuang J, Gao F, Li Y, Cheng ZM, Yao QH (2008) Chemical gene synthesis: strategies, softwares, error corrections, and applications. FEMS microbiology reviews 32:522-540.

Xu L, Ryugo DK, Pongstaporn T, Johe K, Koliatsos VE (2009) Human neural stem cell grafts in the spinal cord of SOD1 transgenic rats: differentiation and structural integration into the segmental motor circuitry. The Journal of comparative neurology 514:297-309.

Yanagisawa K (2005) GM1 ganglioside and the seeding of amyloid in Alzheimer's disease: endogenous seed for Alzheimer amyloid. The Neuroscientist : a review journal bringing neurobiology, neurology and psychiatry 11:250-260.

Yanagisawa K, Ihara Y (1998) GM1 ganglioside-bound amyloid beta-protein in Alzheimer's disease brain. Neurobiology of aging 19:S65-67.

Yoshihara Y, Mizuno T, Nakahira M, Kawasaki M, Watanabe Y, Kagamiyama H, Jishage K, Ueda O, Suzuki H, Tabuchi K, Sawamoto K, Okano H, Noda T, Mori K (1999) A genetic approach to visualization of multisynaptic neural pathways using plant lectin transgene. Neuron 22:33-41.

Yowler BC, Kensinger RD, Schengrund CL (2002) Botulinum neurotoxin A activity is dependent upon the presence of specific gangliosides in neuroblastoma cells expressing synaptotagmin I. The Journal of biological chemistry 277:32815-32819.

Yu YJ, Zhang Y, Kenrick M, Hoyte K, Luk W, Lu Y, Atwal J, Elliott JM, Prabhu S, Watts RJ, Dennis MS (2011) Boosting brain uptake of a therapeutic antibody by reducing its affinity for a transcytosis target. Science translational medicine 3:84ra44.

Yuan T, Ouyang H, Vogel HJ (1999) Surface exposure of the methionine side chains of calmodulin in solution. A nitroxide spin label and two-dimensional NMR study. The Journal of biological chemistry 274:8411-8420.

Yuki N, Taki T, Inagaki F, Kasama T, Takahashi M, Saito K, Handa S, Miyatake T (1993) A bacterium lipopolysaccharide that elicits Guillain-Barre syndrome has a GM1 ganglioside-like structure. The Journal of experimental medicine 178:1771-1775.

Yuki N, Yamada M, Koga M, Odaka M, Susuki K, Tagawa Y, Ueda S, Kasama T, Ohnishi A, Hayashi S, Takahashi H, Kamijo M, Hirata K (2001) Animal model of axonal Guillain-Barre syndrome induced by sensitization with GM1 ganglioside. Annals of neurology 49:712-720.

Yuyama K, Yamamoto N, Yanagisawa K (2008) Accelerated release of exosome-associated GM1 ganglioside (GM1) by endocytic pathway abnormality: another putative pathway for GM1-induced amyloid fibril formation. Journal of neurochemistry 105:217-224.

Zarei S, Carr K, Reiley L, Diaz K, Guerra O, Altamirano PF, Pagani W, Lodin D, Orozco G, Chinea A (2015) A comprehensive review of amyotrophic lateral sclerosis. Surgical neurology international 6:171.

Zha Q, Ruan Y, Hartmann T, Beyreuther K, Zhang D (2004) GM1 ganglioside regulates the proteolysis of amyloid precursor protein. Molecular psychiatry 9:946-952.

Zhang L, Huang Y, Lin Y, Shan Y, Tan S, Cai W, Li H, Zhang B, Men X, Lu Z (2016) Anti-inflammatory effect of cholera toxin B subunit in experimental stroke. Journal of neuroinflammation 13:147.

Zhang Y, Chang S, Sun J, Zhu S, Pu C, Li Y, Zhu Y, Wang Z, Xu RX (2015) Targeted Microbubbles for Ultrasound Mediated Short Hairpin RNA Plasmid Transfection to Inhibit Survivin Gene Expression and Induce Apoptosis of Ovarian Cancer A2780/DDP Cells. Molecular pharmaceutics 12:3137-3145.

Zheng H, Qiao C, Wang CH, Li J, Li J, Yuan Z, Zhang C, Xiao X (2010) Efficient retrograde transport of adeno-associated virus type 8 to spinal cord and dorsal root ganglion after vector delivery in muscle. Human gene therapy 21:87-97.

Zincarelli C, Soltys S, Rengo G, Rabinowitz JE (2008) Analysis of AAV serotypes 1-9 mediated gene expression and tropism in mice after systemic injection. Molecular therapy : the journal of the American Society of Gene Therapy 16:1073-1080.

Zinszner H, Sok J, Immanuel D, Yin Y, Ron D (1997) TLS (FUS) binds RNA in vivo and engages in nucleo-cytoplasmic shuttling. Journal of cell science 110 (Pt 15):1741-1750.